UNIVERSIDADE FEDERAL DO CEARÁ

CENTRO DE TECNOLOGIA

PROGRAMA DE PÓS-GRADUAÇÃO EM ENGENHARIA E CIÊNCIA DE MATERIAIS

RAFAEL LEANDRO FERNANDES MELO

DEVELOPMENT OF A MAGNETIC NANOBIOCATALYST FOR FATTY ACID ESTERIFICATION

FORTALEZA

2025

RAFAEL LEANDRO FERNANDES MELO

DEVELOPMENT OF A MAGNETIC NANOBIOCATALYST FOR FATTY ACID ESTERIFICATION

Doctoral thesis submitted to the Programa de Pós-Graduação em Engenharia e Ciência de Materiais of the Universidade Federal do Ceará as a requeriment for the degree of doctor in engineering and materials sciences.
Concentration area: Physical and mechanical properties of materials.

Supervisor: Prof. Dr. Pierre Basílio Almeida Fechine

Co-supervisor: Prof. Dr. João Maria Soares

FORTALEZA
2025

Dados Internacionais de Catalogação na Publicação
Universidade Federal do Ceará
Sistema de Bibliotecas
Gerada automaticamente pelo módulo Catalog, mediante os dados fornecidos pelo(a) autor(a)

M486d Melo, Rafael Leandro Fernandes.
Development of magnetic nanobiocatalyst for fatty acid esterification / Rafael Leandro Fernandes Melo. – 2025.
174 f. : il. color.

Tese (doutorado) – Universidade Federal do Ceará, Centro de Tecnologia, Programa de Pós-Graduação em Engenharia e Ciência de Materiais, Fortaleza, 2025.
Orientação: Prof. Dr. Pierre Basílio Almeida Fechine.
Coorientação: Prof. Dr. João Maria Soares.

1. Magnetic Biocatalysts. 2. Immobilization. 3. FFA Esterification. 4. Computational Modeling. I. Título.
CDD 620.11

RAFAEL LEANDRO FERNANDES MELO

DEVELOPMENT OF MAGNETIC NANOBIOCATALYST FOR FATTY ACID ESTERIFICATION

Doctoral thesis submitted to the Programa de Pós-Graduação em Engenharia e Ciência de Materiais of the Universidade Federal do Ceará as a requeriment for the degree of doctor in engineering and materials sciences.
Concentration area: Physical and mechanical properties of materials.

Approved on __/__/____

EXAMINATION BOARD

Documento assinado digitalmente
gov.br PIERRE BASILIO ALMEIDA FECHINE
Data: 29/04/2025 11:32:00-0300
Verifique em https://validar.iti.gov.br

PIERRE BASILIO ALMEIDA FECHINE

Documento assinado digitalmente
gov.br JOAO MARIA SOARES
Data: 30/04/2025 09:38:20-0300
Verifique em https://validar.iti.gov.br

JOÃO MARIA SOARES
UERN - Coorientador

Documento assinado digitalmente
gov.br ADONAY RODRIGUES LOIOLA
Data: 29/04/2025 17:48:06-0300
Verifique em https://validar.iti.gov.br

ADONAY RODRIGUES LOIOLA

Documento assinado digitalmente
gov.br TIAGO MELO FREIRE
Data: 29/04/2025 15:25:48-0300
Verifique em https://validar.iti.gov.br

TIAGO MELO FREIRE
UFC - Examinador Externo ao Programa

Documento assinado digitalmente
gov.br FREDERICO RIBEIRO DO CARMO
Data: 29/04/2025 21:34:37-0300
Verifique em https://validar.iti.gov.br

FREDERICO RIBEIRO DO CARMO
UFERSA - Examinador Externo à Instituição

Documento assinado digitalmente
gov.br JOSE CLEITON SOUSA DOS SANTOS
Data: 29/04/2025 12:03:50-0300
Verifique em https://validar.iti.gov.br

JOSÉ CLEITON SOUSA DOS SANTOS
UNILAB - Examinador Externo à Instituição

To my wife and daughter, Bel and Bia, my family and my friends.

ACKNOWLEDGEMENTS

First and foremost, I thank God for granting me the privilege of studying and making this thesis possible.

I am deeply grateful to my wife, Isabel, for her unconditional companionship, patience, and the right words in the moments I needed them most. To my daughter, Beatriz, who brightens my days with her sparkling eyes and warm smile, giving true meaning to my journey. I love you both, Bel and Bia.

To my mother, Ana, I thank you for never sparing any effort to provide me with the best education and values. To my brother, Luciano, thank you for always believing in my abilities and standing by me with encouraging and supportive words. I also extend my gratitude to my sister-in-law, Fernanda, who has always helped me see how capable I am. I also thank my nieces, Valentina and Louise, for reminding me—through their joy and lightness—of the value of small things and the importance of keeping a light heart, even on the most difficult days. I love you all, my dear family.

I express my sincere gratitude to my advisor, Professor Pierre, for welcoming me into his laboratory despite the logistical limitations I faced at the beginning of this research. I am thankful for your outstanding guidance, patience, constant support, and for always leading me with clarity and sensitivity. Your well-structured and challenging thesis proposal was essential for the fruitful outcomes of this research and guided me securely along the path of science. I intend to continue in this field, and I thank you for showing me the way.

To my co-advisor, Professor João Maria, I am grateful for also welcoming me into your laboratory and for helping to ease the logistical difficulties encountered at the beginning of this journey. I am especially thankful for the knowledge shared in the area of material characterization, which was crucial for the development of this thesis.

My heartfelt thanks go to Professor José Cleiton, who, in addition to acting as a co-advisor, shared daily and valuable insights with me in the field of enzyme immobilization. His generous and consistent mentorship guided me smoothly through the world of scientific publishing and was, without a doubt, a great source of inspiration for my path in research and science.

I also thank Professor Tiago Melo, who helped structure the initial steps of this thesis. His guidance was essential in defining the scientific approach and initial methodology. As an exceptional tutor in the field of Chemistry, his support and knowledge were fundamental to me,

especially in the early stages of the research when I needed academic and technical direction the most.

I extend my gratitude to all my laboratory colleagues from the GQMat, CSAMA, GENES, and NPCO2 research groups. You were true partners on this journey, with whom I shared daily discussions, analyses, and scientific reflections. Without your collaboration, support, and constant exchange, this thesis would not have been possible.

To my day-to-day friends, I offer my heartfelt thanks. Thank you for standing by me during moments of fatigue, for the lighthearted conversations that helped me stay balanced, and for the laughter that made the path more bearable. Your friendship was essential for me to carry on with more energy, courage, and joy, even during the most challenging days.

I am grateful to the Federal Institute of Ceará (IFCE) for granting me a leave of absence to pursue my doctoral studies, even after one year into the program. This decision was crucial for me to delve deeper into the research and complete this work with full dedication and quality.

To the Graduate Program in Materials Science and Engineering, I am thankful for the welcoming environment, the infrastructure provided, and the excellence in scientific training. It was within this academic setting that I was able to grow as a researcher and develop this work with the necessary support.

Finally, I extend my gratitude to the Federal University of Ceará (UFC), the State University of Rio Grande do Norte (UERN), and the Federal Rural University of the Semi-Arid Region (UFERSA) — institutions that, directly or indirectly, contributed to my academic formation and to the development of this thesis, whether through partnerships, laboratory access, technical support, or academic collaborations.

RESUMO

Biocatalisadores magnéticos unem as propriedades magnéticas com a atividade catalítica de enzimas, oferecendo vantagens como fácil recuperação e reutilização. Nesse sentido, esta tese foi estruturada em três capítulos principais. No primeiro momento, foi realizada uma análise cienciométrica de 34.949 artigos, sendo refinados para 450. Catalogou-se periódicos, países, instituições, autores e artigos mais citados, identificando os *hotspots*. Palavras-chaves revelaram cinco *clusters*, sendo o mais proeminente relacionado à produção de biocombustíveis a partir de óleos vegetais sustentáveis. No segundo momento, desenvolveu-se um nanobiocatalisador magnético funcionalizado com polietilenimina (PEI) e grupos epóxi, utilizado para imobilizar a lipase Eversa® Transform 2.0 (EVS), formando Fe_3O_4-PEI-DGEBA@EVS. A otimização aconteceu via planejamento Taguchi, alcançando um rendimento de 95,04 ± 0,79% sob as condições: 15 horas, 95 mM, 5 mg/g de carga proteica e 25 °C. O suporte e o nanobiocatalisador foram caracterizados por FRX, MEV, MET, DRX, FTIR, TGA e VSM. A capacidade máxima de carga foi de 25 mg/g, com estabilidade superior a 60 dias, apresentando apenas 9,53% de perda de atividade. O nanobiocatalisador manteve 28% de sua atividade a 70 °C, superando a enzima livre. Foi possível esterificar ácidos graxos livres (AGL) do óleo de babaçu, com eficiência de até 97,91% e reutilização de 10 ciclos com rendimento superior a 50%. A esterificação foi confirmada por RMN. E a viscosidade cinemática e densidade a 40 °C foram de 6,052 mm^2/s e 0,832 g/cm^3. Estudos *in silico* demonstraram uma afinidade de ligação de -5,8 kcal/mol entre a EVS e o ácido oleico, sugerindo uma interação estável substrato-enzima. No terceiro momento, o mesmo suporte foi utilizado para imobilizar a lipase B de *Candida antarctica* (CALB), formando o nanobiocatalisador Fe_3O_4-PEI-DGEBA@CALB. A imobilização foi confirmada pelas mesmas técnicas. A enzima imobilizada apresentou desempenho catalítico de 97% de rendimento e estabilidade operacional de 80% da atividade após 120 dias. O biocatalisador esterificou AGL do óleo de tilápia, com a reação confirmada por RMN e FTIR. Estudos teóricos destacaram que a imobilização promove seletividade da enzima para ácidos graxos saturados de cadeia longa, através de interações hidrofóbicas com resíduos-chave do sítio ativo, como Leu140, Ala141 e Val154.

Palavras-chave: biocatalisadores magnéticas; imobilização; esterificação de AGLs; modelagem computacional.

ABSTRACT

Magnetic biocatalysts combine magnetic properties with the catalytic activity of enzymes, offering advantages such as easy recovery and reuse. In this context, this thesis was structured into three main chapters. Initially, a scientometric analysis of 34,949 articles was conducted and refined to 450. Journals, countries, institutions, authors, and the most cited articles were cataloged, identifying research hotspots. Keyword analysis revealed five clusters, with the most prominent related to the production of biofuels from sustainable vegetable oils. In the second stage, a magnetic nanobiocatalyst functionalized with polyethyleneimine (PEI) and epoxy groups was developed to immobilize the lipase Eversa® Transform 2.0 (EVS), forming Fe_3O_4-PEI-DGEBA@EVS. Optimization was carried out using Taguchi design, achieving a yield of 95.04 ± 0.79% under the following conditions: 15 hours, 95 mM, 5 mg/g protein loading, and 25 °C. The support and nanobiocatalyst were characterized by XRF, SEM, TEM, XRD, FTIR, TGA, and VSM. The maximum loading capacity was 25 mg/g, with stability exceeding 60 days and only 9.53% activity loss. The nanobiocatalyst retained 28% of its activity at 70 °C, surpassing the performance of the free enzyme. It was able to esterify free fatty acids (FFAs) from babassu oil with an efficiency of up to 97.91%, maintaining yields above 50% after 10 reuse cycles. Esterification was confirmed by NMR, and the kinematic viscosity and density at 40 °C were 6.052 mm^2/s and 0.832 g/cm^3, respectively. In silico studies demonstrated a binding affinity of -5.8 kcal/mol between EVS and oleic acid, suggesting a stable substrate-enzyme interaction. In the third stage, the same support was used to immobilize Candida antarctica lipase B (CALB), forming the nanobiocatalyst Fe_3O_4-PEI-DGEBA@CALB. Immobilization was confirmed by the same techniques. The immobilized enzyme exhibited a catalytic performance with 97% yield and operational stability of 80% of its activity after 120 days. The biocatalyst esterified FFAs from tilapia oil, with the reaction confirmed by NMR and FTIR. Theoretical studies highlighted that immobilization promotes enzyme selectivity toward long-chain saturated fatty acids through hydrophobic interactions with key active-site residues such as Leu140, Ala141, and Val154.

Keywords: magnetic biocatalysts; immobilization; FFA esterification; computational modeling.

LIST OF FIGURES

Figure 1 – Representation of the three-dimensional structure of Candida rugosa lipase obtained from PDB, showing its catalytic triad responsible for enzymatic activity. 24
Figure 2 – Annual publications on lipase, immobilization, and magnetic nanoparticles, from 2010 to 2022. 26
Figure 3 – Structure representing the search and analysis criteria. 28
Figure 4 – Main journals that published between 2010 and 2022 in the area of lipases immobilized by magnetic nanoparticles. (A) Ranking of the impact factor H of the ten journals that published the most in the area. (B) Growth in the number of publications of the journals that published the most in the area. 32
Figure 5 – Main countries, institutions and authors who published between 2010 and 2022 in the area of lipases immobilized by magnetic nanoparticles. (A) Geocoded location of each publication. (B) Map of the collaboration network among the countries identified with at least five citations. (C) Publication by each institution, considering collaboration. (D) Map of the collaboration network between institutions identified with at least five citations. (E) Authors publications over the analyzed period. (F) Map of the collaboration network between the authors identified with at least five citations. 34
Figure 6 – Graph of three campuses, listing countries, authors and institutions. 35
Figure 7 – Distributions of research areas for articles on lipases immobilized by magnetic nanoparticles. 38
Figure 8 – Different ways to produce magnetic biocatalysts. The parts of the image depict four variables: selected lipase, immobilization route, type of magnetic nanoparticle and doping of other nanoparticles, and type of functionalization and activation of the nanoparticles. 39
Figure 9 – Different ways of obtaining magnetic biocatalysts. (A) Lipases immobilized by MNPs, (i) Lipases most used in immobilization, (ii) Evolution in the number of articles between 2010 and 2022. (B) Forms of immobilizations, (i) Immobilizations most used in MNPs, (ii) Evolution in the number of articles between 2010 and 2022. (C) Functionalization and activation, (i) Functionalization and activation most used, (ii) Evolution in the number of articles between 2010 and 2022. (D) Magnetic nanoparticles, (i) More magnetic nanoparticles used, (ii) Evolution in the number of articles between 2010 and 2022. 41

Figure 10 – Clusters formed by the main keywords. (A) Mapping of co-citations of keywords in articles in WoS on lipases immobilized by magnetic nanoparticles. (B) Mapping of keyword quotes with period indication. 47
Figure 11 – Thematic map for research on lipases immobilized by magnetic nanoparticles... 52
Figure 12 – Main forms of synthesis of magnetic nanoparticles and main forms of characterization. 54
Figure 13 – (A) Representation of the different applications related to magnetic biocatalysts. (B) Representation of some advantages and disadvantages related to magnetic biocatalysts. 56
Figure 14 – Some reactors based on magnetic biocatalysts. 59
Figure 15 – Patent data related to magnetic biocatalysts. (A) Countries with the most deposited patents. (B) Number of patents filed between 2000 and 2022. 60
Figure 16 – 2D structure of the chemical composition of residual oil from babassu. 75
Figure 17 – Enzyme immobilization (Eversa® lipase Transform 2.0 (EVS) being represented by *Thermomyces lanuginosus* lipase (TLL)) by Fe_3O_4-PEI-DGEBA support. 78
Figure 18 – Response from S/N ratios. 81
Figure 19 – Contour surfaces display the interaction effects between the evaluated factors as a function of immobilization yield (I.Y). 84
Figure 20 – Enzyme immobilization parameters. a) Maximum enzyme load capacity (Maximum load test of Fe_3O_4-PEI-DGEBA@EVS in time 12 h, ionic load 95 mM, temperature 25 °C and protein load 1:1 - 1:50 mg/g); b) Storage capacity (Effect of storage time on the activity of the Fe_3O_4-PEI-DGEBA@EVS biocatalyst over 12 h, ionic load 95 mM, temperature 25 °C and protein load 1:5 mg/g); c) Thermal stability (at different temperatures 25 °C - 80 °C) of the soluble and immobilized EVS enzyme under optimal conditions; d) pH stability (at different pH 4 - 9) of soluble and immobilized EVS enzyme under optimal conditions. 85
Figure 21 – SEM micrographs / XRF maps and elemental spectra a) Fe_3O_4; b) Fe_3O_4-PEI; c) Fe_3O_4-PEI-DGEBA, and d) Fe_3O_4-PEI-DGEBA@EVS. 89
Figure 22 – TEM micrographs/particle size distribution curves a) Fe_3O_4; b) Fe_3O_4-PEI; c) Fe_3O_4-PEI-DGEBA and d) Fe_3O_4-PEI-DGEBA@EVS. 90
Figure 23 – a) XRD; b) FTIR; c) TGA; d) DTG and e) VSM. 93
Figure 24 – Operational stability. Reaction medium: 5% of the biocatalyst Fe_3O_4-PEI-DGEBA@EVS, free fatty acids from babassu oil and octyl alcohol (1:5). The reactions were carried out for 5 hours at 40 °C and 200 rpm. 94

Figure 25 – a) Characterization of the FFA. ^{1}H NMR (500 MHz, $CDCl_3$). b) Characterization of the ^{1}H NMR biolubricant (500 MHz, $CDCl_3$) where R is related to the chemical composition of the residual babassu oil (Fatty acids: lauric, myristic, palmitic, oleic, caprylic, capric, linoleic, stearic). 96
Figure 26 – Interactions of babassu oil composition and the catalytic triad of EVS lipase Ser153-His268-Asp206, together with amino acid residues. 100
Figure 27 – Linoleic acid interactions between the catalytic triad of EVS lipase Ser153-His268-Asp206 (green) and amino acids residues. 101
Figure 28 – Root Mean Square Deviation (RMSD), concerning the initial confirmation of the ligand-enzyme complex versus the simulation time (ns) in the production simulations step of the MD with oil composition babassu/EVS. 103
Figure 29 – Root Mean Square Fluctuation (RMSF), concerning the initial confirmation of the ligand-enzyme complex versus the simulation time (ns) in the production simulations step of the MD with oil composition babassu/EVS. 104
Figure 30 – Hydrogen bonds formed between the protein and the ligand during the simulation steps. 105
Figure 31 – Evaluation of immobilization parameters for CALB using the Fe_3O_4-PEI-DGEBA support. a) Maximum enzyme loading capacity, evaluated by varying the enzyme concentration from 1–50 mg per gram of support; b) Thermal stability assessed at different temperatures (25–80 °C); c) pH activity of soluble and immobilized CALB, tested across a pH range of 4–9 under optimal conditions; d) Storage stability of immobilized CALB. 120
Figure 32 – TEM micrographs, particle size distribution curves, and SEM/XRF analyses of the materials. a) TEM image of Fe_3O_4 with its particle size distribution curve (inset), showing a spherical morphology; b) TEM image of Fe_3O_4-PEI-DGEBA@CALB with its size distribution curve (inset), showing a slightly more aggregated appearance due to the immobilization process; c) SEM image of Fe_3O_4, revealing a laminar surface morphology, and its corresponding XRF map (inset); d) SEM image of Fe_3O_4-PEI-DGEBA@CALB, showing increased surface roughness, indicative of compositional alterations. 123
Figure 33 – Structural characterization of the material. a) X-Ray Diffraction (XRD); b) Fourier Transform Infrared Spectroscopy (FTIR); c) Vibrating Sample Magnetometer (VSM); d) Thermogravimetric Analysis (TGA, solid lines), and Derivative Thermogravimetry (DTG, dash lines). 125

Figure 34 – Operational stability of Fe_3O_4-PEI-DGEBA@CALB. Reaction conditions: 9% biocatalyst, free fatty acids from tilapia oil, and ethanol in a 1:5 molar ratio. Reactions were performed at 25°C and 200 rpm for 5 hours. 126
Figure 35 – FTIR characterization of the biofuel produced from the biocatalysts Fe_3O_4-PEI-DGEBA@CALB and Tilapia oil (red) and commercial biofuel (black). 127
Figure 36 – NMR characterization of the biofuel (500 MHz, in $CDCl_3$). 128
Figure 37 – Optimized binding orientation of fatty acids in the active site of CALB, highlighting key interactions that stabilize substrate binding. Residues within 3 angstroms of each substrate are shown. Non-polar hydrogen atoms are omitted for clarity. ... 130
Figure 38 – Mechanism of acylation catalyzed by CALB. The carbon atoms of the substrate (9O) are shown in orange and enzyme atoms are shown in green. Non-polar hydrogens are omitted for clarity. Bond lengths are displayed in angstroms, and Gibbs free energies are in kcal/mol, relative to the reactant (R_A). 131
Figure 39 – Mechanism of deacylation catalyzed by CALB. The carbon atoms of the substrate (9O) are shown in orange, ethanol (EtOH) is shown in yellow, and enzyme atoms are shown in green. Non-polar hydrogens are omitted for clarity. Bond lengths are displayed in angstroms, and Gibbs free energies are in kcal/mol, relative to the reactant (R_D). 132

LIST OF TABLES

Table 1 – Ranking of the top ten journals, countries, institutions and authors that most published and were most cited, according to the database obtained from WoS with the keywords “lipase” and “immobilization” and “magnetic nanoparticles” in the period from 2010 to 2022. 30
Table 2 – Most cited articles from the last 10 years on lipases immobilized by magnetic nanoparticles. 36
Table 3 – Ranking of the 20 most prominent keywords in the analyzed articles. 45
Table 4 – The top five co-citation clusters based on CiteSpace analysis. 48
Table 5 – Independent variables and their respective levels for EVS immobilization in Fe_3O_4- 68
Table 6 – Experimental design of the Taguchi method. 68
Table 7 – EVS immobilization results in Fe_3O_4-PEI-DGEBA in Taguchi L9 Planning. 79
Table 8 – Response from S/N ratios. 80
Table 9 – ANOVA results for parameters that affect immobilization. 83
Table 10 – Optimal conditions for EVS immobilization by Fe_3O_4-PEI-DGEBA. 84
Table 11 – Biolubricant properties. 98
Table 12 – Oil composition and molecular docking results. 99
Table 13 – Free energy estimation data of Babassu lipid oil composition against EVS. 106

TABLE OF CONTENTS

CHAPTER I 19

1 INTRODUCTION AND OBJECTIVES 19

1.1 Introduction 19

1.2 Thesis objectives 22

CHAPTER II 23

2 RECENT APPLICATIONS AND FUTURE PROSPECTS OF MAGNETIC BIOCATALYSTS 23

2.1 Introduction 24

2.3 Results and Discussion 28

2.3.1 Results concerning publications 28

2.3.2 Distribution of scientific journals, countries, institutions, and authors 29

2.3.3 The most cited articles 35

2.3.4 Research topics 37

2.3.5 Classification by research topic 38

2.3.6 Quantitative analysis of frequent keywords 45

2.3.7 Constant fields of investigation 48

2.3.8 Thematic map 51

2.4 Overview of magnetic biocatalysts 52

2.4.1 Synthesis and characterization of magnetic biocatalysts 52

2.4.2 Applications of magnetic biocatalysts 54

2.4.3 Reactors used in magnetic biocatalysts 56

2.4.3 Patents related to magnetic biocatalysts 59

2.5 Conclusions 60

CHAPTER III 62

3 ENHANCING BIOCATALYST PERFORMANCE THROUGH IMMOBILIZATION OF LIPASE (EVERSA® TRANSFORM 2.0) ON HYBRID AMINE-EPOXY CORE-SHELL MAGNETIC NANOPARTICLES 62

3.1 Introduction 63

3.2 Materials and Methods 66

3.2.1 Materials 66

3.2.2 Synthesis of Fe_3O_4 magnetic nanoparticles functionalized with PEI and activated with DGEBA 66

3.2.3. Experimental design for immobilization of Eversa® lipase Transform 2.0 (EVS) on Fe_3O_4-PEI-DGEBA 67

3.2.4. Determination of enzyme activity and protein content 69

3.2.5. Immobilization parameters 69

3.2.6. Maximum enzyme loading capacity 70

3.2.7 Storage stability 70

3.2.8 Thermal stability 71

3.2.9 Stability in pH 71

3.2.10 Materials characterization 71

3.2.11 Production of biolubricants and operational stability from Babassu oil 72

3.2.12 Nuclear Magnetic resonance spectroscopy (NMR) 73

3.2.13 Evaluation of viscosity and density 74

3.2.14 Molecular docking 74

3.2.15 Molecular docking 76

3.3 Results and Discussion 77

3.3.1. Functionalization of Fe_3O_4 with polyethyleneimine (Fe_3O_4-PEI) and activation with diglycidyl ether of bisphenol A (Fe_3O_4-PEI-DGEBA) 77

3.3.2 Optimization of the immobilization of Eversa® lipase Transform 2.0 (EVS) on Fe_3O_4-PEI-DGEBA 78

3.3.3 Analysis of the immobilization parameters of the biocatalyst Fe_3O_4-PEI-DGEBA@EVS 85

3.3.4 Maximum enzyme loading capacity 86
3.3.5 Storage stability 86
3.3.6 Thermal stability 87
3.3.7 Stability in pH 87
3.3.7 Materials characterization 88
3.3.8 Production of biolubricants and operational stability from Babassu oil 93
3.3.9 Nuclear Magnetic Resonance Spectroscopy (NMR) 95
3.3.10 Biolubricant viscosity and density 97
3.3.9 Molecular docking 98
3.3.10 Molecular dynamics 101
3.3.11 RMSD analysis 102
3.3.12 RMSF analysis 103
3.3.12 H-bonds analysis 104
3.3.13 MM/GBSA calculations 105
3.4 Conclusion 106
CHAPTER IV 108
4 BIOENERGY CONVERSION OF RESIDUAL TILAPIA OIL USING A NOVEL IMMOBILIZED LIPASE: ENHANCED STABILITY, SELECTIVITY, AND COMPUTATIONAL INSIGHTS 108
4.1 Introduction 109
4.2 Materials and Methods 111
4.2.1 Materials 111
4.2.2 Synthesis of the magnetic support Fe_3O_4-PEI-DGEBA 111
4.2.3 Immobilization of CALB on Fe_3O_4-PEI-DGEBA 112
4.2.4 Determination of enzymatic activity and protein concentration 113
4.2.5 Stability of the catalyst 113
4.2.6 Material characterization 114
4.2.7 Production of biodiesel 115

4.2.8 Fourier Transform Infrared Spectroscopy (FTIR) and Nuclear Magnetic Resonance spectroscopy (NMR) of the biodiesel 116

4.2.9 Viscosity and density of the biodiesel 116

4.2.10 Molecular docking and molecular dynamics (MD) simulations 117

4.2.11 Hybrid molecular mechanics and quantum mechanics (QM/MM) simulations 117

4.3 Results and discussion 118

4.3.1 Synthesis and functionalization of the support 118

4.3.2 Enzymatic immobilization and stability of the biocatalyst 119

4.3.3 Characterization of the heterofunctional biocatalyst 122

4.3.4 Characterization of the biodiesel 126

4.3.5 Computational studies 129

4.3 Conclusion 132

CHAPTER V 134

5 GENERAL CONCLUSIONS 134

6 SCIENTIFIC PRODUCTION 135

6.1 Published articles 135

6.2 Submitted articles 137

REFERENCES 138

CHAPTER I

1 INTRODUCTION AND OBJECTIVES

1.1 Introduction

Industrialization and the advancement of new technologies have caused significant impacts on the environment (Jawadi et al., 2025; Kakar et al., 2024). In response to these challenges, various organizations and international agencies have been investing in cleaner and more sustainable solutions, aiming to minimize the environmental damage associated with production processes (Wang et al., 2024). The Sustainable Development Goals (SDGs), established by the United Nations in 2015, form a global agenda with 17 targets aimed at eradicating poverty, protecting the environment, and promoting economic development by 2030 (Winton et al., 2024). The production, development, and optimization of different catalysts directly contribute to achieving some of these goals by enabling more efficient and environmentally responsible processes.

Catalysts are substances that increase the rate of chemical reactions by lowering the activation energy required. They operate through various mechanisms, such as the adsorption of reagents on their surface, formation of intermediate complexes, or temporary changes in oxidation state (Raju et al., 2024; X. Tang et al., 2025). Catalysts can be classified according to their phase in relation to the reaction medium. In homogeneous catalysis, the catalyst is in the same phase as the reactants, usually in solution, allowing for high activity and selectivity. However, catalyst recovery and stability can be limiting factors. In contrast, in heterogeneous catalysis, the catalyst and reactants are in different phases, such as a solid in a liquid or gaseous medium (Fu et al., 2025; Jang et al., 2025). This form is widely used in industry due to its ease of separation and resistance to harsh conditions, although it presents lower selectivity due to limitations in the available active sites on the surface (Khoramian et al., 2024; Li et al., 2025).

In the search for increasingly sustainable processes, biocatalysts stand out due to their biological origin such as enzymes or microorganisms and their high specificity and efficiency even under mild reaction conditions (Bantihun et al., 2025; Katnic & Gupta, 2025). Unlike heterogeneous catalysts, which operate through physicochemical interactions on surfaces, biocatalysts act with molecular precision, leveraging the complex three-dimensional structures of enzymes that enable selective transformations and catalytic specificity (Andrés-Sanz et al., 2024).

The global biocatalyst market was valued at USD 2.12 billion in 2023 and is projected to reach USD 2.23 billion by 2032, exhibiting a compound annual growth rate (CAGR) of 0.6% over the period. This market trend is growing exponentially as international agreements approve measures for the transition to renewable energy sources (BUSINESS RESEARCH INSIGHTS, 2024). Major players in the materials and surface engineering sector already commercialize well-established industrial biocatalysts, such as the Danish company Novozymes A/S, which produces well-known products like Novozym® 435 and Lipozyme® RM IM, both used in the production of biofuels and biolubricants.

In the pursuit of increasingly efficient processes, engineers and scientists research new materials daily. Enzymes are better catalysts when their pH, temperature, and concentration parameters are optimized (Azad et al., 2025; Bezzekhami et al., 2025). In this context, enzyme immobilization on specific materials emerges as a solution for obtaining more efficient biocatalysts. Various materials can be studied for enzyme immobilization, ranging from natural and synthetic polymers to inorganic or hybrid materials. However, one highly researched area is enzyme immobilization on nanometric materials (Patil et al., 2025; Sood et al., 2025). Nanoparticles offer an extremely high surface area, allowing for greater enzyme loading and better substrate accessibility (Ulu et al., 2025; Zhang et al., 2024). This level of control allows nanomaterials to be designed with specific properties through modulation of their synthesis. Furthermore, their small size favors better dispersion in the reaction medium and increases the exposure of active sites. In this sense, these nanocatalysts can be reused through methods such as filtration, centrifugation, or extraction, standing out as versatile and sustainable solutions in catalytic processes (Kaur et al., 2024; Yadav et al., 2024).

Another recovery method for these biocatalysts gaining attention in the scientific community is the use of an external magnetic field, as in the case of magnetic nanoparticles (MNPs) used for immobilization. MNPs exhibit a phenomenon called superparamagnetism, which allows them to behave as temporary magnets in the presence of an external magnetic field typically occurring in nanoparticles smaller than 30 nm (Fan et al., 2025). Due to their small size, each nanoparticle has a single magnetic domain and enough thermal energy to spontaneously flip the direction of its magnetic moment over time, meaning they do not retain permanent magnetism (Yang et al., 2025).

Although this type of separation was initially limited to materials containing elements such as iron, cobalt, and nickel, advances in materials engineering have allowed the expansion of their applications (Sadjadi, 2019; Sadjadi, 2019). Techniques such as chemical functionalization, doping, core-shell structure formation, and conjugation with specific

molecules have enabled the development of nanobiocatalysts with tunable features for different applications (Perera et al., 2024). Nanometric-scale materials engineering is a rapidly evolving field, with numerous possibilities still underexplored, offering enormous potential for enhancing sustainable and efficient catalytic processes.

It is within this thematic line of magnetic biocatalysts that this thesis is constructed. Chapter II presents an advanced bibliometric analysis and an overview of the field of magnetic biocatalysts, highlighting recent research advances. Using the Web of Science (WoS) database, 34,949 publications were analyzed and refined down to 450 relevant articles. The thematic and keyword analysis revealed five main clusters, with the most prominent research area related to obtaining biofuels from different types of sustainable vegetable oils.

Based on this overview, Chapter III presents an experimental investigation proposing a novel magnetic support for enzyme immobilization. Magnetic nanoparticles functionalized with polyethyleneimine (PEI) and activated with epoxy groups were used to immobilize Eversa® Transform 2.0 lipase (EVS), with optimization of the parameters using the Taguchi method. The support and biocatalyst were characterized using various techniques, and the system's performance was evaluated in terms of immobilization efficiency, pH, temperature, storage time, and application in the esterification of fatty acids from babassu oil to produce a biolubricant. The study also included computational analyses using molecular docking and molecular dynamics.

Chapter IV uses the same material developed in the previous chapter for the immobilization of *Candida antarctica* lipase B (CALB). After similar characterizations, the biocatalyst was applied in the esterification of fatty acids from tilapia oil to produce a biofuel. This system was also analyzed through computational tools.

Chapter V presents the general conclusions of the thesis, while Chapter VI compiles the scientific articles published during the development of the research. Finally, the references used throughout the work are presented.

1.2 Thesis objectives

This thesis aimed to develop and apply functionalized magnetic nanobiocatalysts for enzyme immobilization in heterogeneous catalysis reactions focused on the synthesis of biolubricants and biofuels from vegetable oils. The specific objectives were:

i. To perform a bibliometric analysis of the field of magnetic nanobiocatalysts.
ii. To develop and optimize a magnetic nanobiocatalyst with Eversa® lipase (Fe_3O_4-PEI-DGEBA@EVS) and evaluate its catalytic efficiency in the esterification of free fatty acids (FFA) from babassu oil.
iii. To develop a second nanobiocatalyst with *Candida antarctica* lipase B (Fe_3O_4-PEI-DGEBA@CALB) and evaluate its catalytic efficiency in the esterification of FFAs from tilapia oil.
iv. To apply molecular modeling tools (docking and molecular dynamics) to investigate substrate–enzyme interaction mechanisms and elucidate structural aspects related to the selectivity and catalytic efficiency of the immobilized lipases.

CHAPTER II[1]

2 RECENT APPLICATIONS AND FUTURE PROSPECTS OF MAGNETIC BIOCATALYSTS

Abstract

Magnetic biocatalysts combine magnetic properties with the catalytic activity of enzymes, achieving easy recovery and reuse in biotechnological processes. Most are formed by lipases immobilized by magnetic nanoparticles. This review covers an advanced bibliometric analysis and an overview of the area, elucidating research advances. Using WoS 34,949 publications were analyzed and refined to 450. The main journals, countries, institutions and authors that published the most were identified. The most cited articles showed research hotspots. The analysis of the themes and keywords identified five clusters and showed that the main field of research is associated with obtaining biofuels derived from different types of sustainable vegetable oils. The overview on magnetic biocatalysts showed that these materials are also employed in applications related to biosensors, photothermal therapy, environmental remediation and medicine. The industry shows a significant interest with the number of patents increasing over the years. Future studies should focus on the immobilization of new lipases in new materials with magnetic profiles, aiming to improve even more the efficiency of the different applications.

Keywords: magnetic biocatalysts, lipase, immobilization, magnetic nanoparticles, feedstock.

[1] **MELO, RAFAEL LEANDRO FERNANDES**; SALES, MISAEL BESSA ; DE CASTRO BIZERRA, VIVIANE ; DE SOUSA JUNIOR, PAULO GONÇALVES ; CAVALCANTE, ANTÔNIO LUTHIERRE GAMA ; FREIRE, TIAGO MELO ; NETO, FRANCISCO SIMÃO ; BILAL, MUHAMMAD ; JESIONOWSKI, TEOFIL ; SOARES, JOÃO MARIA ; FECHINE, PIERRE BASÍLIO ALMEIDA ; SOUSA. Recent applications and future prospects of magnetic biocatalysts. **International Journal of Biological Macromolecules**, v. 253, p. 126709, 31 dez. 2023. DOI: doi.org/10.1016/j.ijbiomac.2023.126709

2.1 Introduction

Lipases (EC 3.1.1.3) are a class of enzymes that catalyze the hydrolysis of triglyceride acylglycerol, which is a typical single-subunit folded glycoprotein (Liu et al., 2022; Rabbani et al., 2023). Its natural substrate is long-chain fatty acid esters, which can catalyze the hydrolysis of fats and oils to produce glycerol, fatty acids, and glycerol diesters or monoesters (Chen et al., 2023; Nadiah et al., 2022; Nietz et al., 2022). In addition to hydrolysis reactions, this type of enzyme can catalyze esterification, transesterification, and ammonolysis reactions (Harini et al., 2018; Qin et al., 2022; Zhang et al., 2023). Lipase has only one active site in its structure, the catalytic triad, located at the end of the enzyme's surface, as shown in Figure 1. This region enables the lipase to carry out the catalysis process. The enzymatic activity is directly linked to the three-dimensional and chemical integrity of this region (Casas-Godoy et al., 2012; Grochulski et al., 1993; Rodríguez-Salarichs et al., 2021).

Figure 1 – Representation of the three-dimensional structure of Candida rugosa lipase obtained from PDB, showing its catalytic triad responsible for enzymatic activity.

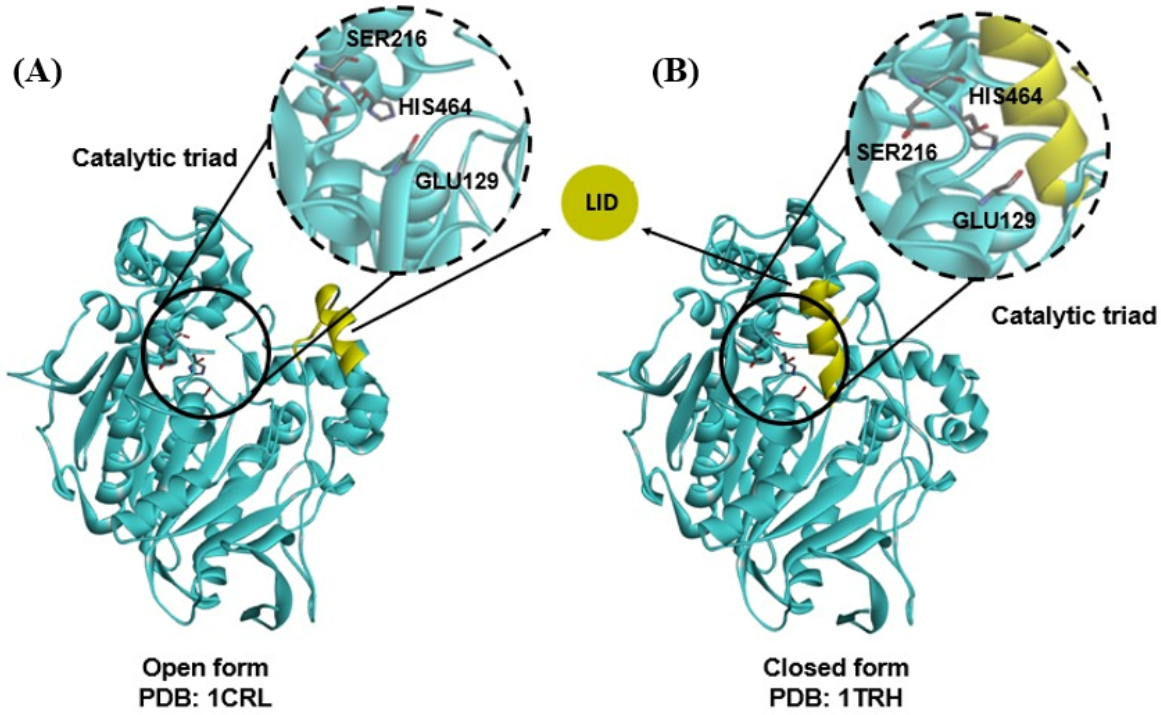

Source: the author.

These catalysts have a range of applications in processing fats and oils, food, cosmetics, pharmaceutical preparations, biosensors, photothermal therapy, environmental

remediation, medicine, biolubricants, and biofuels (An et al., 2015; Califano et al., 2015; Kashefi et al., 2019; Luo et al., 2022; Martínez et al., 2022; Nadar et al., 2020). Such applications mean that the circular bioeconomy based on lipases is continuously growing (Cuadrado-osorio et al., 2022). The global lipase market is projected to grow to US$466.29 million by 2024, with compound growth of approximately 7.6%. In 2019 it already represented approximately $336.09 million, accounting for around 11.6% of the food enzyme market, which was estimated at $29.07 billion (Kim et al., 2023b). The commercial lipases that participate in this circular economy originate mainly from microbial sources (bacteria, yeasts, and fungi), animals, and plants, as such enzymes have good thermostability characteristics, as well as versatility, availability, and ability to be produced on a large scale (Long-yu et al., 2020; Nimkande & Bafana, 2022; Zouari et al., 2005). Microbial lipases have the largest market share, with approximately 92% of total demand (Kim et al., 2023b). However, some economic limitations on the use of lipases result from their being available in free form, making it impossible to recover them from the reaction medium after use (Remonatto et al., 2022).

Enzyme immobilization is a technique that makes it possible to overcome economic barriers related to the cost of enzymatic catalysis, solve problems of enzymatic recovery, and even improve catalytic stability, increasing control of the reaction and avoiding contamination of the products by the enzyme (Remonatto et al., 2022). Several methods and supports for the immobilization of enzymes have been studied. The various immobilization techniques serve to stabilize the enzyme while maintaining its activity (Mehta et al., 2016; Yamaguchi & Miyazaki, 2023). The techniques most studied by scientists are adsorption, covalent bonding, and cross-linked aggregates (Drtina et al., 2005; Panchal et al., 2022; Xing et al., 2022; Zdarta, Jesionowski et al., 2023; Zhou et al., 2022). All of these techniques require the selection of an appropriate support to immobilize the enzyme. These are chosen according to their properties and desired characteristics, including low cost, biocompatibility, free surface, insolubility, thermal stability, and binding sites (Izzati et al., 2021). However, the supports chosen for immobilization can often be modified and coated with other more active materials, thus obtaining more desirable characteristics for lipase binding. An example of this is the use of activated magnetic nanoparticles, which offer low cost and good reusability when attached to a stable surface for enzyme immobilization (Sadeghi et al., 2023).

Magnetic nanoparticles (MNPs) have suitable characteristics for potential enzymatic immobilization, including biocompatibility, low toxicity, and high specific surface area, in addition to superparamagnetic properties, which allow them to be quickly recovered from the reaction medium (Fortes et al., 2017). The use of isolated MNPs for enzyme immobilization is

inefficient, as they do not have a range of active sites where immobilization can take place, in addition to having a high tendency to form agglomerates and thus lose their ability to disperse in the reaction medium (Yu et al., 2022). However, researchers have already found very good solutions to this problem, covering MNPs with polymeric materials such as polyethyleneimine (PEI) (Bezerra et al., 2020; Khoobi, Motevalizadeh et al., 2015) and activating them with several other materials such as glutaraldehyde (Khoobi, Motevalizadeh et al., 2015; Monteiro et al., 2019), epoxy groups (Bezerra et al., 2020; Gennari et al., 2020), and glyoxyl (Santos et al., 2015; Mendes et al., 2014; Morellon-sterling et al., 2021). Thus, MNPs used as supports for enzymes offer exceptional immobilization stability properties, as well as low production cost and low operating costs, since they can be reused (Bezerra et al., 2020; Fortes et al., 2017; Khoobi, Motevalizadeh et al., 2015; Yu et al., 2022).

For these reasons, research interest in lipases immobilized by magnetic nanoparticles has been gradually increasing. A search for free lipases on the Web of Science (WoS) returned an average of approximately 2,688 articles published annually between 2010 and 2022, while searches for immobilized lipases and lipases immobilized by magnetic nanoparticles returned annual averages of approximately 300 and 34 articles, as shown in Figure 2.

Figure 2 – Annual publications on lipase, immobilization, and magnetic nanoparticles, from 2010 to 2022.

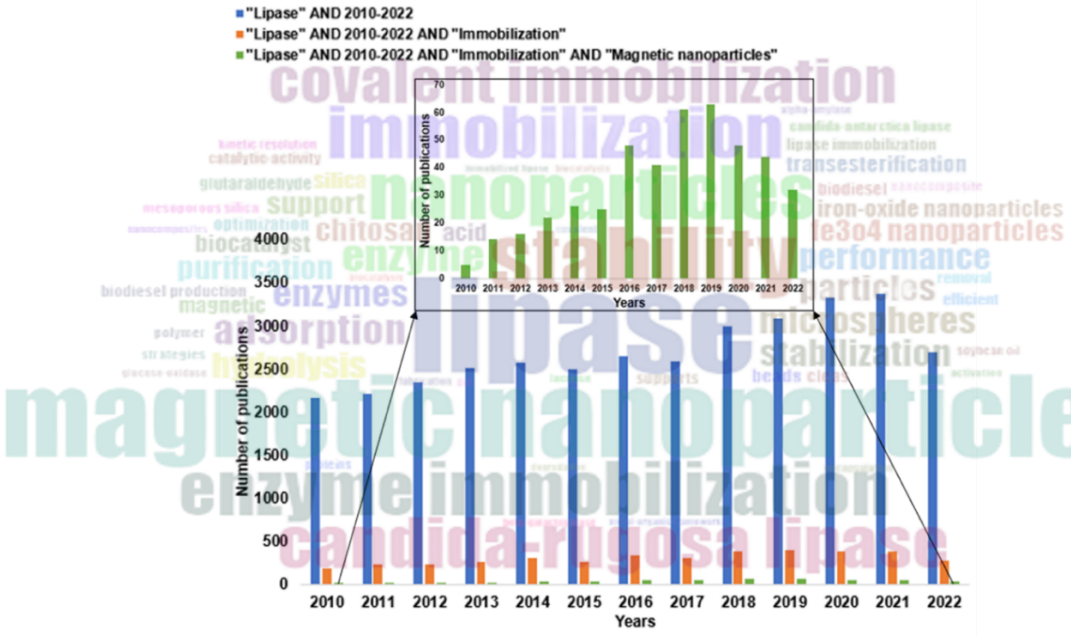

Source: the author.

To understand the development of research on magnetic biocatalysts obtained by lipases, this study aims to map the body of knowledge in this area. For this purpose, an advanced

bibliometric analysis is carried out, observing the performance indicators (newspapers, countries, magazines and authors that publish most in the area) the formation of clusters by analysis of keywords and themes, obtaining a future perspective and paths that the research is following (Mehmood et al., 2023; Ranjbari et al., 2022; Riquelme et al., 2023; Sales et al., 2022). The analysis was based on the WoS database between the years 2010–2022 and evaluated 34,949 publications which was refined to 450 publications, restricting to magnetic biocatalysts obtained by lipases. After this step, an overview of magnetic biocatalysts evaluates the most common synthesis processes and characterizations, applications, advantages and disadvantages, some used reactors and related patent deposits.

2.2 Methodology

In this study, a systematic bibliometric review analysis adapted from previous studies (Sales et al., 2022). The Web of Science (WoS) database (https://www.webofscience.com/) was used to perform the analysis, being considered a high-quality tool and the most useful for generating citation data (van Eck & Waltman, 2010).

The bibliometric analysis began with the identification of an initial database of relevant publications. This was obtained by searching for the keyword “lipase” in documents from the period 2010–2022, defined as “articles”, “review articles” and “procedural papers”, and having English as their language. A set of 34,949 publications was obtained in this initial analysis. Subsequently, two additional screenings were carried out, including the keyword “immobilization”, where the analysis was refined to 3,910 publications, and the keywords “magnetic nanoparticles”, leading to a final set of 445 publications.

Based on these refined result sets, the study aims to answer the following research questions (RQs): What is the pattern of cooperation between journals, countries, institutions, and authors? What are the most influential works in this field? What are the current themes in the existing literature? What might be the agenda for future research in this field?

The search strategy used to identify the most relevant data, the methods of analysis and the research questions are presented in Figure 3.

Figure 3 – Structure representing the search and analysis criteria.

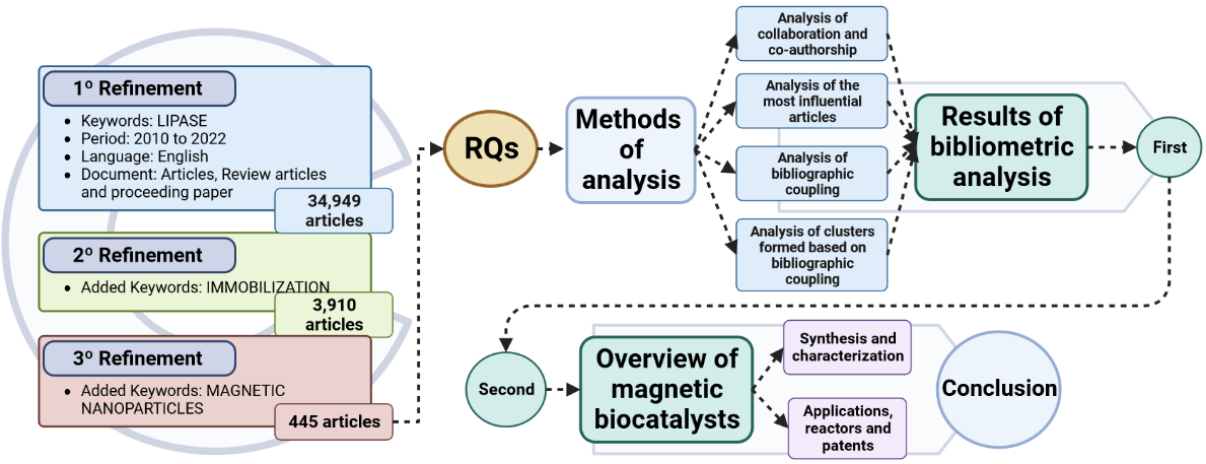

Source: the author.

The software products used to perform and catalog the bibliometric analysis were VOSviewer (version 1.6.18) (https://www.vosviewer.com/), Cite Space (version 6.1.R2) (https://www.citespace.podia.com/), Bibliometrix through the Biblioshiny interface (version 3.0) (https://www.bibliometrix.org/), and Microsoft Excel and Word spreadsheets (Microsoft Office Professional Plus, 2019).

VOSviewer was used to build the bibliometric maps, allowing better visualization of the analyses obtained through database searches (Mehmood et al., 2023). The software allows the import of map data from journals, countries, institutions, and authors, based on citation data, co-citations, and keyword maps, creating clusters capable of being understood and analyzed. CiteSpace predicts trends in research areas using keywords and identified clusters (Riquelme et al., 2023). Bibliometrix works in conjunction with CiteSpace, predicting trends in research areas, in addition to creating a thematic map of the field (Shome, Hassan, Verma, & Ranjan, 2023). Spreadsheets were used to catalog the results obtained.

2.3 Results and Discussion

2.3.1 Results concerning publications

The initial search on the Web of Science for the keyword “lipase” returned a total of 34,949 articles. When the keyword “immobilization” was added, 3,910 articles were found, and on adding the keyword “magnetic nanoparticles” (the final refinement) we obtained 445 articles. The most relevant title was “A general overview of support materials for enzyme

immobilization: characteristics, properties, practical utility" published in February 2018 by Zdart et al. (Characteristics, 2018), which provides an overview of the characteristics and properties of the materials used for the immobilization of enzymes. The number of publications on magnetic nanoparticles (MNPs) as immobilizers of lipases is much lower than for lipases immobilized on other materials. In 2010 the number of publications on MNPs as lipase immobilizers was only 5. A peak was reached in 2019 with 63 articles, and in the last year of the analysis (2022) the total was 33 articles. The increased interest in this type of magnetic support is due to the possibility of recovering it quickly from the reaction mixture by applying an external magnetic field (Cao et al., 2021). The importance of this factor is confirmed in several of the publications identified in this study.

2.3.2 Distribution of scientific journals, countries, institutions, and authors

Articles on lipases immobilized by magnetic nanoparticles were published in 170 journals between 2010 and 2022, giving an average of 2.6 articles per journal per year. There is great interest in research on MNPs as lipase immobilizers, and the variety of the studies undertaken by different research groups shows that the immobilization of lipases on magnetic supports can be approached from different standpoints, especially given that the surface of the nanoparticles can be modified with other materials that are more reactive with enzymes, generating a range of reported products with remarkably different characteristics (Ge et al., 2023).

Table 1 shows the ranking of the ten journals, countries, institutions and authors that published the most. The number of citations and the average citations per publication are also shown. Among the ten journals that published the most, a quantitative analysis shows that these represented 30.5% of the total number of publications in the area studied. The journal with the highest number of publications and citations is the Dutch journal *International Journal of Biological Macromolecules*, with a total of 39 publications, 1430 citations and an average of 36.67 citations per publication. The *Journal of Molecular Catalysis B: Enzymatic*, although having a smaller number of publications, managed to obtain the highest average of citations per publication with a total of 65.86. Database analysis also provides information on the countries of origin declared by the corresponding authors of published articles. The country that obtained the highest number of publications was China with a total of 188 publications (42.2% of the total) and obtaining an impressive 5,489 citations, Iran and India appeared in second and third place with 60 publications and 2,005 citations and 54 publications and 1,252 citations,

respectively. Among the first three countries, Iran obtained the highest average of citations per publication, obtaining 33.42. According to the affiliation of the corresponding authors, the first three institutions that published the most were all Chinese, namely the Chinese Academy of Sciences, Jiangsu University and Lanzhou University, these obtained 19 publications (4.2% of the total) and 676 citations, 15 and 491, 14 and 680, respectively. Lanzhou University was the institution that obtained the highest average of citations per publication, obtaining 48.57. The three authors who published the most were Roberto Fernandez-Lafuente, Mohammad Ali Faramarzi and Ye-Wang Zhang, obtaining 11, 10 and 10 publications (all with approximately 2.2% of the total) and 348, 337 and 259 citations. Among the three, the one with the highest average of citations per article was Mohammad Ali Faramarzi with 33.70.

Figure 4 presents more data on the journal that published the most. Fig. 4 - (A) shows the highest impact factors H of the ten articles that most published in the area of lipases being immobilized by magnetic nanoparticles. The *International Journal of Biological Macromolecules* again led the ranking, having a very high impact factor in the area, with a value of 25. *Catalysts* and the *Journal of Molecular Catalysis B: Enzymatic* were again in second and third place, with the impact factor impact H of 13. From the fourth journal onwards, we observed a difference in the ranking of the impact factor H for the ranking of journals that published the most. Fig. 4 - (B) shows the growth in the number of publications between 2010 and 2022 of the journals that published the most about the area, again we observe the same journals occupying the first three places. In this sense, we can conclude that the *International Journal of Biological Macromolecules*, *Catalysts* and the *Journal of Molecular Catalysis B: Enzymatic* are currently the main journals in the area of lipases immobilized by magnetic nanoparticles.

Table 1 – Ranking of the top ten journals, countries, institutions and authors that most published and were most cited, according to the database obtained from WoS with the keywords “lipase” and “immobilization” and “magnetic nanoparticles” in the period from 2010 to 2022.

Ranking		**NP**	**NC**	**AC**
	Journals			
1	*International Journal of Biological Macromolecules*	39	1430	36,67
2	*Catalysts*	19	797	41,95
3	*Journal of Molecular Catalysis B: Enzymatic*	14	922	65,86
4	*Journal of Chemical Technology and Biotechnology*	13	237	18,23
5	*Applied Biotechemistry and Biotechnology*	12	188	15,67
6	*Bioprocess and Biosystems Engineering*	12	246	20,50
7	*Biochemical Engineering Journal*	11	390	35,45
8	*Journal of Nanoscience and Nonotechnology*	11	109	9,91
9	*Molecules*	9	190	21,11

10	*Process Biochemistry*	9	167	18,56
	Country			
1	China	188	5489	29,20
2	Iran	60	2005	33,42
3	India	54	1252	23,19
4	Brazil	37	1386	37,46
5	Turkey	31	784	25,29
6	USA	22	705	32,05
7	Spain	17	468	27,53
8	Mexico	13	646	49,69
9	South Korea	12	254	21,17
10	Saudi Arabia	12	261	21,75
	Institutions			
1	Chinese Academy of Sciences	19	676	35,58
2	Jiangsu University	15	491	32,73
3	Lanzhou University	14	680	48,57
4	University Tehran	13	285	21,92
5	University Tehran of Medical Sciences	13	391	30,08
6	Universidade Federal do Ceará	11	523	47,55
7	University of Isfahan	11	500	45,45
8	Huaiyin Institute of Technology	10	514	51,40
9	Islamic Azad University	10	306	30,60
10	Nanjing Tech University	10	340	34,00
	Authors			
1	Fernandez-Lafuente, Roberto	11	348	31,64
2	Faramarzi, Mohammad Ali	10	337	33,70
3	Zhang, Ye-Wang	10	259	25,90
4	Bilal, Muhammad	9	508	56,44
5	Hkhoobi, Mehdi	9	350	38,89
6	Yan, Yunjun	9	284	31,56
7	Li, Yanfeng	8	388	48,50
8	Yilmaz, Mustafa	8	196	24,50
9	Shafiee, Abbas	7	315	45,00
10	Hu, Yi	7	243	34,71

Note: NP = number of publications; NC = number of citations; AC = average citations (NC/NP).

Source: the author.

Figure 4 – Main journals that published between 2010 and 2022 in the area of lipases immobilized by magnetic nanoparticles. (A) Ranking of the impact factor H of the ten journals that published the most in the area. (B) Growth in the number of publications of the journals that published the most in the area.

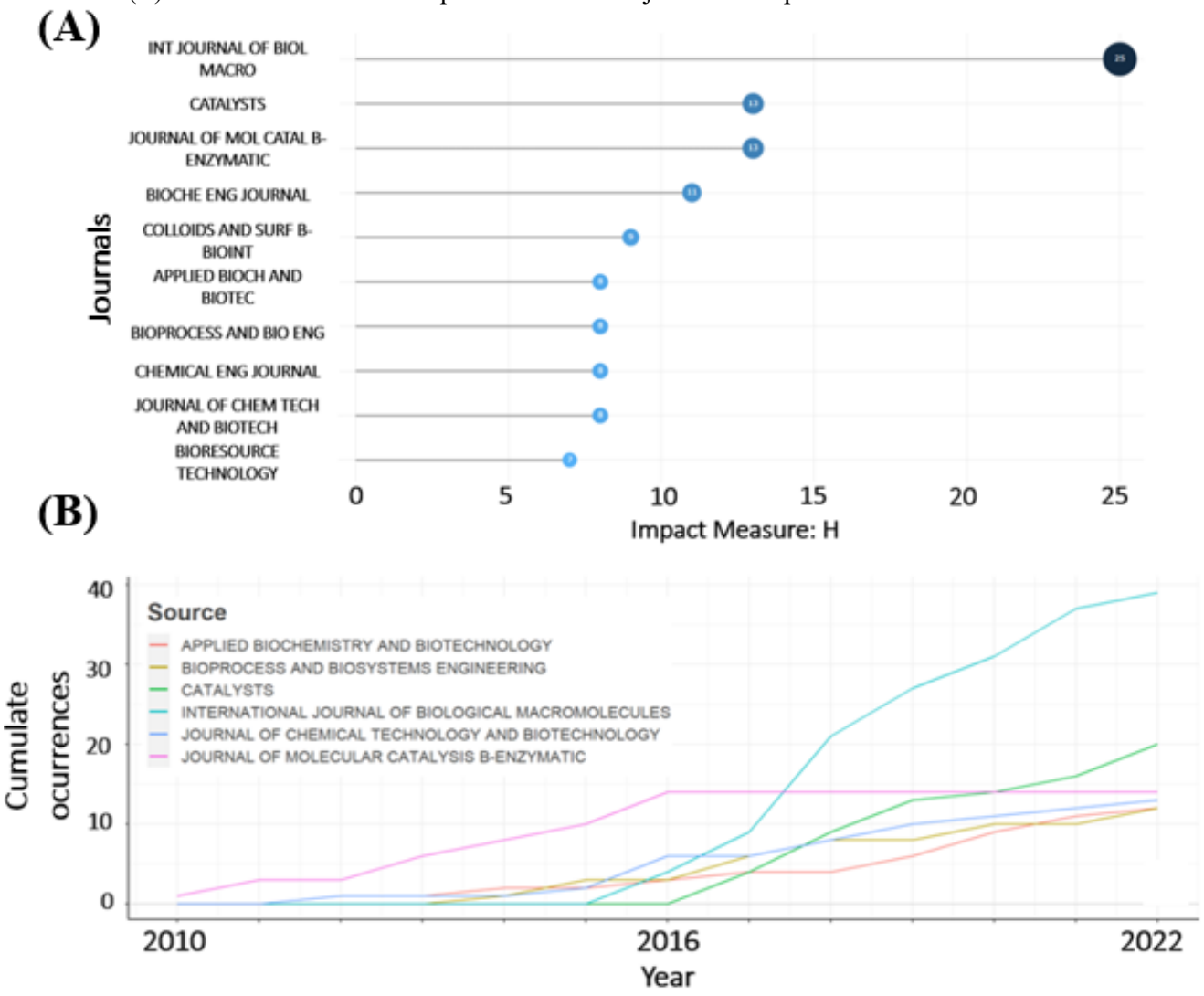

Source: the author.

Figure 5 presents the bibliometric data of the countries, institutions and authors who published the most and who were most cited in the area. Fig. 5 - (A) shows the geocoded location of each publication. The document number is higher than that presented in the database due to the joint publication between the authors. The number of publications is shown with large concentrations in Asia, Europe, North America and South America, especially in Brazil. It also shows the different regions of each country where the articles were published. Fig. 5 - (B) presents a map of the collaboration network between the countries identified with at least five citations. We can see the formation of three large networks, in green, red and blue. China stands out as the country with the highest level of collaboration, followed by Iran, India and Brazil. The authors of the articles on the subject under analysis came from 51 countries and 455

institutions, evidencing the broad interest in the area. Of the 51 countries, only 11 had ten or more publications and only 6 had twenty or more, indicating a concentration of research in a small set of countries: China, Iran, India, Brazil, Turkey and the United States.

Fig. 5 - (C) shows the number of articles published by each institution, considering the collaboration between them (different from that shown in Tab. 1, which considers data from the corresponding authors). Tehran University of Medical Sciences leads with 70 articles, followed by Jiangsu University with 46 articles and Universidade Federal do Ceará with 33 articles. Fig. 5 - (D) shows the collaboration network map between institutions with at least five citations. We can see four large groups, in red with the Chinese Academy of Sciences highlighted, in green with the Lanzhou University highlighted, in blue with the Tehran University of Medical Sciences and in yellow with the Universidade Federal do Ceará. In which, we can conclude that these four institutions are highlighted in the area in question.

Fig. 5 - (E) shows the authors' publications over the analyzed period. It is possible to observe the constancy of publications by the authors on the subject. Yanfeng, for example, appears to be a very constant author in his publications, although not being the author with the highest number of publications, he had publications in almost all years of analysis. Authors Fernandez-Lafuente, and Bilal, authors who presented the highest number of publications, had a higher concentration of articles published in the last 6 years. Fig. 5 - (F) map of the collaboration network among the authors who published the most with at least five citations. Five large groups are observed, denoted by the colors red, green, yellow, blue and purple, consisting of 10, 10, 8, 6 and 6 institutions, respectively, indicating collaborative work between these institutions. In all, 1,736 different authors were identified. However, when refining to authors with at least five citations, the number drops to 32 authors. The authors who published the most significant numbers of articles on the subject were Fernandez Lafuente (11 articles, 348 citations), Mohammad Ali (10 articles, 333 citations) and Ye-Wang (10 articles and 259 citations), being these the authors highlighted in the area in question. The most cited article by the most published author in the area is “Lipase immobilization via cross-linked enzyme aggregates: problems and prospects – A review,” which reviews work on the preparation of cross-linked enzyme aggregates (CLEAs) from lipases, this being a desirable immobilization method due to the simplicity of preparation, non-use of supports, and the possibility of using crude enzymatic extracts (Sampaio et al., 2022).

Figure 6 makes a correlation between the countries, authors and institutions that published the most in the area. We can observe that China leads in an absulative way in the

number of publications, where many authors and institutions, even though they are not declared Chinese, partner with the country in question. Iran and Brazil appear in second and third place.

Figure 5 – Main countries, institutions and authors who published between 2010 and 2022 in the area of lipases immobilized by magnetic nanoparticles. (A) Geocoded location of each publication. (B) Map of the collaboration network among the countries identified with at least five citations. (C) Publication by each institution, considering collaboration. (D) Map of the collaboration network between institutions identified with at least five citations. (E) Authors publications over the analyzed period. (F) Map of the collaboration network between the authors identified with at least five citations.

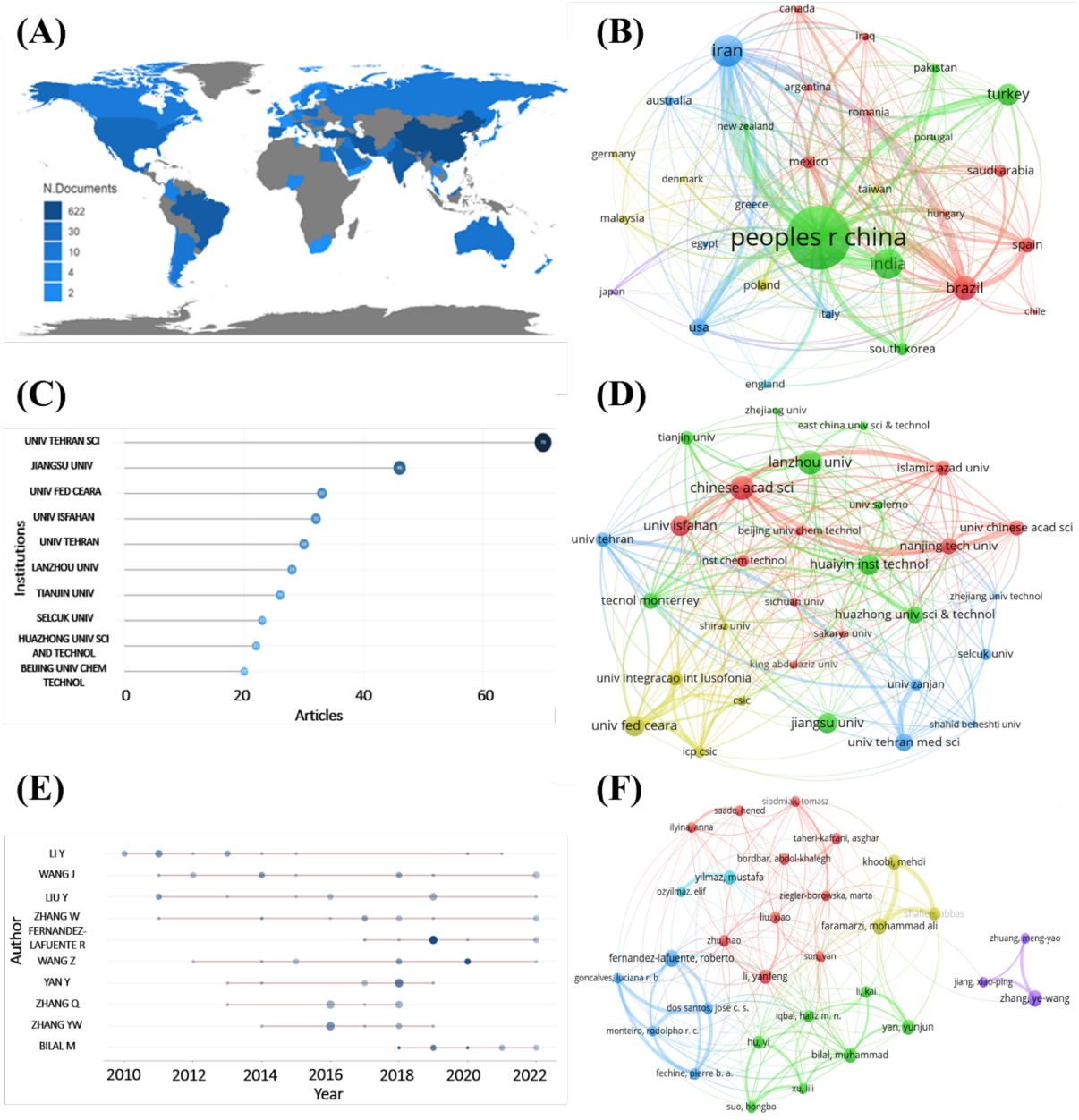

Source: the author.

Figure 6 – Graph of three campuses, listing countries, authors and institutions.

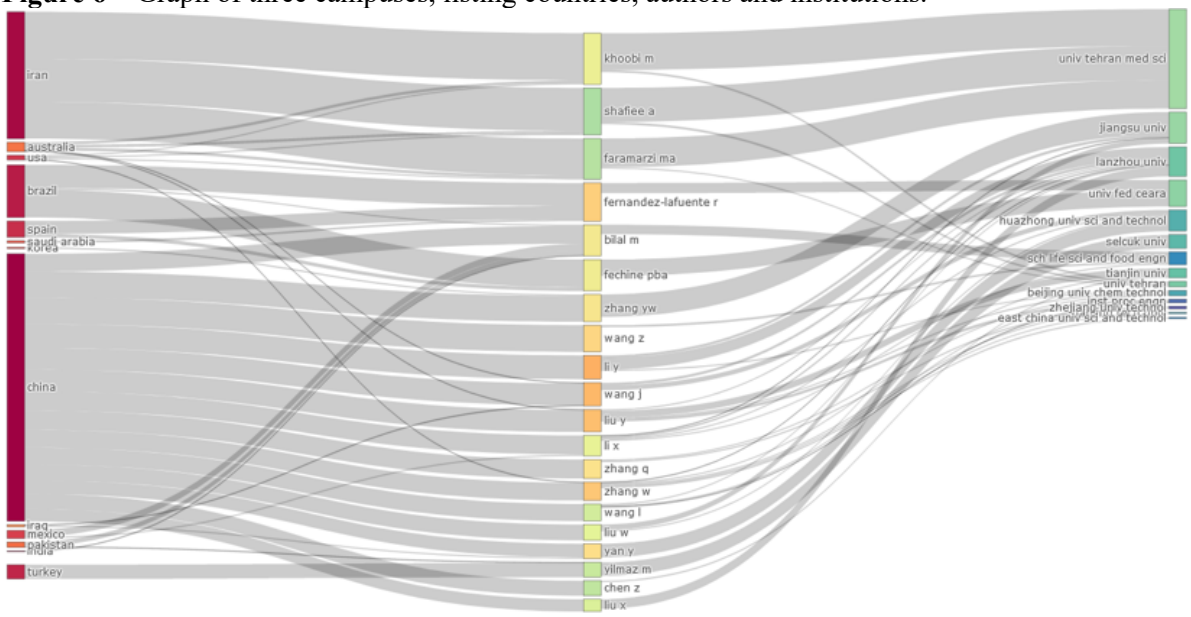

Source: the author.

2.3.3 The most cited articles

The 10 most cited articles on the subject of lipases immobilized by MNPs are listed in Table 3. The most cited article was mentioned above in section 3.1.1. The second most cited article, "Superparamagnetic nanoparticles as versatile carriers and supporting materials for enzymes," was published in 2013 by Netto et al. (Netto et al., 2013) in the *Journal of Molecular Catalysis B: Enzymatic*, and reports on the recent use of superparamagnetic nanoparticles based on magnetite (Fe_3O_4) and maghemite (γ-Fe_2O_3) as support materials for enzymes, exhibiting remarkable properties such as large surface area, mobility, and high mass transfer. The third most cited article was published in 2018 by Bilal et al. (Bilal, Zhao, et al., 2018) in the journal with the most citations in this subject area (see Table 1), the *International Journal of Biological Macromolecules*. That article also presents an updated view on the development and characterization of MNPs, particularly nano constructions derived from MNPs with an iron base as support materials for enzyme immobilization. A relationship may be noted between the most cited articles and the most prolific journals listed in Table 1; however, six journals appearing in Table 3 (those ranked 4, 5, 6, 7, 8 and 10) are not among the most cited. The *Journal of Molecular Catalysis B: Enzymatic* is notable for having two articles among the 10 most cited. One of the notable characteristics of the most cited articles is their time of publication: most of them were published more than five years ago, indicating that interest in work related to lipases immobilized on MNPs remains high.

Table 2 – Most cited articles from the last 10 years on lipases immobilized by magnetic nanoparticles.

Rank	Article Title	Journal	Y.P.	Cit.	Ref.
1	A general overview of support materials for enzyme immobilization: characteristics, properties, practical utility	*Catalysts*	2018	451	(Characteristics, 2018)
2	Superparamagnetic nanoparticles as versatile carriers and supporting materials for enzymes	*Journal Of Molecular Catalysis B: Enzymatic*	2013	230	(Netto, 2013)
3	Magnetic nanoparticles as versatile carriers for enzymes immobilization: a review	*International Journal Of Biological Macromolecule*	2018	215	(Bilal, 2018)
4	Application of magnetic nanoparticles in smart enzyme immobilization	*Biotechnology Letters*	2016	214	(Vaghari, 2016)
5	Facile, high-efficiency immobilization of lipase enzyme on magnetic iron oxide nanoparticles via a biomimetic coating	*Bmc Biotechnology*	2011	213	(Ren, 2011)
6	Current status and trends in enzymatic nanoimmobilization	*Journal Of Molecular Catalysis B-Enzymatic*	2014	196	(Cipolatti et al., 2014)
7	Preparation of magnetic chitosan nanoparticles as support for cellulase immobilization	*Industrial & Engineering Chemistry Research*	2014	159	(Zang et al., 2014)
8	Nanobiotechnology as a novel paradigm for enzyme immobilization and stabilization with potential applications in biodiesel production	*Applied Microbiology And Biotechnology*	2013	158	(Verma, 2013)
9	Immobilization of cellulase enzyme on superparamagnetic nanoparticles and determination of its activity and stability	*Chemical Engineering Journal*	2011	157	(Khoshnevisan, 2011)
10	Enzymatic production of biodiesel from soybean oil by using immobilized lipase on Fe_3O_4/Poly (styrene-methacrylic acid) magnetic microsphere as a biocatalyst	*Energy & Fuels*	2014	149	(Xie & wang, 2014)

Source: the author.

2.3.4 Research topics

The articles from 2010 to 2022 identified in the WoS database as relating to lipases immobilized by MNPs were assigned to 23 different areas of knowledge. Many articles are included in more than one area of research, and 11 of these areas have fewer than ten articles assigned to them. Figure 7 presents the five leading research areas, accounting for around 73% of the published articles. “Chemistry” proved to be the most common research area, with 231 articles involving processes of functionalization and activation of MNPs for the stable immobilization of lipase enzymes. The next research areas were “Biotechnology Applied Microbiology” and “Biochemistry Molecular Biology” with 131 and 111 published articles respectively, involving processes such as transesterification and esterification of fatty acids. “Engineering” ranked fourth with 96 articles, relating to topics in biofuel production and biocatalysis. “Materials Science” included 68 articles related to the doping or modification of MNPs with various other materials, such as silica, carbon nanotubes, and graphene.

There is excellent research potential in biofuels, with several articles in different areas describing proposals for enzymatic catalysis of vegetable oils to obtain biodiesel. The significant relationship between biofuels and engineering shows that the market has been energetically seeking efficient solutions to replace fossil fuels with biodegradable raw materials. An example is the article by Touqeer et al. (Touqeer et al., 2020) published in the journal *Energies* under the title “Fe_3O_4-PDA-lipase as surface functionalized nano biocatalyst for the production of biodiesel using waste cooking oil as feedstock: characterization and process optimization” – this describes a biocatalyst (Fe_3O_4-PDA-lipase) capable of producing biodiesel from cooking oil with an optimized yield of 92%.

Figure 7 – Distributions of research areas for articles on lipases immobilized by magnetic nanoparticles.

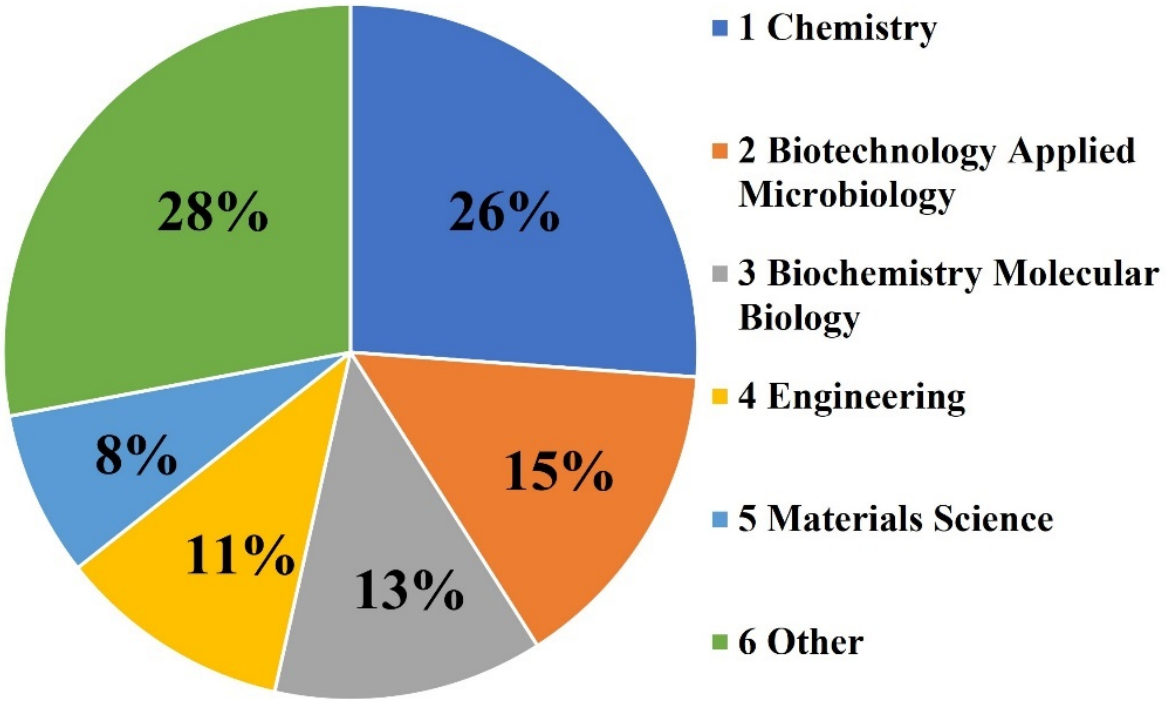

Source: the author.

2.3.5 Classification by research topic

There is a wide variety of materials that directly influence the production of the magnetic biocatalyst. Figure 8 shows biocatalyst production routes, classified by the choice of lipase and how it is to be immobilized, and how the magnetic nanoparticles are functionalized and activated to stabilize the enzyme. Each form of immobilization has its particular properties, as exemplified by the various immobilization yields reported in the literature. Bezerra et al. (Bezerra et al., 2020) immobilized *Thermomyces lanuginosus* lipase (TLL) on an Fe_3O_4 support functionalized with polyethyleneimine (PEI) and activated with divinyl sulfone, and obtained a 100% immobilization yield in phosphate buffer (pH 10 and 1 h), while Silva et al. (Silva et al., 2023) immobilized the same enzyme using as a support a Streamline Phenyl Resin functionalized with PEI and activated with glutaraldehyde, and achieved an immobilization yield of only about 51% in phosphate buffer (pH 7 and 2 h). It can be concluded that the choice of support greatly affects the yield of immobilization.

Figure 8 – Different ways to produce magnetic biocatalysts. The parts of the image depict four variables: selected lipase, immobilization route, type of magnetic nanoparticle and doping of other nanoparticles, and type of functionalization and activation of the nanoparticles.

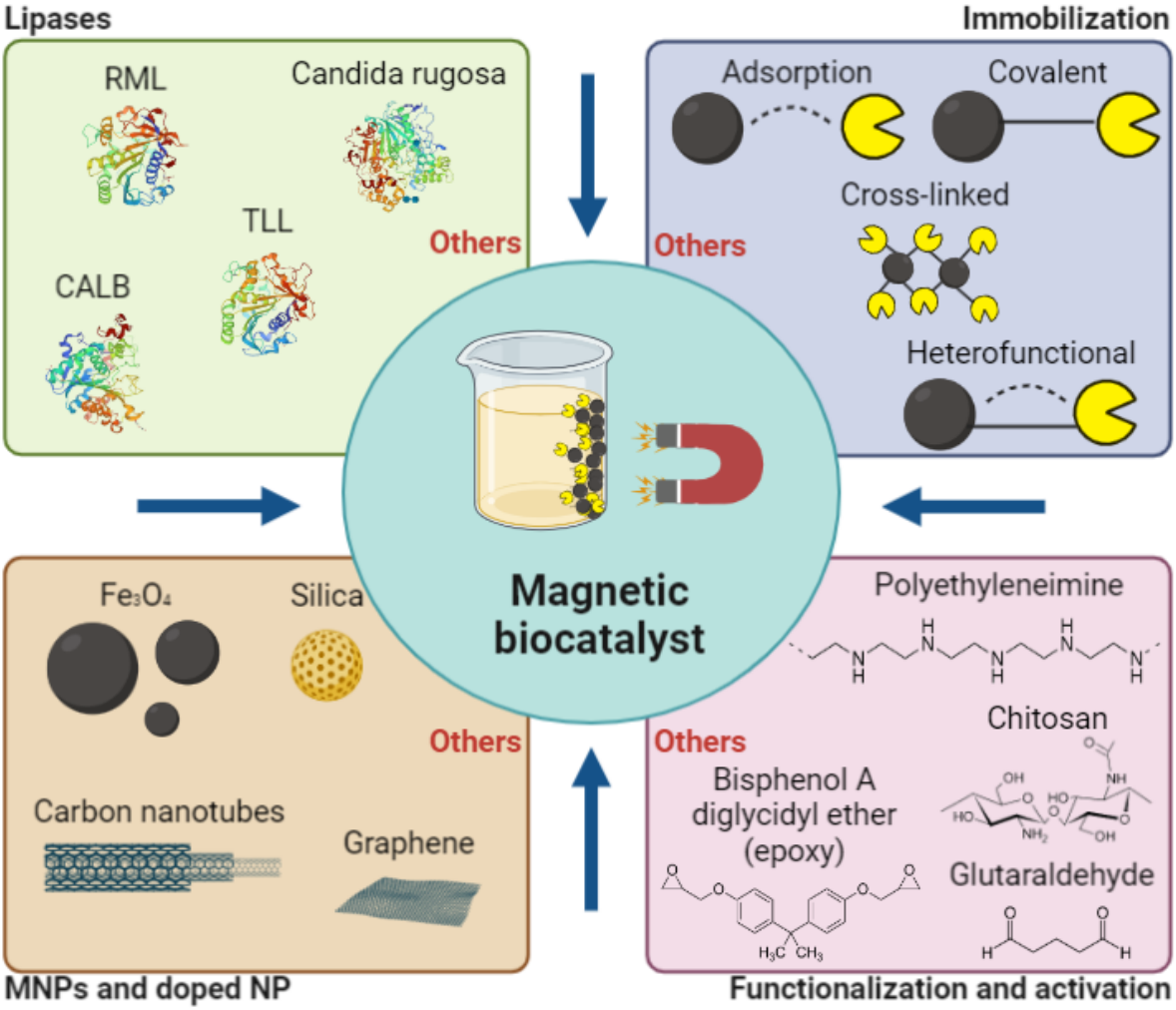

Source: the author.

The ability of lipases to hydrolyze fatty acids at specific positions of the glycerol chain in the structure of triglycerides is related to their regiospecificity, which can be classified as *sn*-1,3-specific, *sn*-2-specific, or nonspecific. The *sn*-1,3-specific lipases hydrolyze ester bonds at the *sn*-1 and *sn*-3 positions (some examples are *Aspergillus niger, Mucos miehei, Rhizomucor miehei*, RML), while the *sn*-2-specific lipases hydrolyze the ester bonds at the position *sn*-2, and the nonspecific enzymes (*Pseudomonas cepacia, Pseudomonas fluorescens* and *Candida rugosa*) act at random positions of the glycerol chain (Kapoor & Gupta, 2012; Monteiro et al., 2021; Remonatto, Miotti, et al., 2022). These different characteristics generate a wide range of options for lipases subject to immobilization on specific supports to form biocatalysts that can be applied in various biotechnological processes (Silva et al., 2020; Palma et al., 2021; Liu et al., 2020; Nájera-Martínez et al., 2022) in the synthesis of esters of industrial interest

(Bayramoglu et al., 2022; Cabezas et al., 2022; Sun et al., 2022), biofuels (Ashwini John et al., 2023; Fan et al., 2016; Zhang et al., 2021) and biolubricants (Abd Wafti et al., 2022; Åkerman et al., 2011; Cavalcanti et al., 2018), among others (Chakraborty et al., 2023; Tan et al., 2023).

In recent years, Novozymes S/A (Denmark) has launched specific enzymes for use in the industrial production of biodiesel, such as Callera™ Trans L and Eversa® Transform 2.0 (both derived from *Thermomyces lanuginosus* lipase, TLL) (Cesarini et al., 2013; Poppe et al., 2015). Eversa® Transform 2.0 has attracted much attention for its low market price (approximately US$20.0/kg) and its ability to act on raw materials regardless of the free fatty acid content, which provides a significant increase in competitiveness and sustainability in the production of enzymatic biodiesel (Monteiro et al., 2021; Remonatto, Miotti, et al., 2022). However, this is not yet one of the enzymes generating the largest number of articles in the WoS database: there were 22 reports on the use of immobilized Eversa® Transform 2.0, and only two articles concerning its immobilization on magnetic supports.

Figure 9 shows the different lipases, immobilization forms, functionalization and activation forms, and the different magnetic or MNP-doped supports for lipase immobilization. *Candida rugosa* lipase was the most common type described in the articles in the refined dataset, with a total of 129 articles, almost 30% of the total (Fig. 9 - (A)). The most cited article on this lipase was also the most cited article in the full set, as commented on above. *Candida antarctica* lipase B (CALB) was the second most researched, with 46 articles, representing 10% of the total. The most cited article in this case was “Catalysis in biodiesel production – a review” published in the journal *Clean Energy* in 2019 by Solomon et al. (Thangaraj et al., 2019). The lipases TLL and RML were the subjects of 26 and 10 articles, respectively.

Figure 9 – Different ways of obtaining magnetic biocatalysts. (A) Lipases immobilized by MNPs, (i) Lipases most used in immobilization, (ii) Evolution in the number of articles between 2010 and 2022. (B) Forms of immobilizations, (i) Immobilizations most used in MNPs, (ii) Evolution in the number of articles between 2010 and 2022. (C) Functionalization and activation, (i) Functionalization and activation most used, (ii) Evolution in the number of articles between 2010 and 2022. (D) Magnetic nanoparticles, (i) More magnetic nanoparticles used, (ii) Evolution in the number of articles between 2010 and 2022.

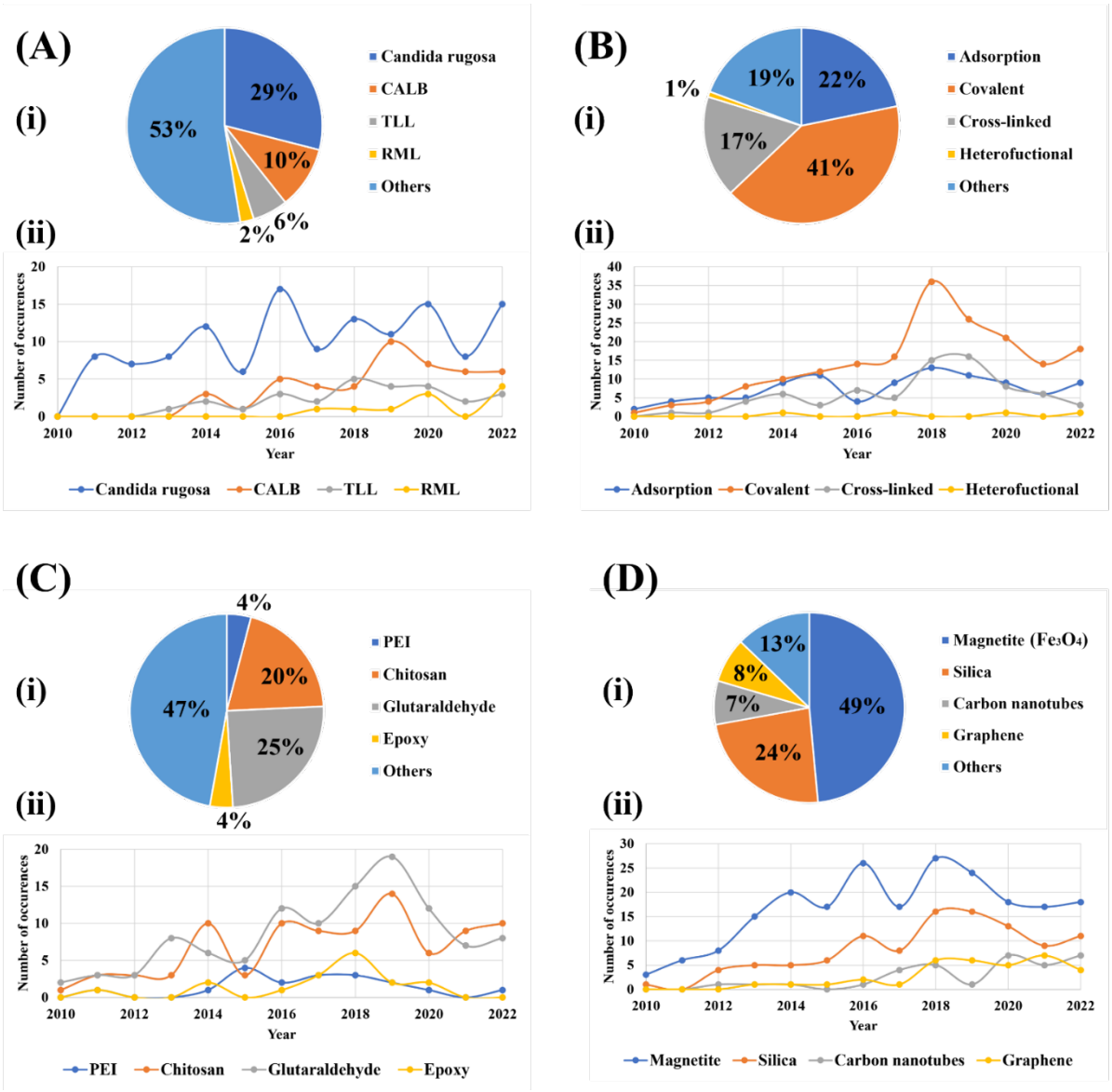

Source: the author.

Immobilizing a specific lipase on a magnetic support produces a biocatalyst. Immobilization is the restriction or confinement of enzymes within a matrix or on the surface of a support material (Bilal et al., 2021; Ismail & Baek, 2020). When considering the design of a magnetic biocatalyst, it is necessary to evaluate the intended application, that is, the operating conditions under which it will be used. The main objectives of immobilization are to improve

the stability of the lipase, to make the lipase insoluble in water, to increase operational stability, to increase control of the process, and to facilitate reuse. The use of MNPs is especially promising for achieving the last of these goals, since it enables faster recovery (Carvalho et al., 2020; Khoobbakht et al., 2020; Vaghari & Mojgan, 2016).

Enzyme stability following immobilization can extend the operational window in terms of the range of temperature, pH, storage, and tolerance to substrate electrochemical components (Sadeghi et al., 2023; H. Xu & Liang, 2022). However, the literature indicates that there is no ideal protocol for enzyme immobilization on supports with universal applicability (Remonattoet al., 2022; Sadeghi et al., 2023; Tan, Bilal et al., 2022; Xu & Liang, 2022). For adequate immobilization, one must consider the support, its functionalization and activation, and its immobilization protocol (Remonatto et al., 2022; Tan et al., 2022). All of these choices directly influence the bonds formed between the support and the enzyme. Immobilization by adsorption consists of interaction between the lipase (adsorbate) and the support (adsorbent) mainly through weaker van der Waals bonds, hydrogen bonds, and acid-base bonding (Wen et al., 2022; J. Xu et al., 2021). This type of immobilization has the great advantage of simplicity. However, it has the disadvantage of lipase leaching, which in the long term can cause reversibility (Hwang & Gu, 2013; Peng et al., 2022; Sheldon, 2007). Covalent immobilization is more stable. It is usually carried out between lipases and supports functionalized and activated with aldehyde, amino, and epoxy groups (Esmi et al., 2021; Huang et al., 2008; Lin & Lin, 2022). Cross-linked immobilization is even more stable; it commonly uses glutaraldehyde with a cross-linker to perform enzymatic (matrix-free) aggregation, causing two aldehyde residues of a glutaraldehyde molecule to act as two reactive amino residues of different lipases (Awad et al., 2018; Guajardo et al., 2021). In heterofunctional immobilization, the support is functionalized and activated with different groups reactive to lipases, causing the enzyme to be immobilized via both adsorption and multipoint covalent bonds. This is a very promising technique according to results for immobilization yields (Bezerra et al., 2020; Zhang et al., 2020).

Figure 9 - (B) illustrates some forms of immobilization of lipases on MNPs reported in the articles analyzed in this bibliometric study. Covalent and adsorption immobilization had the highest numbers of occurrences, with 183 and 97 articles respectively, representing 41% and 22% of the total. However, it should be noted that these two types may also be mentioned in the context of both cross-linked and heterofunctional immobilization. Reports of covalent immobilization increased between 2017 and 2018, a trend that may be related to the increasing representation of cross-linked immobilization in the same period. Heterofunctional

immobilization is poorly represented, with only four articles, although these report immobilization yield results above 95%. The most cited article on heterofunctional immobilization is "A new heterofunctional support for enzyme immobilization: PEI functionalized Fe_3O_4 MNPs activated with divinyl sulfone. Application in the immobilization of lipase *Thermomyces lanuginosus"* by Bezerra et al. (Bezerra et al., 2020), which reports results indicating a 100% yield in the immobilization of TLL.

The functionalization and activation of supports are strategies to generate reactive sites enabling the immobilization of lipases by different types of binding. Numerous materials can be used for enzyme immobilization, each associated with different immobilization protocols, which must be studied and evaluated to obtain the best yields (Mehdi et al., 2019; Sharma, Gupta et al., 2022). For example, Taguchi's orthogonal design is a strategy many researchers use to obtain optimal immobilization points. In this strategy, one of the most widely used variables is the amount of material used to functionalize or activate the support. The reaction groups for enzyme immobilization function in an optimal range, and an increase in quantity above this range only saturates the process and increases the cost of manufacture of the biocatalyst (Sousa et al., 2022).

Thus, in the search for materials for the functionalization and activation of supports, the aim is to find low-cost materials that do not need to be used in excessive quantity (because they have a high concentration of reaction groups). Some materials meeting these requirements are polyethyleneimine (PEI), chitosan, glutaraldehyde, and compounds such as diglycidyl bisphenol A ether (DGEBA) containing epoxy groups. PEI has a large number of primary, secondary, and tertiary amines along the polymeric chain, and offers good biocompatibility and water solubility (Cao et al., 2020; Farshad et al., 2015). Its cost is around US$87.0/kg. Chitosan is an N-deacetylated derivative of chitin obtained from the walls of fungi and mollusk shells. It is a polysaccharide with numerous advantages, such as biodegradability, nontoxicity, and high load capacity due to free amino and hydroxyl groups and can be used to generate one of the best supports for enzyme immobilization (Kandile et al., 2018; Ra & Rezaee, 2021; Younes & Rinaudo, 2015). However, if purchased in pure synthesized form, its cost at Sigma Aldrich (San Luis, USA) is around US$2841.1/kg. Glutaraldehyde is a 5-carbon linear dialdehyde that reacts quickly with terminal amino groups of enzymes, leading to the formation of precipitates. The activation of supports with this material is one of the most commonly used techniques for enzyme immobilization (Li et al., 2018; Luisa et al., 2013; Pal & Khanum, 2011). Its cost is around US$143/liter. Materials such as DGEBA contain epoxy groups with short spacer arms, which can react quickly with many nucleophilic protein groups and more slowly with

carboxylic groups. They can also produce ester linkages, although this process is even slower. The great advantage of activation with epoxy groups is that the immobilization takes place in a heterofunctional manner, involving rapid immobilization by adsorption and subsequent immobilization by multipoint covalent bonding, which leads to a stable system. With only very slight chemical modifications on the surface of the lipase (Cui et al., 2015; Mateo, Grazu, et al., 2007; Thudi et al., 2012; X. Zhang et al., 2020), the cost of DGEBA is around US$280/kg.

Figure 9 - (C) shows some of the materials most commonly used in the analyzed research to functionalize and activate MNPs for the immobilization of lipase. Glutaraldehyde proved to be the most used material, being reported in 110 articles, approximately 25% of the total. It is closely followed by chitosan, with 90 articles (20% of the total). However, it was noted that at certain points in the last 10 years – for example, in 2014 and 2022 – there were more reports on the use of chitosan than glutaraldehyde. PEI and epoxy group materials are the subjects of 18 and 17 articles, respectively. The most cited article concerning the use of glutaraldehyde is “Further stabilization of lipase from Pseudomonas fluorescens immobilized on octyl coated nanoparticles via chemical modification with bifunctional agents” by Rios et al. (Saraiva et al., 2019), in which Pseudomonas fluorescens lipases were immobilized on $NiZnFe_2O_4$ superparamagnetic supports using different concentrations of glutaraldehyde and divinyl sulfone.

Magnetic biocatalysts are so-called when their support contains ferrite nanoparticles (iron oxides) in a magnetite (Fe_3O_4) or maghemite (γ-Fe_2O_3) crystalline structure. These are the most used magnetic supports; their superparamagnetic nature, high surface area, low cost, and low toxicity make them excellent raw materials for the production of biocatalysts (Amruth Maroju et al., 2022; Gennari et al., 2020; Monteiro et al., 2022; Silva et al., 2022; Sousa et al., 2022). Characteristics commonly required of supports for biocatalysts include biocompatibility, high dispersion, ease of manipulation, and the possibility of functionalization and activation to obtain reaction chains with enzymes (Bilal et al., 2021b; Xie & Huang, 2020). Furthermore, materials that are magnetic or can be transformed into a magnetic composite are highly attractive for the biocatalysis industry. Materials described in the literature as forming composites with iron oxides to produce magnetic biocatalysts with exciting characteristics include silica, carbon nanotubes, and graphene.

Mesoporous silica, with fibrous morphology, has aroused great interest among scientists, as this morphology offers a high surface area due to its channels (which can also be adjusted), ample pore diameter, and high mechanical and thermal stability (Malhotra & Ali, 2019). Silica also permits better dispersion of the active sites in the channels, leading to

improved doping with iron oxides, allowing more significant oxide–silica interaction without blocking the channel (Bahari et al., 2021; Ge et al., 2023; Malhotra & Ali, 2019). Carbon nanotubes are another support with similar properties as silica, having a large surface area, high load capacity, and high chemical, mechanical and thermal resistance (Rafiee-pour, 2011; Rasheed et al., 2019; S. Wang et al., 2023). Graphene, on the other hand, has a two-dimensional structure. Its functionalization and activation facilitate the successful binding of many enzymes and surface modulation (Moosavi et al., 2022; Zhang et al., 2023). Various functionalizing and activating agents are used on Fe_3O_4, silica, carbon nanotubes, and graphene supports, and together they can facilitate different forms of immobilization, such as adsorption, covalent bonding, cross-linked and heterofunctional immobilization, and entrapment.

Figure 9 - (D) shows the primary base materials used to form magnetic supports for lipase immobilization. Isolated Fe_3O_4, subjected only to functionalization and activation, was the most commonly reported, appearing in 216 articles, almost 50% of the articles identified in the bibliometric analysis. The other materials – silica, carbon nanotubes, and graphene – were used as composites, being doped with iron oxide to produce magnetic materials. Silica was the second most commonly reported material, with 105 occurrences (24% of the total). Graphene and carbon nanotubes were the subjects of 34 and 33 articles (8% and 7%) respectively.

2.3.6 Quantitative analysis of frequent keywords

Keyword analysis makes it possible to understand better the development of the research, as well as the future challenges to be addressed by researchers in the area. Table 3 gives the ranking and total link strength of the top 20 keywords in this bibliometric analysis. It indicates the most prominent themes in this field of research in the last 10 years. Magnetic nanoparticles (287), lipase (221), immobilization (182), and enzyme immobilization (149) are the central themes of this analysis and are the most prominent keywords. Stability (113), covalent immobilization (96) and *Candida rugosa* lipase (82) are “motor themes” and appear in fifth, sixth and seventh place respectively.

Table 3 – Ranking of the 20 most prominent keywords in the analyzed articles.

Rank	Keyword	Freq.	TLS	Rank	Keyword	Freq.	TLS
1	Magnetic nanoparticles	287	950	11	Chitosan	51	215
2	Lipase	221	794	12	Enzyme	51	187
3	Immobilization	182	604	13	Biodiesel	46	139
4	Enzyme immobilization	149	494	14	Stabilization	44	169

5	Stability	113	438	15	Hydrolysis	42	173
6	Covalent immobilization	96	360	16	Microspheres	42	163
7	*Candida rugosa* lipase	82	284	17	Fe_3O_4 nanoparticles	41	144
8	Nanoparticles	54	199	18	Particles	41	158
9	Adsorption	53	197	19	Performance	38	131
10	Enzymes	52	205	20	Support	34	152

Note: TLS = total link strength.
Source: the author.

Figure 10 shows a visualization network map obtained from VOSviewer for the 90 most important keywords, with at least 10 occurrences. It is seen that six clusters are formed, where the largest cluster (marked in red) consists of the keyword “magnetic nanoparticles” linked to several other areas. The cluster marked in green has “lipase” as the most cited keyword, while for the blue cluster it is “immobilization”. The diagram also shows a yellow cluster around “covalent immobilization”, a purple cluster with the keywords “biocatalysis”, and “design”, and a small cluster marked in orange with the words “glutaraldehyde”, “supports” and “proteins” (Fig. 10 - (A)). All of these clusters are interconnected, and they have several other keywords with solid links. The label of each cluster and how many articles and nodes represented it were investigated in CiteSpace. Fig. 10 - (B) shows the period in which the keywords began to form.

Figure 10 – Clusters formed by the main keywords. (A) Mapping of co-citations of keywords in articles in WoS on lipases immobilized by magnetic nanoparticles. (B) Mapping of keyword quotes with period indication.

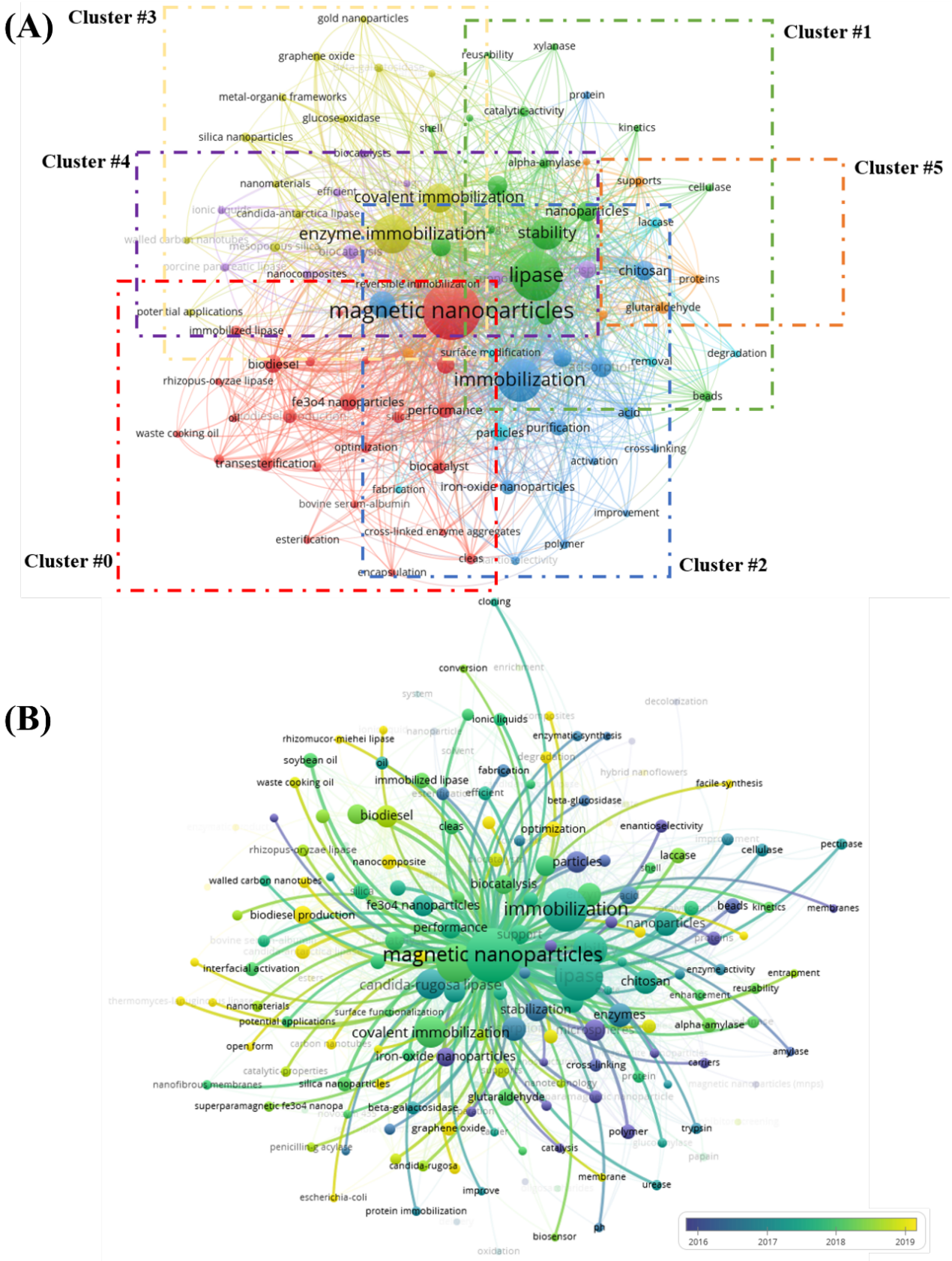

Source: the author.

2.3.7 Constant fields of investigation

CiteSpace software was used to analyze and organize the data obtained in the bibliometric research. It can also indicate which articles and keywords form each cluster and the numbers of links (nodes) being formed (Wang et al., 2022). Keyword analysis is a tool of great importance to determine future paths for research related to lipases immobilized by magnetic nanoparticles.

Table 4 presents the five main clusters, identified by CiteSpace software, of co-citations in research on lipases immobilized by magnetic nanoparticles.

Table 4 – The top five co-citation clusters based on CiteSpace analysis.

CID	Label	Ns	Mean	Top Five Terms	Ref.
#0	Magnetic cross-linked enzyme aggregates	59	2015	Magnetic nanoparticle; *Candida rugosa;* Chitosan-coated magnetic nanoparticle; Using carboxyl-functionalized magnetic nanoparticle; Ester synthesis; Catalytic properties	(Awad, et al., 2018; Lucena et al., 2020)
#1	Superparamagnetic Fe_3O_4 nanoparticles	44	2013	Magnetic nanoparticle; Biodiesel production; *Pseudomonas fluorescens*; *Candida rugosa* lipase; Superparamagnetic Fe_3O_4 nanoparticle	(Kanimozhi, 2013; Khoobi et al., 2015)
#2	Transesterification	36	2014	Magnetic nanoparticle; Biodiesel; Esterification; Ester synthesis, Transesterification	(Cao, et al., 2014; Liu, et al., 2012)
#3	*Candida rugosa*	31	2014	Catalytic properties; Lipolytic lipase; Chitosan-coated magnetic nanoparticle; *Candida rugosa* lipase; Polyamine-induced tannic acid deposition	(Zheng, Ming et al., 2012; Mahmood et al., 2013)
#4	Waste cooking oil	30	2015	Biodiesel production; Waste cooking oil; Magnetic nanoparticle; Enhanced performance; Biodiesel synthesis	(Alikhani et al., 2022; Parandi et al., 2022)

Note: CID = cluster ID, Ns = node size.
Source: the author.

Cluster #0 has the label “Magnetic cross-linked enzyme aggregates” and has magnetic nanoparticles as one of the five most cited keywords, in addition to others such as Candida rugosa and chitosan-coated magnetic nanoparticles. Cluster #0 consists of work on functionalized and activated MNPs capable of immobilizing enzymes through stable immobilization techniques, such as cross-linking. CiteSpace lists each cluster with several representative articles. In cluster #0, the articles report on different ways of immobilizing lipase with bonds that are stable over a range of pH and temperature and in storage. One study shows that disaccharides (maltose, sucrose, and lactose) and polysaccharides such as starch are environmentally friendly additives for tannic acid magnetic crosslinks, functionalized with glutaraldehyde, to immobilize lipase by cross-linking (Özacar et al., 2018). Another article concerned a synthesized magnetic cross-linked enzyme aggregate (MCLEA) from cellulases and a non-magnetic analog (CLEA). MCLEA and CLEA achieved high enzymatic loading efficiency (90% and 88%, respectively). However, MCLEA exhibited 33% greater activity than CLEA, suggesting a catalytic potentiation effect due to the presence of magnetic nanoparticles in the structure of cross-linked cellulose aggregates (Lucena et al., 2020).

Cluster #1 is represented by the term “Superparamagnetic Fe_3O_4 nanoparticles”, which (like the label for Cluster #0) is highly recurrent throughout this bibliometric analysis. The articles in this cluster relate to the use of Fe_3O_4 as the primary material for forming the support, that is, not as a dopant for other materials such as silica, carbon nanotubes, and graphene. The articles also analyze the magnetic capacity retained by Fe_3O_4 after enzyme immobilization. For example, Kanimozhi et al. (Kanimozhi & Perinbam, 2013) used Fe_3O_4 prepared by a chemical coprecipitation method surface-functionalized with 3-aminopropyltriethoxysilane via a silanization reaction to obtain amino functionalized magnetic nanoparticles, on which purified lipase from Pseudomonas fluorescens Lp1 was immobilized using glutaraldehyde as a coupling agent. The saturation magnetization of the nanoparticles was 28.34 emu/g, which fell to 17.07 emu/g after the immobilization. The immobilized lipase displayed more significant activity at 50 °C and thermal stability up to 70 °C. The biocatalyst exhibited excellent reusability over 4 cycles and storage stability for up to 15 days, retaining 75% of its initial activity.

Cluster #2 is labeled “Transesterification”. This cluster contains articles focusing on the enzymatic biocatalysis of processes, whether in biodegradable oils for biodiesel or biolubricants, or even in the production of aromas. Transesterification has become a significant research topic, as lipase-catalyzed transesterification for biodiesel synthesis is clean, efficient, and water-tolerant. In one study, researchers immobilized *Yarrowia lipolytica* lipase (YYL) on a support based on iron oxide and silicon with a pore size of 4.27 nm, capable of trapping the

enzyme. The biocatalyst achieved a relative activity of 197% compared to the free enzyme, and exhibited excellent thermal stability, preserving almost 80% of the initial activity after incubation at 60 °C for 1 h. In addition, the biocatalyst was used for transesterifying olive oil with methanol, producing a conversion yield of 98% (Y. Cao et al., 2014). In another work, *Burkholderia* lipase was immobilized on hydrophobic magnetic particles (HMPs) for application in biodiesel production. Transesterification with the immobilized lipase could be repeated six times without a severe drop-in activity. The optimal conditions for enzymatic transesterification were identified as room temperature, 200 rpm, 10% water content, and a methanol-to-oil molar ratio of 4:1. The yield of conversion of oil to fatty acid methyl esters (FAMEs) reached almost 70% in 12 hours, resulting in a biodiesel production rate of 43.5 g/L/h (C. H. Liu et al., 2012).

Cluster #3 has the label "*Candida rugosa*", this being one of the lipases most commonly immobilized on magnetic nanoparticles and includes studies on the improvement of enzyme catalysis. Zheng et al. (Zheng et al., 2012) synthesized Fe_3O_4 magnetic nanoparticles and functionalized and activated them with allyl glycidyl and ethylene glycol dimethacrylate and epoxy groups. This support was used to immobilize *Candida rugosa* lipase. The resulting biocatalyst offered better resistance to pH and temperature inactivation than the free enzyme, the adaptive pH and temperature ranges of the lipase were widened, and it exhibited good thermal stability and reuse. Phytosterol esters were converted with high yields by transesterification with fatty acid methyl esters (55.3%) or triacylglycerols (above 78.1%) when the biocatalyst was used. In another study, Fe_3O_4 magnetic nanoparticles coated with gum arabic (GAMNP) were prepared by chemical coprecipitation and activated with glutaraldehyde and were used to immobilize *Candida rugosa* lipase that had been coated with various surfactants to stabilize the enzyme in its open form. This system was used as a biocatalyst for producing ethyl isovalerate, a flavor ester. The surfactant-coated and immobilized lipase retained sufficient activity over seven reuse cycles (Mahmood et al., 2013).

Cluster #4 is assigned the label "Waste cooking oil", a driving theme for applications of lipases immobilized by MNPs and also represents many occurrences of the keywords "biodiesel production" and "biodiesel synthesis". CiteSpace lists a number of articles on this topic. Many of them investigate biodiesel production from waste frying oil, catalyzed by different magnetic biocatalysts. Parandi et al. (Parandi et al., 2022) used Fe_3O_4 magnetic nanoparticles synthesized by the coprecipitation technique, and coated with silica (SiO_2) and later functionalized and activated with tetraethyl orthosilicate organic-inorganic hybrid (TEOS) and N-[3-(trimethoxysilyl)propyl] ethylenediamine (TSD), to immobilize *Candida Antarctica*

lipase B (CALB). The biocatalyst achieved a biodiesel yield of 96% at a temperature of 40 °C, a molar ratio of 4:1, a contact time of 30 h, and a catalyst dosage of 1 g. In another article from this cluster, an enzyme co-immobilization approach was applied. A support consisting of magnetic nanoparticles coated with silica and functionalized with amine (Fe_3O_4@SiO_2-NH_2) was used for the immobilization of *Thermomyces lanuginosus* lipase (TLL) and *Candida antarctica* lipase B (CALB) [TLL: CALB], and of *Rhizomucor miehei* lipase (RML) and CALB [RML:CALB]. The immobilization of lipases in different proportions was performed for 3 h under mild conditions and led to specific activities ranging from 29 to 35 U/mg for TLL:CALB and from 21 to 34 U/mg for RML:CALB (Alikhani et al., 2022).

2.3.8 Thematic map

Thematic mapping was performed using R Bibliometrix 3.0 via the biblioshiny interface. This interface allows one to gain insights into current and future potential research topics within the bibliometric analysis and can thus be used together with CiteSpace to obtain a reasonable expectation of how research is developing. The thematic map represents various themes, with centrality on the X axis and density on the Y axis. Centrality measures the extent of correlation between topics, and density measures the degree of cohesion. In thematic maps, centrality indicates the importance of a given theme, while density indicates its capacity for development and sustainability (Verma & Panigrahi, 2023). Figure 11 shows the thematic map for the analysis carried out in this work, which indicates the main topics related to lipases immobilized by magnetic nanoparticles.

The themes “magnetic nanoparticles” and “lipase” are found to have high centrality and low density; that is, they are considered basic themes of research in this area. “Transesterification” and (to some extent) “biodiesel” are considered driving themes; that is, they are vital themes that are drivers for continuing research. In turn, “applications of lipase immobilization” and (to some extent) “cross-linked” are considered emerging themes, currently presenting a growing number of articles. Finally, “cloning conversion” is considered a specialized or niche theme, which is present, but appears in only a small proportion of articles in this research area.

Figure 11 – Thematic map for research on lipases immobilized by magnetic nanoparticles.

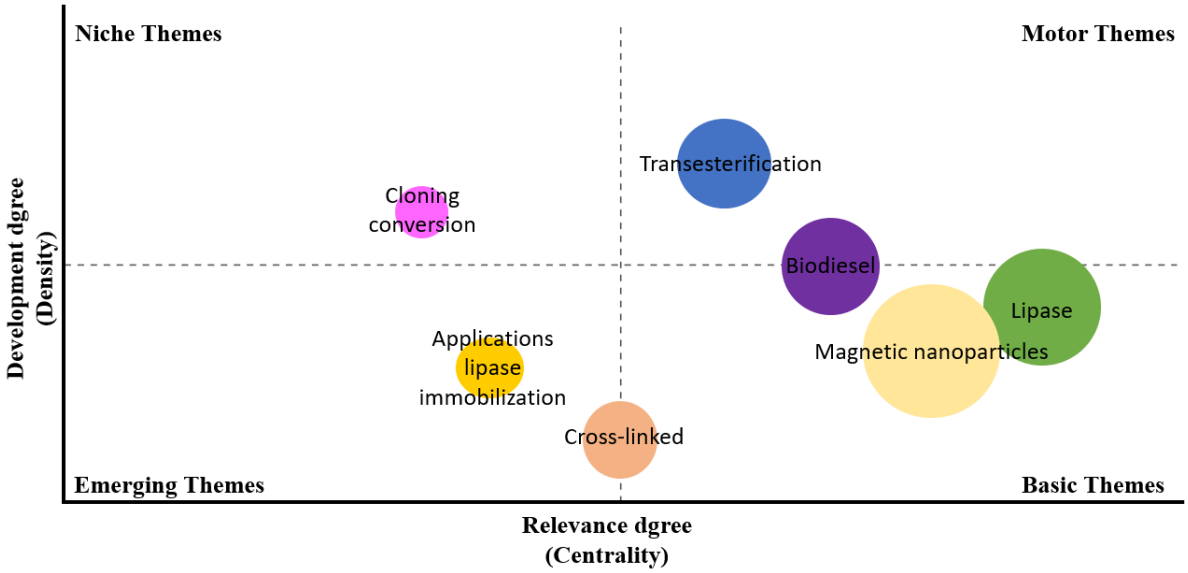

Source: the author.

2.4 Overview of magnetic biocatalysts

2.4.1 Synthesis and characterization of magnetic biocatalysts

The synthesis of magnetic biocatalysts is a research topic in constant evolution, with the objective of developing efficient, controlled and reproducible methods to obtain particles with desired sizes, shapes and magnetic properties (Del Arco et al., 2021; Staudt et al., 2022). Magnetic biocatalysts are obtained after the synthesis of a magnetic support that are later used for the immobilization of the enzyme of interest (Sulman et al., 2019). Magnetic materials, such as iron oxides (Fe_3O_4) and cobalt oxides ($CoFe_2O_4$), are functionalized and activated with biocompatible materials for enzymatic immobilization (Torres et al., 2018a).

There are several approaches for the synthesis of magnetic materials, which can be through a physical method or a chemical method. Sonication synthesis, high temperature evaporation, spputering and high energy milling are characterized as physical methods (Bilal et al., 2023; Teng & Iqbal, 2022). These are generally used to obtain particles with smaller sizes and higher crystalline purity (Salih & Mahmood, 2023). However, these methods are more expensive, as they require more complex equipment (Salih & Mahmood, 2023). Chemical methods are generally more used because they have a lower cost, the most common include coprecipitation, chemical reduction, microemulsion, thermal decomposition and hydrothermal synthesis (Kumar & Gangawane, 2022; Li et al., 2023). These techniques allow for precise

control of particle size and morphology (Kumar & Gangawane, 2022; Li et al., 2023). Chemical methods are commonly the most used for surface functionalization of MNPs. Coprecipitation has been the most used method, both for the synthesis of MNPs and for functionalization (Houshiar et al., 2014; Mote et al., 2023). Basically, the method consists of solubilizing metallic ions in a basic medium and subsequently adding a precipitating agent (Houshiar et al., 2014; Mote et al., 2023).

Several MNPs functionalization strategies exist in the literature, in addition to the continued growth of research in the area, in search of new functionalizing materials and new ways of performing the MNPs interaction with the functionalizing agent. Functionalizations and activations of MNPs are linked to the way in which the support will immobilize the enzyme. As already mentioned in topic 3.3.2. the most common functionalization approaches are the introduction of amino, carboxyl, hydroxyl groups, addition of epoxy materials and/or glutaraldehydes, or even addition of polymeric materials or surfactants (Hamedi et al., 2022; Liu et al., 2020). After proper functionalization and activation of MNPs, they are used to immobilize by covalent, adsorption, cross-linked, heterofunctional, or encapsulation different types of enzymes and thus form the biocatalyst (Kim et al., 2023; Zdarta, Kołodziejczak-Radzimska et al., 2023). After this training, the process of structural and morphological characterization of the magnetic biocatalyst begins.

Numerous forms of structural and morphological characterization are employed in nanoparticle research. The most common structural characterizations in magnetic biocatalysts are X-ray diffraction (XRD), infrared spectroscopy (FTIR), photoelectron spectroscopy (XPS) and Raman spectroscopy. The most used morphological characterizations are scanning microscopy (SEM) and transmission microscopy (TEM). Other characterizations linked to the composition of the biocatalyst are electron scattering spectroscopy (EDS), X-ray fluorescence spectroscopy (XRF) and thermogravimetric analysis (TGA). Vibrating sample magnetometer (VSM) analysis is used to measure the magnetic potential of biocatalysts (Bilal et al., 2023; Salih & Mahmood, 2023; Teng & Iqbal, 2022).

Figure 12 illustrates the main forms of synthesis, functionalization and characterization of magnetic biocatalysts.

Figure 12 – Main forms of synthesis of magnetic nanoparticles and main forms of characterization.

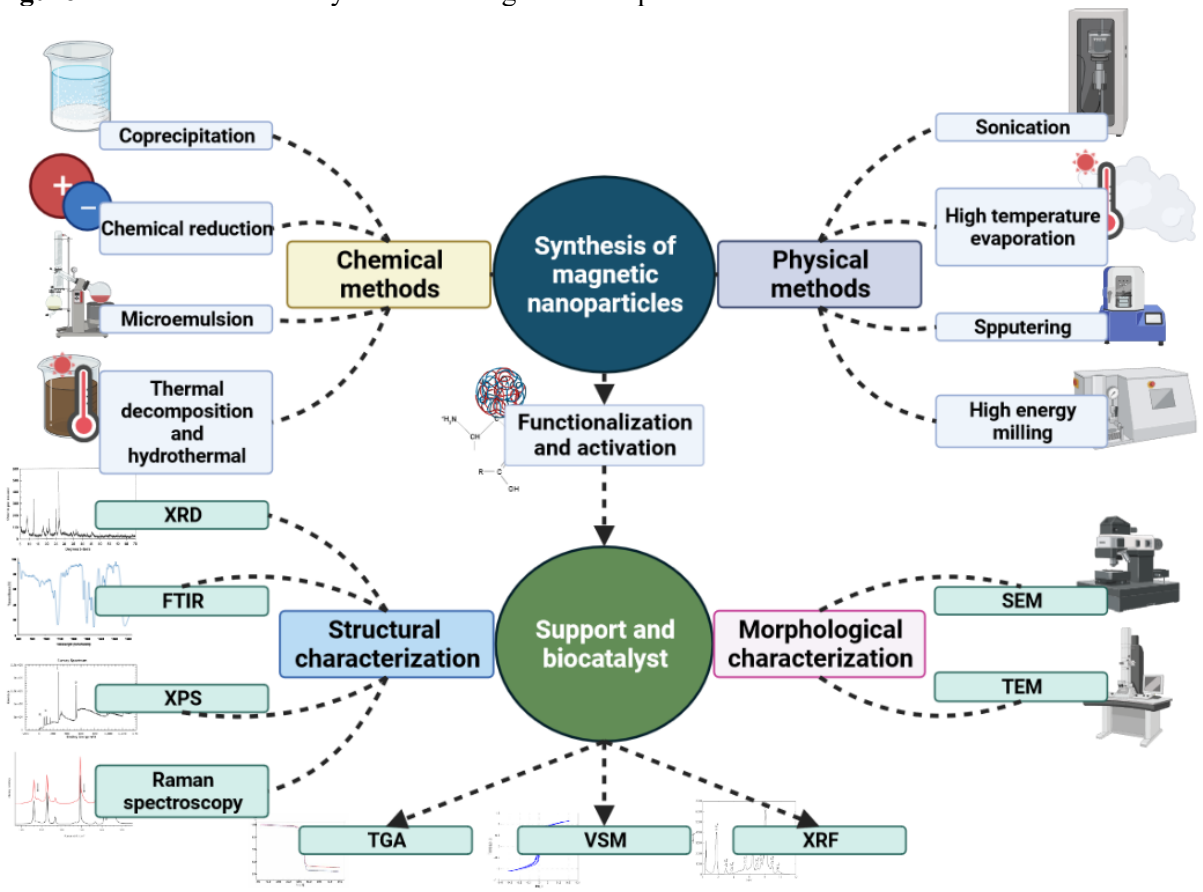

Source: the author.

2.4.2 Applications of magnetic biocatalysts

The applications of magnetic biocatalysts have already been discussed in the course of this work. It is possible to see that applications related to the catalysis of free fatty acids to obtain biofuels and biolubricants are widely explored in the area of biotechnology, which in turn aims to obtain a sustainable energy source (Amruth et al., 2023; Shakeel et al., 2019). Other applications of magnetic biocatalysts that appear in different areas are related to obtaining biosensors (Jimenez-Carretero et al., 2023; Saylan et al., 2022), magnetic therapy (Gunakala et al., 2023; Nain et al., 2023), environmental remediation (Das et al., 2022; Papolu & Bhogi, 2023), medicine (Alexiou, 2022; Borghei et al., 2022), and others.

Magnetic biosensors can be used for detection of biomarkers, toxins, pathogens and environmental pollutants, offering enhanced sensitivity and selectivity (Ghosh, 2020; Pandit et al., 2022). Magnetic biocatalysts also find application in magnetic therapy, where they can be used to direct and concentrate specific therapeutic agents into targeted areas of the human body

(Afzalipour et al., 2021; Tian et al., 2018). The application of magnetic biocatalysts in environmental remediation has gained prominence, especially in the degradation of toxic compounds and organic pollutants (Liu et al., 2023; Pandey et al., 2022). In medicine, magnetic biocatalysts have been investigated for applications such as controlled drug delivery, diagnostic imaging and theranostics (Gorobets et al., 2023; Sivanandan & Saravanan, 2023).

With all these applications, and with prospects for new future applications emerging in the area, it is clear to note that magnetic biocatalysts bring several advantages. As well as the fields of applications, the advantages of magnetic biocatalysts have already been well discussed in this work, to list more succinctly, the advantages related to lipases being immobilized by MNPs are ease of recovery, improvement in stability, increase in catalytic activity, and as already clear, versatility of applications (Chavan et al., 2022; Díez et al., 2022). However, magnetic biocatalysts can also have some disadvantages, which are associated with: limited diffusion, loss of enzymatic activity, limitations in reuse and the complexity of synthesis (Esmaeilnejad-Ahranjani & Lotfi, 2023).

The immobilization of biomolecules on magnetic particles can reduce the mobility of reagent molecules in relation to enzymes, generating limited diffusion (Olusegun et al., 2023). The loss of enzymatic activity due to the particularity of some enzymes (Bilal et al., 2018; Vaghari & Mojgan, 2016). Regarding reuse limitations, although the recovery and reuse of magnetic biocatalysts are outstanding advantages, in some situations, there may be a gradual loss of enzymatic activity after multiple reuse cycles (Gennari et al., 2020; Zang et al., 2014). The complexity of the synthesis appears as the most apparent disadvantage (Fortes et al., 2017; Gao et al., 2018). The synthesis of magnetic biocatalysts can be a complex and challenging process, requiring additional steps for the functionalization of magnetic particles and immobilization of biomolecules, making the process have a high production cost.

Figure 13 shows in a representative way the different possibilities of applications of magnetic biocatalysts, it also shows the advantages and disadvantages of this material.

Figure 13 – (A) Representation of the different applications related to magnetic biocatalysts. (B) Representation of some advantages and disadvantages related to magnetic biocatalysts.

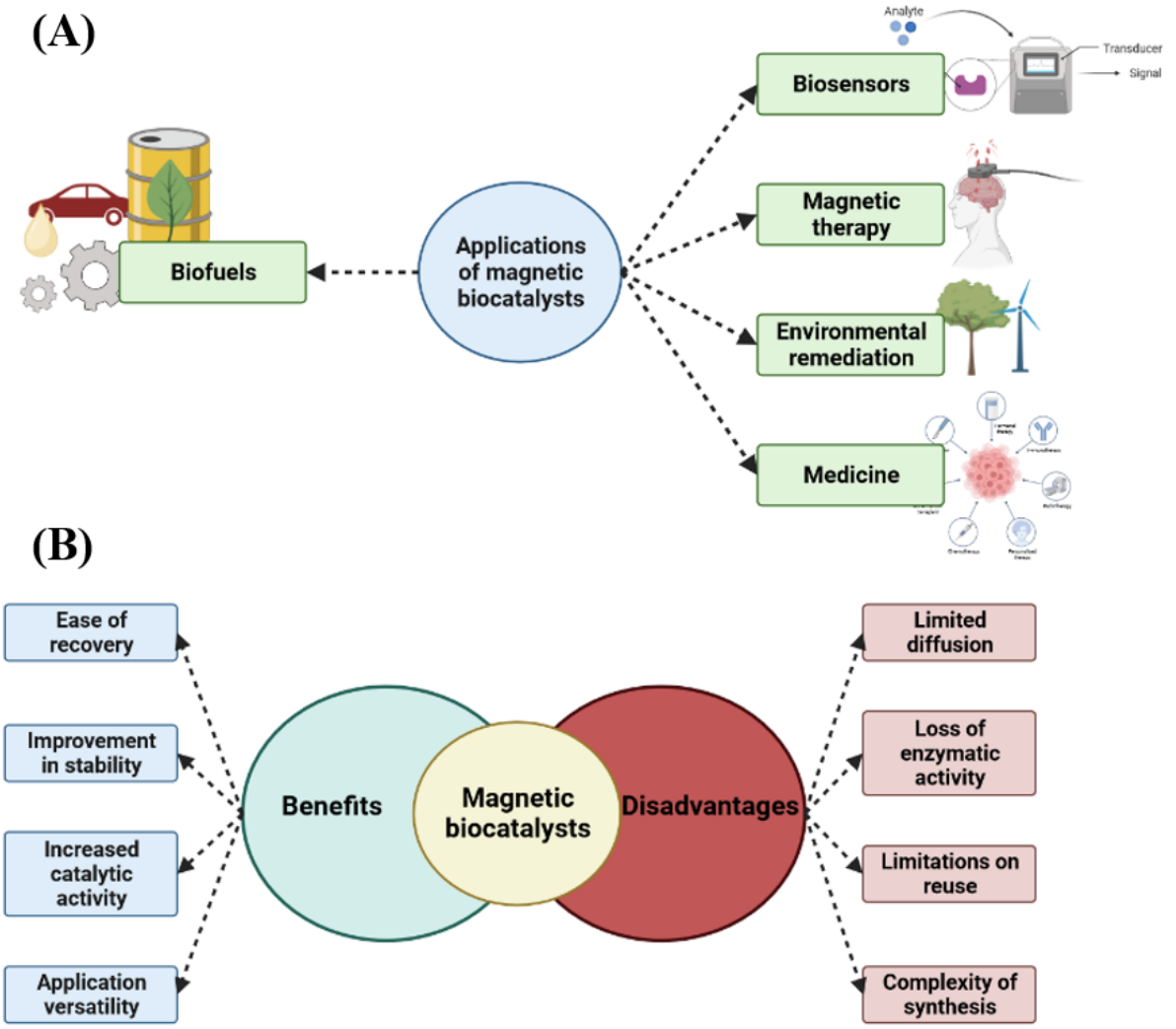

Source: the author.

2.4.3 Reactors used in magnetic biocatalysts

Among the various enzyme immobilization techniques, reactors based on MNPs have emerged as a promising approach in several areas (Bôa Morte et al., 2021; Eom et al., 2022; S. Pal et al., 2023). In the food industry, for example, these reactors are used for the production of immobilized enzymes for the hydrolysis of starch, synthesis of sugars and transformation of oils and fats (Jadhav et al., 2023; Masihi et al., 2023). In the search for more sustainable energy systems, reactors are developed to transform free fatty acids into biofuels and biolubricants (Nagappan & Babu, 2023; Wu et al., 2023). In addition, in the field of biomedicine, magnetic reactors have been used to treat diseases through the controlled release of therapeutic enzymes (Emirik, 2022; Gunakala et al., 2023; Nain et al., 2023; Tian et al., 2018).

Although reactors for enzyme immobilization by MNPs present several advantages, some challenges must be overcome. A challenge is to guarantee the stability and enzymatic reactivity during the immobilization process. It is necessary to avoid the loss of catalytic activity in addition to optimizing reaction conditions, such as pH, temperature, substrate concentration and storage of the biocatalyst, maximizing the efficiency of the system (Bilal et al., 2018b; Torres et al., 2018b; Vaghari; Mojgan, 2016). In this sense, several reactors are being developed and improved by the academic community, such as the reactors: U-Shape magnetic nanoparticle flow reactor (USMNFR), magnetically stabilized fluidized bed reactor (MSFBR), fed-batch stirred tank reactor (FBSTR), micro-reactor with rotating magnetic field (RMF) and the biocatalytic membrane reactor (BMR).

Silva et al. (Imarah et al., 2022) studied the scalability of the U-Shape magnetic nanoparticle flow reactor (USMNFR). The reactor consisted of a polytetrafluoroethylene (PTFE) tube of various internal diameters and moving magnets that allowed mixing of the reaction. The selective acylation of the enantiomer of 4-(morpholin-4-yl) butan-2-ol (±)-1, being the chiral alcohol constituent of the mucolytic drug Fedrylate, was carried out by CALB-MNPs in the U-shaped reactor. results showed that this microreactor can be a simple and flexible instrument for many processes in biocatalysis. The U-shaped permanent magnet design represents a general and easily accessible implementation of MNP-based flow microreactors, being useful for many biotransformations and reducing costly and time-consuming processes downstream.

Hajar et al. (Hajar & Vahabzadeh, 2016) studied the enzymatic conversion of castor oil into biolubricants in a magnetically stabilized fluidized bed reactor (MSFBR). It was shown that the reactor performance depended on the magnetic field strength and the liquid flow rate. A yield of 96.9% of methyl ester was obtained after 24h reaction under optimal conditions. The MSFBR reactor offers advantages that are better than other types of reactors, such as better mass transfer, lower pressure rates, higher efficiency between fluid and particle interactions, especially magnetic nanoparticles, which influence the properties hydrodynamics, as well as the few existing collisions between particles in the MSFBR. The established configurations of the MSFBR appeared to be promising for producing the biolubricant from castor oil.

The configuration of the fed-batch stirred tank reactor (FBSTR) was used from the immobilization by covalent method of lipase Rhizopus oryzae, in which the nanobiocatalysts produced were used in the biodiesel production process, through the extraction of bio-oil from microalgae *Chlorella vulgaris*, in which it was cultivated from glassy tubular photo-bioreactor,

with very positive conclusions the research found the possibility of increasing the productivity and load of the enzyme from the analyzed methods (Nematian et al., 2020).

The micro-reactor with rotating magnetic field (RMF) was used to synthesize butyl oleate with the aim of increasing the industrial scale production of cross-linked enzyme aggregates (CLEAs) together with magnetic nanoparticles (M-CLEAs) (D. Zheng et al., 2018). This micro-reactor, in addition to having a rotating magnetic field (RMF), also has three sand-core sieve plates, which allow the passage of some reaction products, except M-CLEAs, and a magnetic field from two magnets. that were fixed in a part of the structure, which allowed the movement of the M-CLEAs in the microreactor from the projected rotating magnetic field (Zheng et al., 2018). The RMF helped in the promising results obtained, there was an increase in the yield of butyl oleate in 84% in 15h, this result being due to the influence of the distribution of M-CLEAS in the micro-reactor (Zheng et al., 2018).

The biocatalytic membrane reactor (BMR) was designed from Pickering water-in-oil emulsions, in which the entire emulsion process was stabilized with the aid of different colloidal silica nanoparticles (Heyse et al., 2018). The whole process was successful, resulting in smaller emulsions, in addition to no loss of activity, there was better reproducibility and greater filterability, in which the concentrations of both substrates and products remained constant and still reproducible, the lipase enzymes remained active even after 30 hours of reaction (Heyse et al., 2019).

Figure 14 makes a schematic representation of the reactors mentioned in this topic. However, several other reactors based on MNPs have been studied and optimized. Each biocatalysis process has its distinct variables, so that each designed reactor has to have the necessary characteristics to obtain satisfactory results.

Figure 14 – Some reactors based on magnetic biocatalysts.

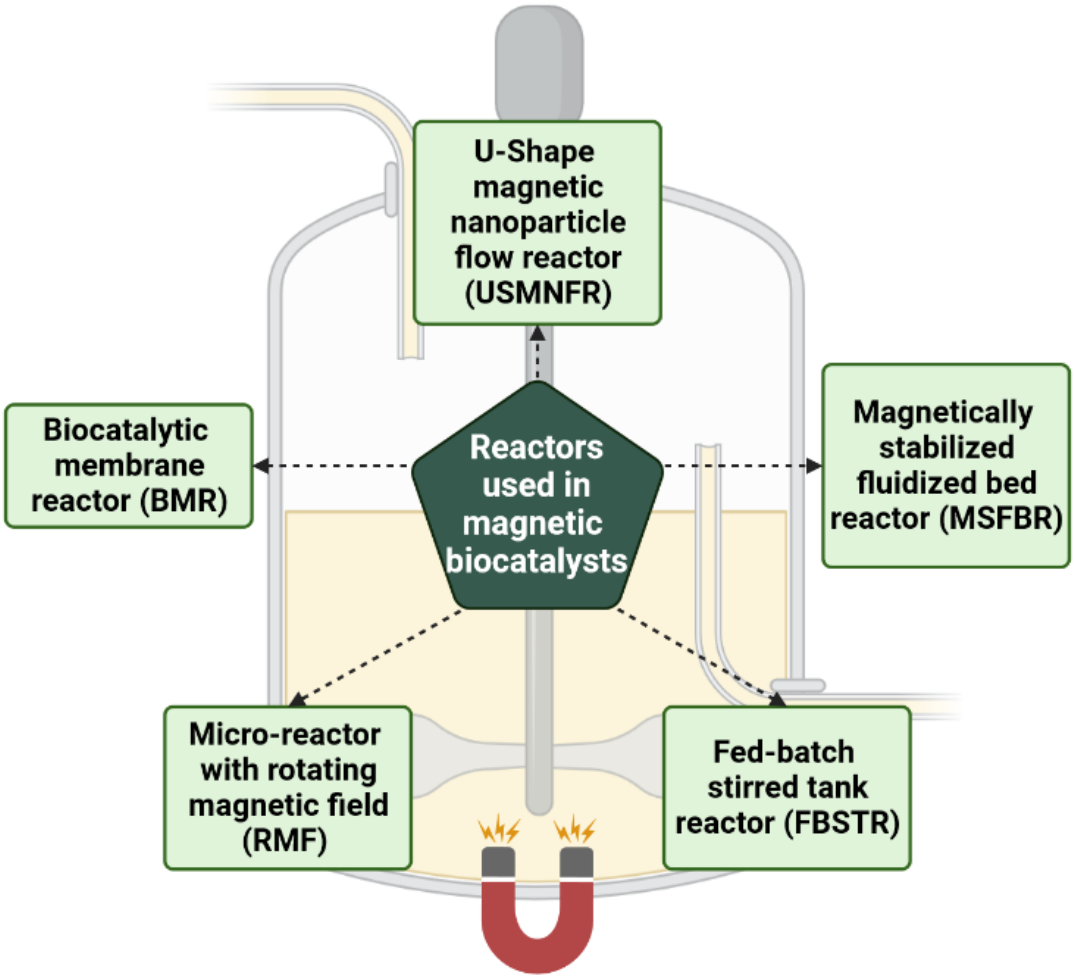

Source: the author.

2.4.3 Patents related to magnetic biocatalysts

Magnetic nanoparticles have interesting properties for industry and characteristics of fine nanoparticles, making them an attractive therapeutic agent. Notably, the volume of bibliographic material on lipase-related magnetic nanoparticles is significant. Some areas are more prominent, such as enzymatic engineering, experimental modeling and building sensory tools for detecting cancer cells. In parallel with academia, industrial research has observed the valuable potential of magnetic nanoparticles for industrial applications. In searches by research platform or robust database on patents such as the United States Patent and Trademark office – USPTO; II. European-Patent Office – EPO, founded in 1994 – 2022, has a volume of 2,618 international patents containing the words nanoparticles, magnetics and lipases in the title. Over the past 20 years, more than 2,000 patents have been filed or granted, representing more than 80% of patents. It is worth mentioning that this theme is current, versatile and still has no limits

in the fields of application of this technological tool (ESPACENET PATENT SEARCH, 2023; WIPO, 2023).

Figure 15 presents the cited data with greater visibility, showing the growth in the volume of patents. It is also worth mentioning that some global potentials stand out when these data are related to the countries where the patent was deposited. United States, China and Europe occupy the 1st, 2nd and 3rd place in the ranking of most deposited patents. With the Americans responsible for about 51.52% of the granted patents, the Europeans for 20.55% and the Chinese responsible for about 10.61% (ESPACENET PATENT SEARCH, 2023; WIPO, 2023).

Figure 15 – Patent data related to magnetic biocatalysts. (A) Countries with the most deposited patents. (B) Number of patents filed between 2000 and 2022.

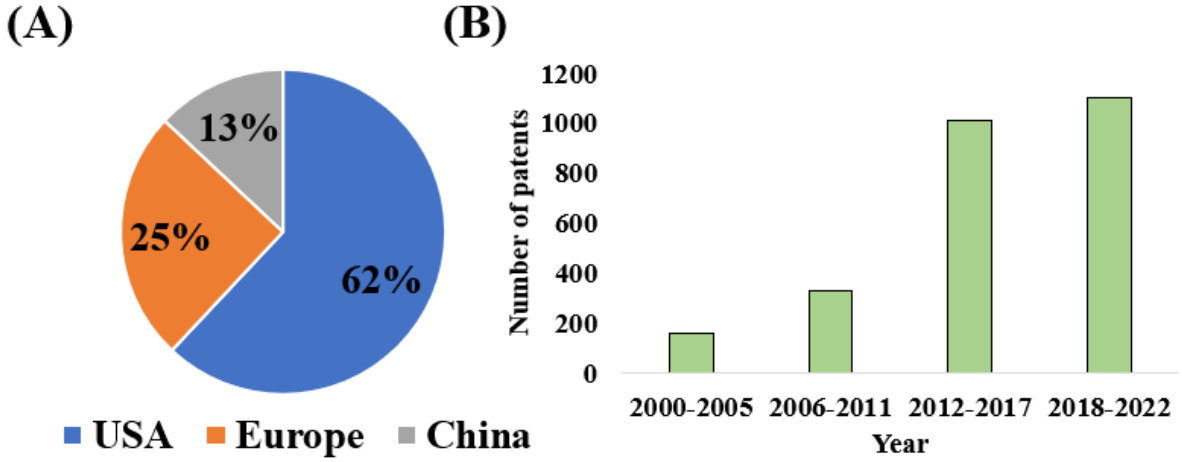

Source: the author.

2.5 Conclusions

Lipase-based magnetic biocatalysts have shown diverse applications and growing interest. Bibliometric analysis showed that cooperation between countries and researchers is growing. Citation between journals and institutions generates high-impact articles and growing citations. The areas where the articles related to lipases immobilized by magnetic nanoparticles are published along with the main keywords showed that the main applications are related to the production of biofuels obtained by enzymatic catalysis of vegetable oils. Showing a great interest in sustainable processes.

The overview of magnetic biocatalysts summarized the main methods of synthesis and characterization of these materials. The coprecipitation method proved to be the most common

synthesis process. Although the most common applications are related to the production of biofuels, applications related to biosensors, photothermal therapy, environmental remediation and medicine are presented as other trends. Magnetic biocatalysts still present some challenges to be overcome. Although the recycling and reuse of these materials is an advantage, the complexity of the synthesis and the different particularities of the lipase immobilization process still require studies. Several reactors are being designed and optimized to enhance the advantages related to magnetic biocatalysts. The industry has also shown a growing interest in these materials, with an increase in patents being filed each year.

Future perspectives related to magnetic biocatalysts are related to the development of better forms of immobilization of lipases, seeking new functionalizing and activating materials for MNPs that can obtain better process stability and catalytic activities, linked to low production costs.

CHAPTER III[2]

3 ENHANCING BIOCATALYST PERFORMANCE THROUGH IMMOBILIZATION OF LIPASE (EVERSA® TRANSFORM 2.0) ON HYBRID AMINE-EPOXY CORE-SHELL MAGNETIC NANOPARTICLES

Abstract

Magnetic nanoparticles were functionalized with polyethylenimine (PEI) and activated with epoxy. This support was used to immobilize Eversa® lipase Transform 2.0 (EVS), optimization using the Taguchi method. XRF, SEM, TEM, XRD, FTIR, TGA, and VSM performed the characterizations. The optimal conditions were immobilization yield (I.Y) of 95.04 ± 0.79%, time of 15 h, ionic load of 95 mM, protein load of 5 mg/g, and temperature of 25 °C. The maximum loading capacity was 25 mg/g, and its stability in 60 days of storage showed a negligible loss of only 9.53% of its activity. The biocatalyst demonstrated better stability at varying temperatures than free EVS, maintaining 28% of its activity at 70 °C. It was feasible to esterify Free Fatty Acids (FFA) from babassu oil with the best reaction of 97.91% and ten cycles having an efficiency above 50%. The esterification of produced biolubricant was confirmed by NMR, and it displayed kinematic viscosity and density of 6.052 mm2/s and 0.832 g/cm3, respectively, at 40 °C. The in-silico study showed a binding affinity of -5.8 kcal/mol between EVS and oleic acid, suggesting a stable substrate-lipase combination suitable for esterification.

Keywords: eversa lipase; heterofunctional immobilization; babassu oil; biofuels.

[2] **MELO, RAFAEL LEANDRO FERNANDES**; FREIRE, TIAGO MELO ; VALÉRIO, ROBERTA BUSSONS RODRIGUES ; NETO, FRANCISCO SIMÃO ; DE CASTRO BIZERRA, VIVIANE ; FERNANDES, BRUNO CAIO CHAVES ; DE SOUSA JUNIOR, PAULO GONÇALVES ; DA FONSECA, ALUÍSIO MARQUES ; SOARES, JOÃO MARIA ; FECHINE, PIERRE BASÍLIO ALMEIDA ; DOS SANTOS, JOSÉ CLEITON SOUSA. Enhancing biocatalyst performance through immobilization of lipase (Eversa® Transform 2.0) on hybrid amine-epoxy core-shell magnetic nanoparticles. **International Journal of Biological Macromolecules**, v. 264, p. 130730, 1 abr. 2024. DOI: doi.org/10.1016/j.ijbiomac.2024.130730.

3.1 Introduction

Enzyme immobilization is a widely used method for preparing enzymatic biocatalysts (Hwang & Gu, 2013; J. Liu et al., 2020; Sheldon, 2007; Tan et al., 2023). It involves fixing them on a solid and insoluble support in a stable way while utilizing the recovery capacity of the reaction system (Luisa et al., 2013; Rueda et al., 2016; J. M. F. Silva et al., 2023b; Zhou et al., 2022). In addition, immobilization improves enzymatic properties, such as activity, selectivity, specificity, and resistance to changes in pH and temperature (Andrades et al., 2019; Ismail & Baek, 2020b; Rios et al., 2016a). The efficiency of each of these characteristics depends on the properties of the materials used to form the support. These attributes can result in different immobilization paths, such as physical, chemical, or heterofunctional interactions (Hwang & Lee, 2019; Jesionowski et al., 2014; Liu et al., 2021; Monteiro et al., 2022). Since enzymatic biocatalysts play an economically exciting role in the industry, the quest for novel materials to develop supports with new and enhanced properties has expanded increasingly (Aguieiras et al., 2016; Chapman, 2018; Nájera-Martínez et al., 2022).

Fe_3O_4 are magnetic nanoparticles (MNP) that have proven to be an excellent support for immobilizing various enzymes (Maroju et al., 2022; Bilal, Zhao, et al., 2018; R. Melo et al., 2023; Vaghari & Mojgan, 2016). Its large surface area, low toxicity, ease of synthesis, paramagnetic potential, and simple separation of the reaction mixture by an external magnetic field simplify the biocatalysis process (Atiroglu, 2020; Melo et al., 2023; Ren et al., 2011; Yu et al., 2022). However, MNPs alone do not have enough reactive surface for immobilization, and they tend to aggregate and oxidize, resulting in the loss of their paramagnetism and dispersibility (Ali et al., 2021; Ashwini John; Samuel; Selvarajan, 2023; Bezarra et al., 2020; Heidarizadeh et al., 2017). Nevertheless, Fe_3O_4 can be easily modified with various surface coating groups, forming a core-shell structure. This overcomes the oxidation problem and enables the enzymatic immobilization process on a more reactive surface (Akhlaghi & Najafpour-darzi, 2022; Kanimozhi & Perinbam, 2013; Sadeghi et al., 2023a).

Polyethyleneimine (PEI) is one of the materials capable of functionalizing the surface of Fe_3O_4 (Bezerra et al., 2020; Cao et al., 2020; Khoobi, Motevalizadeh, et al., 2015). This polymer has a high positive charge density, containing primary, secondary, and tertiary amino groups, with a potent anion exchange capacity under different conditions (Fernandez-Lopez et al., 2017; Mohd Syukri et al., 2021). Together with other anionics, PEI can generate an even more favourable environment for enzyme immobilization (Sun et al., 2022; Zhang et al., 2016). In this regard, covering the MNP with PEI and activating with other agents enables the

development of a heterofunctional support with immobilization by adsorption and multipoint covalent bonds, leading to the creation of a system that is even more stable and has the potential to interact with a broader range of enzymes (Sun et al., 2022; Zhang et al., 2016).

Epoxy groups are reactive and can immobilize proteins and enzymes via multipoint bonding (Mateo et al., 2000a; Mateo, Grazú, et al., 2007; Thudi et al., 2012). These have short spacer arms and can react with several nucleophilic groups (Lys, Cys, His, Tyr) on the protein's surface and slowly with carboxylic groups to form ester linkages (Cui et al., 2015a; Lin & Lin, 2022; X. Liu et al., 2018; Mateo, Grazu, et al., 2007). Epoxy groups promote only mild chemical modifications on the protein surface, creating a very active biocatalyst (Maciel et al., 2019; Mohammadi et al., 2018; Tripathi et al., 2017). Monofunctional epoxy supports require slow immobilization protocols; however, they can be circumvented with other functionalizing agents and support activators (Gandomkar et al., 2015; Ghafar et al., 2019; Habibullah et al., 2014; Heikal et al., 2017; Jing et al., 2015a; Li et al., 2016; Owuna et al., 2020; Tural et al., 2013). Thus, magnetic support with amino functionalization and epoxy activation provides excellent enzymatic immobilization (Cui et al., 2015; Jing et al., 2015; Zhao et al., 2022).

Searching for low-cost biocatalysts with efficient biocatalysis is necessary for industrial viability (Bilal et al., 2021; Gotor-fern, 2006; Torres et al., 2018; Wen et al., 2022). The Eversa® lipase Transform 2.0 (EVS) were developed to be more accessible and effective (Chang et al., 2021; Remonatto, Oliveira, et al., 2022). This is derived from a *Thermomyces lanuginosus* lipase that was produced using a genetically modified strain of *Aspergillus oryzae* (F. Cavalcante et al., 2022; Feedstocks et al., 2021; Sousa et al., 2022). Biocatalysts produced from EVS have already demonstrated promising results in several applications, such as biofuels and biolubricants, topics that are always on the rise due to the suit of sustainability (Bresolin et al., 2020; Sousa et al., 2022; Sun et al., 2021).

Lubricants are substances that reduce friction between the contact surface, reduce wear between mechanical parts, and increase their useful life (Donato et al., 2021; Leang et al., 2022; Rosenkranz et al., 2021; Sarkar & Mandal, 2022; Vaziriserehk et al., 2019). They are produced from mineral oils, with some additives and antioxidants, and are utilized extensively in the mechanical, automotive, naval, and aeronautical industries (Link et al., 2020; Sharma & Singhal, 2019; Tung & McMillan, 2004). The interest in biolubricants has grown significantly due to the rising global need for lubricants and the quest for innovative bioproducts that can replace petroleum derivatives and satisfy industrial demand (Joshi et al., 2023; Li et al., 2022; Wagh et al., 2022; Xiao et al., 2022). According to data, the global market for biolubricants has

reached 44.7 million tons and is expected to continue growing through 2024 at a rate of 5.4% per year (Cavalcante et al., 2022; Kulkarni et al., 2013).

Vegetable oils can be used to produce renewable and biodegradable biolubricants (Heikal et al., 2017; Owuna et al., 2020; Salih, 2021). Since the long-chain fatty acids with the carboxyl group provide a strong attraction with the metallic surface, minimizing abrasion and friction between two parts, the majority of these oils have triacylglycerol in their chain, making them an ideal structure for lubrication (F. Cavalcante et al., 2021; Freschi et al., 2022). However, these oils and fats cannot be used directly as lubricants because the double bonds in triacylglycerol fatty acids are reactive. When reacting with oxygen, they cause an oxidative instability that damages metallic surfaces (Habibullah et al., 2014; Musakhanian et al., 2022; Salih, 2017).

Due to industrial keen interest in biolubricants, numerous studies are being conducted to reduce their oxidative stability drawbacks (Jedrzejczyk et al., 2021; Nogales-delgado et al., 2022; Status, 2022). Processes have been used, such as replacing the glycerol structure with polyols, epoxidation, transesterification, and esterification (Ahmed & Huddersman, 2022; Cao et al., 2023; Tien et al., 2022). The latter has been receiving significant attention from the scientific community. Chemical, enzymatic, or biological catalysts may be used in esterification catalysis (Angulo et al., 2020; Santana, 2021). The difficulty of recovering chemical catalysts from the reaction mixture and reusing them is a drawback (Miceli et al., 2021). On the other hand, the biocatalysts be reused, making the biolubricants produced even more environmentally friendly, proving their superiority to chemical catalysis (García-bofill et al., 2021; Ortiz, Ferreira, Barbosa, Santos, et al., 2019; Torres et al., 2018b).

Babassu (*Orbignya speciosa M.*) emerged as a promising candidate in the search for vegetable oil that might be obtained on an industrial scale to produce biolubricants (Cassia et al., 2020). In 2018, the production of babassu oil was approximately 50,000 tons. Considering the average price of oil, more than 20 million dollars of this oil were traded solely in Brazil (Cassia et al., 2020). Its oil content is higher than other common oilseeds, such as canola and sunflower, having a content of 42% versus 32% and 40%, respectively (Cassia et al., 2020). Babassu oil is resistant to decomposition by hydrolysis and oxidation, having a predominant composition of saturated fatty acids (Melo et al., 2019). The broader composition of refined babassu oil predominantly consists of fatty acids, with a high proportion of lauric acid, a medium-chain saturated fatty acid. Other significant fatty acids in babassu oil include myristic, palmitic, oleic, and linoleic acids, proving its appropriateness as a vegetable oil for biolubricant production (Melo et al., 2019).

This communication evaluated the development of a new heterofunctional support based on Fe_3O_4 magnetic nanoparticles functionalized with PEI and activated with epoxy groups to stably and effectively immobilize Eversa® lipase Transform 2.0. The developed biocatalyst was evaluated regarding its biocatalysis potential of babassu FFA (*Orbignya speciosa M.*). Taguchi's method was applied to optimize the immobilization of the EVS by the support. The supports and the biocatalyst were structurally and magnetically characterized using SEM, XRF, MET, DRX, FTIR, TGA, and VSM techniques. The storage stability, pH, and temperature of the biocatalyst were assessed. The amount of babassu FFA esterification cycles was evaluated by the biocatalyst and confirmed by NMR. Finally, molecular docking and molecular dynamics scrutinised the positions and binding energies between EVS and babassu FFAs.

3.2 Materials and Methods

3.2.1 Materials

Iron (III) chloride hexahydrate ($FeCl_3.6H_2O$) and iron sulfide heptahydrate ($FeSO_4.7H_2O$) were purchased from Vetec Química Ltda (São Paulo, Brazil). Polyethyleneimine (PEI) (10,000 MW) was bought from Sigma-Aldrich (St. Louis, MO, USA). Diglycidyl ether bisphenol A (DGEBA) was purchased commercially from Polipox Ltda (São Paulo, Brazil). Eversa® lipase Transform 2.0 from *Aspergillus oryzae* (EVS), from *Thermomyces lanuginosus* lipase (TLL). Refined babassu oil was obtained commercially from Leve Ltda (Maranhão, Brazil). Other chemical reagents were provided by Synth and Vetec Química (São Paulo, Brazil). All of them were used without further purification. For the elaboration of the experimental method, Taguchi planning was employed with the Statistica® 10 software (Statsoft, USA).

3.2.2 Synthesis of Fe_3O_4 magnetic nanoparticles functionalized with PEI and activated with DGEBA

The synthesis of Fe_3O_4 nanoparticles was carried out using an ultrasonic probe (Ultrasonic Disruptor). This probe operated at a frequency of 20 kHz, a power of 550 W, and had a microtip diameter of 3.2 mm. During the synthesis of Fe_3O_4, sonication was done with a

power of 200 W in a pulse regime of 3 seconds on and 1 second off (Bezerra, Monteiro et al., 2020; Neto et al., 2021). Initially, 1.16 g (4 mmol) of $FeSO_4.7H_2O$, 1.85 g (7 mmol) of $FeCl_3.6H_2O$ and 1.85 g (7 mmol) of $FeCl_3.6H_2O$ were dissolved in 15 mL of deionized water. This solution was then sonicated for 8 minutes under the mentioned pulse regime. After this, 7.0 mL of NH_4OH was slowly added. During the addition of NH_4OH, the colour of the solution changed from orange to black, indicating the formation of Fe_3O_4 nanoparticles. After the formation of the nanoparticles, the Fe_3O_4 was washed with acetone and separated with a magnet until the pH of the solution became neutral.

The functionalization of Fe_3O_4 with PEI was a joint process. 1.0 g of PEI was dissolved in 5 mL of deionized water and added in a drip after forming Fe_3O_4 (8 min of sonication), continuing the sonication for another 4 min, totalling 12 min. After this process, the Fe_3O_4-PEI was washed with ketone and precipitated using a magnet until a neutral pH was obtained (R. M. Bezerra, Monteiro, Neto, et al., 2020a). The Fe_3O_4-PEI were dried in a vacuum until the powder state.

For the activation of Fe_3O_4-PEI with DGEBA, the nanoparticles, after drying and maceration, were mechanically mixed in rotation at 1500 rpm for 2 h in DGEBA (Relative centrifugal force (RCF) of 63xg). The proportion used was 1g of Fe_3O_4-PEI for 12 g of DGEBA. After this process, the system was sonicated with 10 mL of ethyl alcohol for 4 min, washed with a ketone, and precipitated with a magnet to remove excess DGEBA.

3.2.3. Experimental design for immobilization of Eversa® lipase Transform 2.0 (EVS) on Fe_3O_4-PEI-DGEBA

To determine the optimal point of immobilization of the EVS on the Fe_3O_4-PEI-DGEBA support, the Taguchi method was used with an orthogonal matrix L9 (where “L” and “9” represent the Latin square and the experiment number, respectively). Four independent variables (time (h), ionic strength (mM), protein load (mg/g), and temperature (°C)) were used at three levels.

The procedure for each level of the Taguchi method consisted of suspending 100 mg of the support in 1 mL of 5 mM sodium phosphate buffer solution at pH 7 and 25 °C containing the EVS with an enzymatic load of 1 mg/g of support. This was kept mildly agitated. After this step, the solutions were washed in 5 mM sodium phosphate at pH 7.0 and centrifuged, and the initial yield (I.Y) of the supernatant was determined (Cavalcante et al., 2022a; Sousa et al., 2022). Subsequently, the solutions were incubated in 10 mL of 5 mM sodium bicarbonate at

pH 10 and 25 °C for 16 h. The solution was then mixed with 10 mL of 3 M glycine at pH 8.5 and 25 °C for 24 h to block the epoxy groups that failed to immobilize the EVS (García-bofill et al., 2021; Mateo et al., 2000). Finally, the Fe_3O_4-PEI-DGEBA@EVS nanoparticles, now called biocatalysts, were washed with 5 mM sodium phosphate buffer at pH 7.0 and precipitated with the help of a magnet to measure the enzyme activity and protein content of the derivative. Table 5 shows the four independent variables and their corresponding levels used in the Taguchi method.

Table 5 – Independent variables and their respective levels for EVS immobilization in Fe_3O_4-PEI-DGEBA.

	Time (h)	Ionic strength (mM)	Protein load (mg/g)	Temperature (°C)
Level 1 (L1)	6	5	1	25
Level 2 (L1)	15	50	3	30
Level 3 (L1)	24	95	5	35

Source: the author.

For statistical analysis, the Statistica software was used. Table 6 shows the experimental design of the Taguchi method.

Table 6 – Experimental design of the Taguchi method.

Experiment	Time (h)	Ionic strength (mM)	Protein load (mg/g)	Temperature (°C)
1	6	5	1	25
2	6	50	3	30
3	6	95	5	35
4	15	5	3	35
5	15	50	5	25
6	15	95	1	30
7	24	5	5	30
8	24	50	1	35
9	24	95	3	25

Source: the author.

As one of the research objectives was to maximize the response of the biocatalyst activity (Fe_3O_4-PEI-DGEBA@EVS), the question “bigger is better” was used in each reaction of the variables, as shown in Table 6. It was necessary to calculate S/N, corresponding to the signal-to-noise ratios. These correspond to the values of the activity of the biocatalyst. The S/N calculation is shown in Equation (1).

$$\frac{S}{N} = -10\log\left(\frac{1}{n}\sum_{j=1}^{n}\frac{1}{y^2}\right).100 \quad (1)$$

The response variables are given by y, the number of repetitions by I, and the number of experiments by n. Equation (2) determines the S/Np for ideal conditions for biocatalyst activity.

$$\frac{S}{Np} = \frac{S}{N}\sum_{j=1}^{n}\left(\frac{S}{N_i} - \frac{S}{N}\right) \quad (2)$$

Where S/Np is the ideal point for each factor, S/N is the arithmetic mean of the variables.

3.2.4. Determination of enzyme activity and protein content

The activities of EVS and Fe_3O_4-PEI-DGEBA@EVS were assessed using a method previously described in reference (Rios et al., 2016a). The specific activity of soluble EVS is 560 U/mg of protein (Valero et al., 2022). In this study, the activity of EVS was determined by measuring the increase in absorbance at 348 nm, resulting from the hydrolysis of *p*-NPB (p-nitrophenyl butyrate) over 90 s. *p*-NPB is the preferred substrate in lipase/esterase assays due to its efficient hydrolysis and favourable interaction with these enzymes. Being a short-chain ester, p-NPB ensures maximum hydrolytic activity, ideal for more effective enzymes in short-chain substrates (De et al., 2013). The assays were conducted in 2.5 mL of 25 mM sodium phosphate buffer, pH 7.0, at 25°C, using 50 µL of suspended EVS and 50 µL of p-NPB.

3.2.5. Immobilization parameters

To calculate the immobilization parameters of lipase on support, we use the methodologies outlined by previous studies (Cavalcante et al., 2022). These parameters include the Immobilization Yield (I.Y.), Theoretical Activity (At. T), Recovered Activity (At. R), and Derivative Activity (At. D).

The I.Y. is the percentage of enzymatic activity retained after immobilization, calculated by the difference between the initial and final activity of the enzyme. The At. T is the expected activity of the lipase after immobilization, based on the amount of enzyme used and the I.Y. The At. R compares the actual activity of the At. D with the At. T. Finally, the At. D is the

actual measured activity of the immobilized lipase, assessed under specific test conditions. Below are the equations for calculating each of these parameters.

$$\text{I.Y.} = \left(\frac{At_i - At_f}{At_i}\right) 100\% \quad (3)$$

$$\text{At.T} = At_{enz}\ (\text{I.Y.}) \quad (4)$$

$$\text{At.R} = \left(\frac{\text{At.D}}{\text{At.T}}\right) \quad (5)$$

$$\text{At.D} = \frac{\Delta A}{\Delta t}\ f \quad (6)$$

I.Y. and At. D. are expressed as percentages (%), while At. T and At. R. are denoted in U/g. At_i and At_f represent the initial and final activities, respectively. At_{enz} denotes the amount of enzyme offered per gram of support. The term ΔA represents the change in absorbance as measured by a spectrophotometer over the time interval Δt. Additionally, f serves as a conversion factor, establishing a relationship between the observed change in absorbance and the enzymatic activity.

3.2.6. Maximum enzyme loading capacity

In order to measure the EVS immobilization capacity, 100 mg of NPs suspended in 1.0 mL of sodium phosphate buffer solution (95 mM and pH 7) were used, containing EVS with an enzymatic load of 1:1 - 1:50 mg/g of support. The system was kept under constant agitation for 15 h at 25 °C.

3.2.7 Storage stability

The storage activity of the biocatalyst was evaluated by monitoring the hydrolytic activity using *p*-NPB as a reference reagent. After immobilization, the biocatalysts were washed, vacuum-dried, and stored at 4 °C. The activities of the generated biocatalysts were assessed at regular intervals (days). As a result, the behaviour of the reaction over time was measured.

3.2.8 Thermal stability

To evaluate the impact of temperature on enzymatic activity, the biocatalyst and EVS were incubated in phosphate buffer (95 mM and pH 7) at 25, 30, 40, 50, 60, 70, and 80 °C for 10 min. After heating, the samples were cooled in an ice bath and immediately warmed to room temperature (25 °C) in a water bath before analysis. The activity was measured using *p*-NPB, and residual activity was expressed as a percentage of the initial activity described in Section 2.2.4.

3.2.9 Stability in pH

The evaluation of the impact of pH on enzymatic activity was as follows: the biocatalysts and EVS were resuspended in 1.0 mL of 95 mM buffer solution in the pH range 4–9 [sodium acetate buffer (pH 3.6–5.6), sodium phosphate buffer (pH 5.8–8.0) and sodium carbonate buffer (pH 8.9–10.8)], using *p*-NPB as the reference reagent. Thus, the enzyme was incubated in each buffer for about 15 min, and then the activity was measured as described in Section 2.2.4.

3.2.10 Materials characterization

Scanning electron microscopy (SEM) images and X-ray fluorescence spectroscopy (XRF) were performed to assess morphology and chemical composition. SEM was carried out on the QUANTA 450 FEG microscope. The samples were fixed on carbon tape and metalized with silver using the Quorum QT150ES metallization equipment. An electron beam with 20 kV was applied. The XRF was performed using a SHIMADZU model EDX-7000 equipment equipped with a rhodium tube, applying a power of 4 kV to the powder samples.

The morphology and size of the nanoparticles were assessed using transmission electron microscopy (TEM), and X-ray diffraction (XRD) evaluated the crystallinity and size of the nanoparticles, allowing comparison with microscopy analyses. TEM was carried out using a JOEL JEM 1011 microscope operating at 120 kV with a CCD camera. One drop of aqueous dispersion from each sample was deposited onto a carbon-coated copper grid (200 mesh). Distribution curves were obtained manually using ImageJ software. XRD was performed on an X'Pert MPD X-ray powder diffractometer (Panalytical), with a sweep range of $2\theta = 20 - 80°$. A CuKα tube (1.54059 Å) was used for the samples, operating at 40 kV and 30 mA, and scanning

range 20° - 100°. The diffraction patterns were obtained using Brentano Bragg Geometry in continuous mode with a speed of 0.5°/min and a step size of 0.02° (2θ). The Rietveld structure of refinement was used to interpret and analyze diffraction data using the Maud® program. The crystal size of each sample was calculated using the Scherrer equation.

Fourier transform infrared spectroscopy (FTIR) evaluated the presence of organic molecules on the surface of nanoparticles. FTIR was performed on a PerkinElmer 2000 spectrophotometer. Samples were pulverized in an agate mortar and pressed onto kBr discs at a mass ratio 1:10 (sample: KBr). To prevent interference from water and carbon dioxide, spectra were captured in a vacuum using a Vertex 70v. The range used was 4000 - 500 cm^{-1}, with a resolution of 2 cm^{-1} and 128 scans.

Thermogravimetric analysis (TGA) was performed on the Q50 TA Instruments equipment, using a nitrogen atmosphere at 50 cm^3/min, with a heating rate of 10 °C/min between 25 and 900 °C, and the sample mass was 10 mg.

The magnetic curves were obtained using a vibrating sample magnetometer (VSM) at 300 K. To ensure the accuracy of the acquired magnetic moments, the VSM was previously calibrated using standard reference material. For all measurements, the magnetic moment obtained for each applied field was normalized by the mass of the nanoparticles.

3.2.11 Production of biolubricants and operational stability from Babassu oil

Free fatty acids were formed from refined babassu oil via enzymatic hydrolysis using *Thermomyces lanuginosus* lipase (TLL). The soluble TLL has a specific activity greater than 100,000 U/g, being more effective at a pH range of 2 to 5 and temperatures between 30 to 50 °C (Oliveira Cavalcante et al., 2024). The reaction system was developed based on the methodology by previous studies (Souza et al., 2019). The solution containing oil and water in a 1:1 ratio was heated until the system reached a temperature of 40 °C, after which 0.4% TLL was added. The system remained at 40 °C for 4 h under constant stirring.

The solution was transferred to a separatory funnel, and 100 mL of distilled water at 60 °C was added to separate the FFAs. The lower (aqueous) phase was excluded, and the FFAs were washed three times. The mixture was transferred to a beaker and heated at 80 °C for 10 min. At the end of 10 min, the mixture was assigned to a funnel with filter paper and anhydrous sodium at 20% $m.v^{-1}$, which was previously dried in a muffle oven at 250 °C for 4 h (Souza et al., 2019).

The production of the ester biolubricants was carried out using the biocatalysts obtained in this work. The FFAs obtained from babassu oil were esterified in Eppendorf tubes in an orbital shaker incubator at 200 rpm with 2-ethyl-1-hexanol in a 1:1 molar ratio (Moreira et al., 2022). After this process, 2% of the biocatalyst Fe_3O_4-PEI-DGEBA@EVS was added and incubated for 24 h in triplicate. The reaction time and the acid number of the supernatant were determined. 0.2 g aliquots were taken from the reaction volume, diluted in 20 mL of ethyl alcohol and 3 drops of phenolphthalein, and then titrated with sodium hydroxide (40 mM) (Souza et al., 2019). The acidity index (AI) was established according to Equation (7).

$$AI\ \left(\frac{mgNaO}{g}\right) = MM_{NaOH}.Shch_{NaOH}.f.(\frac{V_{NaOH}}{m}) \quad (7)$$

where MM_{NaOH} is the molar mass of $NaOH$, $Shch_{NaOH}$. Is the molarity of the solution, f is the correction factor determined by the standardization of $NaOH$; V_{NaOH} Is the volume of $NaOH$ spent in the titration, m is the mass of the sample to be analyzed. The conversion of FFAs into esters was calculated by Equation (8), considering the acidity at time zero (AI_o) and at time t (AI_t).

$$Conversion\ FFA(\%) = \frac{AI_o - AI_t}{AI_o}.100 \quad (8)$$

Operational stability was verified by consecutive reactions for producing the biolubricating ester using 5% of the biocatalyst, 1:5 for molar ratio (acid: alcohol) octyl alcohol and free fatty acids from babassu oil, 40 °C for temperature, and 5 h of reaction stirred at 200 rpm. Before each cycle, the biocatalyst was separated from the reaction medium by magnetization and washed three times with hexane to remove unreacted substrates.

3.2.12 Nuclear Magnetic resonance spectroscopy (NMR)

NMR was performed to confirm the esterification of free fatty acids. 1 D and 2 D, ^1H, ^{13}C spectra were obtained in Bruker Avance DRX-500 spectrometers, using $CDCL_3$ as solvent. For NMR spectroscopy, chemical shifts were expressed in parts per million (ppm) and referenced in the ^1H NMR spectra by the hydrogen peak belonging to the non-deuterated fraction of the solvent $CDCl_3$ (δH 7.27). The multiplicities of the hydrogen signals in the ^1H

NMR spectra were indicated according to the convention: s (singlet), d (doublet), t (triplet), and m (multiplet).

3.2.13 Evaluation of viscosity and density

To evaluate the lubricity, the dynamic viscosity (η), the kinematic viscosity (ν), and the density (ρ) were determined. The Anton Paar SVM 3000 U-Tube viscometer was used, which was calibrated using a Cannon mineral oil in the temperature range from 273.15 to 393.15 K. These properties were evaluated at atmospheric pressure and the following temperatures: 293.15, 313.15 and 373.15 K. The SVM 3000 equipment was supplied with the sample through a 5 mL syringe, ensuring no bubble air was present. The internal temperature control shows an uncertainty of u(T) = 0.01 K. The uncertainty for density and viscosity was 0.0015 g/cm^3 and 0.35 %, respectively.

3.2.14 Molecular docking

Comparative modelling of the EVS protein involved in four stages was performed. The amino acid sequence of the EVS, with its CAS number 9001-62-1 through the company Sigma-Aldrich, was submitted to a comparative analysis through the BLAST program (Basic Local Alignment Search Tool) (Altschul et al., 1990) and in its PDB database. Thus, a protein related to the amino acid sequence, the lipase enzyme, classified as hydrolase, was identified by the organism *Aspergillus oryzae*, expressed through the *Escherichia coli-Pichia pastoris* shuttle, obtained from the Protein data Bank with the code 5XK2 being the target protein.

The alignment between the sequences was carried out using the Modeller program (http://www.salilab.org/modeller/) (Webb & Sali, 2016).

The Modeller program also constructed the model98], thus obtaining a new EVS, evaluated according to the objective function and stereochemical parameters (Bedoya & Tischer, 2015).

The model was validated at the stereochemical, conformational, and energetic level. The quality of the generated model was validated by the Ramachandran chart (Ramachandran & Sasisekharan, 1963)) with the PROCHECK program (https://saves.mbi.ucla.edu/), which evaluated its three-dimensional structure, indicating the possible stereochemical quality (Laskowski et al., 1993).

The protein created by EVS homology was submitted to a process of load correction, and hydrogen atoms were added through the Program AutoDock Tools (Morris et al., 2009).

Figure 16 shows the structure of the chemical composition of residual oil from babassu. This was drawn in the ChemDraw 3D software and later minimized with an MM2 force field with an RMS gradient of 0.0001 (Ahmadi et al., 2005). For structural optimization purposes, the configuration was performed through the Software Avogadro® (Hanwell et al., 2012), the configuration with the Merk Molecular Force Field (MMFF94), with cycles of 500 interactions and a steeper algorithm, having the convergence limit of $10e^{-7}$ (Halgren, 1996) and later converted to the pdbqt format.

Figure 16 – 2D structure of the chemical composition of residual oil from babassu.

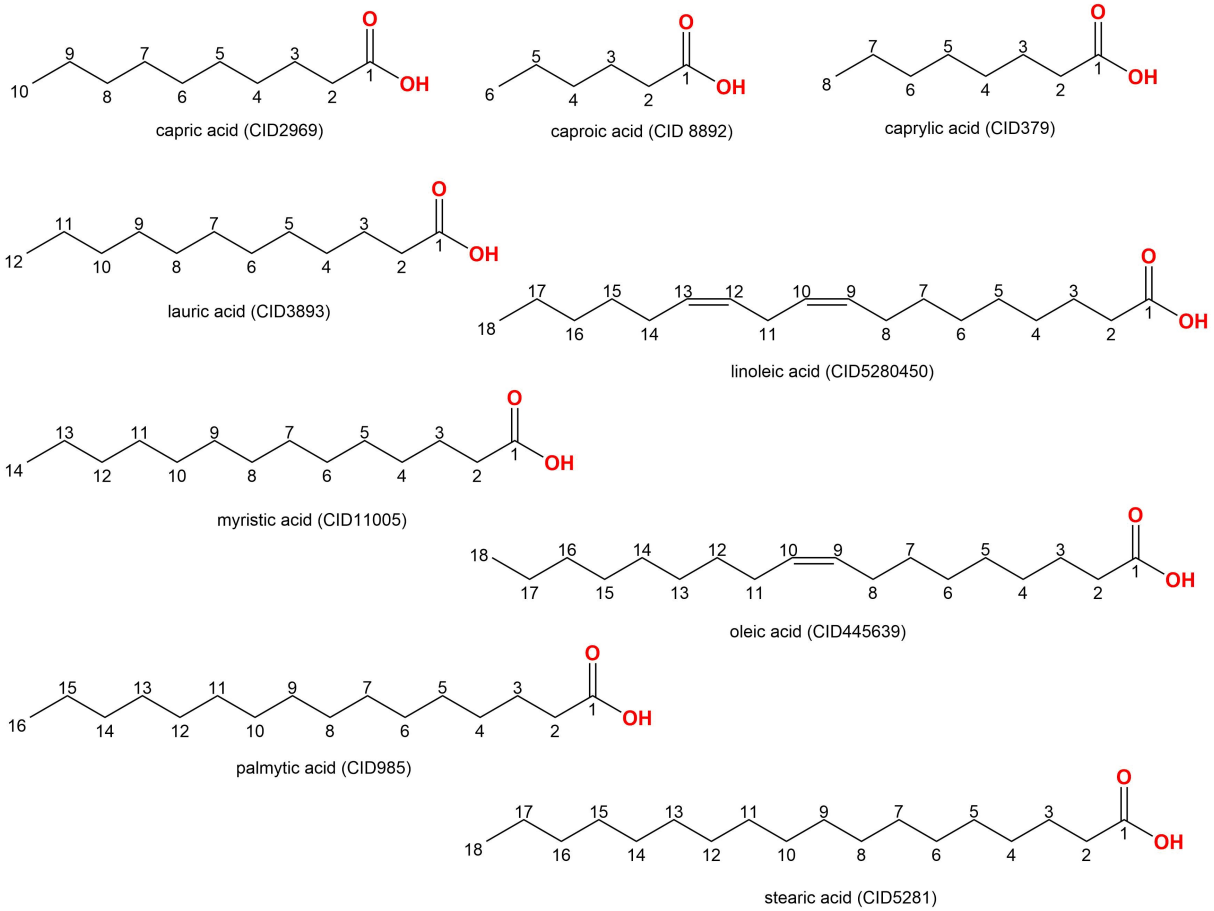

Source: the author.

Molecular coupling simulation was performed with Code AutoDock Vina (Trott & Olson, 2009), considering rigid protein and flexible binders. For both calculations, a grid configuration was performed with parameters of the enzyme active site (Hlima et al., 2021; Cen

et al., 2019). The energy profiles of the ligand-receptor interactions were also evaluated by software, and Pymol visualized the anchored poses (DeLano, 2020).

3.2.15 Molecular docking

Molecular dynamics (MD) simulations were performed with the NAMD program (Phillips et al., 2005a). The best conformations obtained in molecular coupling were solved in water in the TIP3P model (Kato et al., 2021), in the CHARMM36 force field, and in addition to ions to neutralize the total system load. Finally, it was submitted to energy minimization by the Steepest Descent method. The system was then introduced to NVT and NPT balances under conditions described by Langevin (Farago, 2019). The system production simulations were performed with a time of 100 ns. The quality of the structures obtained in MDs was evaluated using the following parameters with NAMD:

a. Potential Energy (kcal/mol) (Diez et al., 2014);
b. Protein-Ligand Interaction Energy (kcal/mol);
c. The mean quadratic deviation of the atomic positions of proteins, binders, and distances between them (RMSD, Å), and the mean quadratic deviation of the nuclear positions of proteins, ligands, and distances between them (RMSD, Å);
d. Hydrogen bonds were evaluated with Visual Molecular Dynamics (VMD) (Humphrey et al., 1996).
e. The mean quadratic fluctuation of the minimum distances between proteins and ligands was observed in MD (RMSF, Å) (Arshia et al., 2021). The graphs were generated using the Qtrace program (Lima et al., 2012).

Based on MD log file of NAMD software (Phillips et al., 2005b), the MM/GBSA was calculated by MolAICal (Bai et al., 2021) and was estimated by Equations (9), (10), and (11).

$$\Delta G_{bind} = \Delta H - T\Delta S \approx \Delta E_{MM} + \Delta G_{sol} - T\Delta S \quad (9)$$

$$\Delta E_{MM} = \Delta E_{internal} + \Delta Ee_{le} + \Delta E_{vdw} \quad (10)$$

$$\Delta G_{sol} = \Delta G_{GB} + \Delta G_{SA} \quad (11)$$

Where ΔEMM, ΔG_{sol}, and TΔS represent the gas phase MM energy, solvation-free energy (sum of polar contribution ΔG_{GB} and nonpolar contribution ΔG_{SA}), and conformational entropy, respectively (Gohlke et al., 2003; Gohlke & Case, 2004). ΔE_{MM} contains Van Der Waals energy ΔE_{vdw}, electrostatic ΔE_{ele}, and $\Delta E_{internal}$ of bond, angle, and dihedral energies. If there are no binding-induced structural changes in the process of MD simulations, the entropy calculation can be omitted (DasGupta et al., 2017).

3.3 Results and Discussion

3.3.1. Functionalization of Fe_3O_4 with polyethyleneimine (Fe_3O_4-PEI) and activation with diglycidyl ether of bisphenol A (Fe3O4-PEI-DGEBA)

This work aims to create a heterofunctional support that would enable very stable immobilization of the enzyme through multipoint covalent connections and adsorption-based physical interactions. For this, the preparation of the support followed 2 steps.

The first step was the functionalization of Fe_3O_4 with polyethyleneimine (PEI). This modification enables Fe_3O_4 to improve its resistance against oxidation and allows the support to have a surface with multiple active amine groups to interact with the enzyme covalently (Bezerra, Monteiro et al., 2020; Zhang et al., 2016). Both the synthesis of Fe_3O_4 and its functionalization with PEI were performed via ultrasound, which has already been proven to be an effective technique with low cost and short operating time (Veisi et al., 2021). In this technique, acoustic waves create bubbles that grow to a specific size and then collapse, releasing concentrated energy quickly. The temperature obtained can reach 5,000 K and pressures of up to 1,000 bar (Neto et al., 2017). Thus, the high energy induced by ultrasonic irradiation allowed covalent interactions between Fe_3O_4 and PEI (Neto et al., 2017, 2021).

The second step was the activation of Fe_3O_4-PEI with diglycidyl ether of bisphenol A (DGEBA). DGEBA has highly active epoxy groups for enzyme immobilization (Liu et al., 2018; Mateo, Grazú et al., 2007; Mihailović et al., 2014). Supports with epoxy groups have the characteristic of first performing a rapid immobilization by physical adsorption on the surface of the enzymes, and later, with increasing incubation time, a chemical reaction is formed between the epoxy group and the nucleophilic groups, giving rise to covalent solid bonds (Mateo, Grazú, et al., 2007; Zaak et al., 2018). Thus, the immobilization with epoxy groups is a heterofunctional immobilization (Bezerra, Monteiro et al., 2020). The activation of Fe_3O_4-PEI with DGEBA happened mechanically, where the rotation of Fe_3O_4-PEI with DGEBA likely

facilitated the covalent interaction between the amine groups of PEI and the epoxy groups of DGEBA, resulting in the formation of Fe_3O_4-PEI-DGEBA support. The creation of this new support probably allowed the immobilization of Eversa® lipase Transform 2.0 (EVS) through the physical adsorption of epoxy groups and covalent bonds of both epoxy groups and free surfaces of amine groups. Figure 17 represents the immobilization of the enzyme by the support obtained in this work.

Figure 17 – Enzyme immobilization (Eversa® lipase Transform 2.0 (EVS) being represented by *Thermomyces lanuginosus* lipase (TLL)) by Fe_3O_4-PEI-DGEBA support.

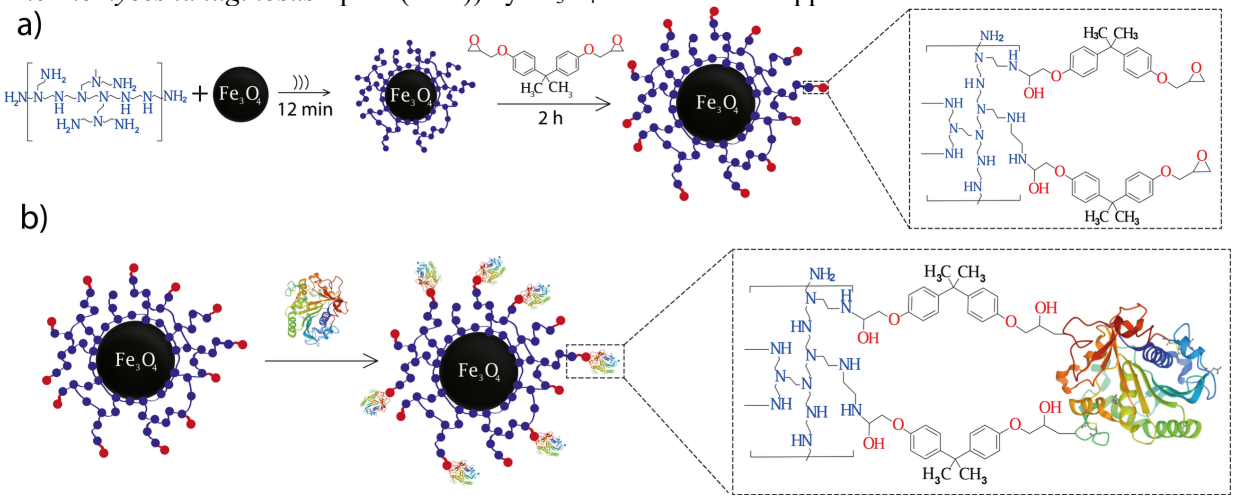

Source: the author.

3.3.2 Optimization of the immobilization of Eversa® lipase Transform 2.0 (EVS) on Fe_3O_4-PEI-DGEBA

In contrast to other statistical designs, the Taguchi technique provides a simple data design and is quite effective (Jankovic et al., 2021). Several authors have already reported that using the Taguchi method in different areas of scientific research (Nemati et al., 2023; Williamson et al., 2022) effectively reduces the experimental cost and provides a reliable assessment of the significance of each factor studied (Hayatzadeh et al., 2022). In enzyme immobilization, the Taguchi method has already shown that conditions of the reaction medium and the concentration of the enzyme have varied influences on the immobilization depending on the support used to develop the biocatalyst (Cavalcante et al., 2022; Monteiro et al., 2022; Rocha et al., 2021). In this study, the Taguchi planning of the L9 orthogonal matrix was used to quantify the effects and the interaction between the factors involved in the process and

identify the parameters that had the most significant influence on the immobilization of the EVS by Fe_3O_4-PEI-DGEBA.

Table 7 shows the results obtained, as shown in Section 2.2.2. up to Section 2.2.4, related to the enzymatic immobilization parameters in terms of percentage immobilization yield (I.Y), theoretical activity in U/g (At. T), derivative activity in U/g (At. D) and recovered activity in % (At. R). Signal noise (S/N) values were calculated according to Equations (1) and (2).

Table 7 – EVS immobilization results in Fe_3O_4-PEI-DGEBA in Taguchi L9 Planning.

Experiment	I.Y (%)	At. T (U/g)	At. D (U/g)	At. R (%)	S/N
1	86.87 ± 4.24	15.38 ± 0.75	6.69 ± 0.67	45.49 ± 5.47	38.777
2	87.81 ± 0.59	50.04 ± 0.33	11.047 ± 0.57	22.074 ±1.01	38.871
3	91.37 ± 1.36	97.25 ± 1.45	12.21 ± 1.29	12.55 ± 1.17	39.216
4	85.15 ± 1.2	50.95 ± 0.71	9.13 ± 1.11	17.92 ± 2.20	38.604
5	92.85 ± 0.55	73.56 ± 0.44	24.57 ± 2.69	33.35 ± 3.74	39.356
6	89.84 ± 0.35	30.44 ± 0.12	9.39 ± 0.30	30.86 ± 0.93	39.069
7	92.59 ± 2.95	88.31 ± 2.81	14.71 ± 3.69	16.59 ± 3.71	39.331
8	80.03 ± 3.43	20.33 ± 0.87	10.84 ± 0.44	53.42 ± 3.88	38.065
9	91.24 ± 1.52	35.98 ± 0.60	13.707 ± 0.37	38.11 ± 1.64	39.204

Note: EVS is measured in U/g and Fe_3O_4-PEI-DGEBA in g.
Source: the author.

Table 7 shows that experiments 3, 5, 7, and 9 obtained approximate values of I.Y, At. D and S/N. However, experiment 5 obtained the best results, with an immobilization yield of 92.85%, a derivative activity of 24.57 U/g, and a recovered activity of 33.35%. The immobilization conditions of experiment 5 were 15 h, ionic strength of 50 mM, protein load of 5 mg/g, and temperature of 25 °C.

Eversa® lipase Transform 2.0 (EVS) has already been immobilized on different support materials by applying varying processing parameters. Remonatto et al. (2022) immobilized EVS on four different hydrophobic supports, Lewatit-DVB, Purolite-DVB, Sepabeads-C18 and Purolite-C18 (Purolite C-18 and Sepabeads C-18 are methacrylic resins functionalized with octadecyl groups, Purolite-DVB and Lewatit DVB are methacrylic resins, non-functionalized divinylbenzene groups) and obtained immobilization yields of 55.5%, 65.1%, 86% and 98%, respectively, using 10% by weight of EVS in 24 h of reaction. Souza et al. (2022) achieved an immobilization yield of 74.2% by immobilizing Eversa® lipase Transform 2.0 (EVS) on hybrid support composed of chitosan (CHI) and agarose (AGA) activated with glutaraldehyde (GLU) under the optimized conditions of 1 h, 5 mM ionic strength, activated with 1% GLU and 5 mg protein load per g of support (Sousa et al., 2022).

Thus, it is possible to note that the immobilization results obtained in this research closely align with those published in the literature.

The literature also shows the effective use of several supports activated with epoxy groups for immobilizing other lipases. Mihailović et al. (2014) immobilized the CALB lipase with epoxy groups activating the Purolite® A109 resin (which is a polystyrene resin with primary amine functional groups) where it obtained immobilization yields of 85% for 2.25 mg/g of support in 10 µl of CALB solution and 95% to 22.5 mg/g of support in 100 µl of CALB solution. The work revealed that the lipase is bound in a more active conformation in the support modified with epoxy, indicating a better spatial arrangement of the lipase due to different groups. Therefore, various regions of enzymes participate in the fixation (Mihailović et al., 2014). The immobilization of enzymes through physical adsorption and covalent bonding with protein amine, thiol, or hydroxyl groups is made possible by activating supports with epoxy groups (Bilal, Rasheed, et al., 2018; Kujawa et al., 2021; Mateo et al., 2000; Rodrigues, Berenguer-Murcia et al., 2021).

The amount of free chains that activate the epoxy groups that allow for the support necessitates a more significant amount of protein to saturate the immobilization (Mateo et al., 2000; Rodrigues, Berenguer-Murcia et al., 2021). Protein concentration was the factor that most influenced EVS immobilization on Fe_3O_4-PEI-DGEBA support. Table 8 shows the ranking of each parameter (time, ionic strength, protein charge, and temperature) based on Delta values (difference in S/N ratio values between the highest and lowest levels of process factors).

Table 8 – Response from S/N ratios.

Level	Time (h)	Ionic strength (mM)	Protein load (mg/g)	Temperature (°C)
1	38.95478	38.90413	38.63728	39.11225
2	39.00957	38.76386	38.89276	39.09052
3	38.86668	39.16306	39.30100	38.62827
Delta	0.142890	0.39920	0.663720	0.48398
Ranking	4°	3°	1°	2°

Source: the author.

The signal-to-noise ratio (S/N) can identify the parameters most influencing an experimental design using the Taguchi method, as shown in Figure 18. In this work, the S/N was created using the greater-is-better ratio.

Figure 18 – Response from S/N ratios.

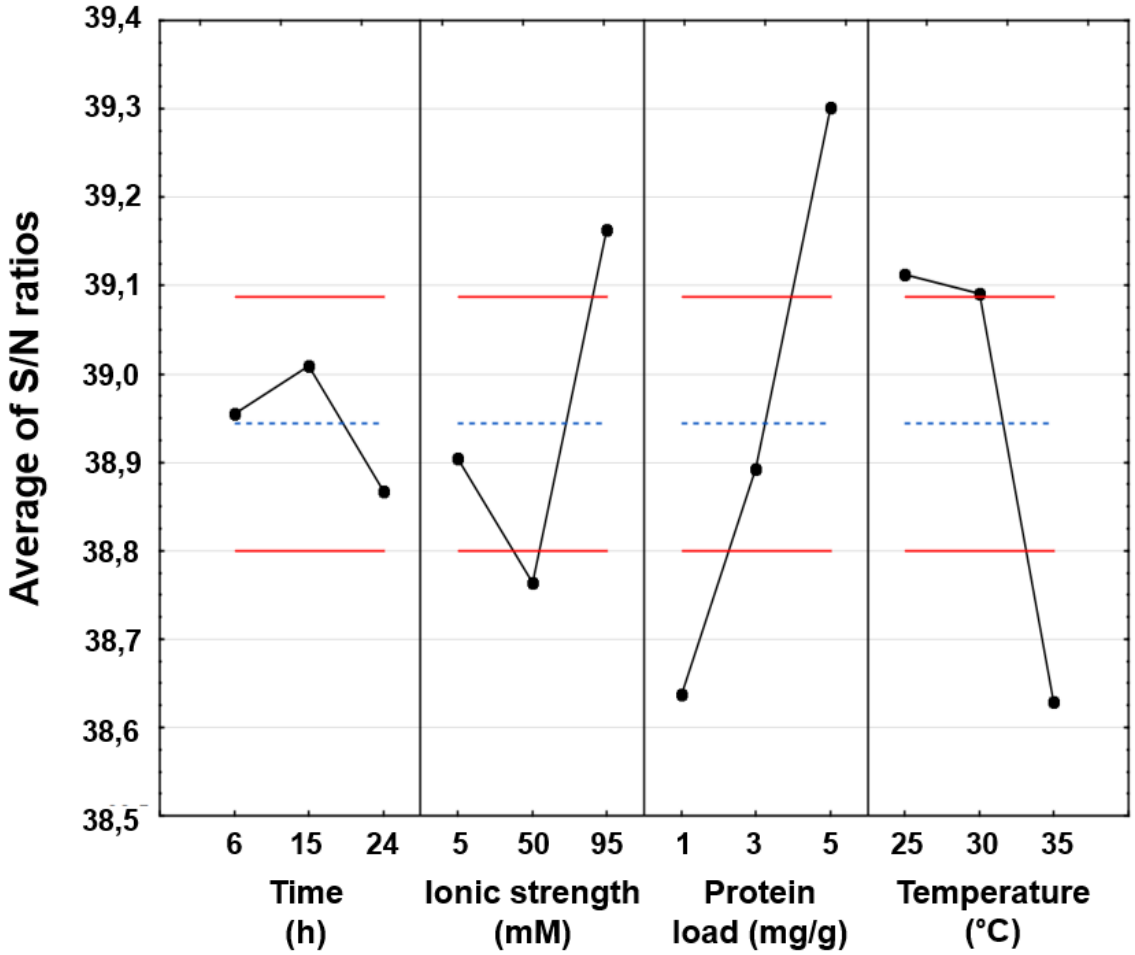

Source: the author.

It is worth noting that protein load had the most significant influence on the immobilization of the EVS on the support, with a considerable difference in the S/N values when the load of 1 mg/g reached 5 mg/g (S/N values came out from 38.65 to 39.3), which can be explained by the number of free reaction sites on the surface of the support that are capable of immobilizing the EVS by multipoint covalent (Liu et al., 2018; Mateo, Grazú, et al., 2007; Rodrigues, Carballares, et al., 2021). The synergistic effect of temperature and ionic charge further enhanced the biocatalytic activity of the formed biocatalyst.

Increasing temperature caused a reduction in S/N values. The free enzyme has distortion agents, such as high temperature and the presence of organic solvents or chaotropic agents (Proc et al., 2010), and multipoint covalent immobilization minimizes the effects of these factors. However, immobilization on supports functionalized with PEI and activated with epoxy groups occurs in two phases, first through physical adsorption and then through the formation of covalent bonds during the incubation period (Bezerra, Monteiro et al., 2020) Thus, we can

assume that a temperature rise reduced the enzyme's immobilization capacity in the initial moments of the process. In contrast, the increase in ionic charge enables a better enzymatic immobilization capacity to a specific extent in physical adsorption (Proc et al., 2010).

In the immobilization conditions of this research, the time we had the lowest significance compared to the others. Better outcomes for immobilization are observed when the duration is increased from 6 to 15 h, which can be attributed to the fact that 6 h is insufficient to allow for a complete first reaction. However, immobilization decreases when the time is increased to 24 h, which can be related to an enzymatic deactivation or leaching process (Han et al., 2021; Ismail & Baek, 2020a). Even with these differences, the S/N values for the time parameter did not have a significant difference, as shown in Figure 1.

The contact time for immobilization is a critical factor in some studies published in the literature using different supports and lipases (Barbosa et al., 2012; Bilal et al., 2021; Silva et al., 2022), where there is a significant difference between the immobilization results obtained with short and long contact times. Highly long periods may confer supersaturation on supports with fewer free reaction surfaces, resulting in mass transfer limitations that affect substrate dispersion and cause a decline in enzymatic activity. In contrast, the enzymatic contact process is limited at short times (Cavalcante et al., 2022; Sousa et al., 2022). Heterofunctional supports, such as the one produced in this research, have the characteristic of starting the immobilization process with rapid physical adsorption and, subsequently, generating covalent interactions with the enzyme (Bezerra, Monteiro et al., 2020; Zaak et al., 2018). Furthermore, supports activated with epoxy groups have the characteristic of having multiple free reaction groups, making it necessary to block after immobilization to prevent damage to enzymatic catalysis (Mateo, Grazu, et al., 2007; Mateo, Grazú, et al., 2007; Mihailović et al., 2014). As a result, it is possible to assume a small sign of the time parameter compared to the other parameters studied in the production of this biocatalyst.

The analysis of variance (ANOVA) in Table 9 shows the statistical significance of each parameter studied in the planning, p-value attests to the impact of each factor for the proposed model, for an importance with a 95% confidence interval p-value must be less than 0.05 (Cavalcante et al., 2022; Sousa et al., 2022).

Table 9 – ANOVA results for parameters that affect immobilization.

Factor	SS	DF	MS	*F-value*	*p-value*	Contribution (%)
Time	-	-	-	-	-	-
Ionic strength	0.246082	2	0.123041	7.89156	0.112466	17.60
Protein load	0.672444	2	0.336222	21.56454	0.044317	48.10
Temperature	0.448372	2	0.224186	14.37879	0.065025	32.07
Residual	0.031183	2	0.015591	-	-	2.23
Total	1.3981	6			0	100

Source: the author.

The protein load had the highest statistical significance, with a 48.10% contribution to the total immobilization result of the four parameters studied. Temperature and ionic strength acted in association with improving immobilization results, obtaining 32.07% and 17.60%, respectively. The synergism between each parameter is of extreme statistical importance to understand the degree of influence of the factors in the joint conditions on the recovered activity (Cavalcante et al., 2022; Sousa et al., 2022). Taguchi planning uses the system of orthogonal matrices that allows for predicting the response of the immobilization yield in the intersection of the parameters used.

Figure 19 shows the response surface of the interaction between protein charge and temperature, parameters that most influenced immobilization. It is possible to observe that the 5 mg/g protein load obtains the best results optimized in the temperature ranges between 25 and 30 °C.

The ionic strength shows that there can still be better immobilization results using the 95 mM values corresponding to design level 3 (Figure 18). Fernandez-Arrojo et al. (2015) showed that the ionic strength is considerably active in the physical protocols of enzymatic immobilization, with considerable changes in the optimization of the experiments.

Time acted as an intermediate parameter in the planning of this research, with level 2 being the most suitable for immobilization, where there is no limited time to start the process but also does not exceed the time of loss of enzyme activity.

Figure 19 – Contour surfaces display the interaction effects between the evaluated factors as a function of immobilization yield (I.Y).

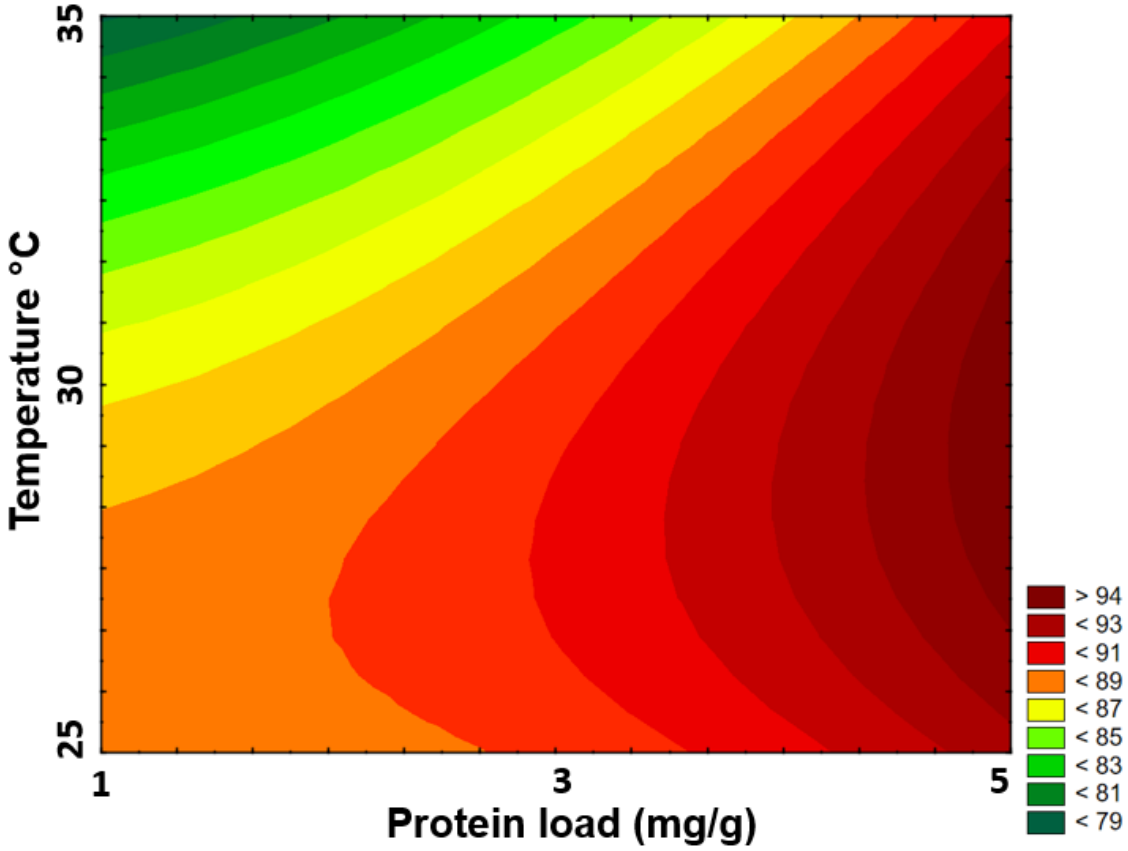

Source: the author.

Table 11 shows the optimized conditions for immobilization of the EVS by the Fe_3O_4-PEI-DGEBA support, which was not tested a priori but verified after the Taguchi planning results.

Table 10 – Optimal conditions for EVS immobilization by Fe_3O_4-PEI-DGEBA.

Factor	Time (h)	Ionic strength (mM)	Protein load (mg/g)	Temperature (°C)
Level	2	3	3	1
Level values	15	95	5	25

Source: the author.

The optimal conditions presented by the Taguchi method showed better immobilization results, with percentage immobilization (I.Y) of 95.04 ± 0.79, theoretical activity in U/g (At. T) of 86.84 ± 8.85, derivative activity in U/g (At. D) of 29.73 ± 0.44 and recovered activity in % (At. R) of 34.48 ± 3.66. Thus, this Fe_3O_4-PEI-DGEBA@EVS biocatalyst was used to obtain the maximum loading capacity, the immobilization course,

thermal stability, pH stability, and storage capacity, and characterized at structural and magnetic levels. Furthermore, this biocatalyst was used to obtain biolubricants from babassu oil.

3.3.3 Analysis of the immobilization parameters of the biocatalyst Fe_3O_4-PEI-DGEBA@EVS

The essential parameters to understand the efficiency of the enzymatic immobilization protocol and the impacts of the enzyme's catalytic activity, as well as the efficiency of the method and the viability of the immobilization, are shown in Figure 20 where all the graphs related to the biocatalyst Fe_3O_4-PEI-DGEBA@EVS are shown.

Figure 20 – Enzyme immobilization parameters. a) Maximum enzyme load capacity (Maximum load test of Fe_3O_4-PEI-DGEBA@EVS in time 12 h, ionic load 95 mM, temperature 25 °C and protein load 1:1 - 1:50 mg/g); b) Storage capacity (Effect of storage time on the activity of the Fe_3O_4-PEI-DGEBA@EVS biocatalyst over 12 h, ionic load 95 mM, temperature 25 °C and protein load 1:5 mg/g); c) Thermal stability (at different temperatures 25 °C - 80 °C) of the soluble and immobilized EVS enzyme under optimal conditions; d) pH stability (at different pH 4 - 9) of soluble and immobilized EVS enzyme under optimal conditions.

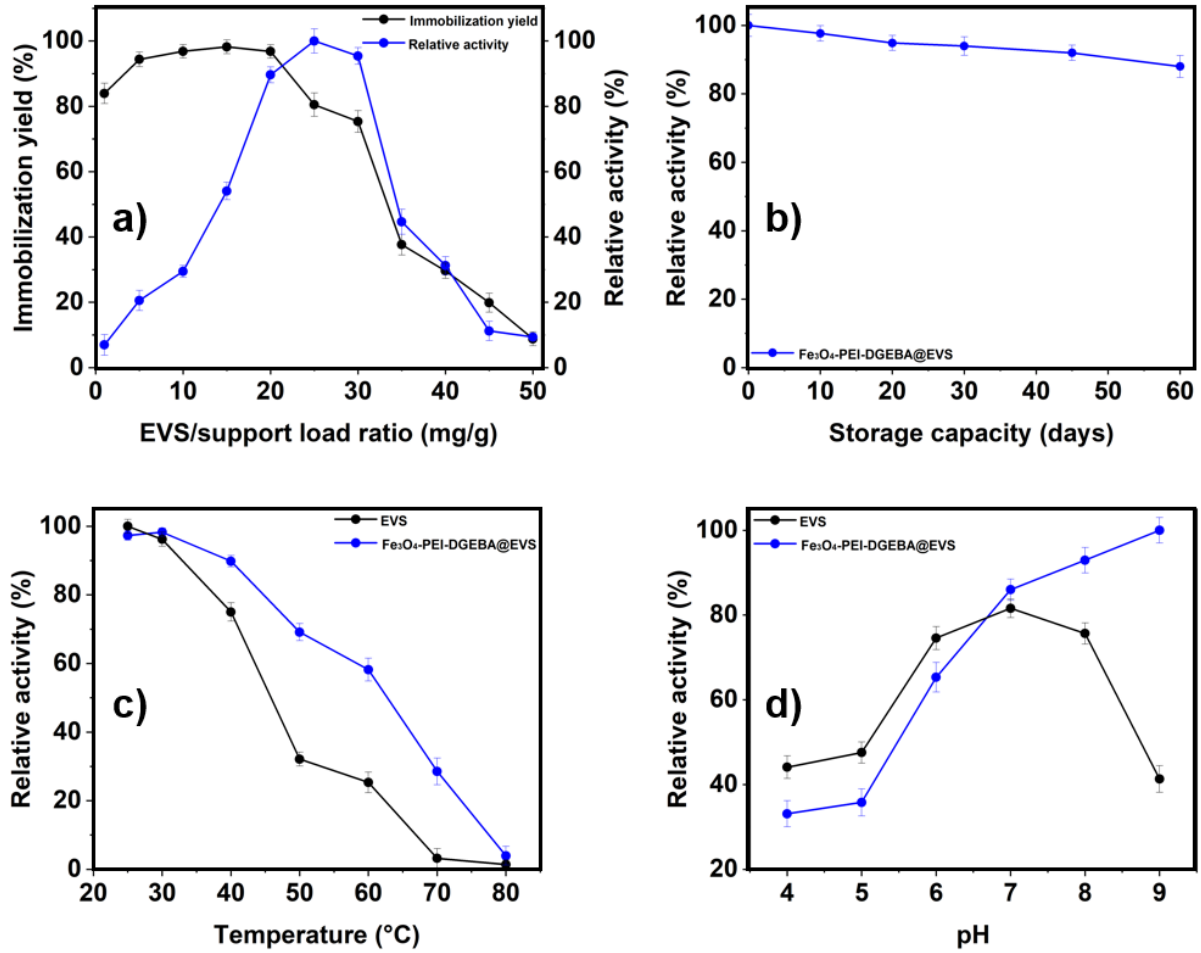

Source: the author.

3.3.4 Maximum enzyme loading capacity

Figure 20 - a) shows the maximum load capacity of the EVS that can efficiently interact with the Fe_3O_4-PEI-DGEBA@EVS support. Analyzing these parameters allows an adequate interpretation and precise assimilation of the maximum capacity of support by the biocatalyst. In this way, it is possible to verify the adhesion of the enzyme to the support, as well as whether all enzymes stabilized on the support remain active or suffer some inactivation caused by structural, conformational modification or formation of enzymatic multilayers, causing the biocatalyst to be partially inactivated by spherical blocking (Arana-Peña et al., 2021; Fernandez-Lopez, Pedrero et al., 2017). The immobilization yield from the optimal point up to 20 mg/g of the enzyme on the support maintained a yield above 98%. From that point on, the yield began to decrease a percentage decrease. The activity of the derivative had its maximum point at 25 mg/g, showing that the support can immobilize 20 mg/g of enzyme more than the optimal point shown (5 mg/g), before obtaining surface saturation and beginning to have its activity diminished. Too much enzyme in the solution can cause interactions between enzymatic molecules, forming conglomerates that inhibit the elastic elongation of the enzymatic conformation, resulting in spherical deficiency and inactivation (Fernandez-Lopez, Pedrero et al., 2017; Okura et al., 2020; Siar et al., 2018).

Superficial saturation of the support by the enzyme also compromises operational, thermal, and pH stability due to possible enzymatic inactivation and leaching (Anwar et al., 2017). The knowledge of the maximum load capacity of Eversa® lipase Transform 2.0 by the Fe_3O_4-PEI-DGEBA support allows us to determine the ideal amount without incurring unnecessary costs. Sousa et al. (2022) immobilized the EVS on support based on chitosan (CHI) and agarose (AGA) activated with glutaraldehyde (GLU). They found that the biocatalyst activity was nearly saturated at 23 mg/g and that the immobilization yield started to drop at about 7 mg/g.

3.3.5 Storage stability

Figure 20 - b) shows the storage stability of the produced biocatalyst over 60 days at 4 °C. The storage capacity of the immobilized enzyme is of considerable importance in the production of biocatalysts (Awad et al., 2020). In general, the enzyme in its soluble form is not stable during storage, gradually reducing its activity over time. The reduction in free lipase activity is associated with its autolysis during storage time or as a time-dependent natural loss

(Aghaei et al., 2021a). After 60 days, the relative activity of this biocatalyst was 90.46%. Heterofunctional immobilization of the scaffold created a favourable activity rate, reducing the influence of autolysis and possibly stabilizing the active free form of lipase. Aghaei et al. (Aghaei et al., 2021a) immobilized Candida rugosa lipase on an epoxy-activated cloisite (ECL) backing and achieved 30-day storage stability of 87.3%.

3.3.6 Thermal stability

Figure 20 - c) analyzes the thermal deactivation of soluble and immobilized EVS against temperature variations. Immobilized enzymes generally have more thermal resistance than the free form, which is related to the restriction of enzyme mobility and increased rigidity (Eslamipour & Hejazi, 2016; Nwagu et al., 2021). In this study, the soluble and immobilized enzymes showed their highest activities at 25 °C and 30 °C, respectively. The soluble enzyme showed a sharp drop in its activity at temperatures above 40 °C, a result that can be observed in studies using EVS (Feedstocks et al., 2021; Remonatto et al., 2022; Remonatto, Oliveira et al., 2022; Sousa et al., 2022). It can be observed that the support of this work contributed to the increase in the thermal stability of the EVS, with better immobilization activities at temperatures above 40 °C, when compared to the soluble enzyme. At 60 °C, the biocatalyst also showed a sharp drop-in activity. However, the biocatalyst still presented a relative activity of approximately 28.55% at 70 °C, while the soluble enzyme no longer showed any significant activity. These results reveal the crucial role of immobilization in protecting enzymatic activity (Mohd Hussin et al., 2020).

3.3.7 Stability in pH

Figure 20 - d) analyzes the effect of pH on enzyme performance over a range of values from 4 to 9. The surface charges of the transporter influence the pH of enzyme activity. The optimal pH is related to hydrogen bonds or ionic interactions between the support and the lipase. Positively charged supports changing the optimal pH to a lower pH, while negatively charged supports carry out the opposite process. In this way, the anions and the cations placed on the supports attract or repel protons from the medium and modify the proton density in the solution around the immobilized enzyme (Binhayeeding et al., 2020; Işik et al., 2019; Poonsin et al., 2020). This work detected the maximum hydrolytic activity for free lipase and biocatalyst at pH 7 and 9, respectively. The immobilization procedure contributed to the increase of

enzymatic activity at alkaline pHs. Reports have shown that the lipases immobilized on organic, inorganic, or hybrid supports are prone to increased activity at pHs between 7.0 and 10 (Ding et al., 2019; Villeneuve et al., 2000). This variation can be explained by several factors associated with immobilization. Changes in enzymatic conformation, improved thermal stability, specific interactions between the enzyme and the support, and the microenvironment created by the support can alter the optimal pH values (Ren et al., 2011; Shuai et al., 2017).

The stability of immobilized enzymes at different pHs may be related to the interaction between the support and the enzyme that stabilizes the active site's structure and reduces the enzyme's mobility after immobilization. The pH stability of the biocatalyst in this research can be conferred by the improved rigidity of the enzyme conformation due to the heterofunctional bonds of the support (Mateo, Grazu et al., 2007; Nezhad & Aghaei, 2021; Zaak et al., 2018).

3.3.7 Materials characterization

The scanning micrographs of the Fe_3O_4, Fe_3O_4-PEI, Fe_3O_4-PEI-DGEBA, and Fe_3O_4-PEI-DGEBA@EVS samples, in addition to the XRF maps (inserts), are presented in Figure 21 - a), b), c), and d). The morphology of the support is shown. A difference in the rugosity of the materials indicates a slight change in the composition of the material. The XRF spectra show slight variations in the elemental compositions, indicating small decreases in Fe atoms and the appearance and increase of other materials such as Cl, S, P. Corroborating the notion that the support is being strengthened with additional materials. All images showed a laminar surface morphology. SEM and XRF served as complementary analyses to determine whether the EVS was immobilized on the surface of the support, thus forming the Fe_3O_4-PEI-DGEBA@EVS biocatalyst.

Figure 21 – SEM micrographs / XRF maps and elemental spectra a) Fe_3O_4; b) Fe_3O_4-PEI; c) Fe_3O_4-PEI-DGEBA, and d) Fe_3O_4-PEI-DGEBA@EVS.

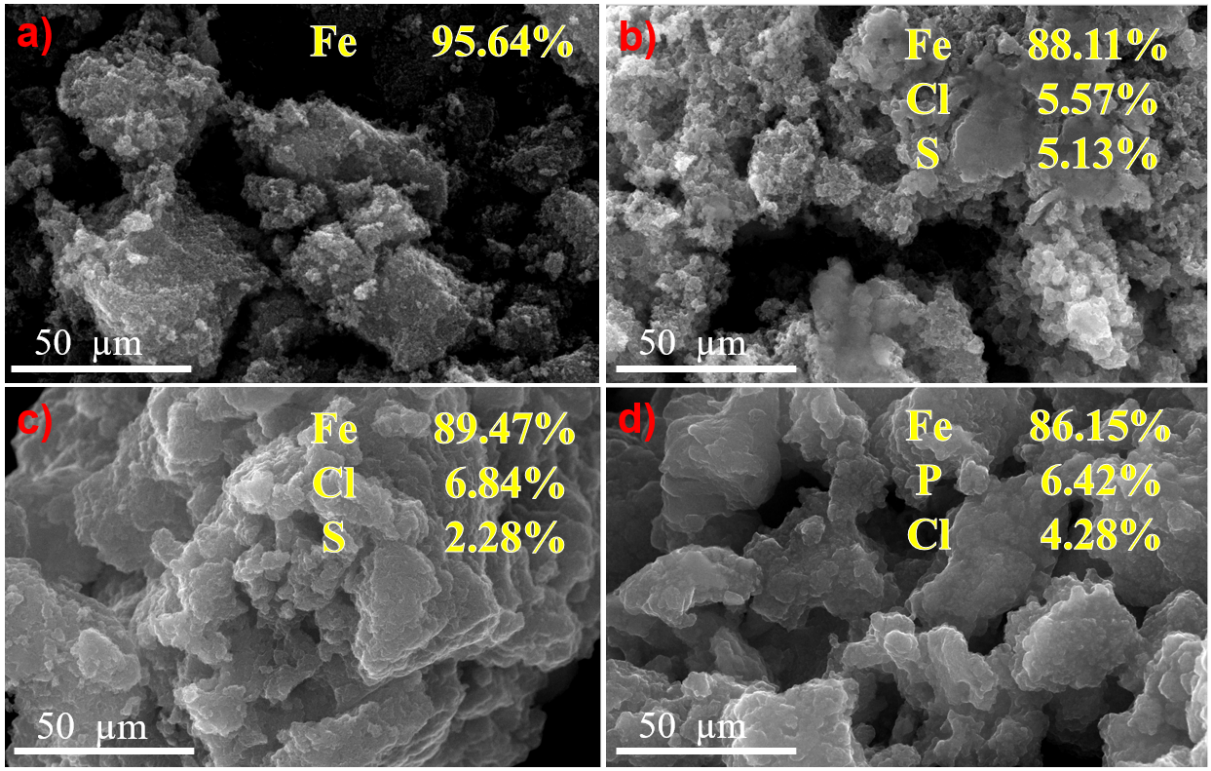

Source: the author.

The transmission micrographs of the Fe_3O_4, Fe_3O_4-PEI, Fe_3O_4-PEI-DGEBA, and Fe_3O_4-PEI-DGEBA@EVS samples and their respective particle size distribution curves (inserts) are shown in Figure 22 - a), b), c) and d). TEM shows that the samples have a spherical morphology, which is normal when Fe_3O_4 is prepared by sonicating Fe^{2+} and Fe^{3+} ions with ammonium hydroxide (Neto et al., 2017, 2021). The size distribution curves had the results of 10.27 ± 2.35, 12.80 ± 2.02, 13.15 ± 2.35 and 12.44 ± 2.16 nm for Fe_3O_4, Fe_3O_4-PEI, Fe_3O_4-PEI-DGEBA and Fe_3O_4-PEI-DGEBA@EVS, respectively. We can consider the average diameters as statistically similar even though there is a little rise in particle size, a finding consistent with the increase in materials. No irregular morphology was observed.

Figure 22 – TEM micrographs/particle size distribution curves a) Fe_3O_4; b) Fe_3O_4-PEI; c) Fe_3O_4-PEI-DGEBA and d) Fe_3O_4-PEI-DGEBA@EVS.

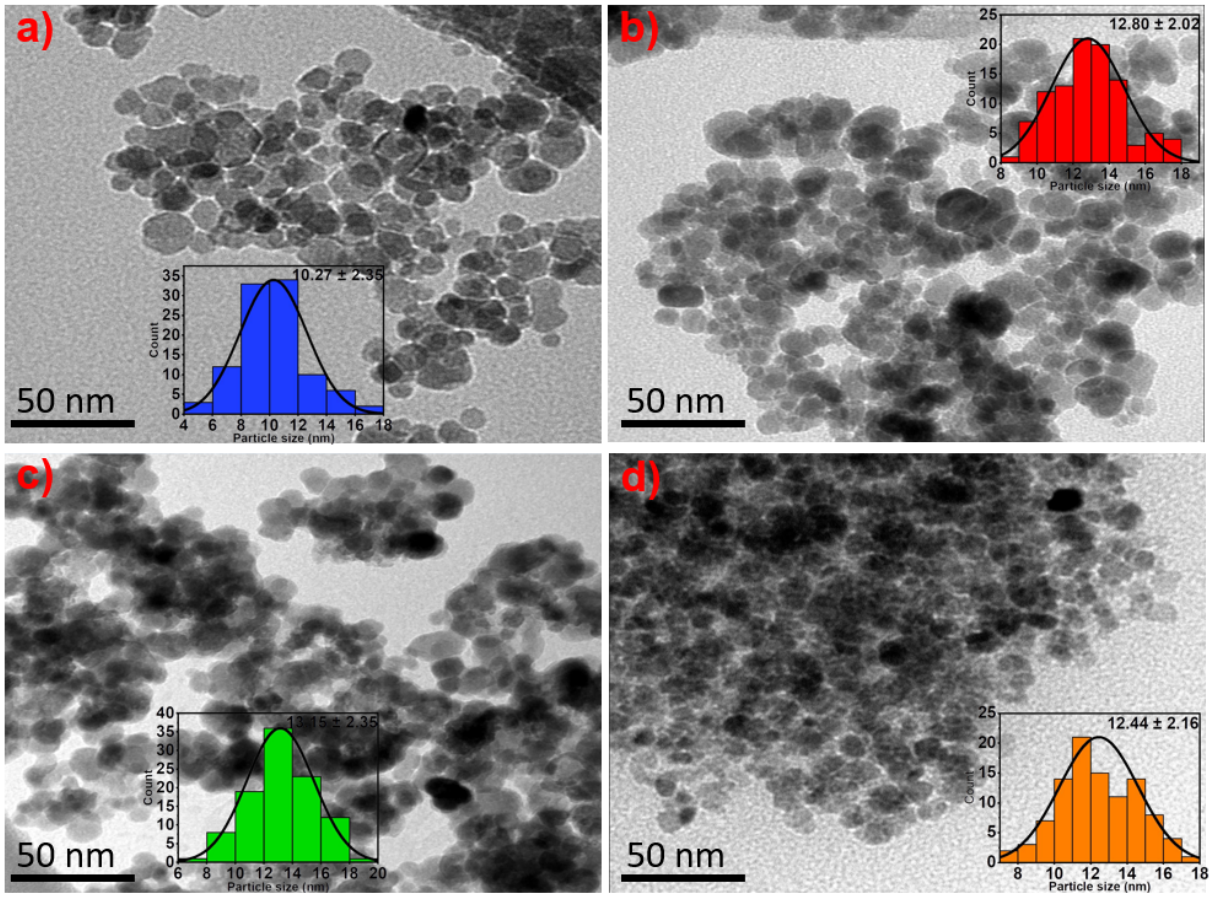

Source: the author.

X-ray diffraction (XRD), Fourier transform infrared spectra (FTIR), thermogravimetric analyses and their respective differential curves (TGA and DTG) and magnetization curves (VSM) are shown in Figure 23 - a), b), c), d) and e).

Figure 23 - a) shows the diffraction profile obtained. A Rietveld analysis using the Maud® program was performed to acquire deeper information about the crystalline structure of the samples phase composition. The blue, red, green, and yellow dots show the experimental data for Fe_3O_4, Fe_3O_4-PEI, Fe_3O_4-PEI-DGEBA, and Fe_3O_4-PEI-DGEBA@EVS. The black line indicates the calculated data. Analysis of the position and intensity of XRD reflections showed that the crystalline structure in all samples can be assigned to inverse cubic spinel Fd3m (ICSD code: 84611), characteristic of Fe_3O_4 (Iyengar et al., 2014). However, it is known that as Fe3O4 decreases below 20 nm, its average particle size and oxidation rate increase, and the γ-Fe_2O_3 maghemite phase can also act (Baaziz et al., 2014; Daou et al., 2006; Santoyo Salazar et al., 2011). However, we believe that PEI functionalization slowed the Fe_3O_4 oxidation rate since high magnetization values were obtained for this sample. PEI is a functionalizing agent for

enzyme immobilization and an agent that supports maintaining a degree of magnetization suitable for reuse in its enzymatic catalysis (Bezerra, Monteiro et al., 2020).

Narrow and well-defined peaks showed high crystallinity in all samples. All diffractograms do not show changes or peak shifts, suggesting that functionalization with PEI, activation with DGEBA, and immobilization with EVS do not change the crystallinity of Fe_3O_4, thus being an interaction on the surface of the nanoparticle (Sousa et al., 2022).

Figure 23 - b) shows infrared spectra with Fourier transform. All spectra showed a band in the range of 600 cm^{-1}, characteristic of Fe-O bond vibrations in the γ-Fe_2O_3 and Fe_3O_4 phases, indicating that the synthesized materials consist of partially oxidized Fe3O4. (Yang et al., 2010; Zhang et al., 2019). In this band, it was possible to verify that the magnetite remained after functionalization with PEI, activation with DGEBA and immobilization of the EVS. The bands around 1600 cm^{-1} and 3500 cm^{-1} also remained. They are related to the presence of hydroxyl groups and are attributed to OH flexion and elongation (Roca et al., 2007; Sharifi Dehsari et al., 2018). The functionalization of Fe_3O_4 with PEI can be observed in the appearance of more bands between 800 cm^{-1} and 1600 cm^{-1}, which can be attributed to C-N stretching vibration, C-H bending vibration and N-H bond bending vibration (Khoobi, Motevalizadeh et al., 2015; Liu et al., 2018; Neto et al., 2017; Silva et al., 2023). After activation of Fe_3O_4-PEI with DGEBA, the FTIR spectra will show a clear distinction with the appearance of other small bands that may be related to vibrations of the epoxy groups (Aghaei et al., 2021; X. Jiang et al., 2016; Sciancalepore et al., 2015; Tripathi et al., 2017). The immobilization of the EVS on the Fe3O4-PEI-DGEBA support can be linked to a distinction in the FTIR bands that can be observed once again in the range of 800 cm^{-1} and 1600 cm^{-1}, suggesting the existence of electrostatic interactions and hydrogen bonds, as well as covalent interactions both with the amine groups of PEI and with the epoxy groups of DGEBA, characterizing a heterofunctional immobilization, which appears as a very stable immobilization for the activity of lipases (Barbosa et al., 2012; Rios et al., 2016; Rodrigues, Carballares et al., 2021).

The thermogravimetric analysis and their respective differential curves are shown in Figure 23 - c) and d), respectively. The Fe_3O_4 sample showed an initial mass loss event of 3% around 80 °C, related to water weakly adsorbed on the surface (humidity) and a volatile composition in the sample. After this event, Fe_3O_4 continues in a continuous mass loss process, stabilizing at a loss of approximately 12.5% around 500 °C. The Fe_3O_4-PEI and Fe_3O_4-PEI-DGEBA samples exhibit two distinct mass loss events, initially around 80 °C like the Fe_3O_4 sample, but with a more pronounced loss of 6% and 4%, respectively. Subsequently, a more pronounced loss at 450 °C stabilizes with 22% and 25% losses, respectively. The Fe_3O_4-PEI-

DGEBA@EVS sample presented the highest percentage of loss, presenting again an initial event with a loss of approximately 7%, an event close to 200 °C, with a loss of 5% and being continuous up to approximately 700 °C where it stabilizes with a mass loss accumulation of 45%. The more pronounced mass losses in the Fe_3O_4-PEI samples may be related to the amine groups that can form hydrogen bonds with water, and in the Fe_3O_4-PEI-DGEBA samples an indication of the reaction of epoxy groups with the amines, decreasing the number of adsorption sites for water (Bezerra, Monteiro et al., 2020; Khoobi, Motevalizadeh et al., 2015; Mateo et al., 2000; Mihailović et al., 2014). The most significant loss in Fe_3O_4-PEI-DGEBA@EVS may be related to the more substantial amount of organic materials, which is revealed as further evidence of EVS immobilization by the support produced in this research (Liu et al., 2018; Mateo, Grazú et al., 2007; Monteiro et al., 2022; Silva et al., 2023; Xu et al., 2021).

Figure 23 - e) shows the magnetization curves. A very low coercivity was presented, highlighting the superparamagnetic nature (Damasceno et al., 2020; Khoobi, Motevalizadeh et al., 2015). The magnetization saturation (Ms) for Fe_3O_4 obtained a 73.26 emu/g. This value is lower than values already exposed in the literature of 92 emu/g for crude Fe_3O_4 (Khoobi, Motevalizadeh et al., 2015). The presence of surface spin disturbances can explain this fact. As the nanoparticle size decreases and the number of oxidized materials increases, the maghemite phase γ-Fe_2O_3, increases the amount of oxidized material, as reported in the analyses XRD and FTIR (Neto et al., 2017), decreasing the magnetic potential of Fe_3O_4. The Fe_3O_4-PEI, Fe_3O_4-PEI-DGEBA, and Fe_3O_4-PEI-DGEBA@EVS samples showed magnetizations of 57.35, 46.75, and 44.15 emu/g, respectively. These results support the idea that the surface of Fe_3O_4 contains non-magnetic elements. In this respect, with the Fe_3O_4-PEI-DGEBA@EVS sample having the lowest magnetization values, we can assume that the EVS immobilization was successful on the heterofunctional support.

Figure 23 – a) XRD; b) FTIR; c) TGA; d) DTG and e) VSM.

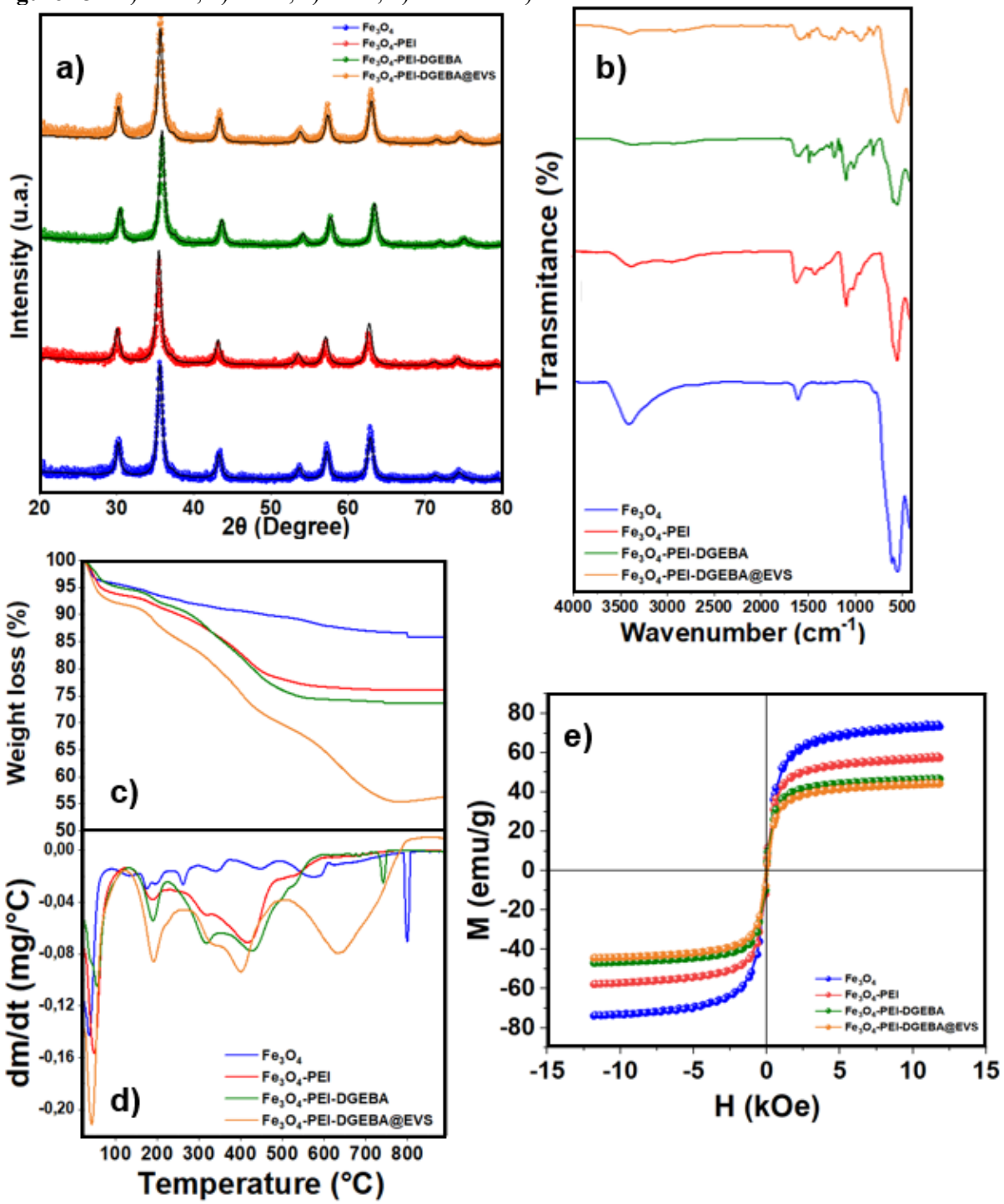

Source: the author.

3.3.8 Production of biolubricants and operational stability from Babassu oil

Figure 24 shows the reuse cycles of the Fe_3O_4-PEI-DGEBA@EVS biocatalyst for the esterification of babassu oil-free fatty acids. Productivity is one of the most critical concerns for the commercial production of biocatalysis using immobilized lipases, with reuse serving as

a means of compensating the higher cost of enzymes than chemical catalysts. Enzymes that can produce good results with the most re-uses can lower the cost of producing biolubricants (Atiroglu, 2020; Babaki, Yousefi et al., 2015). It was possible to carry out ten cycles with the biocatalyst of this work without the esterification yield dropping below 50%. A reduction in yield was observed after each cycle due to lipase deactivation. This deactivation may be due to repeated treatment of the biocatalyst (shaking, washing, and recycling) and contact with hexane, which can alter the lipase conformation (Aguieiras et al., 2016). This work's biocatalyst obtained 97.91% of the yield in its first esterification cycle. After three cycles, the yield was 74.86% and reduced to 58.79% after seven cycles. After the tenth cycle, the yield obtained was 52.86%. Xie and Huang (Xie & Huang, 2018) immobilized *Candida rugosa* biocatalyst on magnetic graphene oxide (activated with carboxylic, hydroxyl, and epoxy groups). They used it to produce biodiesel from commercial soybean oil, obtaining a yield of 92.8% and the ability to perform five cycles above 75% yield. Chang et al (Chang et al., 2021) used free Eversa® lipase Transform 2.0 to produce biodiesel from cooking oil and obtained a 96.7% yield in the highest conversion.

Figure 24 – Operational stability. Reaction medium: 5% of the biocatalyst Fe_3O_4-PEI-DGEBA@EVS, free fatty acids from babassu oil and octyl alcohol (1:5). The reactions were carried out for 5 hours at 40 °C and 200 rpm.

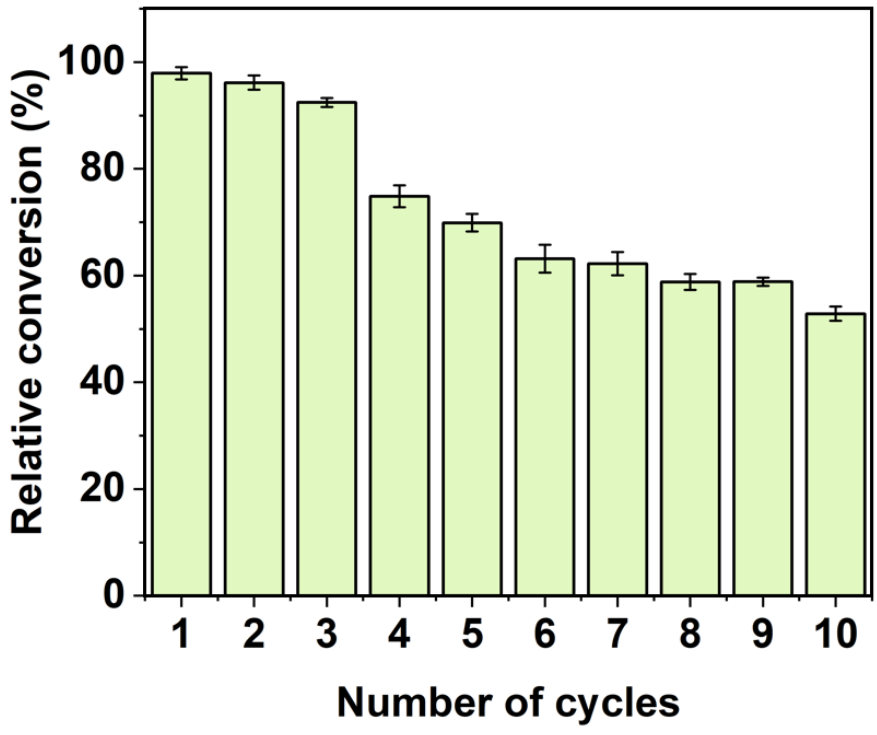

Source: the author.

3.3.9 Nuclear Magnetic Resonance Spectroscopy (NMR)

Figure 25 shows the results of nuclear magnetic spectroscopy. Figure 25 - a) shows Babassu's Free Fatty Acid (FFA) spectrum, which contains the following fatty acids: lauric, myristic, palmitic, oleic, caprylic, capricious, linoleic, and stearic. In the signal at δ 0.88 ppm, we identified a multiplet (m), related to terminal methyl hydrogens. In the δ 1.26 ppm signal, a very intense peak was identified associated with the resonance frequency range of the other methylene groups. At δ 1.52 ppm, we identified a multiplet (m) related to methylene hydrogens in the β-carbonyl position. At δ 2.42 ppm, we identified a multiplet (m) related to methylenes α hydrogens-carbonyl. The δ signals 4.17 ppm and 4.28 ppm identify multiplets (m) associated with allylic hydrogens (Fernandes et al., 2021; Lopes et al., 2017; H. Rodrigues et al., 2023).

In Figure 25 - b), the ^{1}H NMR spectrum shows characteristic signs of biocatalytic esterification of babassu FFA. At δ 0.9 ppm we identified a triplet (t) that refers to terminal methyl hydrogens. The signals close to δ 1.26 and 1.36 ppm are multiplets (m) related to the remaining methylene hydrogens of the carbon chain, as they have very close resonance frequencies, where the peaks can overlap in this chemical shift region. At δ 1.62 and 1.73 ppm, we have singlets (s) and at δ 2.31 ppm we have a triplet (t), all related to the methylene hydrogens located in the α and β -carbonyl positions of the ester, highlighting that there was alcohol conversion. The δ 3.56 ppm signal is associated with the singlet (s) of the methylene hydrogens linked to hydroxyl, referring to the substrate in the reaction medium, octyl alcohol. At δ 3.98 ppm we have a triplet (t) associated with the methylene hydrogens directly linked to the oxygen of the ester, suggesting that there was enzymatic esterification of the alcohol (Bezerra et al., 2020; Caroline et al., 2014; Kamalakar et al., 2013; Nery et al., 2019; Sousa et al., 2022).

Figure 25 – a) Characterization of the FFA. ^{1}H NMR (500 MHz, $CDCl_3$). b) Characterization of the ^{1}H NMR biolubricant (500 MHz, $CDCl_3$) where R is related to the chemical composition of the residual babassu oil (Fatty acids: lauric, myristic, palmitic, oleic, caprylic, capric, linoleic, stearic).

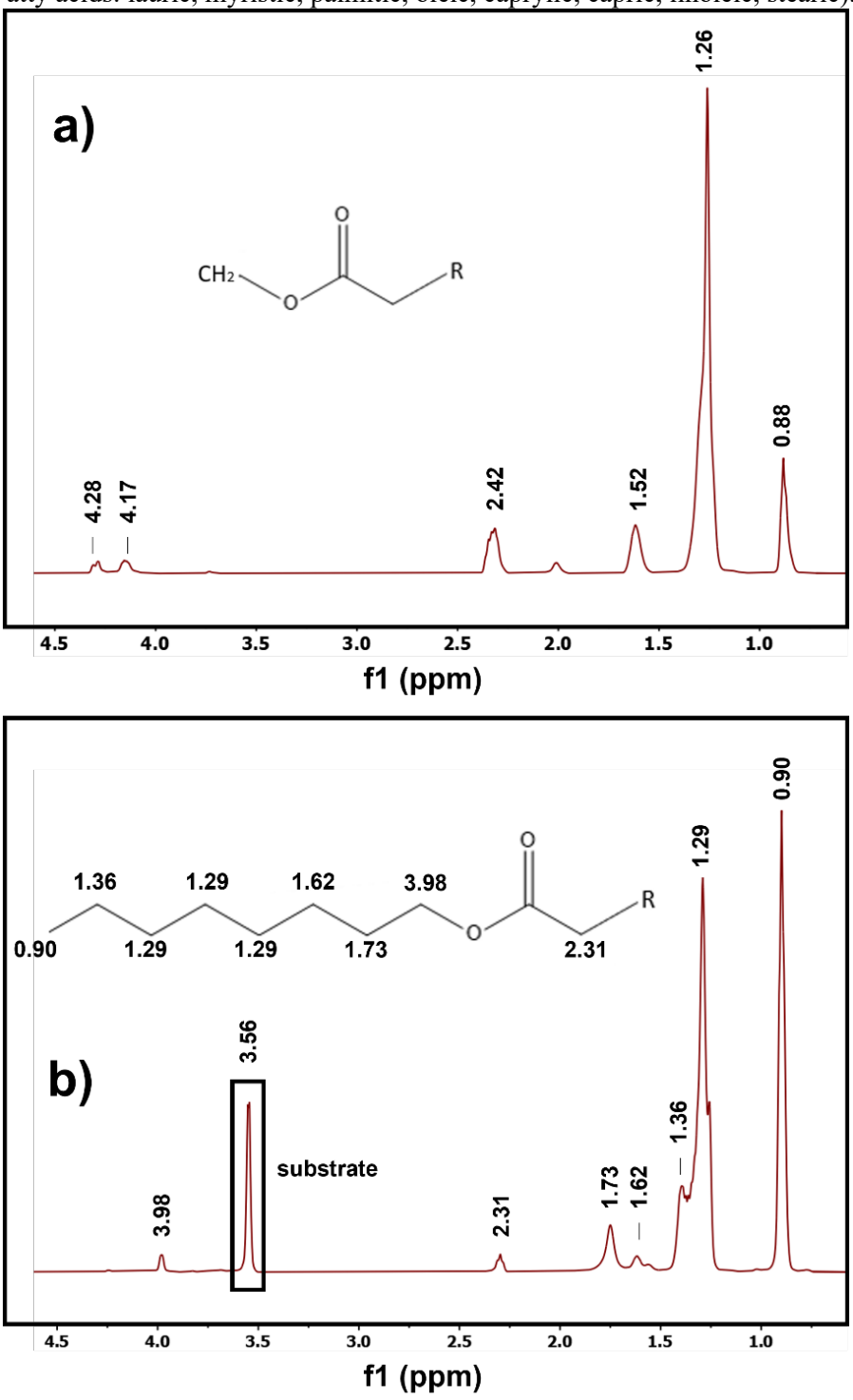

Source: the author.

3.3.10 Biolubricant viscosity and density

Table 11 presents the attractive viscosity and density evaluation for using babassu esters as a biolubricant. The kinematic viscosity showed 12.736, 6.0520, and 1.3879 mm²/s at 20, 40, and 100 °C, respectively, following reports on babassu esters and conforming to ASTM D 341. At 40 °C, the biolubricant falls into the ISO VG (Viscosity Grade) 7 category. ISO VG 7 oils are generally considered low-viscosity oils, and their application is more directed towards low-load and low-speed systems (Bezerra et al., 2020; Coelho et al., 2022).

The kinematic viscosity values of babassu oil were not suitable for calculating the Viscosity Index (VI) according to ASTM D2270 and ISO 2909, as these standards are defined only for petroleum products with kinematic viscosity more significant than 2 mm²/s at 100 °C (Brêda et al., 2022; Kurre & Yadav, 2023; Noguchi et al., 2023). There is no universally accepted specific standard for calculating the VI of vegetable oils (Sousa et al., 2023; Kurre & Yadav, 2023). When dealing with particular vegetable oils, it is advisable to check for specific standards or test methods for this type of material. Depending on the application or industry, particular standards or procedures may define methods for measuring viscosity and calculating the VI of vegetable oils (Brêda et al., 2022; Sousa et al., 2023; Kurre & Yadav, 2023; Noguchi et al., 2023). In this sense, when dealing with vegetable oil, which does not have kinematic viscosity greater than 2 mm²/s at 100 °C, it is advisable to compare dynamic viscosity, kinematic viscosity, density, and acidity index data with other biolubricants already studied in the literature.

The density of babassu oil showed values of 0.8472, 0.8328, and 0.7864 g/cm^3 at 20, 40, and 100 °C, respectively, low values consistent with those required for lubrication in low-load and low-speed systems (Franco, 2020; Owuna, 2020). The acidity index is another essential physicochemical measure to be presented in a biolubricant. For the biolubricant in question, an acidity index of 0.14 mg KOH/g was obtained, according to data obtained in the literature and with the Brazilian legislation ANP, 1999 (Bezerra et al., 2020).

Comparing the kinematic viscosity at 40 and 100 °C with other vegetable oils studied as biolubricants obtained by enzymatic esterification, palm oil esters showed values of 4.7 ± 0.3 and 1.8 ± 0.1 mm²/s, respectively (Abd Wafti et al., 2022b). In this study, enzymes were used to synthesise trimethylolpropane ester (TMP), a component of biolubricants, from high-oleic palm oil methyl ester (HO-PME). The enzyme used was lipase 435, an immobilized form of *Candida antarctica* B lipase (CALB) (Abd Wafti et al., 2022). In contrast, soybean oil esters showed kinematic viscosity at 40 and 100 °C of 8.9 and 2.9 mm²/s, respectively (Sabi et al.,

2022). In this study, the oil esterification occurred using a biocatalyst based on Octyl-SiO_2 immobilizing Candida rugosa (Sabi et al., 2022). Under certain conditions, the produced biolubricant aligns with other biolubricants mentioned in the literature.

Table 11 – Biolubricant properties.

Properties	Temperature (°C)		
	20	40	100
η (mPa.s)	10.790	5.0398	1.0915
ν (mm^2/s)	12.736	6.0520	1.3879
ρ (g/cm^3)	0.8472	0.8328	0.7864

Note: η = Dynamic viscosity; ν = Kinematic viscosity; ρ = Density.
Source: the author.

3.3.9 Molecular docking

Molecular coupling studies were conducted to support the theories used to explain the results observed for lipase. In order to forecast its affinity, orientation, and surrounding surfaces for immobilization purposes, it was structurally analyzed by molecular modelling by a study of lipase coupling EVS (modelled) using the software AutoDock Vina and DS. According to the literature, the van der Waals forces and hydrogen bonds were favourable with the binding affinities predicted by molecular coupling studies (Chaturvedi et al., 2015).

The catalytic site of the EVS, a triad represented by Ser 153, His 268, and Asp 206, with serine residue acting as a nucleophile, is located inside the substrate pouch. Only substrates of appropriate molecular forms can occupy these subsites to undergo catalysis. The strict substrate conformation requirements for active EVS sites and substrate binding sites offer the possibility of finding specific binding sites in the inactive regions of the enzyme surface to guide the direction of immobilization.

The binding affinity for the anchored composition oil with the enzyme was estimated to be between -4.6 kcal/mol and -6.0 kcal/mol, as shown in Table 12. The lower binding energy suggests that the combination of substrate and lipase was more stable and suitable for esterification. The simulation results are displayed in 2D in Figure 26.

Table 12 – Oil composition and molecular docking results.

Compounds	PubChem number	Energy (kcal/mol)	RMSD (Å)
Capric acid	CID 2969	-4.9	2.1
Caproic acid	CID 8892	-4.6	2.0
Caprylic acid	CID 379	-4.6	1.7
Lauric acid	CID 3893	-4.9	0.9
Linoleic acid	CID 5280450	-6.0	1.9
Myristic acid	CID 11005	-5.7	1.9
Oleic acid	CID 445639	-5.8	1.2
Palmytic acid	CID 985	-4.7	1.7
Stearic acid	CID 5281	-5.6	2.0

Source: the author.

According to the molecular docking study, only the structures of caproic acid, caprylic acid, lauric acid, linoleic acid, and stearic acid interacted with the catalytic triad, more precisely with the approximation of the carboxylic acid region to serine 153 or His 268, which, according to the literature, slightly favours the formation of an ester in the esterification reaction (Ben Hlima et al., 2021; Cen et al., 2019).

Figure 26 – Interactions of babassu oil composition and the catalytic triad of EVS lipase Ser153-His268-Asp206, together with amino acid residues.

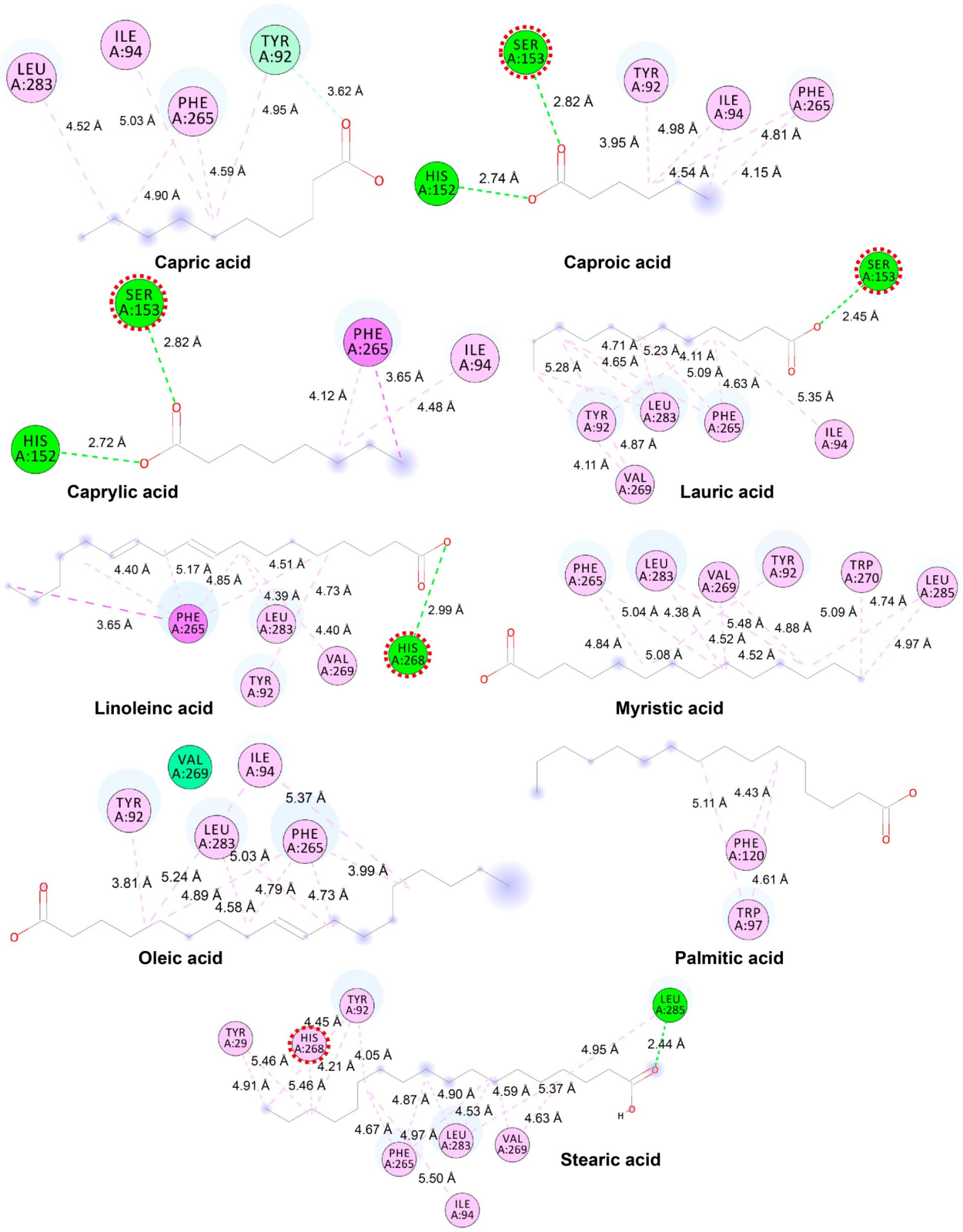

Source: the author.

Linoleic acid showed one hydrogen bridge at His 268, regions where an esterification reaction can occur. In addition, hydrophobic interactions were observed at Tyr 92, Phe 265, Val 269, and Leu 283 all of which were alkyl and π-alkyl types. In addition, an interaction of the pi-stack type with the Phe 265 residue was also observed in Figure 27.

Figure 27 – Linoleic acid interactions between the catalytic triad of EVS lipase Ser153-His268-Asp206 (green) and amino acids residues.

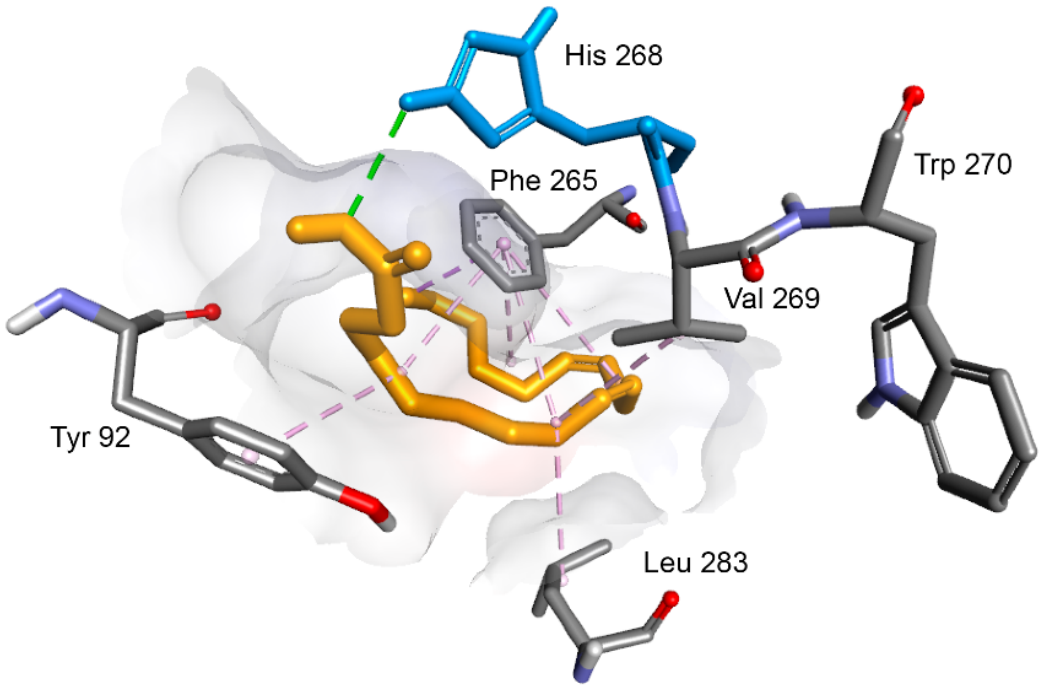

Source: the author.

3.3.10 Molecular dynamics

A thermodynamic system consisting of solute and solvent can be represented by a complex involving protein, ligand, solvent, and ion. Within this system, various types of intermolecular forces contribute to the interactions between the molecules, in addition to thermal exchanges between the molecules and ions present. According to the laws of thermodynamics, the relationship between these molecules and how heat transfer occurs is determined by several energy changes, as reported by numerous sources (Arcon et al., 2017; Beretta, 2020; Chinaka, 2021; Struchtrup, 2020).

Considering this, molecular dynamics simulations were conducted on protein-ligand complexes using NAMD to investigate the possible occurrence of global conformational changes and protein stability after each conformational change and to obtain insights into the

mechanism of interaction of the complexes at the molecular level. These simulations were carried out to provide a better understanding of the thermodynamics of the system and the factors that influence the stability and behaviour of the protein-ligand complexes (Byléhn et al., 2021; Du et al., 2016).

The outcomes of these simulations can help design drugs and therapeutics and develop new chemical processes that can improve the efficiency of chemical reactions. Therefore, the results of these simulations have significant implications for a wide range of scientific and industrial fields, such as drug development, biotechnology, and materials science (Vamathevan et al., 2019).

3.3.11 RMSD analysis

After molecular docking, the composition of babassu oil was selected based on its binding solid energies for further molecular dynamics studies at the catalytic site of Eversa® lipase Transform 2.0 (EVS), as shown in Figure 28. The simulations revealed that the average RMSD values for EVS remained around 0.63 Å throughout the 100 ns production stages. Caprilic, Lauric, and Caproic acid showed stable values with an average RMSD of 1.9 Å. However, other acids exhibited stable values with RMSD above 2.0 Å, which is consistent with previous studies, who used MD simulations to evaluate the stability of a viral protease enzyme in an aqueous solution with different ligands containing varying levels of α helix and β sheets. The long-range interactions were calculated using the SPME procedure and a Langevin thermal bath at 310 K (Miyamoto et al., 2014). The mean quadratic deviations (RMSD) were used to describe the conformational changes of the protein observed during MD simulations.

Figure 28 – Root Mean Square Deviation (RMSD), concerning the initial confirmation of the ligand-enzyme complex versus the simulation time (ns) in the production simulations step of the MD with oil composition babassu/EVS.

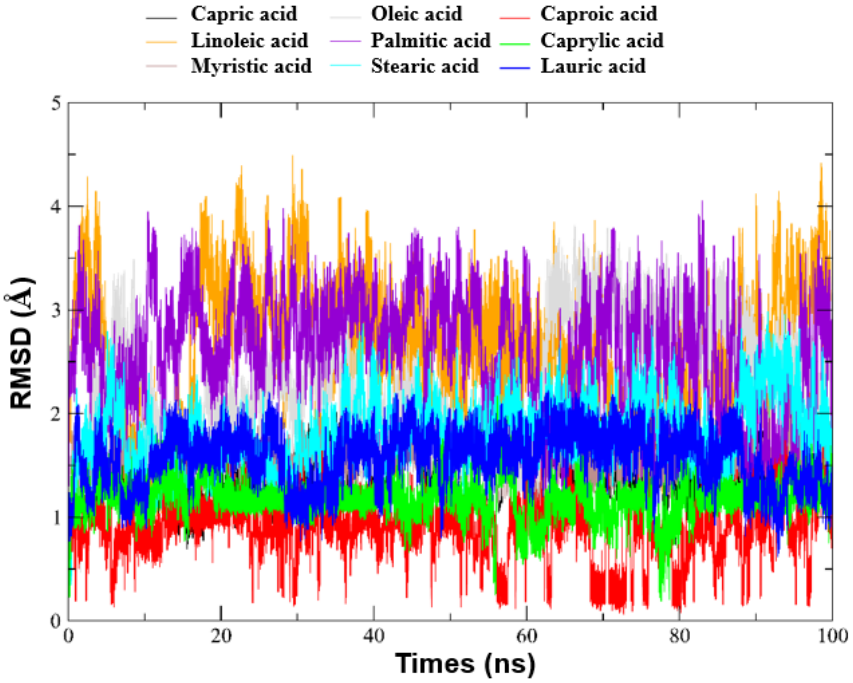

Source: the author.

3.3.12 RMSF analysis

The stability of the complexes was verified through the RMSD analysis. However, to comprehend the conformational changes observed during MD simulations, fluctuations in the mean atomic quadratic deviations (RMFS) were used to express the fluctuations in the mean structure of the protein. RMSF of the system was performed to assess the displacement and stability of each protein residue during the 100 ns trajectory. Figure 29 illustrates the main interactions of the leading complexes (babassu oil composition) studied, suggesting significant conformational changes of the compound-EVS complexes during the simulation. The results indicate that all complexes' molecular dynamics simulation trajectories showed mean oscillations with substantial correlations with critical residues in replication (Qin et al., 2021; Roe & Brooks, 2020). Only the complexes formed between Stearic acid, Oleic acid, and Lauric acid with EVS presented values higher than 2.0 Å for residues 53, 64, 115, 146, 163, 198, 235, and 267. Despite the fluctuations observed, the results showed stable structures in an aqueous solution. The conformations obtained from MD simulations for both proteins were complexed with various ligands through docking techniques, generating meaningful information about small molecules' binding modes in different enzyme folding states (Thirumalai et al., 2020).

Figure 29 – Root Mean Square Fluctuation (RMSF), concerning the initial confirmation of the ligand-enzyme complex versus the simulation time (ns) in the production simulations step of the MD with oil composition babassu/EVS.

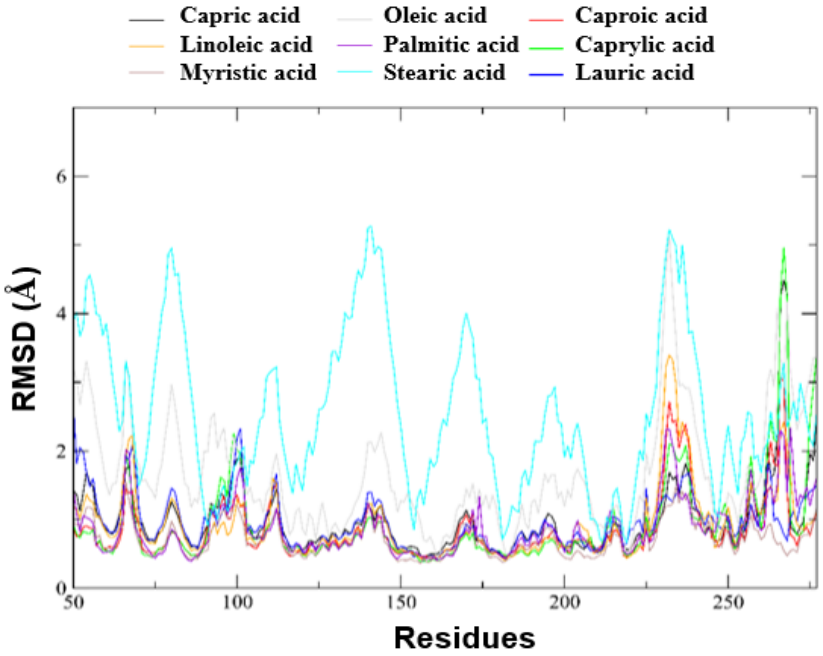

Source: the author.

3.3.12 H-bonds analysis

The number of hydrogen bonds is essential to verify whether a complex has reached stability in a dynamic system (Mascoli et al., 2021; Ragunathan et al., 2018). After the 100 ns, it was possible to verify the hydrogen bonds formed between EVS with their respective simulated ligands in long stages of production in molecular dynamics (Figure 30). During the simulation, there were changes in hydrogen binding networks, and the number of interactions for the lipase fluctuated between 2 and 4. In the EVS with linoleic acid complex, the isolated hydrogen bonds and the moderate average number of hydrogen bonds per period (up to 4) suggested that hydrogen bonding networks were relatively adequate and median. It was forming reasonable connections during its trajectory. Myristic, Caproic and Stearic acid MD were shown to have more interactions along the course (3 links), suggesting another hydrogen binding network, moderately more significant than the previous one.

For the simulation of Oleic, Lauric, Caprylic, Palmitic, and Capric acid with EVS, a maximum of 2 hydrogen bonds were formed, characterizing a relatively weaker network of interactions. The moment when these connections were very present suggests that this

interaction maintained the stability of the complex beyond the size of the compounds and their functionalities (Qin et al., 2021).

Therefore, complementary correlations can be observed in comparing hydrogen bonds formed in molecular dynamics with those previously obtained by the coupling process, indicating the convergence of a static method for a continuous system process.

Figure 30 – Hydrogen bonds formed between the protein and the ligand during the simulation steps.

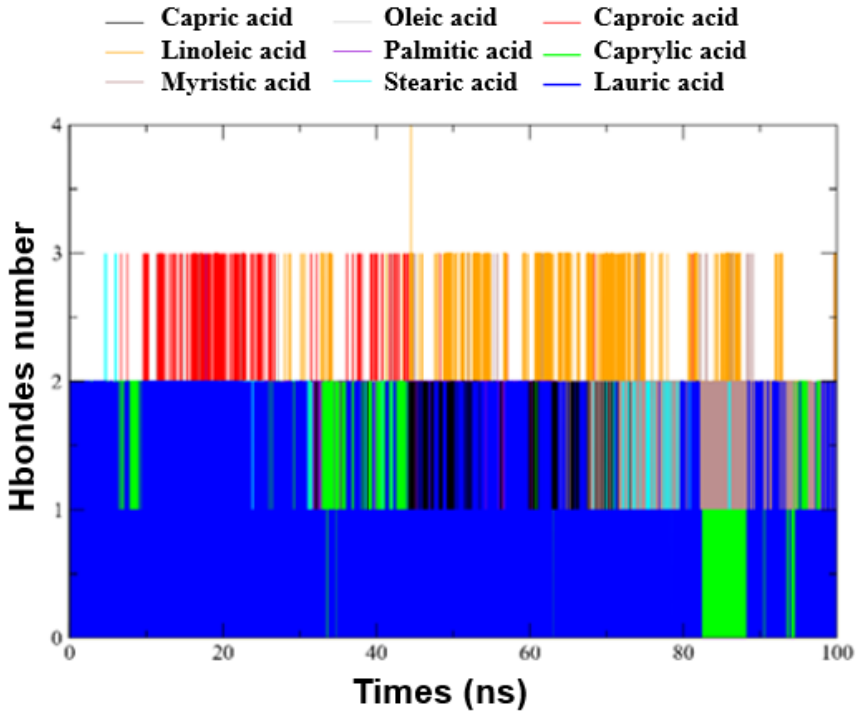

Source: the author.

3.3.13 MM/GBSA calculations

The generalized Born and surface area continuum solvation (MM/GBSA) and molecular mechanics energies can be used to calculate the free energies of a receptor complex (Genheden & Ryde, 2015). MolAICal is a computational tool that quickly estimates the free energy of a system without ligand entropy based on the approach of three trajectories obtained by molecular dynamics. The Myristic acid/EVS complex was the best result, based on its free energy, with -27.03 kcal/mol, about the other linker under study, Oleic acid/EVS, which presented a free energy of -24.42 kcal/mol. Soon after, the complexes formed by the Lauric acid/EVS and linoleic acid/EVS presented almost similar values -20.82kcal/mol and -20.70kcal/mol. In the other current simulation, the Capric acid, Caproic acid, Stearic acid, and Palmitic acid/EVS complex gave free energy, ranging from -17 to -13 kcal/mol. These results are shown in Table

13. The term entropy variation concerns the loss of degrees of freedom resulting from forming one or more interactions because previously, only two molecules (ligand and protein) could access any degree of rotational, translational, or vibrational freedom. Now, there is a complex where the movement of molecules is much more limited (Ben-Tal et al., 2000; Wright et al., 2014).

This estimate can then be obtained from the calculations of normal modes for the two systems. Thus, for a macromolecular complex with a target and a ligand, the interaction energy must be estimated according to Equations 10, 11, and 12 (Emirik, 2022; Šponer et al., 1999).

$$\Delta A_{interaction}^{(vac)} = \left(E_{complex}^{MM} - E_{target}^{MM}\right) - \left(E_{complex}^{MM} - E_{ligand}^{MM}\right) + T\Delta S_{NORMODS} \quad (10)$$

$$\Delta A_{interaction}^{(vac)} = E_{complex}^{MM} - E_{target}^{MM} - E_{complex}^{MM} + E_{ligand}^{MM} + T\Delta S_{NORMODS} \quad (11)$$

$$\Delta A_{interaction}^{(vac)} = E_{ligand}^{MM} - E_{target}^{MM} + T\Delta S_{NORMODS} \quad (12)$$

Table 13 – Free energy estimation data of Babassu lipid oil composition against EVS.

Complex	$\Delta E_{ele} + \Delta G_{sol}$ (kcal/mol)	ΔE_{vdw} (kcal/mol)	ΔG_{bind} (kcal/mol)	Standard deviation
Capric acid/EVS	5.73	-22.97	-17.24	+/- 0.0115
Caproic acid/EVS	1.19	-18.64	-17.45	+/- 0.0079
Caprylic acid/EVS	2.97	-19.00	-16.03	+/- 0.0109
Lauric acid/EVS	3.94	-24.76	-20.82	+/- 0.0107
Linoleic acid/EVS	3.76	-24.47	-20.70	+/- 0.0166
Myristic acid/EVS	3.61	-30.63	-27.03	+/- 0.0091
Oleic acid/EVS	8.45	-32.87	-24.42	+/- 0.0170
Palmitic acid/EVS	5.80	-19.21	-13.41	+/- 0.0244
Stearic acid/EVS	7.46	-21.88	-14.41	+/- 0.0130

Source: the author.

3.4 Conclusion

Fe_3O_4 nanoparticles produced in this work by sonication synthesis managed to be functionalized and activated with polyethyleneimine (PEI) and the epoxy bisphenol A diglycidyl ether (DGEBA), creating a magnetic support that was capable of efficiently immobilizing lipase enzymes. The Taguchi L9 planning identified the most favourable reaction environment within the working conditions and levels for the Fe_3O_4-PEI-DGEBA support to

heterofunctionally immobilize the Eversa® lipase Transform 2.0 (EVS), forming the Fe_3O_4-PEI-DGEBA@EVS biocatalyst. The time of 15 h, ionic strength of 95 mM, protein load of 5 mg/g of the support, and temperature of 25 °C proved optimal immobilization conditions. Under these conditions, we had immobilization yield (I.Y) 95.04%, theoretical activity (At. T) 86.84 U/g, derived activity (At. D) 29.73 U/g and recovered activity (At. R) 34.48%. The most significant factors for immobilization were protein charge and temperature, time, and ionic strength, which worked synergistically for punctual improvements. The maximal load capacity of the support is 25 mg/g of protein, according to the examination of the biocatalyst's immobilization parameters. The immobilization yield and the biocatalyst activity rapidly decrease after that value. A storage time of 60 days showed that the biocatalyst had an activity decay of less than 10% during this period. Compared to the free EVS, the biocatalyst was more stable when exposed to temperature and pH changes.

The structural and magnetic characterization results corroborated the EVS immobilization hypothesis by the Fe3O4-PEI-DGEBA support. Even with non-magnetic materials anchored to Fe_3O_4, the biocatalyst Fe_3O_4-PEI-DGEBA@EVS showed a magnetization of 44.15 emu/g, allowing its reuse in enzymatic catalysis. The Fe_3O_4-PEI-DGEBA@EVS biocatalyst has proven itself in its proposal for reuse in esterification cycles, obtaining 10 esterification cycles with yields more significant than 50% and a better esterification yield of babassu oil of 97.91%. The results obtained by NMR confirmed the esterification of FFA, with peaks at δ 1.62, 1.73, and 2.31 ppm that are associated with methylene hydrogens located at positions α and β -carbonyl of the ester, proving alcohol conversion, in addition to the peak δ 3.98 ppm, where it is associated with the methylene hydrogens directly linked to the oxygen of the ester, suggesting that there was enzymatic esterification.

The in-silico results demonstrated stability between the EVS and the acids, emphasizing oleic and linoleic acid, which obtained -5.8 kcal/mol and -6.0 kcal/mol, respectively. As a result, the novel support produced an efficient biocatalyst for the enzymatic catalysis of babassu FFA, resulting in esters that might be employed as biolubricants. Future research may involve using the produced biocatalyst to catalyze the reactions of other acids in quest of other biotechnological applications.

CHAPTER IV

4 BIOENERGY CONVERSION OF RESIDUAL TILAPIA OIL USING A NOVEL IMMOBILIZED LIPASE: ENHANCED STABILITY, SELECTIVITY, AND COMPUTATIONAL INSIGHTS

Abstract

The immobilization of lipase B from *Candida antarctica* (CALB) on an amino-epoxy functionalized magnetic support (Fe_3O_4-PEI-DGEBA) yielded a highly efficient biocatalyst with enhanced selectivity and stability. Structural and compositional analyses, including TEM, SEM, XRD, FTIR, TGA, and VSM, confirmed the successful immobilization and preservation of the magnetic core's integrity, while characterizing the biocatalyst's dual functionality with residual amino and epoxy groups. The immobilized enzyme demonstrated superior catalytic performance, achieving a 97% immobilization yield and remarkable operational stability, retaining over 80% activity after 120 days of storage and maintaining consistent activity through multiple reuse cycles. Computational docking and molecular dynamics studies highlighted the role of immobilization in promoting the enzyme's selectivity for long-chain saturated fatty acids through enhanced hydrophobic interactions with key active site residues, such as Leu140, Ala141, and Val154. QM/MM simulations further revealed that the nucleophilic attack step, with an energy barrier of 17.5 kcal/mol, remains the rate-limiting step, consistent with the enzyme's optimized catalytic efficiency post-immobilization. The results demonstrate that the heterofunctional immobilization significantly stabilizes CALB while enhancing its specificity and adaptability under industrially relevant conditions. This study provides a robust framework for the development of advanced biocatalytic systems aimed at sustainable bioprocesses and expands the understanding of enzyme-substrate interactions under immobilized states.

Keywords: magnetic biocatalyst; heterofunctional immobilization, selectivity enhancement, structural stability, hydrophobic interactions.

4.1 Introduction

The global transition to renewable energy has become a critical objective in addressing climate change (Aljashaami et al., 2024; Uzar, 2020). Initiatives like the Paris Agreement have united nations in the goal of limiting global temperature rise to 1.5 °C and achieving carbon neutrality by the second half of the century (Gong et al., 2024; Singh et al., 2023; Yang et al., 2024). Biofuels are key contributors to this effort, as they can generate up to 90% less carbon dioxide (CO_2) and significantly lower emissions of pollutants such as sulfur dioxide (SO_2), compared to fossil fuels (Joshiba et al., 2024; Pandey et al., 2023). Derived from vegetable and animal oils through chemical and biological processes (Seibel et al., 2024), biofuels exhibit diverse characteristics and environmental impacts, which are based on the pathway and raw material employed in their production (Srivastava et al., 2023; Tagami-Kanada et al., 2022).

Among the many developed processes of converting oils into biofuels, enzymatic catalysis presents a sustainable and versatile approach (Noraini et al., 2014). Operating under mild conditions of temperature, pressure and pH, enzymatic processes are highly selective and minimize the formation of toxic byproducts, unlike conventional chemical processes that rely on strong acids (H2SO4) and bases (NaOH) (Cai et al., 2024; Tunio et al., 2024; Wang et al., 2024). These attributes reduce both the environmental impact, and the costs associated with waste treatment, positioning enzymatic catalysis as a green alternative for biofuel production (Torres-Mayanga et al., 2019; Valle et al., 2024; Wancura et al., 2024).

The lipase B from *Candida antarctica* (CALB) offers several advantages in biofuel production (Kamel & Idris, 2022; Shahedi et al., 2019). The high catalytic specificity of this enzyme enables the efficient conversion of free fatty acids (FFA) into biofuels, with minimal by-product formation (Mehrasbi et al., 2017; Vásquez-Garay et al., 2018). CALB is active within a temperature range of 25 to 60 °C, under neutral or slightly alkaline conditions (Silva et al., 2024; Li et al., 2024), and its performance can be further enhanced through immobilization on suitable supports (Li et al., 2024; Zeng et al., 2024). The immobilization improves enzyme stability, allows for reuse, and simplifies downstream processing, thereby increasing the economic feasibility and sustainability of the process (Melo et al., 2023).

Magnetic supports, particularly Fe_3O_4 (magnetite) nanoparticles, are promising materials for enzyme immobilization (Menezes et al., 2024; Wang et al., 2015). These nanoparticles offer a high surface area, strong magnetization properties and tunable surface chemistry (Niu et al., 2024; Yang et al., 2024). They exhibit a saturation magnetization between 60 and 100 emu/g, which is strongly dependent on their size (Damasceno et al., 2020; Touqeer

et al., 2020). When synthesized below 20 nm, they tend to exhibit superparamagnetism, where they do not retain magnetization in the absence of an external magnetic field (Santos et al., 2024; Rani & Varma, 2015; Wan et al., 2022). However, as the particle size increases, they transition to a ferromagnetic state, exhibiting positive coercivity (Hc) (Saraçoğlu et al., 2023). The heterofunctional activation of magnetic nanoparticles can further enhance immobilization stability, shielding the enzyme from fluctuations in temperature and pH (Aghaei et al., 2021; Bezerra et al., 2020). For instance, the activation of magnetite with polymeric and epoxy compounds enhances their surface with a higher density of positive charges, facilitating electrostatic interactions between the support and the enzyme (Melo et al., 2024). Additionally, the epoxy groups allow the formation of covalent bonds, increasing the biocatalysts stability under varying conditions (Melo et al., 2023; Liu et al., 2024). These features make functionalized magnetic supports ideal for applications in biofuel production through enzymatic catalysis (Mekuriaw & Abera, 2024; Monteiro et al., 2024).

The utilization of animal-derived raw materials, such as fishery by-products, in biofuel production provides an additional environmental benefit by addressing waste disposal challenges (Laos et al., 2002; Mota et al., 2019). The tilapia oil (from *Oreochromis niloticus*) is particularly promising due to its high yield (15-40 % of residue weight) and cost-effectiveness. (Afedzi et al., 2023; El-Dakar et al., 2023; Magbanua & Ragaza, 2024). Tilapia oil has demonstrated potential for producing bio-oil and biodiesel, with significant reductions in pollutant emissions (up to 44% in diesel engines) (Lin & Huang, 2012). Despite its economic and environmental importance, effective methods for valorizing fishery waste are underexplored in the literature.

This study evaluates biofuel production from tilapia oil using an enzymatic pathway. The lipase B from *Candida antarctica* was immobilized on Fe_3O_4 nanoparticles functionalized with polyethyleneimine (PEI) and epoxy groups, creating a stable and efficient biocatalyst for the esterification of tilapia oil derived free fatty acids (FFA). The structural, magnetic, and catalytic properties of the support were characterized through Scanning Electron Microscopy (SEM), X-ray Fluorescence (XRF), Transmission Electron Microscopy (TEM), X-ray Diffraction (XRD), Fourier Transform Infrared Spectroscopy (FTIR), Thermogravimetric Analysis (TGA) and Vibrating Sample Magnetometry (VSM). The biocatalyst performance was evaluated through stability tests (temperature, pH and storage), esterification efficiency, and cycles of reuse. Finally Molecular Docking, Molecular Dynamics (MD), and Quantum Mechanics/Molecular Mechanics (QM/MM) simulations provides mechanistic insights into CALB interactions with tilapia oil, complementing experimental observations.

4.2 Materials and Methods

4.2.1. Materials

Ferric chloride hexahydrate ($FeCl_3 \cdot 6H_2O$) and ferrous sulfate heptahydrate ($FeSO_4 \cdot 7H_2O$) were purchased from Vetec Química Ltda (São Paulo, Brazil). Polyethyleneimine (PEI) (10,000 MW) was obtained from Sigma-Aldrich (St. Louis, MO, USA). Diglycidyl ether of bisphenol A (DGEBA) was acquired from Polipox Ltda (São Paulo, Brazil). Soluble Lipase B from *Candida antarctica* (CALB) (10.9 mg protein/mL) was purchased from Codexis (Redwood, USA). The commercial TLL extract (25 mg protein per mL) was obtained from Novozymes (Spain). Tilapia oil (*Oreochromis niloticus*) was acquired from the Department of Chemical Engineering at the Federal University of Ceará (Fortaleza, Brazil). Other chemical reagents were supplied by Synth (São Paulo, Brazil).

4.2.2. Synthesis of the magnetic support Fe_3O_4-PEI-DGEBA

The synthesis of the magnetic support was carried out following the methodology from Melo et al. (2023). The synthesis of Fe_3O_4 was carried out using an ultrasonic probe with a frequency of 20 kHz, 550 W, and a microtip of 3.2 mm in diameter. Sonication was performed at 200 W in pulsed mode, with 3 seconds on and 1 second off. A total of 1.16 g (4 mmol) of $FeSO_4 \cdot 7H_2O$ and 1.85 g (7 mmol) of $FeCl_3 \cdot 6H_2O$ were dissolved in 15 mL of deionized water. The mixture was sonicated for 8 minutes under the described pulsing regime. Then, 7.0 mL of NH_4OH was slowly added, causing a color change from orange to black, indicating the formation of nanoparticles. After formation of the Fe_3O_4 nanoparticles, 1.0 g of PEI was dissolved in 5 mL of deionized water and slowly added to the mixture, which was then sonicated for an additional 4 minutes. The Fe_3O_4-PEI was then washed with acetone and separated using a magnet until the solution reached neutral pH (Neto et al., 2017). For activation with epoxy groups, diglycidyl ether of bisphenol A (DGEBA) was used. The Fe_3O_4-PEI nanoparticles were dried, ground, and mixed mechanically at a rotation speed of 1500 rpm for 2 hours in the presence of DGEBA, with a relative centrifugal force (RCF) of 617 m/s^2, using a ratio of 1 g Fe_3O_4-PEI to 12 g DGEBA. The system was then sonicated in 10 mL of ethanol for 4 minutes, washed with acetone, and precipitated with the aid of a magnet, resulting in the Fe_3O_4-PEI-DGEBA support.

4.2.3. Immobilization of CALB on Fe_3O_4-PEI-DGEBA

The immobilization parameters for CALB on the Fe_3O_4-PEI-DGEBA support were determined based on the optimal point identified by Melo et al. (2024) in previous studies, where the lipase Eversa® Transform 2.0 was immobilized on the same support used in this article. 100 mg of Fe_3O_4-PEI-DGEBA was suspended in 1 mL of 95 mM sodium phosphate buffer at pH 7.0 containing CALB, at a ratio of 5 mg of protein per g of support. The system was kept under constant stirring for 12 hours at 25 °C (Santos et al., 2015). Subsequently, the solution was washed with 5 mM sodium phosphate at pH 7.0 and centrifuged to determine the initial immobilization yield (IY) of the supernatant. Then, the solution was incubated for 16 hours at 25 °C in 10 mL of 5 mM sodium bicarbonate pH 10. Subsequently, the mixture was treated with 10 mL of 3 M glycine at pH 8.5 and maintained at 25 °C for 24 hours, to cap the epoxy groups that did not participate in the immobilization of CALB (Niu et al., 2024). Finally, the biocatalyst Fe_3O_4-PEI-DGEBA@CALB was washed with 5 mM sodium phosphate buffer at pH 7.0, and isolated with a magnet.

To evaluate the loading capacity of CALB, 100 mg of Fe_3O_4-PEI-DGEBA were suspended in 1.0 mL of a sodium phosphate buffer solution (95 mM, pH 7), containing CALB with an enzyme loading varying from 1:1 to 1:50 mg/g of support. The system was kept under constant stirring for 15 hours at a temperature of 25 °C (Cavalcante et al., 2022).

The lipase immobilization parameters were determined by following the methodologies established by previous studies (Cavalcante et al., 2022). The key parameters assessed include Immobilization Yield (I.Y.), Theoretical Activity (At. T), Recovered Activity (At. R), and Derivative Activity (At. D).

I.Y. represents the percentage of enzymatic activity retained after immobilization, calculated as the difference between initial and final enzyme activity. At. T is the expected activity of lipase post-immobilization, based on the enzyme amount and I.Y. At. R compares the actual activity of At. D with At. T, while At. D is the measured activity of the immobilized lipase under specific test conditions. Below are the equations for calculating each parameter (Eq. 13 to Eq. 16).

$$\text{I.Y.} = \left(\frac{At_i - At_f}{At_i}\right) 100\% \tag{13}$$

$$\text{At.T} = At_{enz}\ (\text{I.Y.}) \tag{14}$$

$$\text{At. R} = \left(\frac{\text{At.D}}{\text{At.T}}\right) \quad (15)$$

$$\text{At. D} = \frac{\Delta A}{\Delta t}\ \text{f} \quad (16)$$

I.Y. and At. D are expressed as percentages (%), while At. T and At. R are measured in U/g. Ati and Atf refer to the initial and final activities, respectively. Atenz indicates the amount of enzyme provided per gram of support. ΔA represents the change in absorbance measured by a spectrophotometer over the time interval Δt. Additionally, f is a conversion factor that relates the observed change in absorbance to enzymatic activity.

4.2.4. Determination of enzymatic activity and protein concentration

The activity of CALB, in its soluble and immobilized forms, was analyzed through the hydrolysis of *p*-NPB (Rios et al., 2016). The quantification of the released p-nitrophenol was performed using spectrophotometry at 348 nm. Activity measurements were conducted in a sodium phosphate buffer (25 mM, pH 7.0) under constant stirring at 25 °C for 90 seconds, monitoring the release of p-nitrophenol from the hydrolysis of 50 mM *p*-NPB. To initiate the reaction process, 50 µL of the CALB suspension was combined with 50 µL of *p*-NPB and 2.5 mL of the buffer solution. One international unit of activity (U) was defined as the amount of enzyme capable of hydrolyzing 1 µmol of *p*-NPB per minute under the established conditions. The protein concentration was determined using the Bradford method (Miguel Júnior et al., 2022).

4.2.5. Stability of the catalyst

The effect of the pH in the activity of the catalyst was assessed as follows: the immobilized and free CALB were resuspended in 1.0 mL of 95 mM buffer solution, with varying pH (4-9). Acetate buffers (pH 3.6-5.6), sodium phosphate buffer (pH 5.8-8.0), and sodium carbonate buffer (pH 8.9-10.8) were employed, and p-NPB was used as a substrate. The enzyme was incubated in each buffer for approximately 15 minutes, after which the activity was measured (Pinheiro et al., 2019).

The effect of temperature was assessed as follows: the immobilized and free CALB were incubated in phosphate buffer (95 mM, pH 7) at 25, 30, 40, 50, 60, 70, and 80 °C for 10

minutes. After heating, the samples were cooled in an ice bath (approximately 10 min) and then reheated to room temperature (25 °C) in a water bath (approximately 5 min) before analysis. Activity was measured using *p*-NPB, and the residual activity was expressed as a percentage of the initial activity (Bezerra et al., 2020).

The storage activity of the biocatalyst was evaluated by monitoring the hydrolytic activity towards *p*-NPB. After immobilization, the biocatalysts were washed, vacuum-dried, and stored at 4 °C. The activity of the biocatalysts was assessed at regular intervals from 0 to 120 days (Bezerra et al., 2020).

4.2.6. Material characterization

Transmission Electron Microscopy (TEM), Scanning Electron Microscopy (SEM), and X-ray Fluorescence Spectroscopy (XRF) analyses were performed to investigate the morphology and chemical composition of the samples. The TEM analysis was conducted using a JOEL JEM 1011 microscope operating at 120 kV, equipped with a CCD camera. The distribution curves were analyzed using ImageJ. SEM was performed with a QUANTA 450 FEG microscope and a Quorum QT150ES metallizer, utilizing a 20 kV electron beam. XRF analysis was conducted using a SHIMADZU EDX-7000 system equipped with a rhodium tube, applying a power of 4 kV to the powdered samples.

X-ray Diffraction (XRD) was employed to assess the crystallinity and the size of the nanoparticles, allowing for comparison with the TEM results. The analyses were conducted using a PANalytical X'Pert MPD powder X-ray diffractometer, with a scanning range of 2θ from 20° to 80°. A CuKα tube (1.54059 Å) was utilized, operating at 40 kV and 30 mA, with a scanning range between 20° and 100°. The refinement of the analyses was performed using the Maud software.

The Fourier-Transform Infrared Spectroscopy (FTIR) technique was employed to identify organic molecules present on the surface of the nanoparticles. The analyses were conducted using a PerkinElmer 2000 spectrophotometer, utilizing KBr disks, with the spectra captured under vacuum on a Vertex 70v instrument. Thermogravimetric analysis (TGA) was performed using a Q50 instrument from TA Instruments in a nitrogen atmosphere with a flow rate of 50 cm^3/min. Magnetic curves were determined using a Vibrating Sample Magnetometer (VSM) at 300 K. To ensure the accuracy of the measured magnetic moment values, the equipment was previously calibrated with a standard reference material. For all measurements,

the recorded magnetic moments for each applied field were normalized by the mass of the nanoparticles.

4.2.7. Production of biodiesel

Free fatty acids were extracted from tilapia oil through an enzymatic hydrolysis process using lipase derived from *Thermomyces lanuginosus* (TLL). This soluble lipase exhibits a specific activity greater than 100,000 U/g and is widely employed in the breakdown of triglycerides due to its thermostability (up to 60-70°C), effectiveness in organic solvents, and high specificity for triglycerides. It is extensively utilized in various hydrolytic reactions (Alexandre et al., 2022; Moreira et al., 2020; Petro et al., 2023; Rocha et al., 2021). A mixture of oil and water in a 1:1 ratio was heated to 40 °C, at which point TLL was added at a concentration of 0.4%. The reaction was maintained at 40 °C with continuous stirring for a period of 4 hours. The solution was then placed in a separation funnel, and 100 mL of distilled water at 60 °C was added to promote the separation of the free fatty acids (FFAs), followed by three washings. Next, the mixture was transferred to a beaker and heated to 80 °C for 10 minutes. After this period, the mixture was poured into a funnel containing filter paper and a preheated 20% ($m \cdot V^{-1}$) anhydrous sodium solution.

The Fe_3O_4-PEI-DGEBA biocatalysts were used for the synthesis of the biofuel. The free fatty acids (FFAs) were esterified using ethyl alcohol in a 1:5 ratio (acid:alcohol), with 9% of the biocatalyst, at a temperature of 25 °C and with constant stirring for 5 hours. Aliquots of 0.2 g were taken from the reaction system, diluted in 20 mL of ethanol, and three drops of phenolphthalein were added, followed by titration with a 40 mM sodium hydroxide solution to measure the acidity index and determine the biocatalyst's reaction cycles. The acidity index (AI) was calculated according to Eq. (17).

$$AI\left(\frac{mgNaO}{g}\right) = MM_{NaOH}.Shch_{NaOH}.f.(\frac{V_{NaOH}}{m}) \quad (17)$$

MM_{NaOH} represents the molar mass of NaOH. $Shch_{NaOH}$ indicates the molarity of the solution, while f is the correction factor obtained through the standardization of NaOH. V_{NaOH} corresponds to the volume of NaOH consumed in the titration, and m is the mass of the sample under analysis. The conversion of FFAs to esters was determined using Eq. (18), considering the initial acidity index AI_0 and the index at the final time AI_t.

$$Conversion\ FFA(\%) = \left(\frac{AI_0 - AI_t}{AI_o}\right) .100 \quad (18)$$

Operational stability was assessed through consecutive reactions to produce the esters. Before each new cycle, the biocatalyst was separated from the reaction medium using magnetization and washed three times with hexane to remove any residual substrates.

4.2.8. Fourier Transform Infrared Spectroscopy (FTIR) and Nuclear Magnetic Resonance spectroscopy (NMR) of the biodiesel

FTIR was performed on the samples to identify specific functional groups, such as carbonyl (1740 cm^{-1}, C=O) and hydroxyl (3000–3500 cm^{-1}, O-H), which can be used to track the chemical reaction (Ong et al., 2020; So & Eberhardt, 2018). Additionally, the samples were compared with the FTIR of a commercial biodiesel obtained through a chemical route. The equipment used was the Cary 630 with a diamond ATR from Agilent. NMR was also conducted to confirm the esterification of the free fatty acids (Ben-Youssef et al., 2021). 1D and 2D spectra, including ^{1}H and ^{13}C, were obtained using a Bruker Avance DRX-500 spectrometer with $CDCl_3$ as the solvent. Chemical shifts were measured in parts per million (ppm), and in the ^{1}H NMR spectra, the reference peak was the hydrogen of the non-deuterated fraction of $CDCl_3$ (δH 7.27). The multiplicities of the hydrogen signals in the ^{1}H NMR spectrum were indicated according to the convention: s (singlet), d (doublet), t (triplet), and m (multiplet).

4.2.9. Viscosity and density of the biodiesel

To verify compatibility and performance with engines and injection systems, the kinematic viscosity (ν) and density (ρ) of the biodiesel were measured. The measurements were performed using the Anton Paar SVM 3000 U-tube viscometer, previously calibrated with Cannon mineral oil for the temperature range of 273.15 to 393.15 K. The properties were evaluated at atmospheric pressure and at temperatures of 293.15, 313.15, and 373.15 K. The sample was introduced into the SVM 3000 equipment using a 5 mL syringe, ensuring the absence of air bubbles. The temperature control system of the apparatus has an uncertainty of u(T) = 0.01 K.

4.2.10. Molecular docking and molecular dynamics (MD) simulations

The computational model of CALB was created from its x-ray structure (PDB identification code: 1TCA) (Uppenberg et al., 1994). The geometry of the fatty acid substrates were optimized at the B3LYP/6-311G+(d,p) level of the DFT without any geometric constraints using the Gaussian software package (Pudzianowski, 1995). Their charges and electrostatic potentials (ESP) were computed at the HF/-311G+(d,p) level of theory, and their force field parameters were developed using the antechamber software from the AmberTools package (Salomon-Ferrer et al., 2013). The enzyme-substrate complexes were built through molecular docking using the AutoDock software (Trott & Olson, 2010). In the rigid docking protocol utilized, the structure of the enzyme was kept fixed, but the substrate was allowed to adopt any conformations. This procedure provided 20 poses, which were ranked based on their energies (Eberhardt et al., 2021). The 3 poses with the lowest energies for each substrate were selected for all-atom MD simulations.

The classical MD simulations were performed using the PMEMD module of the Amber software package (Salomon-Ferrer et al., 2013). The enzyme-substrate complex was then placed in a cubic box of 100 × 100 × 100 Å dimensions. The minimal distance from the edge of the box to the surface of the protein complex was not shorter than 10 Å. The AMBER ff14SB force field was employed for the protein and the TIP3P water model was used as the solvent. The total charge of the system was neutralized with Na^+ and Cl^- ions. After minimization, the system was heated up to 300 K over 10 ns at constant volume (NVT), while imposing positional restraints of 100 kcal/mol. $Å^2$ on the heavy atoms. Subsequently, restraints were slowly removed, and a production MD run of 200 ns was performed in the isothermal-isobaric ensemble (NPT). The temperature control (300 K) was performed by a Langevin thermostat with a collision frequency of 1/ps, and the pressure control (1 atm) was accomplished by a Monte Carlo barostat (Harger & Ren, 2019). The SHAKE algorithm was used to constrain the bonds involving hydrogen atoms, and the particle mesh Ewald method was used to compute the electrostatic interactions. A 10 Å short range non-bonded interaction cutoff distance and a 1fs time step were used for the simulations.

4.2.11. Hybrid molecular mechanics and quantum mechanics (QM/MM) simulations

The hybrid two-layer QM/MM (ONIOM) calculations were performed by using the

Gaussian software package. This method utilizes a subtractive method in which the MM energy [EMM(High)] of the QM (high layer) part is subtracted from the sum of the QM energy of the high layer [EQM(High)] and the MM energy of the whole system [EMM(Total)]. This subtraction method corrects the artifacts introduced by using link atoms. The ONIOM optimization procedure uses macro/micro interactions, and the electrostatic interactions between the QM and the MM part were treated by mechanical embedding. The QM region (model) was defined as the catalytic triad (Ser105, His224 and Asp187), the second coordination shell residue Thr40, and the substrates. The remaining atoms of the system were treated in the classic MM region. The QM region was optimized without any geometric constraint by using the hybrid B3LYP exchange correlation DFT functional (Yanai et al., 2004). The 6-31G(d,p) basis set was used to implement the computations, and the Grimme's function with the Becke-Johnsons damping effect (GD3BJ) was used to take into account the dispersive effects (Grimme et al., 2011). Hessians were calculated at the same level of theory as those of the optimizations to confirm the nature of the stationary points along the reaction coordinate. The transition states were confirmed to have only one imaginary frequency corresponding to the reaction coordinates. Single point calculations were performed using the larger 6-311+G(d,p) basis set with the M06-2X and mPW1PW91 functionals (Park et al., 2014). In these calculations, the electrostatic interactions between the QM and the MM parts were treated by electronic embedding. Zero-point vibrational, thermal and entropy corrections were added to the final energies (at 298.15 K and 1 atm). The MM region was modeled using the AMBER force field as implemented in Gaussian software.

4.3 Results and discussion

4.3.1. Synthesis and functionalization of the support

This study utilized the sonication technique for synthesizing Fe_3O_4 nanoparticles (magnetite), a method that enhances chemical reactions by generating microbubbles. The collapse of these bubbles release significant energy, creating extreme conditions of localized temperatures exceeding 5000 K and pressures up to 1000 atm (Neto et al., 2021). These extreme conditions facilitate the crystalline organization of nanoparticles, reduce impurities and agglomeration, and increase the specific surface area, yielding highly functional magnetite particles (Zheng et al., 2020). Following synthesis, the magnetite was successfully activated with polyethyleneimine (PEI), also using the sonication process.

Polyethyleneimine is rich in amino groups, which can be protonated in solution to impart a positive charge. On the other hand, the hydroxyl groups (-OH) present on the surface of Fe_3O_4 can generate negative charges under specific pH conditions (Cao et al., 2020). This electrostatic attraction between PEI and magnetite is intensified by the high-energy conditions generated during sonication (Verma & Moholkar, 2023). The energy from this process enhances the reactivity of functional groups on both PEI and Fe_3O_4, promoting the formation of stable covalent bonds between the amino groups of PEI and the -OH groups on the magnetite surface (Ning et al., 2024; Wang et al., 2022). This protocol results in a more stable and durable bond between the polymer and the nanoparticle (Ping et al., 2019).

Sonication also plays a critical role in dispersing Fe_3O_4 nanoparticles, ensuring homogenous PEI distribution across their surface (Echeverría et al., 2021; Taghizadeh et al., 2023). The rapid dissipation of energy prevents particle agglomeration, facilitating the formation of a uniform PEI coating. Neto et al. (2017) reported similar outcomes, functionalizing Fe_3O_4 with PEI via sonochemistry. Their study demonstrated a single inverse spinel phase with nanoparticles averaging 9-11 nm in diameter, confirmed by XRD and TEM. Mössbauer spectroscopy and magnetic measurements revealed superparamagnetic behavior and high saturation magnetization (59-77 emu/g), aligning with the properties desired for immobilization platforms.

Nevertheless, the main goal of this study is to immobilize the lipase B from *Candida antarctica* (CALB) through diverse anchoring strategies to preserve its active conformation and enhance catalytic activity. To this end, a heterofunctional support was developed, building on our group's prior success with immobilizing the lipase from *Thermomyces lanuginosus* (TLL) (R. L. F. Melo, Freire, et al., 2024). The heterofunctional support was achieved by activating Fe_3O_4-PEI with bisphenol A diglycidyl ether (DGEBA), a compound that binds to amino groups on the support surface through epoxy ring opening or multipoint interactions (Babaki, Yousefi, 2015; Gandomkar et al., 2015). The resulting Fe_3O_4-PEI-DGEBA support offers dual functionality, leveraging residual amine groups and active epoxy groups for enzyme immobilization (Mateo et al., 2007). This innovative support system demonstrated its efficacy with CALB immobilization, resulting in a biocatalyst with superior activity compared to the free enzyme.

4.3.2. Enzymatic immobilization and stability of the biocatalyst

To evaluate the efficiency of lipase immobilization on the Fe_3O_4-PEI-DGEBA support,

key parameters such as immobilization yield (IY), theoretical activity (TA), recovered activity (RA), and derived activity (DA) were analyzed. These metrics provide critical insights into the immobilization process, with IY representing the percentage of enzymatic activity retained post immobilization. The parameter TA estimates the expected enzyme activity based on the IY, while RA and DA assess the actual performance and effectiveness of the immobilized enzyme under experimental conditions (Cavalcante et al., 2022; Sousa et al., 2024). Figure 31 shows the effects of the immobilization parameters and operational conditions on the catalytic performance of free and immobilized CALB.

Figure 31 – Evaluation of immobilization parameters for CALB using the Fe_3O_4-PEI-DGEBA support. a) Maximum enzyme loading capacity, evaluated by varying the enzyme concentration from 1–50 mg per gram of support; b) Thermal stability assessed at different temperatures (25–80 °C); c) pH activity of soluble and immobilized CALB, tested across a pH range of 4–9 under optimal conditions; d) Storage stability of immobilized CALB.

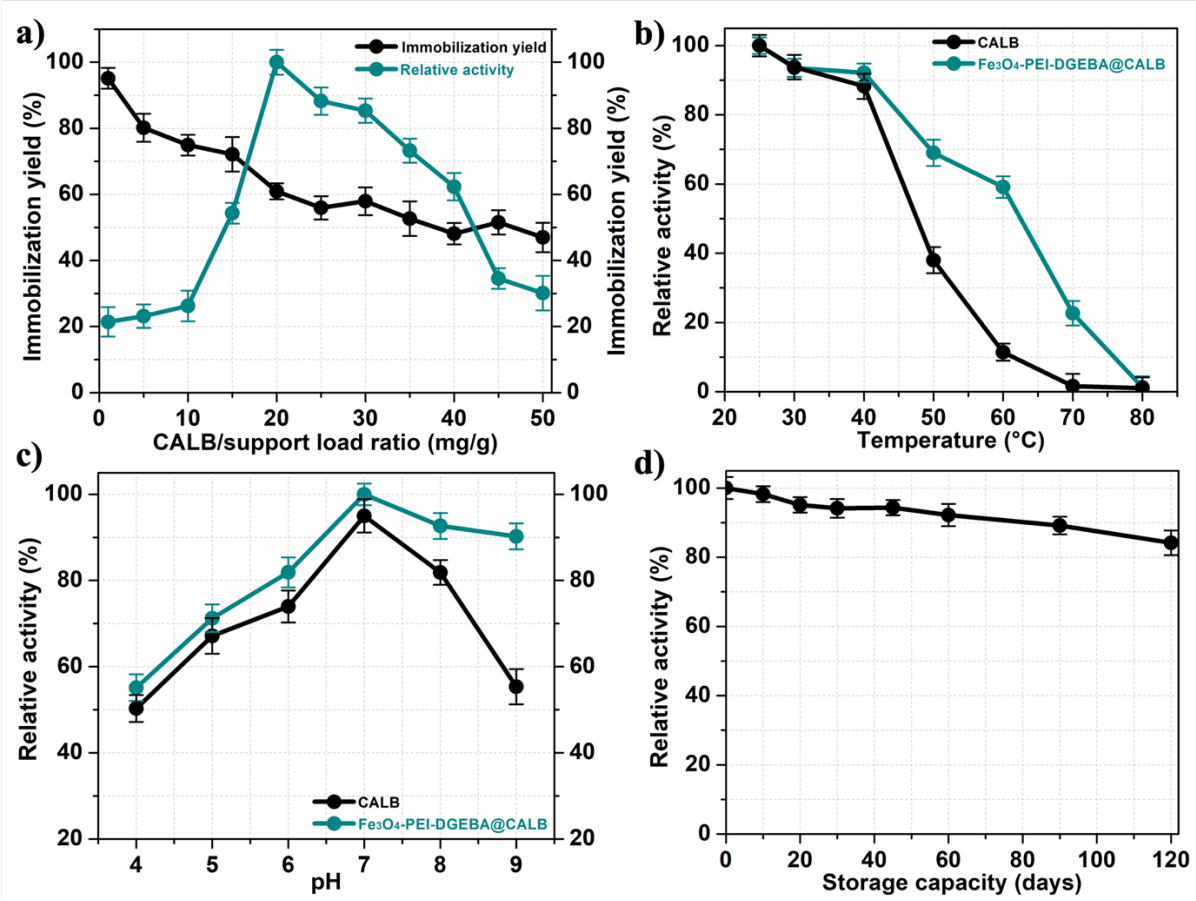

Source: the author.

The analysis of CALB loading on the Fe_3O_4-PEI-DGEBA support (Figure 31 - a)) shows the support's capacity to immobilize up to 20 mg/g of enzyme without significant loss in activity. At lower concentrations (1-15 mg/g), immobilization yields remained high, reaching

up to 97%. However, at higher enzyme concentrations (20-50 mg/g), IY decreased sharply, indicating surface saturation and potential multilayer formation. This clustering likely reduces accessibility to the enzyme's active site, emphasizing the importance of optimizing enzyme-to-support rations to maximize catalytic efficiency (Pinheiro et al., 2019). The heterofunctional nature of the support played a key role in enhancing enzyme immobilization capacity, providing multiple interaction sites through both adsorption and covalent bonding (Bezerra et al., 2020; Almeida et al., 2024).

Thermal stability tests (Figure 31 - b)) revealed the susceptibility of CALB to thermal denaturation above 60 °C, in line with previous studies that indicate that CALB has an optimal temperature range between 35 °C and 50 °C (Ren et al., 2024). While free CALB showed significant activity loss at elevated temperatures, immobilized CALB demonstrated remarkable resistance, maintaining over 60% relative activity at 60 °C. The multipoint anchoring provided by the heterofunctional support likely minimized structural disruptions caused by thermal stress, preserving the enzyme's catalytic efficiency (Cruz-Martínez et al., 2024; Santos et al., 2015; Silva et al., 2023).

The impact of pH variations on CALB activity and stability was analyzed across a range of pH (4-9), as shown in Figure 31 - c). The results confirm that CALB exhibits maximum activity at neutral to slightly alkaline conditions (pH 7-8). Under extreme pH conditions, activity decreased, likely due to alterations in the ionization state of residues critical for substrate binding and catalysis (Song & Chang, 2022). Notably, immobilized CALB retained higher activity across the tested pH range compared to its free counterpart. The immobilization process likely provided structural stability, mitigating conformational changes under unfavorable conditions (Guajardo et al., 2015; Mittersteiner et al., 2017; Salman Sajid et al., 2020; Wang et al., 2022).

The storage stability of Fe_3O_4-PEI-DGEBA@CALB was evaluated over 120 days at 4 °C, as shown in Figure 31 - d). Free CALB exhibited a significant decline in activity due to leaching and denaturation, whereas immobilized CALB maintained over 80% of its initial activity. The stability provided by the immobilization matrix likely prevented structural degradation, ensuring long-term enzyme functionality (Santos et al., 2015; Thudi et al., 2012).

Across all assessments, CALB immobilized on Fe_3O_4-PEI-DGEBA magnetic support consistently outperformed its free form in terms of stability, activity, and resistance to environmental stresses. The magnetic nature of the support also offers practical advantages, such as facile recovery and reuse of the biocatalyst, enhancing the economic feasibility of the processes. These characteristics make this immobilization strategy highly promising for

industrial applications.

4.3.3. Characterization of the heterofunctional biocatalyst

The TEM analysis (Figure 32 - a) and b)) confirms the spherical morphology of Fe_3O_4 nanoparticles, characteristics of sonochemical synthesis methods. Embedded size distribution curves reveal a small increase in particle size from 12.48 ± 1.62 nm for Fe_3O_4 to 13.40 ± 2.50 nm for Fe_3O_4-PEI-DGEBA@CALB. This increase, statistically insignificant, suggests successful coating of the magnetic core without altering its morphology. Aggregation observed in the biocatalysts reflects typical nanoparticle clustering due to enzyme immobilization. Melo et al. (Melo et al., 2024) used this support for the immobilization of TLL. The study also demonstrated that after activation with PEI and DGEBA, the magnetic core did not undergo significant morphological changes.

The SEM images (Figure 32 - c) and d)) display a laminar morphology for both Fe_3O_4 and Fe_3O_4-PEI-DGEBA@CALB. The biocatalyst shows rougher surfaces compared to the core, indicating successful immobilization of CALB. Complementary XRF mapping confirms enrichment with elements such as Cl and P, consistent with PEI-DGEBA coating and CALB adherence. These results demonstrate that CALB immobilization modified the surface properties while preserving the core structural integrity.

Figure 32 – TEM micrographs, particle size distribution curves, and SEM/XRF analyses of the materials. a) TEM image of Fe_3O_4 with its particle size distribution curve (inset), showing a spherical morphology; b) TEM image of Fe_3O_4-PEI-DGEBA@CALB with its size distribution curve (inset), showing a slightly more aggregated appearance due to the immobilization process; c) SEM image of Fe_3O_4, revealing a laminar surface morphology, and its corresponding XRF map (inset); d) SEM image of Fe_3O_4-PEI-DGEBA@CALB, showing increased surface roughness, indicative of compositional alterations.

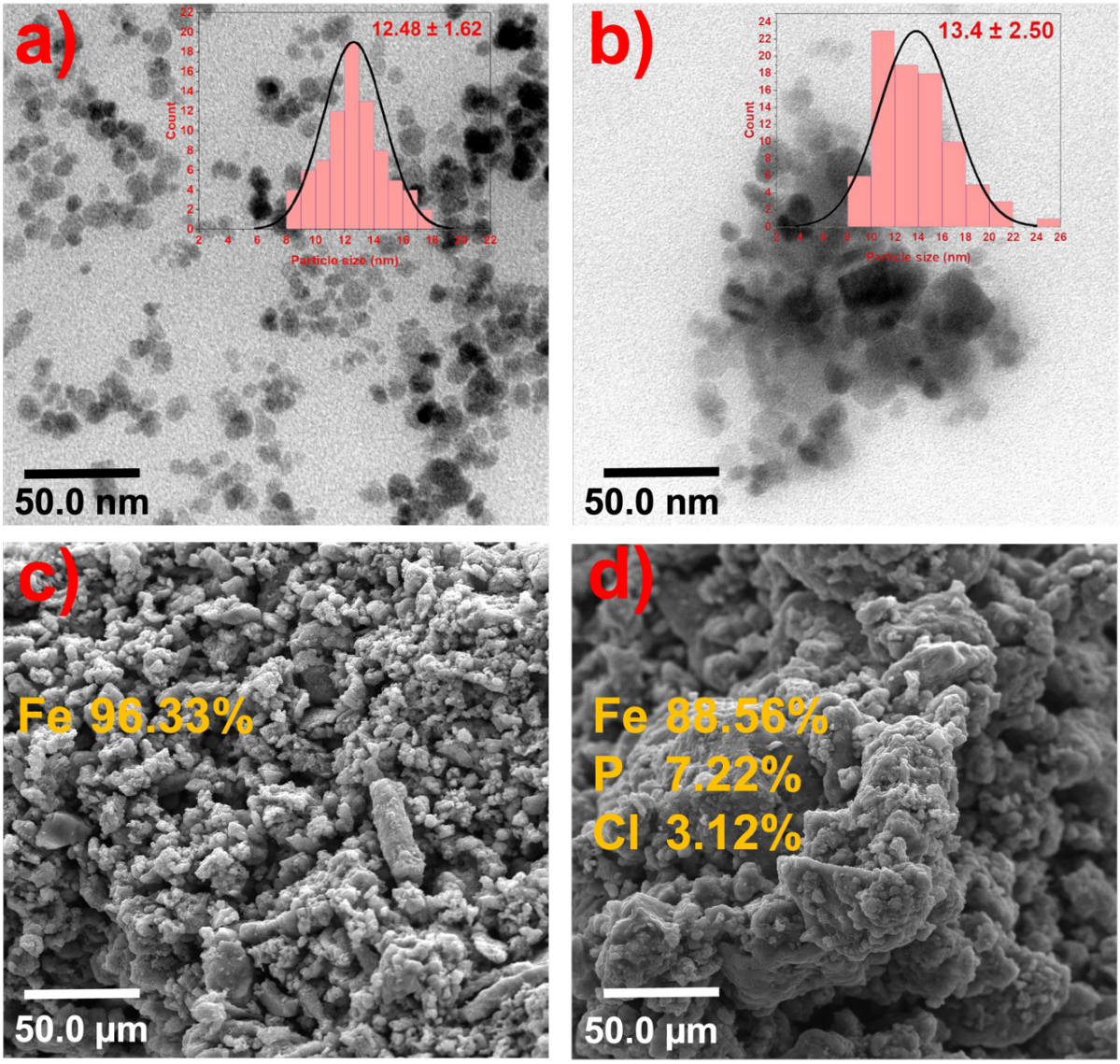

Source: the author.

The XRD patterns, shown in Figure 33 - a), reveal peaks characteristic of the inverse spinel structure of magnetite, corresponding to crystallographic planes of Fe_3O_4. For magnetite, the most prominent peaks include one at approximately 30° (2θ), corresponding to the (220) crystal plane. This peak is among the most intense and is characteristic of the magnetite structure. Another notable peak appears at around 35° (2θ), associated with the (311) plane, indicating the presence of additional crystal planes. Additionally, a peak at approximately 45° (2θ) corresponds to the (400) plane, while a peak near 60° (2θ) is related to the (511) plane.

The persistence of these peaks in Fe_3O_4-PEI-DGEBA@CALB confirms that structural integrity is retained post-functionalization and immobilization. Crystallite sizes calculated via the Scherrer equation: 13.66±1.11 nm for Fe_3O_4 to 14.11±0.89 nm for Fe_3O_4-PEI-DGEBA@CALB, align closely with TEM data). It is important to note that when Fe_3O_4 is reduced to particle sizes smaller than 20 nm, its oxidation rate tends to increase, with the possible formation of the maghemite (γ-Fe_2O_3) phase (Nnadozie & Ajibade, 2022; Ouda et al., 2020). Functionalization with PEI appears to reduce oxidation rates, as evidenced by preserved magnetite crystallinity and high magnetization values (W. Jiang et al., 2024; Y. Tang et al., 2024).

The FTIR spectra, shown in Figure 33 - b), highlight distinctive features of both Fe_3O_4 and Fe_3O_4-PEI-DGEBA@CALB. Stretching vibrations of Fe-O bonds (500-600 cm^{-1}) remain detectable but decrease in intensity for the biocatalyst, indicating surface coverage by PEI-DGEBA (Yang et al., 2010; Zhang et al., 2019). Additional absorption bands at 1600-1650 cm^{-1} associated with N-H (PEI) and C=O or C-O-C (DGEBA) further confirm successful functionalization (Ng et al., 2024; Singh et al., 2023). The observed changes suggest that the immobilization involves multiple interactions, including electrostatic, hydrogen bonding, and covalent mechanisms, enhancing enzyme stability and activity (Sharma et al., 2022; Tardioli et al., 2011).

The magnetic properties evaluated using VSM (Figure 33 - c)), show a reduction in saturation magnetization (Ms) from 70.8 emu/g for Fe_3O_4 to 52.3 emu/g for Fe_3O_4-PEI-DGEBA@CALB. This reduction is attributed to the addition of non-magnetic organic layers during functionalization and immobilization. Other authors have observed similar decrease after adding activators to magnetite. Kumar et al. (Kumar et al., 2025) synthesized Fe_3O_4 and coated it with PEI and silver using ultrasound techniques. The authors obtained a magnetization of approximately 72.5 emu/g for Fe_3O_4, 62.1 emu/g for Fe_3O_4@PEI, and 32.3 emu/g for Fe_3O_4@PEI@Ag (Liu et al., 2011; Suo et al., 2018). Despite this decrease, the biocatalyst retains sufficient magnetization for efficient recovery and reuse, making it suitable for industrial applications.

Thermal stability analysis through TGA and DTGA, shown in Figure 33 - d), reveals distinct decomposition profiles for Fe_3O_4 and Fe_3O_4-PEI-DGEBA@CALB. Fe_3O_4 shows an 8% mass loss around 70 °C due to adsorbed water, stabilizing at approximately 15% by 450 °C. In contrast, the biocatalyst exhibits greater mass losses, 12% initially, followed by a sharp 25% loss around 450 °C, culminating in 34% by 700 °C. These losses are associated with the amine groups, epoxy groups, and organic content of CALB presents in Fe_3O_4-PEI-

DGEBA@CALB (Mateo et al., 2000b; Uzun et al., 2013).

Figure 33 – Structural characterization of the material. a) X-Ray Diffraction (XRD); b) Fourier Transform Infrared Spectroscopy (FTIR); c) Vibrating Sample Magnetometer (VSM); d) Thermogravimetric Analysis (TGA, solid lines), and Derivative Thermogravimetry (DTG, dash lines).

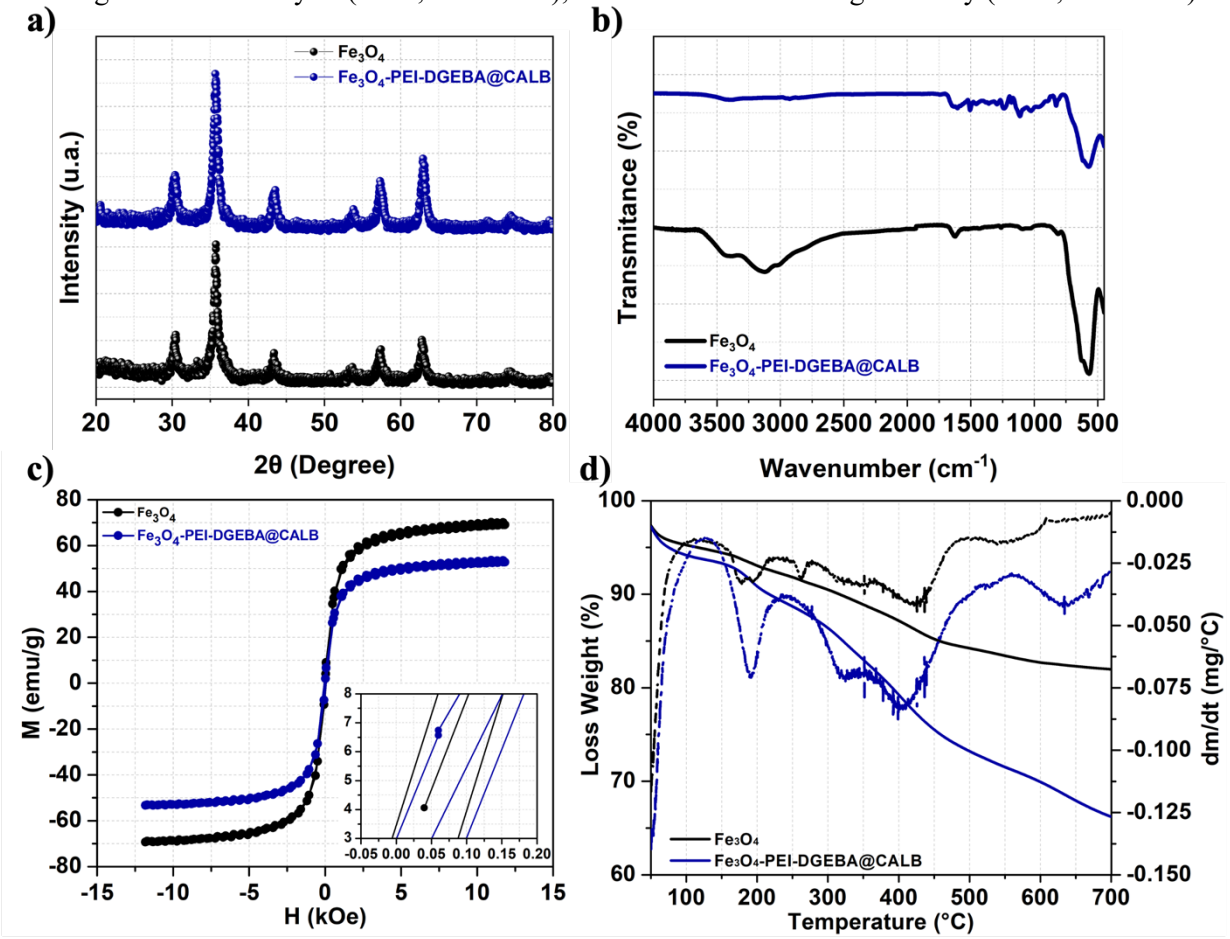

Source: the author.

The reuse cycles of the Fe₃O₄-PEI-DGEBA@CALB biocatalyst in the esterification of FFAs derived from tilapia oil demonstrated high stability, with an initial yield of 98.8%, remaining above 95% for the first three cycles. By the fifth cycle, the yield dropped to 85.2%, stabilizing above 65% after ten cycles. The decline in activity is primarily attributed to enzyme leaching and incomplete recovery during magnetic separation (Figure 34). These results align with previous studies (Melo et al., 2024), who achieved an initial yield of 97.91% and maintained over 50% after ten cycles using a similar support and TLL.

Figure 34 – Operational stability of Fe_3O_4-PEI-DGEBA@CALB. Reaction conditions: 9% biocatalyst, free fatty acids from tilapia oil, and ethanol in a 1:5 molar ratio. Reactions were performed at 25°C and 200 rpm for 5 hours.

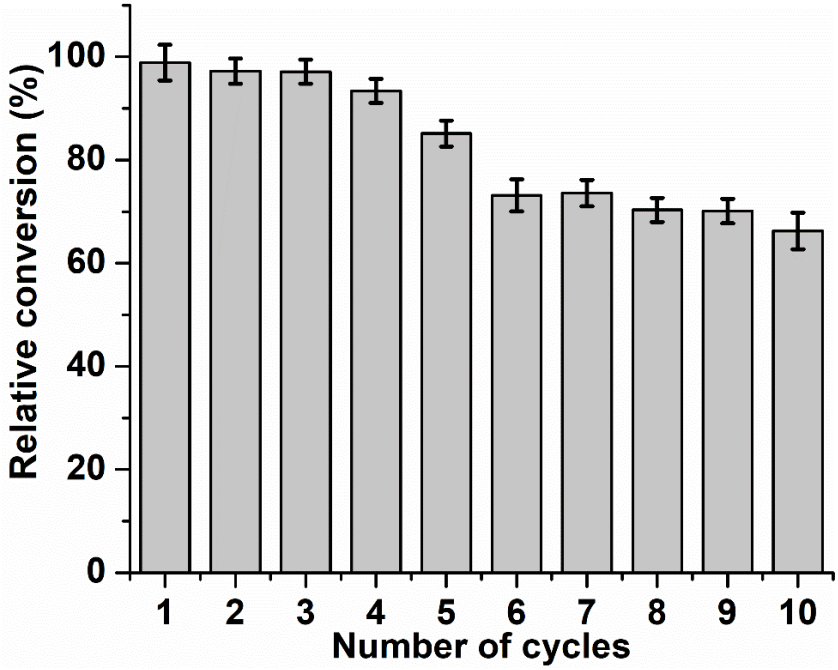

Source: the author.

Comparing the biocatalyst of this study with Novozym 435 (N435), a commercial biocatalyst widely used in academia and industry, which consists of CALB immobilized on a macroporous support of poly(methyl methacrylate) cross-linked with divinylbenzene, we observe that N435 exhibits superior stability over reuse cycles (Santos et al., 2019). In previus studies, N435 achieved an initial yield of 97.68% to 98.29% in three parallel tests (Zhao et al., 2023). After six cycles, the yield remained at 90%, and even after 16 cycles, it still reached 75%. The decline in N435 activity is primarily associated with the breakdown of enzyme particles, which hinders the complete recovery of the enzyme after repeated cycles. This physical degradation is the main cause of the reduction in yield over prolonged cycles.

4.3.4. Characterization of the biodiesel

The FTIR spectra of biofuel produced using the Fe_3O_4-PEI-DGEBA@CALB biocatalyst and tilapia oil, compared to commercial biodiesel, reveal key similarities in ester functional groups, as shown in Figure 35. Both biofuels exhibit an intense absorption band around 1740 cm^{-1}, characteristic of the C=O stretching vibrations of esters (Arokiaraj et al., 2022; Kanthasamy, 2021), confirming successful esterification. Additional bands at 1465 cm^{-1} (C-H bending in methylene), 1375 cm^{-1} (methyl bending), and 1240–1170 cm^{-1} (C-O

stretching) support the formation of ester bonds. Minor variations in band intensities, such as at 1740 cm^{-1}, suggest differences in fatty acid composition or purity between the biofuels. Previous studies used crude oil from tilapia heads to produce biodiesel through a chemical transesterification reaction using potassium hydroxide (KOH) and ethanol (Moraes et al., 2020). The FTIR spectrum presented by the author was similar to that in this research, showing the same important bands (1740 cm^{-1} and 1240-1170 cm^{-1}). These findings align with previous studies on biodiesel from tilapia oil, confirming that biocatalysis does not significantly alter the chemical structure of esters compared to chemically produced biodiesel. Note that while we did not conduct FFA purity tests on the tilapia oil, the esterification process yielded a product similar to commercial biodiesel.

Figure 35 – FTIR characterization of the biofuel produced from the biocatalysts Fe_3O_4-PEI-DGEBA@CALB and Tilapia oil (red) and commercial biofuel (black).

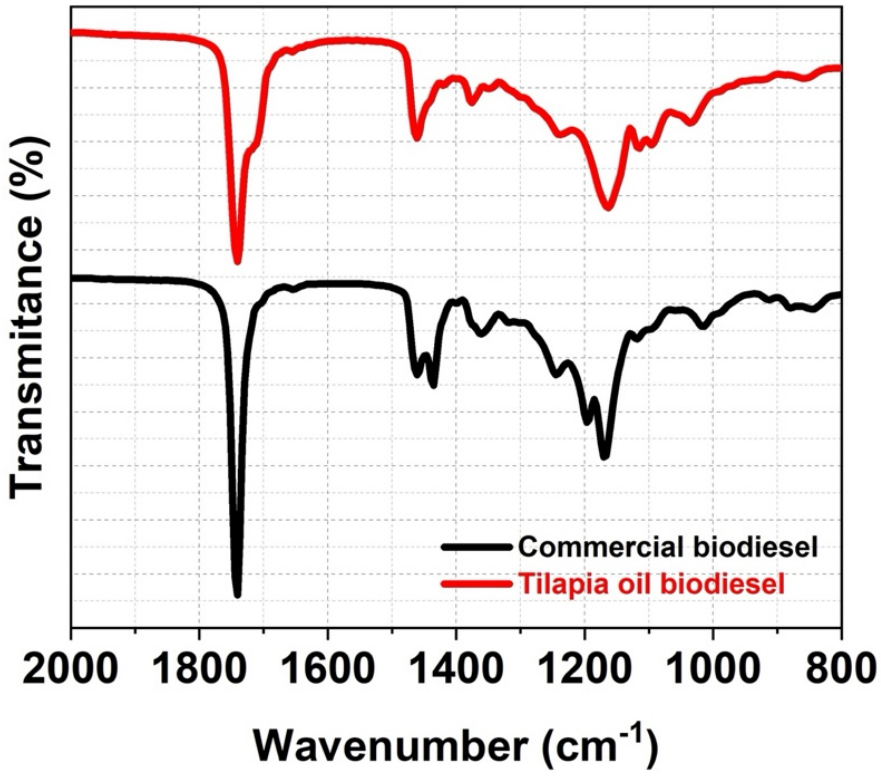

Source: the author.

The ^1H NMR spectrum (500 MHz, $CDCl_3$) further validates the esterification process (Figure 36). A key peak at 4.10 ppm corresponds to methylene hydrogens adjacent to the ester oxygen (O-CH_2), indicative of ester formation (Valle et al., 2018). The peak at 2.28 ppm, attributed to alpha protons near the carbonyl group (C=O), also confirms the ester structure.

Peaks at 5.33 ppm and 2.00 ppm reflect unsaturated fatty acid residues, demonstrating that the biocatalytic process preserved the fatty acid structure while converting carboxylic acids into esters.

Figure 36 – NMR characterization of the biofuel (500 MHz, in $CDCl_3$).

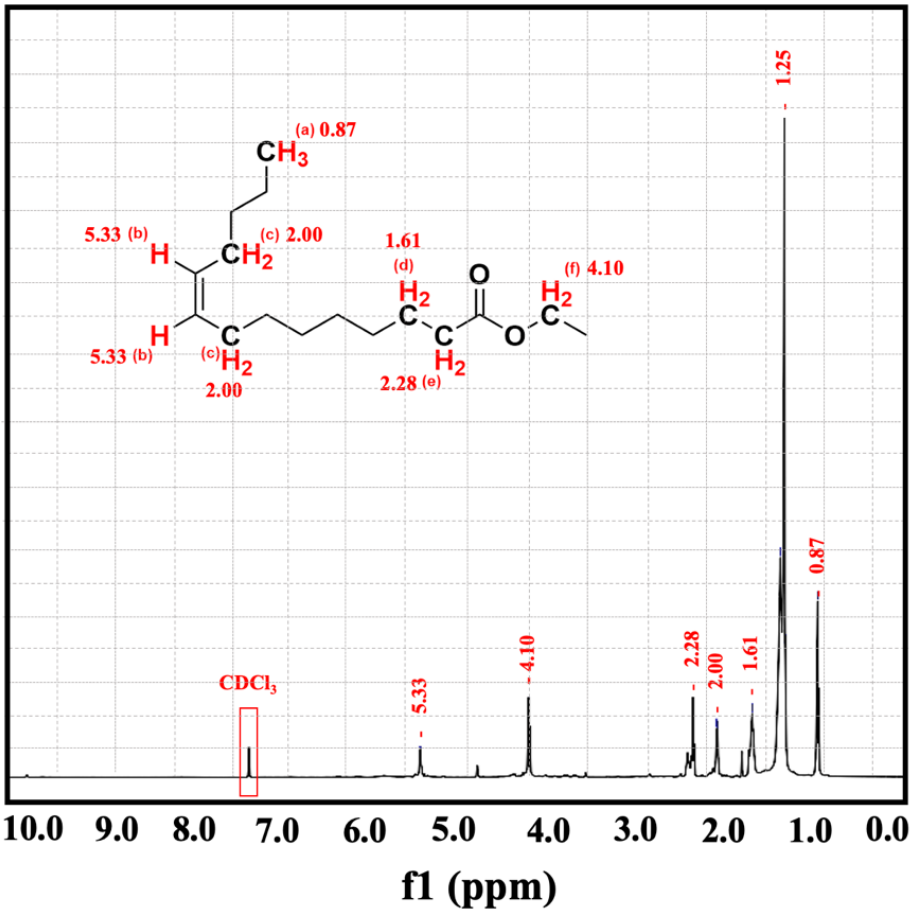

Source: the author.

The produced biodiesel exhibited a kinematic viscosity of 38 mm²/s (cSt) at 40 °C and a density of 0.90 g/cm³ at 20 °C. While the density aligns with ASTM D6751 and ANP Resolution No. 798 of 2019 (Brazilian resolution) standards, the viscosity exceeds the acceptable range for conventional biodiesel. According to the same resolution, the kinematic viscosity of biodiesel should be between 1.9 and 6.0 mm²/s at 40 °C. The higher viscosity may stem from the significant presence of saturated fatty acids and long-chain fatty acids like oleic acid in tilapia oil, which produce heavier esters (Valle et al., 2018; Mota et al., 2019). In addition, the presence of long-chain fatty acids, such as oleic acid, may also contribute to the increased viscosity of the biodiesel (Skowroń et al., 2015; Taherinia et al., 2024).

Although the produced biodiesel does not meet the ASTM and ANP requirements for

use in conventional combustion engines, it can be blended with biodiesel of lower viscosity and density (such as soybean oil biodiesel) to adjust its properties, a practice that is already applied in other biodiesel optimization processes (He et al., 2024; Sun et al., 2024). Another point is that in industrial or agricultural applications where the fuel is used in stationary engines with lower performance requirements, high-viscosity biodiesel may be viable (Alosius et al., 2022; Mendoza-Casseres et al., 2021).

4.3.5. Computational studies

Theoretical studies were conducted to explain the experimental results of esterification of a tilapia oil. According to gas chromatography-mass spectrometry (GC-MS) analysis, the content of the tilapia oil is: 6.3% octadecanoic acid (OD), 8.7% tetradecanoic acid (TD), 16% 9-hexadecenoic acid (9D), 27.1% 129exadecenoic acid (HD), and 41.9% 9-octadecenoic (9O or oleic) acid.

To investigate the binding affinity and structural interactions of CALB with various substrates, docking studies were performed using key fatty acids present in fish oil, as shown in Figure 37. The docking results reveal a clear trend: the binding affinity tends to increase with the length of the fatty acid chain. This pattern is due to the increasing number of hydrophobic interactions as chain length extends. The octadecanoic acid (OD) is the longest saturated fatty acid and exhibited the highest binding affinity, with a binding energy of -67.6 kcal/mol. It formed stable interactions with the hydrophobic residues Leu140, Ala141, Leu144, Val154, Ile189, Leu278, Ala281, Ala282 and Ile285. The 129exadecenoic (HD) and tetradecanoic (TD) acids, with shorter saturated chains, displayed binding energies of -59.9 and -55.1 kcal/mol respectively. The resulting reduction in hydrophobic contacts (Leu140 in HD, Leu140 and Val154 in TD) corresponds to their lower binding affinity compared to OD, supporting a trend where fewer hydrophobic interactions are associated with decreased binding energies as the chain length shortens.

Figure 37 – Optimized binding orientation of fatty acids in the active site of CALB, highlighting key interactions that stabilize substrate binding. Residues within 3 angstroms of each substrate are shown. Non-polar hydrogen atoms are omitted for clarity.

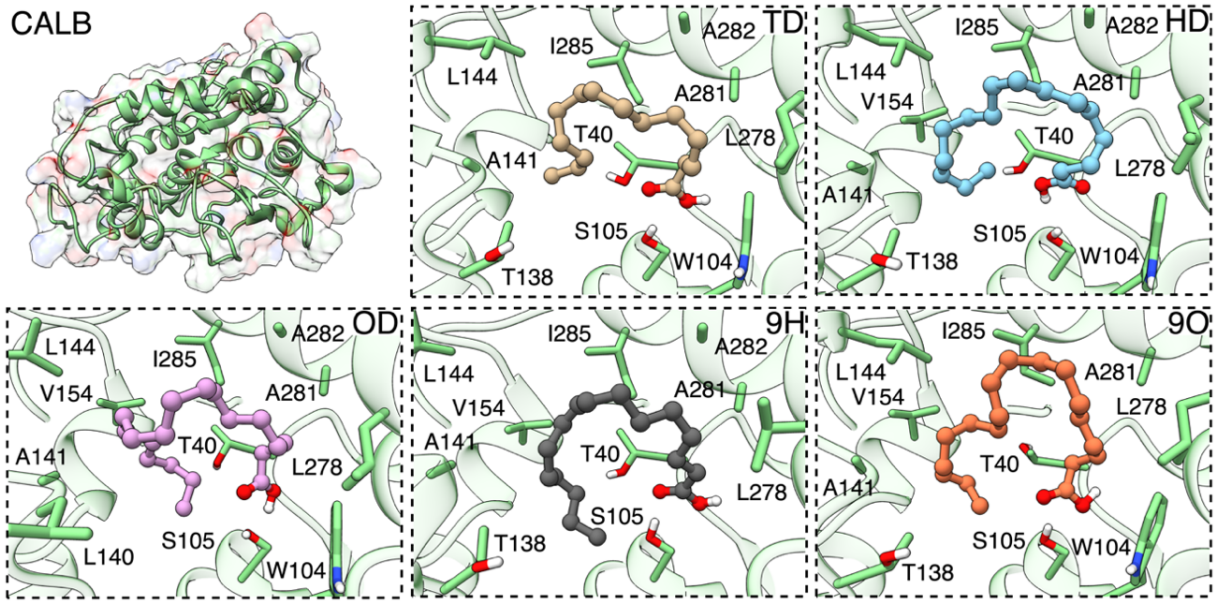

Source: the author.

The unsaturated fatty acids (9H and 9O) revealed a different binding orientation, primally due to the cis-double bond in their structure. This feature induced slight reorientation in the binding interaction, involving residues Thr138 (methyl group) and Val190. The unsaturated acids 9H and 9O displayed slightly lower binding affinities than their saturated counterpart (-57.3 kcal/mol and -61.1 kcal/mol, respectively). Their inferior binding energies are mostly due to loss of contact with the hydrophobic residues Leu144 and Ala141, in 9H, and Leu140 in 9O.

To identify the rate limiting step of the esterification mechanism catalyzed by CALB, we conducted QM/MM calculations using 9-octadecenoic acid (9O, oleic acid) as the substrate, given its high abundance in the original fish oil mixture. Ethanol (EtOH) was employed as the alcohol (acyl acceptor), since the esterification reaction produces the ester ethyl oleate, which is a known standard molecule for biodiesel (Zheng et al., 2017).

The esterification reaction begins with the nucleophilic residue Ser105 initiating an attack on the electrophilic carbonyl carbon atom of 9O, as shown in Figure 38. This step has a calculated Gibbs free energy barrier of 17.5 kcal/mol (associated with T1A) which is the rate limiting step of the entire mechanism. In this first transition state, residue His224 acts as a base, abstracting a proton from Ser105, and activating it as a nucleophile, while Asp187 assists by stabilizing His224 through hydrogen bonding (Uppenberg et al., 1994). This coordinated action

facilitates the formation of the intermediate IA, which is endergonic by 13.4 kcal/mol. In the unstable gem-diol intermediate IA structure, one additional hydrogen bond is formed with Thr40, which is the residue responsible for stabilizing the oxyanion hole.

Figure 38 – Mechanism of acylation catalyzed by CALB. The carbon atoms of the substrate (9O) are shown in orange and enzyme atoms are shown in green. Non-polar hydrogens are omitted for clarity. Bond lengths are displayed in angstroms, and Gibbs free energies are in kcal/mol, relative to the reactant (R_A).

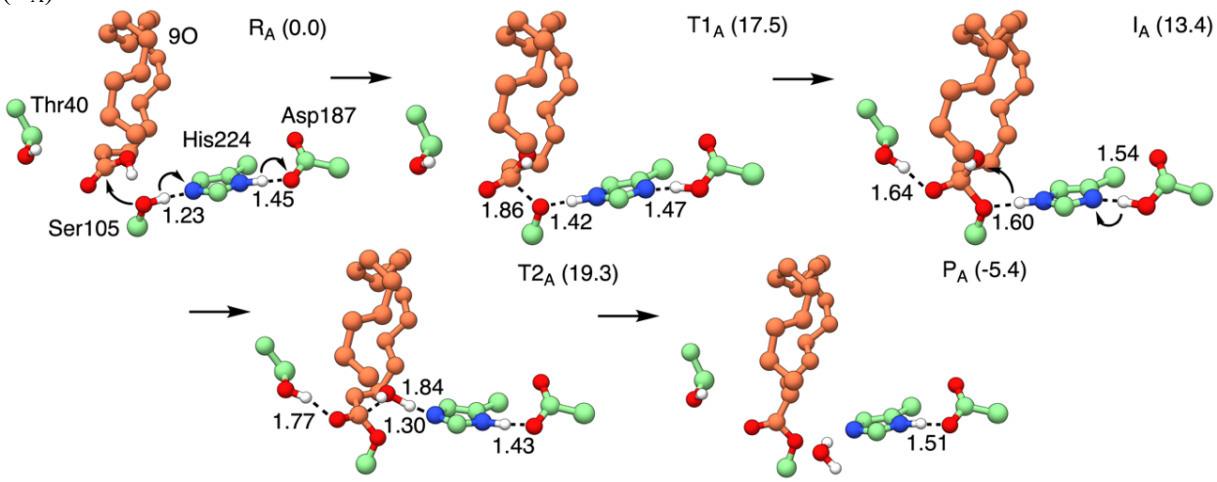

Source: the author.

In the second step of the acylation mechanism, the *gem*-diol intermediate undergoes a collapse to form the acyl-enzyme intermediate P_A. The transition state associated with this process ($T2_A$ in Figure 39) has a calculated Gibbs free energy of 19.3 kcal/mol (5.9 kcal/mol barrier from I_A). In $T2_A$, His224 now acts as a general acid, transferring a proton (previously acquired from Ser105 in $T1_A$) to the oxygen atom of the substrate, which causes water to be released. The acylation reaction is exergonic by 5.4 kcal/mol, indicating a thermodynamically favourable pathway for forming the acyl-enzyme intermediate.

In the deacylation step, the acyl-enzyme binds one molecule of ethanol (EtOH), which acts as the acyl acceptor to drive product formation, as shown in R_D in Figure 10. In the first stage of deacylation, EtOH performs a nucleophilic attack on the electrophilic carbonyl carbon atom of the acyl-enzyme intermediate. The transition state associated with this step ($T1_D$ in Figure 10) is endergonic by 16.8 kcal/mol. The electrophile-nucleophile distance in $T1_D$ resembles that in T1A (1.86 and 1.89 Å, respectively), accounting for their free energy values. Similarly to the acylation mechanism, this step also produces a *gem*-diol intermediate. However, I_D is endergonic by 8.8 kcal/mol, and 4.6 kcal/mol is more stable than I_A. Subsequently, the diol intermediate I_D collapses, requiring an additional free energy barrier of

3.3 kcal/mol ($T2_D$) to complete the reaction. Compared to acylation, the lower free energy barriers in the deacylation step can be attributed to the enhanced electrophilicity of the carbonyl carbon in the acyl-enzyme intermediate and the superior leaving group ability of the formed product. After this step, the catalytic cycle is completed, yielding the ester product (ethyl oleate P_D), which is 10.4 kcal/mol exergonic energy.

Figure 39 – Mechanism of deacylation catalyzed by CALB. The carbon atoms of the substrate (9O) are shown in orange, ethanol (EtOH) is shown in yellow, and enzyme atoms are shown in green. Non-polar hydrogens are omitted for clarity. Bond lengths are displayed in angstroms, and Gibbs free energies are in kcal/mol, relative to the reactant (R_D).

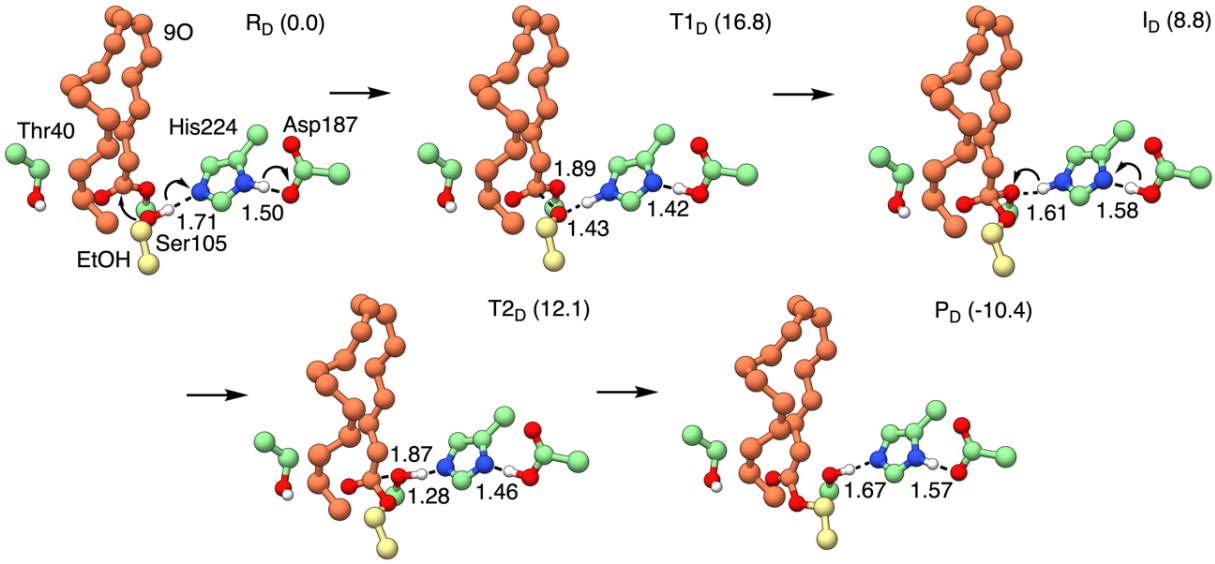

Source: the author.

4.3 Conclusion

The Fe_3O_4-PEI-DGEBA@CALB biocatalyst demonstrated excellent immobilization efficiency and catalytic performance, making it a promising tool for biodiesel production. The immobilization method achieved an immobilization yield of 97% using a protein loading of 20mg/g. The biocatalyst displayed exceptional stability, operating under varying pH and temperature conditions, retaining above 80% activity after 120 days of storage, and maintaining yields above 65% over ten reaction cycles, highlighting its reusability and economic viability.

Characterization techniques confirmed successful immobilization and the retention of desirable magnetic properties, enabling efficient separation and reuse. Characterization by TEM, SEM, XRF, XRD, FTIR, TGA, DTGA, and VSM confirmed the immobilization of CALB. The biocatalyst showed a magnetization of 52.3 emu/g and superparamagnetic

behaviour, with very low hysteresis (0.05 kOe), indicating negligible remanent magnetization and an insignificant coercive field, desirable characteristics for catalytic and magnetic separation applications.

The esterification of tilapia oil using the biocatalyst resulted in biodiesel with properties comparable to commercial standards, including key FTIR and NMR signals indicative of ester formation. The biocatalyst esterified tilapia oil with an initial yield of 98.8%, achieving ten esterification cycles with yields more significant than 65%. The kinematic viscosity and density of the biodiesel were 38 mm^2/s at 40°C and 0.90 g/cm^3 at 20°C. Although the produced biodiesel's viscosity exceeded ASTM and ANP standards for direct use in combustion engines, it holds significant potential for blending with less viscous biodiesels or for application in stationary engines, furnaces, and boilers.

Molecular docking and QM/MM calculations revealed CALB's substrate specificity, favouring long-chain saturated fatty acids due to enhanced hydrophobic interactions with key residues. These findings emphasize CALB's substrate promiscuity and efficiency in catalyzing esterification reactions. Hybrid QM/MM calculations identified the nucleophilic attack step in the acylation mechanism as the rate-limiting step in biodiesel synthesis catalyzed by CALB, with a free energy activation barrier of 17.5 kcal/mol. The insights gained underscore the potential of Fe_3O_4-PEI-DGEBA@CALB as a sustainable and effective biocatalyst for biodiesel production, supporting its broader application in green chemistry and industrial biocatalysis.

CHAPTER V

5 GENERAL CONCLUSIONS

This thesis integrated theoretical, experimental, and computational approaches for the development of magnetic biocatalysts based on lipases, focusing on environmentally relevant reactions such as the production of sustainable biofuels and biolubricants.

Chapter II, demonstrated the growing scientific and industrial interest in the field, with emphasis on applications in biofuel production through enzymatic catalysis of vegetable oils. Emerging application areas were also identified, including biosensors, medicine, and environmental remediation. Despite advancements, challenges such as synthesis complexity and efficient enzyme immobilization remain, encouraging the development of new functional supports.

Chapter III, a magnetic nanobiocatalyst (Fe_3O_4-PEI-DGEBA@EVS) was developed, showing high immobilization yield (95.04%) and excellent stability, maintaining over 90% of its activity after 60 days. The system performed efficiently in the esterification of fatty acids from babassu oil, reaching up to 97.91% yield and maintaining performance over ten reuse cycles. In silico studies confirmed the stability of enzyme–substrate interactions.

Chapter IV, *Candida antarctica* lipase B (CALB) was immobilized on the same support, forming the biocatalyst Fe_3O_4-PEI-DGEBA@CALB. The system achieved 97% immobilization, high stability with 80% activity after 120 days, and yields above 65% over ten esterification cycles of tilapia oil. Computational analyses revealed selectivity for long-chain saturated fatty acids and an energy barrier consistent with the observed catalytic efficiency.

The results confirm the potential of the developed biocatalysts as viable solutions for sustainable enzymatic catalysis. The combination of efficiency, stability, reusability, and magnetic separation reinforces their industrial applicability. Future studies may explore new magnetic materials and co-immobilization strategies to further expand the scope and applications of these systems.

6 SCIENTIFIC PRODUCTION

6.1 Published articles

1. **Melo, Rafael Leandro Fernandes**; Nascimento Dari, Dayana; Da Silva Aires, Francisco Izaias; Simão Neto, Francisco; Freire, Tiago Melo; Fernandes, Bruno Caio Chaves; Fechine, Pierre Basílio Almeida; Soares, João Maria; Sousa Dos Santos, José Cleiton. *Global Advancements in Bioactive Material Manufacturing for Drug Delivery: A Comprehensive Study*. **ACS Omega**, v. 10, p. 1207-1225, 2025.
2. De Castro Bizerra, Viviane; Sales, Misael Bessa; **Fernandes Melo, Rafael Leandro**; Andrade Do Nascimento, Jean Gleison; Junior, João Brandão; França Silva, Michael Pablo; Moreira Dos Santos, Kaiany; Da Silva Sousa, Patrick; Marques Da Fonseca, Aluísio; De Souza, Maria Cristiane Martins; Sousa Dos Santos, José Cleiton. *Opportunities for cleaner leather processing based on protease enzyme: Current evidence from an advanced bibliometric analysis*. **RENEWABLE & SUSTAINABLE ENERGY REVIEWS**, v. 191, p. 114162, 2024.
3. **Melo, Rafael Leandro Fernandes**; Neto, Francisco Simão; Dari, Dayana Nascimento; Fernandes, Bruno Caio Chaves; Freire, Tiago Melo; Fechine, Pierre Basílio Almeida; Soares, João Maria; Dos Santos, José Cleiton Sousa. *A comprehensive review on enzyme-based biosensors: Advanced analysis and emerging applications in nanomaterial-enzyme linkage*. **INTERNATIONAL JOURNAL OF BIOLOGICAL MACROMOLECULES**, v. 264, p. 130817, 2024.
4. **Melo, Rafael Leandro Fernandes**; Freire, Tiago Melo; Valério, Roberta Bussons Rodrigues; Neto, Francisco Simão; De Castro Bizerra, Viviane; Fernandes, Bruno Caio Chaves; De Sousa Junior, Paulo Gonçalves; Da Fonseca, Aluísio Marques; Soares, João Maria; Fechine, Pierre Basílio Almeida; Dos Santos, José Cleiton Sousa. *Enhancing biocatalyst performance through immobilization of lipase (Eversa® Transform 2.0) on hybrid amine-epoxy core-shell magnetic nanoparticles*. **INTERNATIONAL JOURNAL OF BIOLOGICAL MACROMOLECULES**, v. 264, p. 130730, 2024.
5. Lima, Paula; Silva, Jouciane; **Melo, Rafael**; Neto, Francisco; Fechine, Pierre; Rocha, Maria; Gonçalves, Luciana; Dos Santos, José. *Dimensioning of vinylsulfonic supports from cashew apple bagasse biomass in the immobilization of lipases*. **QUIMICA NOVA**, v. 47, p. 1-11, 2024.
6. Dos Santos, Kaiany Moreira; De França Serpa, Juliana; De Castro Bizerra, Viviane; Melo, **Rafael Leandro Fernandes**; Sousa Junior, Paulo Gonçalves De; Santos Alexandre, Valdilane; Da Fonseca, Aluísio Marques; Fechine, Pierre Basílio Almeida; Lomonaco, Diego; Sousa Dos Santos, José Cleiton; Martins De Souza, Maria Cristiane. *Enhanced Biodiesel Production with Eversa Transform 2.0 Lipase on Magnetic Nanoparticles*. **LANGMUIR**, v. 40, p. 26835-26851, 2024.
7. De Menezes, Fernando Lima; Freire, Tiago Melo; De Castro Monteiro, Rodolpho Ramilton; Antunes, Renato Altobelli; Melo, **Rafael Leandro Fernandes**; Freire, Rafael Melo; Dos Santos, José Cleiton Sousa; Fechine, Pierre Basílio Almeida. *L-cysteine-*

coated magnetite nanoparticles as a platform for enzymes immobilization: Amplifying biocatalytic activity of Candida antarctica Lipase A. **MATERIALS RESEARCH BULLETIN**, v. 177, p. 112882, 2024.

8. Sales, Misael Bessa; Neto, José Gadelha Lima; De Sousa Braz, Ana Kátia; De Sousa Junior, Paulo Gonçalves; **Melo, Rafael Leandro Fernandes**; Valério, Roberta Bussons Rodrigues; Serpa, Juliana De França; Da Silva Lima, Ana Michele; De Lima, Rita Karolinny Chaves; Guimarães, Artemis Pessoa; De Souza, Maria Cristiane Martins; Lopes, Ada Amélia Sanders; Rios, Maria Alexsandra De Sousa; Serafim, Leonardo Farias; Dos Santos, José Cleiton Sousa. *Trends and Opportunities in Enzyme Biosensors Coupled to Metal-Organic Frameworks (MOFs): An Advanced Bibliometric Analysis*. **Electrochem**, v. 4, p. 181-211, 2023.
9. Da Silva, Jessica Lopes; Sales, Misael Bessa; De Castro Bizerra, Viviane; Nobre, Millena Mara Rabelo; De Sousa Braz, Ana Kátia; Da Silva Sousa, Patrick; Cavalcante, Antônio L. G.; **Melo, Rafael L. F**.; Gonçalves De Sousa Junior, Paulo; Neto, Francisco S.; Da Fonseca, Aluísio Marques; Santos, José Cleiton Sousa Dos. *Lipase from Yarrowia lipolytica: Prospects as an Industrial Biocatalyst for Biotechnological Applications*. **Fermentation-Basel**, v. 9, p. 581, 2023.
10. Nobre, Millena Mara Rabelo; Silva, Ananias Freire Da; Menezes, Amanda Maria; Silva, Francisco Lennon Barbosa Da; Lima, Iesa Matos; Colares, Regilany Paulo; Souza, Maria Cristiane Martins De; Marinho, Emmanuel Silva; Melo, **Rafael Leandro Fernandes**; Santos, José Cleiton Sousa Dos; Da Fonseca, Aluísio Marques. *Ester Production Using the Lipid Composition of Coffee Ground Oil (Coffea arabica): A Theoretical Study of Eversa® Transform 2.0 Lipase as an Enzymatic Biocatalyst*. **Compounds**, v. 3, p. 411-429, 2023.
11. Neto, Francisco Simão; Melo Neta, Maria; Sousa, Ana; Damasceno, Luana; Sousa, Bruna; Medeiros, Samuel; **Melo, Rafael**; Lopes, Ada; Santos, José; Rios, Maria. *Analysis of the Fuel Properties of the Seed Shell of the Neem Plant (Azadirachta indica)*. **PROCESSES**, v. 11, p. 2442, 2023.
12. **Melo, Rafael Leandro Fernandes**; Sales, Misael Bessa; De Castro Bizerra, Viviane; De Sousa Junior, Paulo Gonçalves; Cavalcante, Antônio Luthierre Gama; Freire, Tiago Melo; Neto, Francisco Simão; Bilal, Muhammad; Jesionowski, Teofil; Soares, João Maria; Fechine, Pierre Basílio Almeida; Dos Santos, José Cleiton Sousa. *Recent applications and future prospects of magnetic biocatalysts*. **INTERNATIONAL JOURNAL OF BIOLOGICAL MACROMOLECULES**, v. 253, p. 126709, 2023.

6.2 Submitted articles

1. **Melo, Rafael Leandro Fernandes**; Neto, Francisco Simão; Fernandes, Bruno Caio Chaves; Sousa Junior, Paulo Gonçalves; Freire, Tiago Melo; Valença, Raniere Dantes; Do Carmo, Frederico Ribeiro; Da Silva, Marcos Reinaldo; Serafim, Leonardo Farias; Soares, João Maria; Fechine, Pierre Basílio Almeida; Dos Santos, José Cleiton Sousa. *Bioenergy Conversion Of Residual Tilapia Oil Using A Novel Immobilized Lipase: Enhanced Stability, Selectivity, And Computational Insights. MOLECULAR CATALYSIS.*

REFERENCES

ABD WAFTI, N. S. et al. Enzymatic synthesis of palm oil-based trimethylolpropane ester as biolubricant base stock catalyzed by Lipozyme 435. **Energy**, v. 260, n. July, p. 125061, 2022.

AFEDZI, A. E. K. et al. Valorization of Ghanaian cocoa processing residues as extractives for value-added functional food and animal feed additives – A review. **Biocatalysis and Agricultural Biotechnology**, v. 52, p. 102835, 2023.

AFZALIPOUR, R. et al. Thermosensitive magnetic nanoparticles exposed to alternating magnetic field and heat-mediated chemotherapy for an effective dual therapy in rat glioma model. **Nanomedicine: Nanotechnology, Biology, and Medicine**, v. 31, 2021.

AGHAEI, H.; YASINIAN, A.; TAGHIZADEH, A. Covalent immobilization of lipase from Candida rugosa on epoxy-activated cloisite 30B as a new heterofunctional carrier and its application in the synthesis of banana flavor and production of biodiesel. **International Journal of Biological Macromolecules**, v. 178, p. 569–579, 2021.

AGUIEIRAS, E. C. G. et al. Investigation of the Reuse of Immobilized Lipases in Biodiesel Synthesis: Influence of Different Solvents in Lipase Activity. **Applied Biochemistry and Biotechnology**, v. 179, n. 3, p. 485–496, 2016.

AHMADI, M. et al. Chem3D 15.0 User Guide. **Macromolecules**, v. 24, n. 2, p. 1–61, 2005.

AHMED, R.; HUDDERSMAN, K. Journal of Industrial and Engineering Chemistry Review of biodiesel production by the esterification of wastewater containing fats oils and grease (FOGs). **Journal of Industrial and Engineering Chemistry**, v. 110, p. 1–14, 2022.

ÅKERMAN, C. O. et al. Biolubricant synthesis using immobilised lipase: Process optimisation of trimethylolpropane oleate production. **Process Biochemistry**, v. 46, n. 12, p. 2225–2231, 2011.

AKHLAGHI, N.; NAJAFPOUR-DARZI, G. Preparation of immobilized lipase on Co 2 + - chelated carboxymethyl cellulose based $MnFe_2O_4$ magnetic nanocomposite particles. **Molecular Catalysis**, v. 519, n. December 2021, p. 112118, 2022.

ALEXANDRE, J. Y. N. H. et al. A theoretical and experimental study for enzymatic biodiesel production from babassu oil (Orbignya sp.) using Eversa lipase. **Catalysts**, v. 12, n. 11, p. 1322, 2022.

ALEXIOU, C. Emerging applications of magnetic nanoparticles in medicine – a personal perspective. **Biochemical and Biophysical Research Communications**, v. 633, p. 1–5, 2022.

ALI, A. et al. Review on recent progress in magnetic nanoparticles: synthesis, characterization, and diverse applications. **Nanomaterials**, v. 9, n. 7, p. 1–25, 2021.

ALIKHANI, N. et al. A multi - component approach for co - immobilization of lipases on silica - coated magnetic nanoparticles: improving biodiesel production from waste cooking oil. **Bioprocess and Biosystems Engineering**, v. 45, n. 12, p. 2043–2060, 2022.

ALJASHAAMI, B. A. et al. Recent improvements to heating, ventilation, and cooling technologies for buildings based on renewable energy to achieve zero-energy buildings: A systematic review. **Results in Engineering**, v. 23, p. 102769, 2024.

ALTSCHUL, S. F. et al. Basic local alignment search tool. **Journal of Molecular Biology**, v. 215, n. 3, 1990.

AMRUTH MAROJU, P.; GANESAN, R.; RAY DUTTA, J. Biofuel generation from food waste through immobilized enzymes on magnetic nanoparticles. **Materials Today: Proceedings**, v. 72, p. 62–66, 2023.

DELANO, W. L. Immobilization of enzymes on clay minerals for biocatalysts and biosensors. **Applied Clay Science**, v. 114, p. 283–296, 2015.

ANDRADES, D. DE et al. International Journal of Biological Macromolecules Immobilization and stabilization of different β -glucosidases using the glutaraldehyde chemistry: Optimal protocol depends on the enzyme Observed activity. **International Journal of Biological Macromolecules**, v. 129, p. 672–678, 2019.

ANDRÉS-SANZ, D. et al. Enantiodivergent biosynthesis of β-hydroxy esters by self-sufficient heterogeneous biocatalysts in a continuous flow. **Green Chemistry**, v. 26, n. 8, p. 4563–4573, 2024.

ANGULO, B. et al. Comparison of chemical and enzymatic methods for the transesterification of waste fish oil fatty ethyl esters with different alcohols. **Fuel Processing Technology**, v. 206, p. 106–122, 2020.

ANTO ALOSIUS, M. et al. Effects of injection parameters on CRDI-equipped stationary diesel engine fuelled with neat biodiesel mix derived from waste feedstocks. **Transactions of The Canadian Society for Mechanical Engineering**, v. 47, n. 1, p. 54–61, 2022.

ANWAR, M. Z. et al. SnO2 hollow nanotubes: A novel and efficient support matrix for enzyme immobilization. **Scientific Reports**, v. 7, n. 1, p. 1–11, 2017.

ARANA-PEÑA, S. et al. Immobilization of lipases via interfacial activation on hydrophobic supports: Production of biocatalysts libraries by altering the immobilization conditions. **Catalysis Today**, v. 362, n. April 2020, p. 130–140, 2021.

ARCON, J. P. et al. Molecular Dynamics in Mixed Solvents Reveals Protein-Ligand Interactions, Improves Docking, and Allows Accurate Binding Free Energy Predictions. **Journal of Chemical Information and Modeling**, v. 57, n. 4, p. 846–863, 2017.

AROKIARAJ, R. G. et al. Excess thermodynamic properties and FTIR studies of binary mixtures of aniline with esters at different temperatures. **Chemical Data Collections**, v. 37, p. 100807, 2022.

ARSHIA, A. H. et al. De novo design of novel protease inhibitor candidates in the treatment of SARS-CoV-2 using deep learning, docking, and molecular dynamic simulations. **Computers in Biology and Medicine**, v. 139, 2021.

ASHWINI JOHN, J.; SAMUEL, M. S.; SELVARAJAN, E. Immobilized cellulase on Fe_3O_4/GO/CS nanocomposite as a magnetically recyclable catalyst for biofuel application. **Fuel**, v. 333, n. P1, p. 126364, 2023.

ATİROĞLU, V. Lipase immobilization on synthesized hyaluronic acid-coated magnetic nanoparticle-functionalized graphene oxide composites as new biocatalysts: Improved reusability, stability, and activity. **International Journal of Biological Macromolecules**, v. 145, p. 456–465, 2020.

AWAD, A. et al. Evaluation of different saccharides and chitin as eco-friendly additive to improve the magnetic cross-linked enzyme aggregates (CLEAs) activities. **International Journal of Biological Macromolecules**, v. 118, p. 2040–2050, 2018.

AWAD, G. E. A. et al. Functionalized κ-carrageenan/hyperbranched poly(amidoamine)for protease immobilization: Thermodynamics and stability studies. **International Journal of Biological Macromolecules**, v. 148, p. 1140–1155, 2020.

AZAD, S. AL et al. Machine learning-driven optimization of pretreatment and enzymatic hydrolysis of sugarcane bagasse: Analytical insights for industrial scale-up. **Fuel**, v. 390, p. 134682, 2025.

BAAZIZ, W. et al. Magnetic iron oxide nanoparticles: Reproducible tuning of the size and nanosized-dependent composition, defects, and spin canting. **Journal of Physical Chemistry C**, v. 118, n. 7, p. 3795–3810, 2014.

BABAKI, M. et al. Effect of water, organic solvent and adsorbent contents on production of biodiesel fuel from canola oil catalyzed by various lipases immobilized on epoxy-functionalized silica as low-cost biocatalyst. **Journal of Molecular Catalysis B: Enzymatic**, v. 120, p. 93–99, 2015.

BABAKI, M. et al. Preparation of highly reusable biocatalysts by immobilization of lipases on epoxy-functionalized silica for production of biodiesel from canola oil. **Biochemical Engineering Journal**, v. 101, p. 23–31, 2015.

BAHARI, M. B. et al. Materials Today: Proceedings Development of fibrous mesoporous silica for catalytic reaction: A short review. **Materials Today: Proceedings**, v. 42, p. 33–38, 2021.

BAI, Q. et al. MolAICal: a soft tool for 3D drug design of protein targets by artificial intelligence and classical algorithm. **Briefings in bioinformatics**, v. 22, n. 3, p. 1–12, 2021.

BANTIHUN, G. et al. Biocatalyst application of newly isolated Enterococcus species using microbial fuel cell (MFC) in wastewater treatment. **Environmental Technology & Innovation**, v. 38, p. 104090, 2025.

BARBOSA, O. et al. Versatility of glutaraldehyde to immobilize lipases: Effect of the immobilization protocol on the properties of lipase B from Candida antarctica. **Process Biochemistry**, v. 47, n. 8, p. 1220–1227, 2012.

BAYRAMOGLU, G. et al. Immobilization of Candida rugosa lipase on magnetic chitosan beads and application in flavor esters synthesis. **Food Chemistry**, v. 366, n. July 2021, p. 130699, 2022.

BEDOYA, O. F.; TISCHER, I. Detección de homología remota de proteínas usando modelos 3D enriquecidos con propiedades fisicoquímicas. **INGENIERÍA Y COMPETITIVIDAD**, v. 17, n. 1, 2015.

BEN HLIMA, H. et al. Molecular and Structural Characterizations of Lipases from Chlorella by Functional Genomics. **Marine drugs**, v. 19, n. 2, p. 1–16, 2021.

BEN-TAL, N. et al. Association entropy in adsorption processes. **Biophysical Journal**, v. 79, n. 3, p. 1180–1187, 2000.

BEN-YOUSSEF, C. et al. Simultaneous esterification/transesterification of waste cooking oil and Jatropha curcas oil with MOF-5 as a heterogeneous acid catalyst. **International Journal of Environmental Science and Technology**, v. 18, n. 11, p. 3313–3326, 2021.

BERETTA, G. P. The fourth law of thermodynamics: Steepest entropy ascent. **Philosophical Transactions of the Royal Society A: Mathematical, Physical and Engineering Sciences**, v. 378, n. 2170, p. 1–17, 2020.

BEZERRA, R. DE C. DE F. et al. Babassu-oil-based biolubricant: Chemical characterization and physicochemical behavior as additive to naphthenic lubricant NH-10. **Industrial Crops and Products**, v. 154, n. June, p. 112624, 2020.

BEZERRA, R. M. et al. Enzyme and Microbial Technology A new heterofunctional support for enzyme immobilization: PEI functionalized Fe_3O_4 MNPs activated with divinyl sulfone . Application in the immobilization of lipase from Thermomyces lanuginosus. **Enzyme and Microbial Technology**, v. 138, n. March, p. 109560, 2020.

BEZZEKHAMI, M. A. et al. Facile and eco-friendly method of starch nanocrystals esterified with oleic acid using natural clay as a catalyst: Synthesis, Box-Behnken optimization, characterization and analysis of thermal and antioxidant properties. **International Journal of Biological Macromolecules**, v. 292, p. 139295, 2025.

BILAL, M. et al. Magnetic nanoparticles as versatile carriers for enzymes immobilization: A review. **International Journal of Biological Macromolecules**, v. 120, p. 2530–2544, 2018.

BILAL, M. et al. “Smart” chemistry and its application in peroxidase immobilization using different support materials. **International Journal of Biological Macromolecules**, v. 119, p. 278–290, 2018.

BILAL, M. et al. Immobilized lipases-based nano-biocatalytic systems — A versatile platform with incredible biotechnological potential. **International Journal of Biological Macromolecules**, v. 175, p. 108–122, 2021.

BINHAYEEDING, N. et al. Immobilisation of Candida rugosa lipase on polyhydroxybutyrate via a combination of adsorption and cross-linking agents to enhance acylglycerol production. **Process Biochemistry**, v. 95, n. January, p. 174–185, 2020.

BÔA MORTE, E. F. et al. Modified magnetite nanoparticle as biocatalytic support for magnetically stabilized fluidized bed reactors. **Journal of Materials Research and Technology**, v. 14, p. 1112–1125, 2021.

BORGHEI, Y. S.; HOSSEINKHANI, S.; GANJALI, M. R. Engineering in modern medicine using magnetic nanoparticles in understanding physicochemical interactions at the nano–bio interfaces. **Materials Today Chemistry**, v. 24, p. 100870, 2022.

BRÊDA, G. C. et al. Current approaches to use oil crops by-products for biodiesel and biolubricant production: Focus on biocatalysis. **Bioresource Technology Reports**, v. 18, p. 101030, 2022.

BRESOLIN, D. et al. Immobilization of lipase Eversa Transform 2.0 on poly(urea–urethane) nanoparticles obtained using a biopolyol from enzymatic glycerolysis. **Bioprocess and Biosystems Engineering**, v. 43, n. 7, 2020.

BUSINESS RESEARCH INSIGHTS. Biocatalysis – biocatalysts market. Available at: https://www.businessresearchinsights.com/market-reports/biocatalysis-biocatalysts-market-114967. Accessed on: 28 mar. 2025.

BYLÉHN, F. et al. Modeling the Binding Mechanism of Remdesivir, Favilavir, and Ribavirin to SARS-CoV-2 RNA-Dependent RNA Polymerase. **ACS Central Science**, v. 7, n. 1, p. 164–174, 2021.

CABEZAS, J. T. et al. Combining the mechanical ball milling of the carbohydrate and the use of low solvent reaction media for the synthesis of fructose fatty acid esters by immobilized lipases. **New Biotechnology**, v. 70, n. April, p. 93–101, 2022.

CAI, J. et al. Enzymatic biofuel cell: A potential power source for self-sustained smart textiles. **iScience**, v. 27, n. 2, p. 108998, 2024.

CALIFANO, V. et al. m-DOPA addition in MAPLE immobilization of lipase for biosensor applications. **Sensing and Bio-Sensing Research**, v. 6, p. 103–108, 2015.

CAO, J. et al. Tuning the electronic properties of supported Cu catalysts for efficient epoxidation of long-chain α -olefins. **Fuel**, v. 342, n. December 2022, p. 127829, 2023.

CAO, X. et al. One-step direct transesterification of wet yeast for biodiesel production catalyzed by magnetic nanoparticle-immobilized lipase. **Renewable Energy**, v. 171, p. 11–21, 2021.

CAO, Y. et al. Rationally designed Fe-MCM-41 by protein size to enhance lipase immobilization, catalytic efficiency and performance. **Applied Catalysis A: General**, v. 478, p. 175–185, 2014.

CAO, Y. et al. Colloids and Surfaces B: Biointerfaces PEI-crosslinked lipase on the surface of magnetic microspheres and its characteristics. **Colloids and Surfaces B: Biointerfaces**, v. 189, n. February, p. 110874, 2020.

CAROLINE, P. et al. Biodiesel from babassu oil: Characterization of the product obtained by enzymatic route accelerated by microwave irradiation. **Industrial Crops & Products**, v. 52, p. 313–320, 2014.

CARVALHO, T. et al. Simple physical adsorption technique to immobilize Yarrowia lipolytica lipase purified by different methods on magnetic nanoparticles: adsorption isotherms and thermodynamic approach. **International Journal of Biological Macromolecules**, v. 160, p. 889–902, 2020.

CASAS-GODOY, L.; DUQUESNE, S.; BORDES, F. Lipases and Phospholipases. **Methods Mol Biol**, v. 861, p. 3–30, 2012.

CASSIA, R. DE et al. Industrial Crops & Products Babassu-oil-based biolubricant: Chemical characterization and physicochemical behavior as additive to naphthenic lubricant NH-10. **Industrial Crops & Products**, v. 154, n. November 2019, p. 112624, 2020.

CATUMBA, B. D. et al. Sustainability and challenges in hydrogen production: an advanced bibliometric analysis. **International Journal of Hydrogen Energy**, v. 47, n. 63, p. 26789–26809, 2022.

CAVALCANTE, A. L. G. et al. Chemical modification of clay nanocomposites for the improvement of the catalytic properties of Lipase A from Candida antarctica. **Process Biochemistry**, v. 120, p. 1–14, 2022.

CAVALCANTE, F. et al. A stepwise docking and molecular dynamics approach for enzymatic biolubricant production using lipase Eversa® Transform as a biocatalyst. **Industrial Crops & Products**, v. 187, p. 115498, 2022.

CAVALCANTI, E. D. C. et al. Improved production of biolubricants from soybean oil and different polyols via esterification reaction catalyzed by immobilized lipase from Candida rugosa. **Fuel**, v. 215, n. October 2017, p. 705–713, 2018.

CAVALLARI, M. et al. Partially folded states of HIV-1 protease: Molecular dynamics simulations and ligand binding. **Journal of Molecular Structure: THEOCHEM**, v. 769, n. 1–3, p. 111–121, 2006.

CEN, Y. et al. Artificial cysteine-lipases with high activity and altered catalytic mechanism created by laboratory evolution. **Nature Communications**, v. 10, n. 1, 2019.

CESARINI, S.; DIAZ, P.; NIELSEN, P. M. Exploring a new, soluble lipase for FAMEs production in water-containing systems using crude soybean oil as a feedstock. **Process Biochemistry**, v. 48, n. 3, p. 484–487, 2013.

CHAKRABORTY, D. et al. Sustainable enzymatic treatment of organic waste in a framework of circular economy. **Bioresource Technology**, v. 370, n. October 2022, p. 128487, 2023.

CHANG, M. Y.; CHAN, E. S.; SONG, C. P. Biodiesel production catalysed by low-cost liquid enzyme Eversa® Transform 2.0: Effect of free fatty acid content on lipase methanol tolerance and kinetic model. **Fuel**, v. 283, n. August 2020, p. 119266, 2021.

CHARACTERISTICS, I. A general overview of support materials for enzyme immobilization: characteristics, properties, practical utility. **International Journal of Molecular Sciences**, v. 19, n. 2, p. 412, 2018.

CHATURVEDI, S. K. et al. Unraveling comparative anti-amyloidogenic behavior of pyrazinamide and D-Cycloserine: A mechanistic biophysical insight. **PLoS ONE**, v. 10, n. 8, p. 1–21, 2015.

CHAVAN, N. et al. Magnetic nanoparticles – a new era in nanotechnology. **Journal of Drug Delivery Science and Technology**, v. 77, p. 103799, 2022.

CHEN, J. et al. Efficient and sustainable preparation of cinnamic acid flavor esters by immobilized lipase microarray. **LWT**, v. 173, n. September 2022, p. 114322, 2023.

CIPOLATTI, E. P. et al. Journal of Molecular Catalysis B: Enzymatic Current status and trends in enzymatic nanoimmobilization. **Journal of Molecular Catalysis. B, Enzymatic**, v. 99, p. 56–67, 2014.

COELHO, G. et al. Current approaches to use oil crops by-products for biodiesel and biolubricant production: focus on biocatalysis. **Bioresource Technology Reports**, v. 18, p. 101037, 2022.

CRUZ-MARTÍNEZ, Y. A. et al. Effect of adsorption/desorption of substrates/products during isobutyl propionate synthesis over CalB Immo Plus^{TM} in solid/gas biocatalysis. **Biochemical Engineering Journal**, v. 208, p. 109341, 2024.

CUADRADO-OSORIO, P. D. et al. Bioresource Technology Reports Agro-industrial residues for microbial bioproducts: A key booster for bioeconomy. **Bioresource Technology Reports**, v. 20, n. September, p. 101232, 2022.

CUI, C. et al. Colloids and Surfaces B: Biointerfaces Synergistic effects of amine and protein modified epoxy-support on immobilized lipase activity. **Colloids and Surfaces B: Biointerfaces**, v. 133, p. 51–57, 2015.

DA SILVA, G. A. R. et al. Ethyl esters synthesis catalyzed by lipase B from Candida antarctica immobilized on $NiFe_2O_4$ magnetic nanoparticles. **Catalysis Today**, p. 115099, 2024.

DA SILVA, M. V. C. et al. Synthesis of 2-ethylhexyl oleate catalyzed by Candida antarctica lipase immobilized on a magnetic polymer support in continuous flow. **Bioprocess and Biosystems Engineering**, v. 43, n. 4, p. 615–623, 2020.

DAMASCENO, B. S.; DA SILVA, A. F. V.; DE ARAÚJO, A. C. V. Dye adsorption onto magnetic and superparamagnetic Fe3O4nanoparticles: A detailed comparative study. **Journal of Environmental Chemical Engineering**, v. 8, n. 5, p. 103994, 2020.

DAOU, T. J. et al. Hydrothermal synthesis of monodisperse magnetite nanoparticles. **Chemistry of Materials**, v. 18, n. 18, p. 4399–4404, 2006.

DASGUPTA, D.; MANDALAPARTHY, V.; JAYARAM, B. A component analysis of the free energies of folding of 35 proteins: A consensus view on the thermodynamics of folding at the molecular level. **Journal of Computational Chemistry**, v. 38, n. 32, p. 2791–2801, 2017.

DE, H. et al. Influence of ammonium salts on the lipase/esterase activity assay using p-nitrophenyl esters as substrates. **International Union of Biochemistry and Molecular Biology, Inc**, v. 60, n. 3, p. 343–347, 2013.

DE MELO, D. W.; FERNANDEZ-LAFUENTE, R.; RODRIGUES, R. C. Enhancing biotechnological applications of l-asparaginase: Immobilization on amino-epoxy-agarose for improved catalytic efficiency and stability. **Biocatalysis and Agricultural Biotechnology**, v. 52, p. 102821, 2023.

DE MENEZES, F. L. et al. L-cysteine-coated magnetite nanoparticles as a platform for enzymes immobilization: Amplifying biocatalytic activity of Candida antarctica Lipase A. **Materials Research Bulletin**, v. 177, p. 112882, 2024.

DE SOUSA, I. G. et al. Renewable processes of synthesis of biolubricants catalyzed by lipases. **Journal of Environmental Chemical Engineering**, v. 11, n. 1, p. 109006, 2023.

DEL ARCO, J. et al. Magnetic micro-macro biocatalysts applied to industrial bioprocesses. **Bioresource Technology**, v. 323, p. 124603, 2021.

DELANO, W. L. The PyMOL molecular graphics system. Version 2.3. Schrödinger LLC, 2020. Available at: https://pymol.org/2/. Accessed on: 15 Aug. 2023.

DÍEZ, A. G. et al. Multicomponent magnetic nanoparticle engineering: the role of structure-property relationship in advanced applications. **Materials Today Chemistry**, v. 26, p. 101106, 2022.

DIEZ, M. et al. Insights into mechanism kinematics for protein motion simulation. **BMC Bioinformatics**, v. 15, n. 1, 2014.

DING, C. et al. Photothermal enhanced enzymatic activity of lipase covalently immobilized on functionalized Ti_3C_2TX nanosheets. **Chemical Engineering Journal**, v. 378, n. May, p. 122205, 2019.

DO VALLE, C. P. et al. Chemical modification of Tilapia oil for biolubricant applications. **Journal of Cleaner Production**, v. 191, p. 158–166, 2018.

DONATO, M. T. et al. A review on alternative lubricants: Ionic liquids as additives and deep eutectic solvents. **Journal of Molecular Liquids**, v. 333, p. 116004, 2021.

DOS SANTOS, J. C. S. et al. Characterization of supports activated with divinyl sulfone as a tool to immobilize and stabilize enzymes via multipoint covalent attachment. Application to chymotrypsin. **RSC Advances**, v. 5, n. 27, p. 20639–20649, 2015.

DOS SANTOS, J. C. S. et al. Bovine trypsin immobilization on agarose activated with divinylsulfone: Improved activity and stability via multipoint covalent attachment. **Journal of Molecular Catalysis B: Enzymatic**, v. 117, p. 38–44, 2015.

DOS SANTOS, J. C. S. et al. Versatility of divinylsulfone supports permits the tuning of CALB properties during its immobilization. **RSC Advances**, v. 5, n. 45, p. 35801–35810, 2015.

DOS SANTOS, K. M. et al. Enhanced Biodiesel Production with Eversa Transform 2.0 Lipase on Magnetic Nanoparticles. **Langmuir**, 2024.

DRTINA, G. J. et al. Azlactone-reactive polymer supports for immobilizing synthetically useful enzymes. II. Important preliminary hydrogen bonding effects in the covalent coupling of penicillin Gacylase. **Enzyme and Microbial Technology**, v. 64, p. 13–24, 2005.

DU, X. et al. Insights into protein–ligand interactions: Mechanisms, models, and methods. **International Journal of Molecular Sciences**, v. 17, n. 2, p. 1–34, 2016.

EBERHARDT, J. et al. AutoDock Vina 1.2.0: New Docking Methods, Expanded Force Field, and Python Bindings. **Journal of Chemical Information and Modeling**, v. 61, n. 8, p. 3891–3898, 2021.

ESPACENET PATENT SEARCH. Available at: https://worldwide.espacenet.com/advancedSearch?locale=en_EP. Accessed on: 15 Jan. 2023.

ECHEVERRÍA, J. C. et al. Steering the synthesis of Fe3O4 nanoparticles under sonication by using a fractional factorial design. **Materials Chemistry and Physics**, v. 270, p. 124760, 15 set. 2021.

EL-DAKAR, A. Y. et al. Evaluation of fermented soybean meal by Bacillus subtilis as an alternative to fishmeal on the growth, and physiological status of Nile tilapia Oreochromis niloticus fingerlings. **Heliyon**, v. 9, n. 9, p. e19602, 2023.

EMIRIK, M. Potential therapeutic effect of turmeric contents against SARS-CoV-2 compared with experimental COVID-19 therapies: in silico study. **Journal of Biomolecular Structure and Dynamics**, v. 40, n. 5, p. 2024–2037, 2022.

EOM, Y. et al. In-line monitoring of magnetic nanoparticles synthesis using reactor integrated on-chip magnetometer. **Journal of Science: Advanced Materials and Devices**, v. 7, n. 4, 2022.

ESLAMIPOUR, F.; HEJAZI, P. Evaluating effective factors on the activity and loading of immobilized α-amylase onto magnetic nanoparticles using a response surface-desirability approach. **RSC Advances**, v. 6, n. 24, p. 20187–20197, 2016.

ESMAEILNEJAD-AHRANJANI, P.; LOTFI, M. Surfactant-assisted combustion synthesis of agglomerated-free, size- and shape-controlled magnetic iron oxide nanoparticles for biomedical applications. **Ceramics International**, 2023.

ESMI, F. et al. Amine and aldehyde functionalized mesoporous silica on magnetic nanoparticles for enhanced lipase immobilization, biodiesel production, and facile separation. **Fuel**, v. 291, n. February 2020, p. 120126, 2021.

FAN, Y. et al. Lipase oriented-immobilized on dendrimer-coated magnetic multi-walled carbon nanotubes toward catalyzing biodiesel production from waste vegetable oil. **Fuel**, v. 178, p. 172–178, 2016.

FAN, Z. et al. Hyaluronidase-responsive hydrogel loaded with magnetic nanoparticles combined with external magnetic stimulation for spinal cord injury repair. **Materials Today Bio**, v. 30, p. 101378, 2025.

FARAGO, O. Langevin thermostat for robust configurational and kinetic sampling. **Physica A: Statistical Mechanics and its Applications**, v. 534, n. 122210, 2019.

FARSHAD, S. et al. Journal of Molecular Catalysis B: Enzymatic Lipase immobilization onto polyethylenimine coated magnetic nanoparticles assisted by divalent metal chelated ions. **Journal of Molecular Catalysis. B, Enzymatic**, v. 120, p. 75–83, 2015.

FEEDSTOCKS, L. A. et al. Performance of liquid Eversa on fatty acid ethyl esters production by simultaneous esterification/transesterification. **Fuel**, v. 285, p. 119106, 2021.

FERNANDES, D. M. et al. Polymeric membrane based on polylactic acid and babassu oil for wound healing. **Materials Today Communications**, v. 26, p. 101922, 2021.

FERNANDEZ-ARROJO, L. et al. Micro-scale procedure for enzyme immobilization screening and operational stability assays. **Biotechnology Letters**, v. 37, n. 8, p. 1593–1600, 2015.

FERNANDEZ-LOPEZ, L. et al. Physical crosslinking of lipase from Rhizomucor miehei immobilized on octyl agarose via coating with ionic polymers: Avoiding enzyme release from the support. **Process Biochemistry**, v. 54, p. 81–88, 2017.

FERNANDEZ-LOPEZ, L. et al. Effect of protein load on stability of immobilized enzymes. **Enzyme and Microbial Technology**, v. 98, p. 18–25, 2017.

FORTES, C. C. S. et al. Optimization of enzyme immobilization on functionalized magnetic nanoparticles for laccase biocatalytic reactions. **Chemical Engineering and Processing: Process Intensification**, v. 117, n. March, p. 1–8, 2017.

FRANCO, J. M. Applied Clay Science Tunable rheological-tribological performance of "green" gel-like dispersions based on sepiolite and castor oil for lubricant applications. **Applied Clay Science**, v. 192, n. February, p. 105632, 2020.

FRESCHI, M. et al. The twelve principles of green tribology: studies, research, and case studies — a brief anthology. **Frontiers in Mechanical Engineering**, v. 8, p. 1–14, 2022.

FU, R. et al. Recent advance in metal-organic frameworks-based catalysts for production of fine chemicals via thermal catalysis. **Molecular Catalysis**, v. 573, p. 114811, 2025.

G. PALMA, B. et al. Immobilization of lipases on lignocellulosic bamboo powder for biocatalytic transformations in batch and continuous flow. **Catalysis Today**, v. 381, n. March 2020, p. 280–287, 2021.

GANDOMKAR, S. et al. Enantioselective resolution of racemic ibuprofen esters using different lipases immobilized on epoxy-functionalized silica. **Biocatalysis and Agricultural Biotechnology**, v. 4, p. 550–554, 2015.

GAO, J. et al. Preparation of epoxy-functionalized magnetic nanoparticles for immobilization of glycerol dehydrogenase. **Molecules**, v. 23, n. 3, p. 4852–4857, 2018.

GARCÍA-BOFILL, M. et al. Biocatalytic synthesis of vanillin by an immobilised eugenol oxidase: high biocatalyst yield by enzyme recycling. **Applied Catalysis A: General**, v. 610, p. 1–7, 2021.

GE, H. et al. Biomimetic one-pot preparation of surface biofunctionalized silica-coated magnetic composites for dual enzyme-oriented immobilization without pre-purification. **Enzyme and Microbial Technology**, v. 164, n. December 2022, p. 110169, 2023.

GENHEDEN, S.; RYDE, U. The MM/PBSA and MM/GBSA methods to estimate ligand-binding affinities. **Expert Opinion on Drug Discovery**, v. 10, n. 5, p. 449–461, 2015.

GENNARI, A. et al. Magnetic cellulose: Versatile support for enzyme immobilization - A review. **Carbohydrate Polymers**, v. 246, n. March, p. 116646, 2020.

GERMANO DE SOUSA, I. et al. A novel hybrid biocatalyst from immobilized Eversa® Transform 2.0 lipase and its application in biolubricant synthesis. **Biocatalysis and Biotransformation**, v. 42, n. 2, p. 151–172, 2024.

GHAFAR, F. et al. ScienceDirect Study on The Potential of Waste Cockle Shell Derived Calcium Oxide for Biolubricant Production. **Materials Today: Proceedings**, v. 19, p. 1346–1353, 2019.

GHOSH, G. Early detection of cancer: Focus on antibody coated metal and magnetic nanoparticle-based biosensors. **Sensors International**, v. 1, 1 jan. 2020.

GOHLKE, H.; CASE, D. A. Converging Free Energy Estimates: MM-PB(GB)SA Studies on the Protein-Protein Complex Ras-Raf. **Journal of Computational Chemistry**, v. 25, n. 2, p. 238–250, 2004.

GOHLKE, H.; KIEL, C.; CASE, D. A. Insights into protein-protein binding by binding free energy calculation and free energy decomposition for the Ras-Raf and Ras-RalGDS complexes. **Journal of molecular biology**, v. 330, n. 4, p. 891–913, 2003.

GONG, X. et al. The impact of U.S. political decisions on renewable and fossil energy companies in the era of the Paris Agreement. **Finance Research Letters**, v. 69, p. 106165, 1 nov. 2024.

GOROBETS, O. et al. Interaction of magnetic fields with biogenic magnetic nanoparticles on cell membranes: Physiological consequences for organisms in health and disease. **Bioelectrochemistry**, v. 151, 1 jun. 2023.

GOTOR-FERNÁNDEZ, V. Lipases: useful biocatalysts for the preparation of pharmaceuticals. **Journal of Molecular Catalysis B: Enzymatic**, v. 40, p. 111–120, 2006.

GRIMME, S.; EHRLICH, S.; GOERIGK, L. Effect of the damping function in dispersion corrected density functional theory. **Journal of Computational Chemistry**, v. 32, n. 7, p. 1456–1465, 2011.

GROCHULSKI, P. et al. Insights into interfacial activation from an open structure of Candida rugosa lipase. **Journal of Biological Chemistry**, v. 268, n. 17, p. 12843–12847, 1993.

GUAJARDO, N. et al. Selectivity of R-α-monobenzoate glycerol synthesis catalyzed by Candida antarctica lipase B immobilized on heterofunctional supports. **Process Biochemistry**, v. 50, n. 11, p. 1870–1877, 2015.

GUAJARDO, N. et al. Immobilization of Pseudomonas stutzeri lipase through Cross-linking Aggregates (CLEA) for reactions in Deep Eutectic Solvents. **Journal of Biotechnology**, v. 337, n. March, p. 18–23, 2021.

GUNAKALA, S. R. et al. In-silico investigation of intratumoural magnetic hyperthermia for breast cancer therapy using FePt or FeCrNbB magnetic nanoparticles. **International Journal of Thermal Sciences**, v. 192, 2023.

HABIBULLAH, M. et al. Effect of bio-lubricant on tribological characteristics of steel. **Procedia Engineering**, v. 90, p. 740–745, 2014.

HAJAR, M.; VAHABZADEH, F. Biolubricant production from castor oil in a magnetically stabilized fluidized bed reactor using lipase immobilized on Fe3O4 nanoparticles. **Industrial Crops and Products**, v. 94, p. 544–556, 2016.

HALGREN, T. A. Merck molecular force field. I. Basis, form, scope, parameterization, and performance of MMFF94. **Journal of Computational Chemistry**, v. 17, n. 5–6, p. 490–519, 1996.

HAMEDI, H.; REZAEI, N.; ZENDEHBOUDI, S. A comprehensive review on demulsification using functionalized magnetic nanoparticles. **Journal of Cleaner Production**, v. 382, p. 135375, 2022.

HAN, Y.; ZHANG, X.; ZHENG, L. Engineering actively magnetic crosslinked inclusion bodies of Candida antarctica lipase B: An efficient and stable biocatalyst for enzyme-catalyzed reactions. **Molecular Catalysis**, v. 504, n. February, p. 111467, 2021.

HANWELL, M. D. et al. Avogadro: an advanced semantic chemical editor, visualization, and analysis platform. **Journal of Cheminformatics**, v. 4, n. 1, p. 17, 2012.

HARGER, M.; REN, P. Virial-based Berendsen barostat on GPUs using AMOEBA in Tinker-OpenMM. **Results in Chemistry**, v. 1, p. 100004, 2019.

HARINI, T. et al. Ammonolysis of (5S)-N-(tert-butoxycarbonyl)-5-(methoxycarbonyl)-2-pyrroline with immobilized Candida antarctica lipase B (CALB) in a packed bed reactor. **Process Biochemistry**, v. 65, p. 109–114, 2018.

HAYATZADEH, M.; MOOSAVI, V.; ALIRAMAEE, R. Assessment and prioritization of soil erosion triggering factors using analytical hierarchy process and Taguchi method. **International Journal of Sediment Research**, n. November, p. 1–10, 2022.

HE, L. et al. Tailpipe emissions and fuel consumption of a heavy-duty diesel vehicle using palm oil biodiesel blended fuels. **Science of The Total Environment**, v. 955, p. 177048, 2024.

HEIDARIZADEH, M. et al. International Journal of Biological Macromolecules Dithiocarbamate to modify magnetic graphene oxide nanocomposite (Fe_3O_4-GO): A new strategy for covalent enzyme (lipase) immobilization to fabrication a new nanobiocatalyst for enzymatic hydrolysis. **International Journal of Biological Macromolecules**, v. 101, p. 696–702, 2017.

HEIKAL, E. K. et al. Manufacturing of environment friendly biolubricants from vegetable oils. **Egyptian Journal of Petroleum**, v. 26, n. 1, p. 53–59, 2017.

HEYSE, A. et al. Impact of enzyme properties on drop size distribution and filtration of water-in-oil Pickering emulsions for application in continuous biocatalysis. **Process Biochemistry**, v. 72, n. December 2017, p. 86–95, 2018.

HEYSE, A. et al. Continuous two-phase biocatalysis using water-in-oil Pickering emulsions in a membrane reactor: Evaluation of different nanoparticles. **Catalysis Today**, v. 331, n. November 2017, p. 60–67, 2019.

HOUSHIAR, M. et al. Synthesis of cobalt ferrite ($CoFe_2O_4$) nanoparticles using combustion, coprecipitation, and precipitation methods: A comparison study of size, structural, and magnetic properties. **Journal of Magnetism and Magnetic Materials**, v. 371, p. 43–48, 2014.

HUANG, J.; LIU, Y.; WANG, X. Influence of differently modified palygorskites in the immobilization of a lipase. **Journal of Molecular Catalysis B: Enzymatic**, v. 55, p. 49–54, 2008.

HUMPHREY, W.; DALKE, A.; SCHULTEN, K. VMD: Visual molecular dynamics. **Journal of Molecular Graphics**, v. 14, n. 1, p. 33–38, 1996.

HWANG, E. T.; GU, M. B. Enzyme stabilization by nano/microsized hybrid materials. **International Journal of Molecular Sciences**, v. 14, n. 1, p. 49–61, 2013.

HWANG, E. T.; LEE, S. Multienzymatic cascade reactions via enzyme complex by immobilization. **Catalysts**, v. 9, n. 7, p. 1–18, 2019.

IMARAH, A. O. et al. A Convenient U-Shape Microreactor for Continuous Flow Biocatalysis with Enzyme-Coated Magnetic Nanoparticles-Lipase-Catalyzed Enantiomer Selective Acylation of 4-(Morpholin-4-yl) butan-2-ol. **Catalysts**, v. 12, n. 9, 1 set. 2022.

IŞIK, C. et al. Synthesis and characterization of electrospun PVA/Zn 2+ metal composite nanofibers for lipase immobilization with effective thermal, pH stabilities and reusability. **Materials Science and Engineering C**, v. 99, n. March 2018, p. 1226–1235, 2019.

ISMAIL, A. R.; BAEK, K. Lipase immobilization with support materials, preparation techniques, and applications: Present and future aspects. **International Journal of Biological Macromolecules**, v. 163, p. 1624–1639, 2020.

IYENGAR, S. J. et al. Magnetic, X-ray and Mössbauer studies on magnetite/maghemite core-shell nanostructures fabricated through an aqueous route. **RSC Advances**, v. 4, n. 110, p. 64919–64929, 2014.

IZZATI, N.; MOHAMMAD, R.; ABU, S. Low cost and eco-friendly nanoparticles from cockle shells as a potential matrix for the immobilisation of urease enzyme. **Arabian Journal of Chemistry**, v. 14, n. 4, p. 103056, 2021.

JADHAV, R. et al. An overview of antimicrobial nanoparticles for food preservation. **Materials Today: Proceedings**, v. 72, p. 204–216, 2023.

JANG, Y. S. et al. Flow heterogeneous catalysis via stable dispersion of silica gel-supported catalysts. **Chemical Engineering Journal**, v. 509, p. 161346, 2025.

JANKOVIC, A.; CHAUDHARY, G.; GOIA, F. Designing the design of experiments (DOE) – An investigation on the influence of different factorial designs on the characterization of complex systems. **Energy and Buildings**, v. 250, p. 111298, 2021.

JAWADI, F.; PONDIE, T. M.; CHEFFOU, A. I. New challenges for green finance and sustainable industrialization in developing countries: A panel data analysis. **Energy Economics**, v. 142, p. 108120, 2025.

JEDRZEJCZYK, M. A. et al. Lignin-based additives for improved thermo-oxidative stability of biolubricants. **Tribology International**, v. 155, p. 106780, 2021.

JESIONOWSKI, T.; ZDARTA, J.; KRAJEWSKA, B. Enzyme immobilization by adsorption: A review. **Adsorption**, v. 20, n. 5–6, p. 801–821, 2014.

JIANG, W. et al. Enhanced electrochemiluminescence immunosensor using MIL-53(Fe) as co-reaction promoter of Ru(bpy)32+/PEI system for the detection of carcinoembryonic antigen. **Sensors and Actuators B: Chemical**, v. 407, p. 135498, 2024.

JIANG, X. et al. Immobilization of dehydrogenase onto epoxy-functionalized nanoparticles for synthesis of (R)-mandelic acid. **International Journal of Biological Macromolecules**, v. 88, p. 9–17, 2016.

JIMENEZ-CARRETERO, M. et al. Nanoassemblies of acetylcholinesterase and β-lactamase immobilized on magnetic nanoparticles as biosensors to detect pollutants in water. **Talanta**, v. 258, p. 124406, 2023.

JING, G. et al. Immobilization of carbonic anhydrase on epoxy-functionalized magnetic polymer microspheres for CO_2 capture. **Process Biochemistry**, v. 50, n. 12, p. 2234–2241, 2015.

JORDAN, J.; CHAPMAN, A. E. I.; AND, C. Z. D. Industrial applications of enzymes: recent advances, techniques, and outlooks. **Catalysts**, v. 8, n. 1, p. 20–29, 2018.

JOSHI, J. R.; BHANDERI, K. K.; PATEL, J. V. A review on bio-lubricants from non-edible oils-recent advances, chemical modifications and applications. **Journal of the Indian Chemical Society**, v. 100, n. 1, p. 100849, 2023.

JOSHIBA GANESAN, J. et al. Low-carbon biofuels from macroalgae towards a sustainable circular bioeconomy and green future. **Biomass and Bioenergy**, v. 190, p. 107389, 2024.

KAKAR, S. K. et al. Exploring the impact of industrialization and electricity use on carbon emissions: The role of green FinTech in Asian countries using an asymmetric panel quantile ARDL approach. **Journal of Environmental Management**, v. 370, p. 122970, 2024.

KAMALAKAR, K. et al. Rubber seed oil-based biolubricant base stocks: A potential source for hydraulic oils. **Industrial Crops & Products**, v. 51, p. 249–257, 2013.

KAMEL ARIFFIN, M. F.; IDRIS, A. Fe_2O_3/Chitosan coated superparamagnetic nanoparticles supporting lipase enzyme from Candida Antarctica for microwave assisted biodiesel production. **Renewable Energy**, v. 185, p. 1362–1375, 2022.

KANDILE, N. G. et al. Extraction and characterization of chitosan from shrimp shells. **International Journal of Biological Macromolecules**, v. 111, p. 33–42, 2018.

KANIMOZHI, S.; PERINBAM, K. Synthesis of amino silane modified superparamagnetic Fe 3 O 4 nanoparticles and its application in immobilization of lipase from Pseudomonas fluorescens Lp1. **Materials Research Bulletin**, v. 48, n. 5, p. 1830–1836, 2013.

KANTHASAMY, P.; ARUL MOZHI SELVAN, V. FTIR and GCMS analysis on useful methyl ester compound from industrial waste animal fleshing oil (WAFO). **Materials Today: Proceedings**, v. 46, p. 10072–10078, 2021.

KAPOOR, M.; GUPTA, M. N. Lipase promiscuity and its biochemical applications. **Process Biochemistry**, v. 47, n. 4, p. 555–569, 2012.

KASHEFI, S.; BORGHEI, S. M.; MAHMOODI, N. M. Superparamagnetic enzyme-graphene oxide magnetic nanocomposite as an environmentally friendly biocatalyst: Synthesis and biodegradation of dye using response surface methodology. **Microchemical Journal**, v. 145, p. 547–558, 2019.

KATNIC, S. P.; GUPTA, R. K. From biofilms to biocatalysts: Innovations in plastic biodegradation for environmental sustainability. **Journal of Environmental Management**, v. 374, p. 124192, 2025.

KATO, K. et al. Molecular dynamics simulations for the protein–ligand complex structures obtained by computational docking studies using implicit or explicit solvents. **Chemical Physics Letters**, v. 781, n. 139022, 2021.

KAUR, G. et al. Fungal cellulolytic enzyme complex immobilized on chitosan-functionalised magnetic nanoparticles for paddy straw saccharification. **Process Safety and Environmental Protection**, v. 185, p. 533–544, 2024.

KHOOBBAKHT, G.; KHEIRALIPOUR, K.; YUAN, W. Desirability function approach for optimization of enzymatic transesterification catalyzed by lipase immobilized on mesoporous magnetic nanoparticles. **Renewable Energy**, v. 158, p. 167–178, 2020.

KHOOBI, M. et al. Polyethyleneimine-modified superparamagnetic Fe_3O_4 nanoparticles for lipase immobilization: Characterization and application. **Materials Chemistry and Physics**, v. 149, p. 77–86, 2015.

KHORAMIAN, R. et al. Surface modification of nanoparticles for enhanced applicability of nanofluids in harsh reservoir conditions: A comprehensive review for improved oil recovery. **Advances in Colloid and Interface Science**, v. 333, p. 103296, 2024.

KHOSHNEVISAN, K. et al. Immobilization of cellulase enzyme on superparamagnetic nanoparticles and determination of its activity and stability. **Chemical Engineering Journal**, v. 171, n. 2, p. 669–673, 2011.

KIM, B. H.; HWANG, J.; AKOH, C. C. Current opinion in food science. **Current Opinion in Food Science**, v. 52, p. 100987, 2023.

KIM, B. H.; HWANG, J.; AKOH, C. C. Liquid microbial lipase — recent applications and expanded use through immobilization. **Current Opinion in Food Science**, v. 51, p. 100902, 2023.

KUJAWA, J. et al. Highly effective enzymes immobilization on ceramics: Requirements for supports and enzymes. **Science of the Total Environment**, v. 801, 2021.

KULKARNI, R. D. et al. Epoxidation of mustard oil and ring opening with 2-ethylhexanol for biolubricants with enhanced thermo-oxidative and cold flow characteristics. **Industrial Crops & Products**, v. 49, p. 586–592, 2013.

KUMAR, A.; GANGAWANE, K. M. Synthesis and effect on the surface morphology & magnetic properties of ferrimagnetic nanoparticles by different wet chemical synthesis methods. **Powder Technology**, v. 410, 2022.

KUMAR, D. et al. Versatile hybrid magnetic core silver-shell (Fe_3O_4@PEI@Ag) microspheres-based SERS substrates for detection of organic dyes pollutant. **Journal of Molecular Structure**, v. 1322, p. 140522, 2025.

KURRE, S. K.; YADAV, J. A review on bio-based feedstock, synthesis, and chemical modification to enhance tribological properties of biolubricants. **Industrial Crops and Products**, v. 193, p. 116122, 2023.

LAOS, F. et al. Composting of fish offal and biosolids in northwestern Patagonia. **Bioresource Technology**, v. 81, n. 3, p. 179–186, 2002.

LASKOWSKI, R. A. et al. PROCHECK: a program to check the stereochemical quality of protein structures. **Journal of Applied Crystallography**, v. 26, n. 2, 1993.

LEANG, J. et al. A review on the properties and tribological performance of recent non-aqueous miscible lubricants. **Journal of Molecular Liquids**, v. 366, p. 120274, 2022.

NOYONS, E. C. M. Bibliometric mapping of science in a policy context. **Scientometrics**, v. 50, n. 1, p. 83–98, 2001.

LI, D. et al. Preparation of highly stable immobilized Candida antarctica lipase B (CALB) through adjusting the surface properties of carrier: Preparation, characterization and performance evaluation. **International Journal of Biological Macromolecules**, v. 280, p. 136356, 2024.

LI, J. et al. Improved lipase performance by covalent immobilization of Candida antarctica lipase B on amino acid modified microcrystalline cellulose as green renewable support. **Colloids and Surfaces B: Biointerfaces**, v. 235, p. 113764, 2024.

LI, K. et al. Enhancing enzyme activity and enantioselectivity of Burkholderia cepacia lipase via immobilization on melamine-glutaraldehyde dendrimer modified magnetic nanoparticles. **Chemical Engineering Journal**, v. 351, p. 258–268, 2018.

LI, K. et al. Burkholderia cepacia lipase immobilized on heterofunctional magnetic nanoparticles and its application in biodiesel synthesis. **Scientific Reports**, v. 7, p. 1–11, 2017.

LI, M. S. et al. Breaking barriers in membrane separation: Power of functional coatings. **Separation and Purification Technology**, v. 360, p. 131173, 2025.

LI, X. et al. Journal of Molecular Catalysis B: Enzymatic Immobilization of SMG1-F278N lipase onto a novel epoxy resin: Characterization and its application in synthesis of partial glycerides. **Journal of Molecular Catalysis. B, Enzymatic**, v. 133, p. 154–160, 2016.

LI, Y. et al. Choline amino acid ionic Liquids: A novel green potential lubricant. **Journal of Molecular Liquids**, v. 360, p. 119539, 2022.

LIMA, A. H. et al. Molecular Modeling of T. rangeli, T. brucei gambiense, and T. evansi Sialidases in Complex with the DANA Inhibitor. **Chemical Biology and Drug Design**, v. 80, n. 1, p. 114–120, 2012.

LIN, C. Y.; HUANG, T. H. Cost–benefit evaluation of using biodiesel as an alternative fuel for fishing boats in Taiwan. **Marine Policy**, v. 36, n. 1, p. 103–107, 2012.

LIN, T.; LIN, S. Metal chelate-epoxy bifunctional membranes for selective adsorption and covalent immobilization of a His-tagged protein. **Journal of Bioscience and Bioengineering**, v. 133, n. 3, p. 258–264, 2022.

LINK, J. M. et al. The tribology of cartilage: Mechanisms, experimental techniques, and relevance to translational tissue engineering. **Clinical Biomechanics**, v. 79, n. December 2018, p. 104880, 2020.

LIU, C. H. et al. Biodiesel production by enzymatic transesterification catalyzed by Burkholderia lipase immobilized on hydrophobic magnetic particles. **Applied Energy**, v. 100, p. 41–46, 2012.

LIU, G. et al. An antifouling epoxy coated metal surface containing silica-immobilized carbonic anhydrase supraparticles for CO_2 capture through microalgae. **International Journal of Biological Macromolecules**, v. 269, p. 132075, 2024.

LIU, J. et al. Applications of functional nanoparticle–stabilized surfactant foam in petroleum-contaminated soil remediation. **Journal of Hazardous Materials**, v. 447, p. 130833, 2023.

LIU, J.; MA, R. T.; SHI, Y. P. Recent advances on support materials for lipase immobilization and applicability as biocatalysts in inhibitors screening methods-A review. **Analytica Chimica Acta**, v. 1101, p. 9–22, 2020.

LIU, S. et al. Preparation, surface functionalization and application of Fe_3O_4 magnetic nanoparticles. **Advances in Colloid and Interface Science**, v. 281, p. 102165, 2020.

LIU, X. et al. Electrospun nanofibrous membranes containing epoxy groups and hydrophilic polyethylene oxide chain for highly active and stable covalent immobilization of lipase. **Chemical Engineering Journal**, v. 336, n. September 2017, p. 456–464, 2018.

LIU, Y. et al. Studies of Fe3O4-chitosan nanoparticles prepared by co-precipitation under the magnetic field for lipase immobilization. **Catalysis Communications**, v. 12, n. 8, p. 717–720, 2011.

LIU, Y.; WEIZHUO, X.; WEI, X. A review on lipase-catalyzed synthesis of geranyl esters as flavor additives for food, pharmaceutical and cosmetic applications. **Food Chemistry Advances**, v. 1, n. March, p. 100052, 2022.

LONG-YU, Y. et al. Pancreatic triglyceride lipase is involved in the virulence of the brown planthopper to rice plants. **Journal of Integrative Agriculture**, v. 19, n. 11, p. 2758–2766, 2020.

LOPES, T. R. et al. Journal of Environmental Chemical Engineering Multinuclear magnetic resonance study on the occurrence of phosphorus in activated carbons prepared by chemical activation of lignocellulosic residues from the babassu production. **Journal of Environmental Chemical Engineering**, v. 5, n. 6, p. 6016–6029, 2017.

LUCENA, G. N. et al. Journal of Magnetism and Magnetic Materials Synthesis and characterization of magnetic cross-linked enzyme aggregate and its evaluation of the alternating magnetic field (AMF) effects in the catalytic activity. **Journal of Magnetism and Magnetic Materials**, v. 516, n. August, p. 167326, 2020.

LUISA, O. et al. Optimization of the immobilization of sweet potato amylase using glutaraldehyde-agarose support. Characterization of the immobilized enzyme. **Process Biochemistry**, v. 48, n. 7, p. 1054–1058, 2013.

LUO, B. et al. CuS NP-based nanocomposite with photothermal and augmented-photodynamic activity for magnetic resonance imaging-guided tumor synergistic therapy. **Journal of Inorganic Biochemistry**, v. 235, 2022.

MACIEL, R. et al. Co-immobilization of dextransucrase and dextranase in epoxy-agarose-tailoring oligosaccharides synthesis. **Process Biochemistry**, v. 78, n. July 2018, p. 71–81, 2019.

MAGBANUA, T. O.; RAGAZA, J. A. Selected dietary plant-based proteins for growth and health response of Nile tilapia Oreochromis niloticus. **Aquaculture and Fisheries**, v. 9, n. 1, p. 3–19, 2024.

MAHMOOD, I. et al. A surfactant-coated lipase immobilized in magnetic nanoparticles for multicycle ethyl isovalerate enzymatic production. **Biochemical Engineering Journal**, v. 73, p. 72–79, 2013.

MALHOTRA, R.; ALI, A. 5-Na/ZnO doped mesoporous silica as reusable solid catalyst for biodiesel production via transesterification of virgin cottonseed oil. **Renewable Energy**, v. 133, p. 606–619, 2019.

MARTÍNEZ, S. A. H. et al. Magnetic nanomaterials assisted nanobiocatalysis systems and their applications in biofuels production. **Fuel**, v. 312, 2022.

MASCOLI, V. et al. Uncovering the interactions driving carotenoid binding in light-harvesting complexes. **Chemical Science**, v. 12, n. 14, p. 5113–5122, 2021.

MASIHI, F. et al. Optimization and enhancement of biohydrogen production in a single-stage hybrid (dark/photo) fermentation reactor using Fe_3O_4 and TiO_2 nanoparticles. **International Journal of Hydrogen Energy**, v. 48, n. 3, p. 849–860, 2023.

MATEO, C. et al. Multifunctional epoxy supports: A new tool to improve the covalent immobilization of proteins. The promotion of physical adsorptions of proteins on the supports before their covalent linkage. **Biomacromolecules**, v. 1, n. 4, p. 739–745, 2000.

MATEO, C. et al. Multifunctional Epoxy Supports: A New Tool To Improve the Covalent Immobilization of Proteins. The Promotion of Physical Adsorptions of Proteins on the Supports before Their Covalent Linkage. **Biomacromolecules**, v. 1, n. 4, p. 739–745, 2000.

MATEO, C. et al. Advances in the design of new epoxy supports for enzyme immobilization-stabilization. **Biochemical Society Transactions**, v. 35, n. 6, p. 1593–1601, 2007.

MEHDI, S. et al. Lipase-immobilized chitosan-crosslinked magnetic nanoparticle as a biocatalyst for ring opening esterification of itaconic anhydride. **Biochemical Engineering Journal**, v. 143, n. October 2018, p. 141–150, 2019.

MEHMOOD, A.; ZUNAID, M.; KUMAR, A. A bibliometric analysis of cold spray coating process using VOSviewer. **Materials Today: Proceedings**, v. 72, p. 3059–3066, 2023.

MEHRASBI, M. R. et al. Covalent immobilization of Candida antarctica lipase on core-shell magnetic nanoparticles for production of biodiesel from waste cooking oil. **Renewable Energy**, v. 101, p. 593–602, 2017.

MEHTA, J. et al. Recent advances in enzyme immobilization techniques: Metal-organic frameworks as novel substrates. **Coordination Chemistry Reviews**, v. 322, p. 30–40, 2016.

MEKURIAW, T. A.; ABERA, M. K. CaO -catalyzed trans-esterification of brassica carinata seed oil for biodiesel production. **Heliyon**, v. 10, n. 13, p. e33790, 2024.

MELO, E. et al. First study on the oxidative stability and elemental analysis of babassu (Attalea speciosa) edible oil produced in Brazil using a domestic extraction machine. **Journal of Food Science and Technology**, v. 56, n. 6, p. 3256–3265, 2019.

MELO, R. L. F. et al. Recent applications and future prospects of magnetic biocatalysts. **International Journal of Biological Macromolecules**, v. 253, p. 126709, 2023.

MELO, R. L. F. et al. A comprehensive review on enzyme-based biosensors: Advanced analysis and emerging applications in nanomaterial-enzyme linkage. **International Journal of Biological Macromolecules**, v. 264, p. 130817, 2024.

MELO, R. L. F. et al. Enhancing biocatalyst performance through immobilization of lipase (Eversa® Transform 2.0) on hybrid amine-epoxy core-shell magnetic nanoparticles. **International Journal of Biological Macromolecules**, v. 264, p. 130730, 2024.

MENDOZA-CASSERES, D.; VALENCIA-OCHOA, G.; DUARTE-FORERO, J. Experimental assessment of combustion performance in low-displacement stationary engines operating with biodiesel blends and hydroxy. **Thermal Science and Engineering Progress**, v. 23, p. 100883, 2021.

MICELI, M.; FRONTERA, P.; MACARIO, A. Recovery/reuse of heterogeneous supported spent catalysts. **Catalysts**, v. 11, n. 4, p. 1–23, 2021.

MIGUEL JÚNIOR, J. et al. Improved Catalytic Performance of Lipase Eversa® Transform 2.0 via Immobilization for the Sustainable Production of Flavor Esters—Adsorption Process and Environmental Assessment Studies. **Catalysts**, v. 12, n. 11, p. 1412, 2022.

MIHAILOVIĆ, M. et al. Immobilization of lipase on epoxy-activated Purolite® A109 and its post-immobilization stabilization. **Process Biochemistry**, v. 49, n. 4, p. 637–646, 2014.

MITTERSTEINER, M. et al. Easy and Simple SiO 2 Immobilization of Lipozyme CaLB-L: Its Use as a Catalyst in Acylation Reactions and Comparison with Other Lipases. **Article J. Braz. Chem. Soc**, v. 28, n. 7, p. 1185–1192, 2017.

MIYAMOTO, Y. et al. Langevin description of gauged scalar fields in a thermal bath. **Physical Review D - Particles, Fields, Gravitation and Cosmology**, v. 89, n. 8, 2014.

MOHAMMADI, M. et al. International Journal of Biological Macromolecules Immobilization of laccase on epoxy-functionalized silica and its application in biodegradation of phenolic compounds. **International Journal of Biological Macromolecules**, v. 109, p. 443–447, 2018.

MOHD HUSSIN, F. N. N.; ATTAN, N.; WAHAB, R. A. Taguchi design-assisted immobilization of Candida rugosa lipase onto a ternary alginate/nanocellulose/montmorillonite composite: Physicochemical characterization, thermal stability and reusability studies. **Enzyme and Microbial Technology**, v. 136, n. January, p. 109506, 2020.

MOHD SYUKRI, M. S. et al. Optimization strategy for laccase immobilization on polyethylene terephthalate grafted with maleic anhydride electrospun nanofiber mat. **International Journal of Biological Macromolecules**, v. 166, p. 876–883, 2021.

MONTEIRO, R. R. C. et al. Ethyl butyrate synthesis catalyzed by lipases a and b from candida antarctica immobilized onto magnetic nanoparticles. Improvement of biocatalysts' performance under ultrasonic irradiation. **International Journal of Molecular Sciences**, v. 20, n. 22, 2019.

MONTEIRO, R. R. C. et al. Liquid lipase preparations designed for industrial production of biodiesel. Is it really an optimal solution? **Renewable Energy**, v. 164, p. 1566–1587, 2021.

MONTEIRO, R. R. C. et al. Improvement of enzymatic activity and stability of lipase A from Candida antarctica onto halloysite nanotubes with Taguchi method for optimized immobilization. **Applied Clay Science**, v. 228, p. 106228, 2022.

MONTEIRO, R. R. C. et al. Optimizing the enzymatic production of biolubricants by the Taguchi method: Esterification of the free fatty acids from castor oil with 2-ethyl-1-hexanol catalyzed by Eversa Transform 2.0. **Enzyme and Microbial Technology**, v. 175, p. 110409, 2024.

MOOSAVI, F. et al. Sortase-mediated immobilization of Candida antarctica lipase B (CalB) on graphene oxide; comparison with chemical approach. **Biotechnology Reports**, v. 34, n. April, p. e00733, 2022.

MORAES, P. S. et al. Biodiesel produced from crude, degummed, neutralized and bleached oils of Nile tilapia waste: Production efficiency, physical-chemical quality and economic viability. **Renewable Energy**, v. 161, p. 110–119, 2020.

MOREIRA, K. S. et al. Optimization of the Production of Enzymatic Biodiesel from Residual Babassu Oil (Orbignya sp.) via RSM. **Catalysts 2020, Vol. 10, Page 414**, v. 10, n. 4, p. 414, 2020.

MORELLON-STERLING, R. et al. Effect of amine length in the interference of the multipoint covalent immobilization of enzymes on glyoxyl agarose beads. v. 329, n. February, p. 128–142, 2021.

MORRIS, G. M. et al. Software news and updates AutoDock4 and AutoDockTools4: Automated docking with selective receptor flexibility. **Journal of Computational Chemistry**, v. 30, n. 16, p. 2785–2791, 2009.

MOTA, F. A. S.; COSTA FILHO, J. T.; BARRETO, G. A. The Nile tilapia viscera oil extraction for biodiesel production in Brazil: An economic analysis. **Renewable and Sustainable Energy Reviews**, v. 108, p. 1–10, 2019.

MOTE, V. D. et al. Structural, optical and magnetic properties of Mn-doped CuO nanoparticles by coprecipitation method. **Materials Science and Engineering B: Solid-State Materials for Advanced Technology**, v. 289, 2023.

MUSAKHANIAN, J.; DAVID, J.; MASUMI, R. Oxidative Stability in Lipid Formulations: a Review of the Mechanisms, Drivers, and Inhibitors of Oxidation. **AAPS PharmSciTech**, 2022.

NADAR, S. S.; PATIL, P. D.; ROHRA, N. M. Magnetic nanobiocatalyst for extraction of bioactive ingredients: a novel approach. **Trends in Food Science and Technology**, v. 106, p. 333–342, 2020.

NADIAH, N. et al. Kinetics and hydrodynamics of Candida antarctica lipase-catalyzed synthesis of glycerol dioleate (GDO) in a continuous flow packed-bed millireactor. **Chemical Engineering and Processing – Process Intensification**, v. 173, p. 108804, 2022.

NAGAPPAN, M.; BABU, J. M. In ternary blend fuelled diesel engines, nanoparticles are used as an additive in biofuel production and as a fuel additive: A review. **Materials Today: Proceedings**, 2023.

NAIN, S. et al. The SLP estimation of the nanoparticle systems using size-dependent magnetic properties for the magnetic hyperthermia therapy. **Journal of Magnetism and Magnetic Materials**, v. 565, 2023.

NÁJERA-MARTÍNEZ, E. F. et al. Lignocellulosic residues as supports for enzyme immobilization, and biocatalysts with potential applications. **International Journal of Biological Macromolecules**, v. 208, n. February, p. 748–759, 2022.

NEMATI, H. et al. Design and Taguchi-based optimization of the latent heat thermal storage in the form of structured porous-coated pipe. **Energy**, v. 263, n. PD, p. 125947, 2023.

NEMATIAN, T.; SALEHI, Z.; SHAKERI, A. Conversion of bio-oil extracted from Chlorella vulgaris micro algae to biodiesel via modified superparamagnetic nano-biocatalyst. **Renewable Energy**, v. 146, p. 1796–1804, 2020.

NERY, E. et al. Investigation of the thermal degradation of the biolubricant through TG-FTIR and characterization of the biodiesel – Pequi (Caryocar brasiliensis) as energetic raw material. **Fuel**, v. 245, n. February, p. 398–405, 2019.

NETO, D. M. A. et al. Rapid Sonochemical Approach Produces Functionalized Fe_3O_4 Nanoparticles with Excellent Magnetic, Colloidal, and Relaxivity Properties for MRI Application. **Journal of Physical Chemistry C**, v. 121, n. 43, p. 24206–24222, 2017.

NETO, D. M. A. et al. A novel amino phosphonate-coated magnetic nanoparticle as MRI contrast agent. **Applied Surface Science**, v. 543, 2021.

NETTO, C. G. C. M.; TOMA, H. E.; ANDRADE, L. H. Journal of Molecular Catalysis B : Enzymatic Superparamagnetic nanoparticles as versatile carriers and supporting materials for enzymes. **Journal of Molecular Catalysis. B, Enzymatic**, v. 85–86, p. 71–92, 2013.

NEZHAD, M. K.; AGHAEI, H. Tosylated cloisite as a new heterofunctional carrier for covalent immobilization of lipase and its utilization for production of biodiesel from waste frying oil. **Renewable Energy**, v. 164, p. 876–888, 2021.

NG, J. X. Y. et al. A study on the surface responses and degradation mechanisms of epoxy-amine coating subjected to UV accelerated weathering and hygrothermal ageing using ToF-SIMS and FTIR analysis. **Polymer Degradation and Stability**, v. 228, p. 110930, 2024.

NIETZ, D. et al. Enzyme and Microbial Technology A new lipase (Alip2) with high potential for enzymatic hydrolysis of the diester diethyladipate to the monoester monoethyladipate. **Enzyme and Microbial Technology**, v. 153, n. August 2021, p. 109898, 2022.

NIMKANDE, V. D.; BAFANA, A. Journal of Water Process Engineering A review on the utility of microbial lipases in wastewater treatment. **Journal of Water Process Engineering**, v. 46, n. 3, p. 102591, 2022.

NING, S. et al. Study on Magnetic and Plasmonic Properties of Fe3O4-PEI-Au and Fe_3O_4-PEI-Ag Nanoparticles. **Materials 2024, Vol. 17, Page 509**, v. 17, n. 2, p. 509, 2024.

NIU, J. et al. Acetate-based ionic liquid immobilized Fe-MIL-101-NH2: A highly efficient heterogeneous catalyst for the conversion of CO_2 into oxazolidinones with N-aryl epoxy amines. **Journal of Environmental Chemical Engineering**, v. 12, n. 5, p. 113503, 2024.

NIU, Y. et al. Magnetic microcapsules based on Fe_3O_4 nanoparticles: Preparation, properties, and applications. **Materials Today Communications**, v. 39, p. 108660, 2024.

NNADOZIE, E. C.; AJIBADE, P. A. Preparation, phase analysis and electrochemistry of magnetite (Fe3O4) and maghemite (γ-Fe_2O_3) nanoparticles. **International Journal of Electrochemical Science**, v. 17, n. 12, p. 22124, 2022.

NOGALES-DELGADO, S.; MARTÍN, E.; MERCEDES, S. Use of mild reaction conditions to improve quality parameters and sustainability during biolubricant production. **Biomass and Bioenergy**, v. 161, p. 106465, 2022.

NOGUCHI, S. et al. Fetal outcomes with and without the use of sugammadex in pregnant patients undergoing non-obstetric surgery: a multicenter retrospective study. **International Journal of Obstetric Anesthesia**, v. 53, p. 103620, 2023.

NORAINI, M. Y. et al. A review on potential enzymatic reaction for biofuel production from algae. **Renewable and Sustainable Energy Reviews**, v. 39, p. 24–34, 2014.

NWAGU, T. N.; OKOLO, B.; AOYAGI, H. Immobilization of raw starch saccharifying amylase on glutaraldehyde activated chitin flakes increases the enzyme operation range. **Bioresource Technology Reports**, v. 13, n. December 2020, p. 100645, 2021.

OKURA, N. S. et al. Improved immobilization of lipase from Thermomyces lanuginosus on a new chitosan-based heterofunctional support: Mixed ion exchange plus hydrophobic interactions. **International Journal of Biological Macromolecules**, v. 163, p. 550–561, 2020.

OLIVEIRA CAVALCANTE, I. et al. Evolving sustainable energy technologies and assessments through global research networks: advancing the role of blue hydrogen for a cleaner future. **Journal of Cleaner Production**, v. 430, p. 139746, 2024.

OLUSEGUN, S. J. et al. Synthesis and characterization of Sr^{2+} and Gd^{3+} doped magnetite nanoparticles for magnetic hyperthermia and drug delivery application. **Ceramics International**, v. 49, n. 12, p. 19375–19386, 2023.

ONG, H. C. et al. A state-of-the-art review on thermochemical conversion of biomass for biofuel production: A TG-FTIR approach. **Energy Conversion and Management**, v. 209, p. 112634, 2020.

ORTIZ, C. et al. Novozym 435: the “perfect” lipase immobilized biocatalyst? **Catalysis Science & Technology**, v. 9, n. 10, p. 2380–2420, 2019.

OUDA, M. et al. Oily wastewater treatment via phase-inverted polyethersulfone-maghemite (PES/γ-Fe_2O_3) composite membranes. **Journal of Water Process Engineering**, v. 37, p. 101545, 2020.

OWUNA, F. J. et al. Chemical modification of vegetable oils for the production of biolubricants using trimethylolpropane: A review. **Egyptian Journal of Petroleum**, v. 29, n. 1, p. 75–82, 2020.

OWUNA, F. J. Stability of vegetable-based oils used in the formulation of ecofriendly lubricants – a review q. **Egyptian Journal of Petroleum**, v. 29, n. 3, p. 251–256, 2020.

PAL, A.; KHANUM, F. Covalent immobilization of xylanase on glutaraldehyde activated alginate beads using response surface methodology: Characterization of immobilized enzyme. **Process Biochemistry**, v. 46, n. 6, p. 1315–1322, 2011.

PAL, S. et al. Self-seeded coprecipitation flow synthesis of iron oxide nanoparticles via triphasic reactor platform: optimising heating performance under alternating magnetic fields. **Chemical Engineering Journal**, v. 462, p. 141110, 2023.

PANCHAL, B. et al. Functionalized mesoporous polymer ionic liquids for efficient immobilization of lipase: Effects of ethyl oleate. **Journal of Catalysis**, v. 416, p. 186–197, 2022.

PANDEY, A.; SRIVASTAVA, S.; KUMAR, S. Carbon dioxide fixation and lipid storage of Scenedesmus sp. ASK22: A sustainable approach for biofuel production and waste remediation. **Journal of Environmental Management**, v. 332, p. 117350, 2023.

PANDEY, K.; SHARMA, S.; SAHA, S. Advances in design and synthesis of stabilized zero-valent iron nanoparticles for groundwater remediation. **Journal of Environmental Chemical Engineering**, v. 10, n. 3, 2022.

PANDIT, C. et al. Development of magnetic nanoparticle assisted aptamer-quantum dot-based biosensor for the detection of Escherichia coli in water samples. **Science of the Total Environment**, v. 831, 2022.

PAPOLU, P.; BHOGI, A. Green synthesis of various metal oxide nanoparticles for the environmental remediation – an overview. **Materials Today: Proceedings**, v. 84, p. 157–162, 2023.

PARANDI, E. et al. Biodiesel production from waste cooking oil using a novel biocatalyst of lipase enzyme immobilized magnetic nanocomposite. **Fuel**, v. 313, n. December 2021, p. 123057, 2022.

PARK, K.; SON, H. J.; CHOE, J. I. mPW1PW91 study for conformational isomers of methylene bridge-monosubstituted tetramethoxycalix[4]arenes. **Journal of Industrial and Engineering Chemistry**, v. 20, n. 5, p. 3276–3282, 2014.

PATIL, P. D. et al. Designable metal–organic frameworks for enzyme immobilization: The reality of controlled architecture. **Chemical Engineering Journal**, v. 508, p. 160994, 2025.

PENG, Y. et al. Chemosphere Interception of fertile soil phosphorus leaching with immobilization materials: Recent progresses, opportunities and challenges. **Chemosphere**, v. 308, n. P2, p. 136337, 2022.

PERERA, M. et al. Improved performance of Pseudomonas fluorescens lipase immobilized on a magnetic mesoporous solvothermal hybrid-nanocarrier and its application in

ultrasonication assisted estolide synthesis. **Journal of Industrial and Engineering Chemistry**, v. 140, p. 258–268, 2024.

PETRO, P. et al. Production, characterization, and exergy analysis of the soybean biodiesel produced by laboratory scale. **Petroleum & Petrochemical Engineering Journal**, v. 7, n. 1, p. 1–9, 2023.

PHILLIPS, J. C. et al. Scalable molecular dynamics with NAMD. **Journal of Computational Chemistry**, v. 26, n. 16, p. 1781–1802, 2005.

PING, T. et al. Reducing oxygen inhibition by Fe_3O_4@PEI nanoparticles co-initiator. **Journal of Photochemistry and Photobiology A: Chemistry**, v. 373, p. 171–175, 2019.

PINHEIRO, B. B. et al. Chitosan activated with divinyl sulfone: a new heterofunctional support for enzyme immobilization. Application in the immobilization of lipase B from Candida antarctica. **International Journal of Biological Macromolecules**, v. 130, p. 798–809, 2019.

POONSIN, T. et al. Optimal immobilization of trypsin from the spleen of albacore tuna (Thunnus alalunga) and its characterization. **International Journal of Biological Macromolecules**, v. 143, p. 462–471, 2020.

POPPE, J. K. et al. Enzymatic reactors for biodiesel synthesis: Present status and future prospects. **Biotechnology Advances**, v. 33, n. 5, p. 511–525, 2015.

PROC, J. L. et al. A quantitative study of the effects of chaotropic agents, surfactants, and solvents on the digestion efficiency of human plasma proteins by trypsin. **Journal of Proteome Research**, v. 9, n. 10, p. 5422–5437, 2010.

PUDZIANOWSKI, A. T. MP2/6-311++G(d,p) study of ten ionic hydrogen-bonded binary systems: Structures, normal modes, thermodynamics, and counterpoise energies. **The Journal of Chemical Physics**, v. 102, n. 20, p. 8029–8039, 1995.

QIN, X.; ZHONG, J.; WANG, Y. A mutant T1 lipase homology modeling, and its molecular docking and molecular dynamics simulation with fatty acids. **Journal of Biotechnology**, v. 337, n. February, p. 24–34, 2021.

QIN, Z. et al. Journal of Colloid and Interface Science Hydrogen-bonded lipase-hydrogel microspheres for esterification application. **Journal of Colloid and Interface Science**, v. 606, p. 1229–1238, 2022.

RA, F.; REZAEE, M. Different strategies for the lipase immobilization on the chitosan-based supports and their applications. **International Journal of Biological Macromolecules**, v. 179, p. 170–195, 2021.

RABBANI, G. et al. International Journal of Biological Macromolecules Structural features, temperature adaptation and industrial applications of microbial lipases from psychrophilic, mesophilic and thermophilic origins. **International Journal of Biological Macromolecules**, v. 225, n. June 2022, p. 822–839, 2023.

RAFIEE-POUR, M. T. H. Amine functionalized TiO_2–carbon nanotube composite: synthesis, characterization and application to glucose biosensing. **Materials Science and Engineering: C**, v. 31, n. 2, p. 189–195, 2011.

RAGUNATHAN, A.; MALATHI, K.; ANBARASU, A. MurB as a target in an alternative approach to tackle the Vibrio cholerae resistance using molecular docking and simulation study. **Journal of Cellular Biochemistry**, v. 119, n. 2, p. 1726–1732, 2018.

RAJU, U. et al. Irreversible and reversible chemical reaction impacts on convective Maxwell fluid flow over a porous media with activation energy. **Case Studies in Thermal Engineering**, v. 61, p. 104821, 2024.

RAMACHANDRAN, G. N. R. C.; SASISEKHARAN, V. Stereochemistry of Polypeptide Chain Conformations. **Journal of Molecular Biology**, v. 7, p. 95–99, 1963.

RANI, S.; VARMA, G. D. Superparamagnetism and metamagnetic transition in Fe_3O_4 nanoparticles synthesized via co-precipitation method at different pH. **Physica B: Condensed Matter**, v. 472, p. 66–77, 2015.

RANJBARI, M. et al. Biomass and organic waste potentials towards implementing circular bioeconomy platforms: a systematic bibliometric analysis. **Fuel**, v. 318, p. 123635, 2022.

RASHEED, T. et al. Carbon nanotubes-based cues: a pathway to future sensing and detection of hazardous pollutants. **Journal of Hazardous Materials**, v. 292, p. 207–222, 2019.

REMONATTO, D. et al. Applications of immobilized lipases in enzymatic reactors: A review. **Process Biochemistry**, v. 114, n. August 2021, p. 1–20, 2022.

REMONATTO, D. et al. Immobilization of Eversa Lipases on Hydrophobic Supports for Ethanolysis of Sunflower Oil Solvent - Free. **Applied Biochemistry and Biotechnology**, p. 2151–2167, 2022.

REN, Y. et al. Facile, high efficiency immobilization of lipase enzyme on magnetic iron oxide nanoparticles via a biomimetic coating. **BMC Biotechnology**, v. 11, p. 63, 2011.

REN, Y. et al. Molecular insight into the enhanced performance of CALB toward PBDF degradation. **International Journal of Biological Macromolecules**, v. 262, p. 130181, 2024.

RIOS, N. S. et al. Strategies of covalent immobilization of a recombinant Candida antarctica lipase B on pore-expanded SBA-15 and its application in the kinetic resolution of (R,S)-Phenylethyl acetate. **Journal of Molecular Catalysis B: Enzymatic**, v. 133, p. 246–258, 2016.

RIQUELME, M. et al. (Paleo) glacier studies in Patagonia over the past decades (1976–2020): a bibliometric perspective based on the Web of Science. **Journal of South American Earth Sciences**, v. 122, p. 104036, 2023.

ROCA, A. G. et al. Effect of nature and particle size on properties of uniform magnetite and maghemite nanoparticles. **Journal of Physical Chemistry C**, v. 111, n. 50, p. 18577–18584, 2007.

ROCHA, T. G. et al. Lipase Cocktail for Optimized Biodiesel Production of Free Fatty Acids from Residual Chicken Oil. **Catalysis Letters**, v. 151, n. 4, p. 1155–1166, 2021.

ROCHA, T. G. et al. Lipase Cocktail for Optimized Biodiesel Production of Free Fatty Acids from Residual Chicken Oil. **Catalysis Letters**, v. 151, n. 4, p. 1155–1166, 1 abr. 2021.

RODRIGUES, A. F. S. et al. A scientometric analysis of research progress and trends in the design of laccase biocatalysts for the decolorization of synthetic dyes. **International Journal of Biological Macromolecules**, v. 126, p. 272–291, 2023.

RODRIGUES, H. et al. Innovative hydrogels made from babassu mesocarp for technological application in agriculture. **Journal of Molecular Liquids**, v. 376, p. 121463, 2023.

RODRIGUES, R. C. et al. Stabilization of enzymes via immobilization: multipoint covalent attachment and other stabilization strategies. **Biotechnology Advances**, v. 52, p. 107522, 2021.

RODRÍGUEZ-SALARICHS, J. et al. Versatile Lipases from the Candida rugosa-like Family: A Mechanistic Insight Using Computational Approaches. **Journal of Chemical Information and Modeling**, v. 61, n. 2, p. 913–920, 2021.

ROE, D. R.; BROOKS, B. R. A protocol for preparing explicitly solvated systems for stable molecular dynamics simulations. **Journal of Chemical Physics**, v. 153, n. 5, p. 1–9, 2020.

ROSENKRANZ, A. et al. Synergetic effects of surface texturing and solid lubricants to tailor friction and wear – A review. **Tribology International**, v. 155, n. November 2020, 2021.

RUEDA, N. et al. Chemical amination of lipases improves their immobilization on octyl-glyoxyl agarose beads. **Catalysis Today**, v. 259, p. 107–118, 2016.

SABI, G. J. et al. Decyl esters production from soybean-based oils catalyzed by lipase immobilized on differently functionalized rice husk silica and their characterization as potential biolubricants. **Enzyme and Microbial Technology**, v. 157, p. 110019, 1 jun. 2022.

SADEGHI, M.; MOGHIMIFAR, Z.; JAVADIAN, H. Fe_3O_4@SiO_2 nanocomposite immobilized with cellulase enzyme: Stability determination and biological activity. **Chemical Physics Letters**, v. 811, n. June 2022, p. 140161, 2023.

SADJADI, S. et al. Magnetic covalent hybrid of graphitic carbon nitride and graphene oxide as an efficient catalyst support for immobilization of Pd nanoparticles. **Inorganica Chimica Acta**, v. 488, p. 62–70, 2019.

SADJADI, S. et al. Magnetic hybrid of cyclodextrin nanosponge and polyhedral oligomeric silsesquioxane: Efficient catalytic support for immobilization of Pd nanoparticles. **International Journal of Biological Macromolecules**, v. 128, p. 638–647, 2019.

SALES, M. B. et al. Sustainable Feedstocks and Challenges in Biodiesel Production: An Advanced Bibliometric Analysis. **Bioengineering**, v. 9, n. 10, 2022.

SALIH, N. physicochemical properties of ricinoleic acid based-diester biolubricants. **Arabian Journal of Chemistry**, v. 10, p. S2273–S2280, 2017.

SALIH, N. A Review on Eco-Friendly Green Biolubricants from Renewable and Sustainable Plant Oil Sources. v. 11, n. 5, p. 13303–13327, 2021.

SALIH, S. J.; MAHMOOD, W. M. Review on magnetic spinel ferrite (MFe_2O_4) nanoparticles: from synthesis to application. **Heliyon**, v. 9, n. 6, e16716, 2023.

SALMAN SAJID, M. et al. Glycosylation heterogeneity and low abundant serum glycoproteins MS analysis by boronic acid immobilized Fe_3O_4@1,2-Epoxy-5-Hexene/DVB magnetic core shell nanoparticles. **Microchemical Journal**, v. 159, p. 105351, 2020.

SALOMON-FERRER, R.; CASE, D. A.; WALKER, R. C. An overview of the Amber biomolecular simulation package. **Wiley Interdisciplinary Reviews: Computational Molecular Science**, v. 3, n. 2, p. 198–210, 2013.

SAMPAIO, C. S. et al. International Journal of Biological Macromolecules Lipase immobilization via cross-linked enzyme aggregates: Problems and prospects – A review. **International Journal of Biological Macromolecules**, v. 215, n. May, p. 434–449, 2022.

SANTANA, V. Simplified method to optimize enzymatic esters syntheses in solvent-free systems: validation using literature and experimental data. **Biotechnology Progress**, v. 37, n. 2, e3132, 2021.

SANTOYO SALAZAR, J. et al. Magnetic iron oxide nanoparticles in 10-40 nm range: Composition in terms of magnetite/maghemite ratio and effect on the magnetic properties. **Chemistry of Materials**, v. 23, n. 6, p. 1379–1386, 2011.

SARAÇOĞLU, M. et al. Challenging the frontiers of superparamagnetism through strain engineering: DFT investigation and co-precipitation synthesis of large aggregated Fe_3O_4 (magnetite) powder. **Journal of Alloys and Compounds**, v. 968, p. 171895, 2023.

SARAIVA, N. et al. International Journal of Biological Macromolecules Further stabilization of lipase from Pseudomonas fluorescens immobilized on octyl coated nanoparticles via chemical modi fi cation with bifunctional agents. **International Journal of Biological Macromolecules**, v. 141, p. 313–324, 2019.

SARKAR, M.; MANDAL, N. Solid lubricant materials for high temperature application: a review. Materials Today: **Proceedings**, v. 62, p. 2134–2139, 2022.

SAYLAN, Y.; AKGÖNÜLLÜ, S.; DENIZLI, A. Preparation of magnetic nanoparticles-assisted plasmonic biosensors with metal affinity for interferon-α detection. **Materials Science and Engineering B: Solid-State Materials for Advanced Technology**, v. 280, p. 115665, 2022.

SCIANCALEPORE, C. et al. Epoxy nanocomposites functionalized with in situ generated magnetite nanocrystals: Microstructure, magnetic properties, interaction among magnetic particles. **Polymer**, v. 59, p. 278–289, 2015.

SEIBEL, J.; CABRAL WANCURA, J. H.; DIAS MAYER, F. Process simulation and technology prospection to the hydrotreating of vegetable oils and animal fats. **Energy Conversion and Management**, v. 315, p. 118811, 2024.

SHAHEDI, M. et al. Co-immobilization of Rhizomucor miehei lipase and Candida antarctica lipase B and optimization of biocatalytic biodiesel production from palm oil using response surface methodology. **Renewable Energy**, v. 141, p. 847–857, 2019.

SHAKEEL, N. et al. Functionalized magnetic nanoparticle-reduced graphene oxide nanocomposite for enzymatic biofuel cell applications. **International Journal of Hydrogen Energy**, v. 44, n. 52, p. 28294–28304, 2019.

SHARIFI DEHSARI, H. et al. Determining Magnetite/Maghemite Composition and Core-Shell Nanostructure from Magnetization Curve for Iron Oxide Nanoparticles. **Journal of Physical Chemistry C**, v. 122, n. 49, p. 28292–28301, 2018.

SHARMA, R.; SINGHAL, P. Demand forecasting of engine oil for automotive and industrial lubricant manufacturing company using neural network. **Materials Today: Proceedings**, v. 18, p. 2308–2314, 2019.

SHARMA, S. et al. Enzyme immobilization: Implementation of nanoparticles and an insight into polystyrene as the contemporary immobilization matrix. **Process Biochemistry**, v. 120, n. November 2021, p. 22–34, 2022.

SHELDON, R. A. Enzyme immobilization: the quest for optimum performance. **Advanced Synthesis & Catalysis**, v. 349, n. 8–9, p. 1289–1307, 2007.

SHOME, S. et al. Impact investment for sustainable development: a bibliometric analysis. **International Review of Economics and Finance**, v. 84, p. 770–800, 2023.

SHUAI, W. et al. A review on the important aspects of lipase immobilization on nanomaterials. **Biotechnology Advances**, v. 64, n. 4, p. 496–508, 2017.

SIAR, E. H. et al. Immobilization/stabilization of ficin extract on glutaraldehyde-activated agarose beads. Variables that control the final stability and activity in protein hydrolyses. **Catalysts**, v. 8, n. 4, 2018.

SILVA ALMEIDA, C. et al. Enhancing lipase immobilization via physical adsorption: advancements in stability, reusability, and industrial applications for sustainable biotechnological processes. **ACS Omega**, v. 9, n. 2, p. 1234–1245, 2024.

SILVA, J. M. F. et al. Immobilization of Thermomyces lanuginosus lipase on a new hydrophobic support (Streamline phenyl™): strategies to improve stability and reusability. **Enzyme and Microbial Technology**, v. 163, p. 110139, 2023.

SILVA, T. D. A. et al. Impact of immobilization strategies on the activity and recyclability of lipases in nanomagnetic supports. **Scientific Reports**, v. 12, p. 1–11, 2022.

SINGH, K. et al. India's renewable energy research and policies to phase down coal: Success after Paris agreement and possibilities post-Glasgow Climate Pact. **Biomass and Bioenergy**, v. 177, p. 106944, 2023.

SINGH, S. et al. Synthesis of PEI functionalized silica microsphere loaded polymeric network for simultaneous removal of Cr (III) & Cr (VI) from aquatic medium. **Materials Today Communications**, v. 35, p. 105706, 2023.

SIVANANDAN, T.; SARAVANAN, S. Effects of calcination temperatures on structural, functional, morphological, and magnetic properties of strontium ferrite ($SrFe_2O_4$) nanoparticles. **Kuwait Journal of Science**, v. 50, n. 2, p. 1–12, 2023.

SKOWROŃ, J.; MIRANOWICZ-DZIERZAWSKA, K.; ZAPOR, L. Cytotoxicity of biofuels produced by esterification of waste materials: Vegetable oils or animal fats on A431 skin cells. **Toxicology Letters**, v. 238, n. 2, p. S345, 2015.

SO, C. L.; EBERHARDT, T. L. FTIR-based models for assessment of mass yield and biofuel properties of torrefied wood. **Wood Science and Technology**, v. 52, n. 1, p. 209–227, 2018.

SONG, M.; CHANG, J. Thermally stable and reusable ceramic encapsulated and cross-linked CalB enzyme particles for rapid hydrolysis and esterification. **Catalysts**, v. 12, n. 2, p. 185, 2022.

SOOD, A. et al. An overview of additive manufacturing strategies of enzyme-immobilized nanomaterials with application incatalysis and biomedicine. **International Journal of Biological Macromolecules**, v. 292, p. 139174, 2025.

SOUSA, I. G. DE et al. A novel hybrid biocatalyst from immobilized Eversa Transform 2. 0 lipase and its application in biolubricant synthesis. **Biocatalysis and Biotransformation**, v. 0, n. 0, p. 1–22, 2022.

SOUZA, M. C. M. de; SANTOS, C. S.; FERNANDEZ-LAFUENTE, R. Immobilization of lipase A from Candida antarctica onto chitosan-coated magnetic nanoparticles. **International Journal of Molecular Sciences**, v. 17, n. 3, p. 4018, 2016.

ŠPONER, J.; HOBZA, P.; LESZCZYNSKI, J. Computational approaches to the studies of the interactions of nucleic acid bases. **Theoretical and Computational Chemistry**, v. 8, p. 85–117, 2001.

SRIVASTAVA, E. et al. Binary blending of different types of biofuels with diesel, and study of engine performance, combustion and exhaust emission characteristics. **Materials Today: Proceedings**, v. 78, p. 378–389, 2023.

STATUS, C. Current status and future prospects of biolubricants: properties and applications. **Lubricants**, v. 10, n. 1, p. 1–21, 2022.

STAUDT, A. et al. Biocatalytic synthesis of monoterpene esters – a review study on the phylogenetic evolution of biocatalysts. **Molecular Catalysis**, v. 526, p. 112422, 2022.

STRUCHTRUP, H. Entropy and the second law of thermodynamics-The nonequilibrium perspective. **Entropy**, v. 22, n. 7, p. 1–61, 2020.

SULMAN, E. M.; MATVEEVA, V. G.; BRONSTEIN, L. M. Design of biocatalysts for efficient catalytic processes. **Current Opinion in Chemical Engineering**, v. 26, p. 1–8, 2019.

SUN, B. et al. Enhanced MOF-immobilized lipase CAL-A with polyethylene glycol for efficient stereoselective hydrolysis of aromatic acid esters. **Biochemical Engineering Journal**, v. 189, n. October, p. 108707, 2022.

SUN, S.; GUO, J.; CHEN, X. Industrial Crops & Products Biodiesel preparation from Semen Abutili (Abutilon theophrasti Medic.) seed oil using low-cost liquid lipase Eversa® transform 2.0 as a catalyst. **Industrial Crops & Products**, v. 169, n. November 2020, p. 113643, 2021.

SUN, W. et al. Optical diagnosis on combustion characteristics and flame development process of Fischer-Tropsch diesel/biodiesel blends. **Journal of the Energy Institute**, v. 117, p. 101900, 2024.

SUO, H. et al. Enhancement of catalytic performance of porcine pancreatic lipase immobilized on functional ionic liquid modified Fe3O4-Chitosan nanocomposites. **International Journal of Biological Macromolecules**, v. 119, p. 624–632, 2018.

TAGAMI-KANADA, N. et al. Combustion characteristics of densified solid biofuel with different aspect ratios. **Renewable Energy**, v. 197, p. 1174–1182, 2022.

TAGHIZADEH, A. et al. Palladium immobilized in Fe_3O_4@PEG/cryptand 222 core-shell nanostructure for enhanced cross-coupling reactions under sonication. **Colloids and Surfaces A: Physicochemical and Engineering Aspects**, v. 675, p. 132009, 2023.

TAHERINIA, Z.; GHORBANI-CHOGHAMARANI, A.; LEMRASKI, E. G. Biodiesel production from spirulina algae oil over cobalt microsphere through esterification reaction. **Materials Today Sustainability**, v. 25, p. 100647, 2024.

TAN, Z. et al. Nanomaterial-immobilized lipases for sustainable recovery of biodiesel – a review. **Renewable and Sustainable Energy Reviews**, v. 316, p. 110877, 2022.

TAN, Z. et al. Designing multifunctional biocatalytic cascade system by multi-enzyme co-immobilization on biopolymers and nanostructured materials. **International Journal of Biological Macromolecules**, v. 227, n. December 2022, p. 535–550, 2023.

TANG, X. et al. Efficient lithium-oxygen batteries with low charge overpotential via solid-state design and thermal catalyst activation. **Chemical Engineering Journal**, v. 505, p. 159351, 2025.

TANG, Y. et al. A mild one-step method to fabricate graphene oxide cross-linked with dopamine/polyethyleneimine (GO@DA/PEI) composite membranes with an ultrahigh flux for heavy metal ion removal. **Separation and Purification Technology**, v. 339, p. 126618, 2024.

TARDIOLI, P. W. et al. Immobilization–stabilization of glucoamylase: Chemical modification of the enzyme surface followed by covalent attachment on highly activated glyoxyl-agarose supports. **Process Biochemistry**, v. 46, n. 1, p. 409–412, 2011.

THANGARAJ, B. et al. Catalysis in biodiesel production - A review. **Clean Energy**, v. 3, n. 1, p. 2–23, 2019.

THIRUMALAI, D.; LORIMER, G. H.; HYEON, C. Iterative annealing mechanism explains the functions of the GroEL and RNA chaperones. **Protein Science**, v. 29, n. 2, p. 1–18, 2020.

THUDI, L. et al. Journal of Molecular Catalysis B: Enzymatic Enzyme immobilization on epoxy supports in reverse micellar media: Prevention of enzyme denaturation. **Journal of Molecular Catalysis. B, Enzymatic**, v. 74, n. 1–2, p. 54–62, 2012.

TIAN, Z. et al. Magnetic mesoporous silica nanoparticles coated with thermo-responsive copolymer for potential chemo- and magnetic hyperthermia therapy. **Microporous and Mesoporous Materials**, v. 256, p. 1–9, 2018.

TIEN, N. et al. Fundamental understanding of in-situ transesterification of microalgae biomass to biodiesel: A critical review. **Energy Conversion and Management**, v. 270, n. August, p. 116212, 2022.

TORRES, J. A. et al. International Journal of Biological Macromolecules Development of a reusable and sustainable biocatalyst by immobilization of soybean peroxidase onto magnetic adsorbent. **International Journal of Biological Macromolecules**, v. 114, p. 1279–1287, 2018.

TORRES, J. A. et al. Development of a reusable and sustainable biocatalyst by immobilization of soybean peroxidase onto magnetic adsorbent. **International Journal of Biological Macromolecules**, v. 114, p. 1279–1287, 2018.

TORRES-MAYANGA, P. C. et al. Production of biofuel precursors and value-added chemicals from hydrolysates resulting from hydrothermal processing of biomass: A review. **Biomass and Bioenergy**, v. 130, p. 105397, 2019.

TOUQEER, T. et al. Fe_3O_4-PDA-lipase as surface functionalized nano biocatalyst to produce biodiesel using waste cooking oil as feedstock: Characterization and process optimization. **Energies**, v. 13, n. 1, 2020.

TRIPATHI, M.; KUMAR, D.; KUMAR, P. Mesoporous silica as amine immobiliser for endowing healing functionality to epoxy resin. **Composites Communications**, v. 4, n. November 2016, p. 20–23, 2017.

TROTT, O.; OLSON, A. J. AutoDock Vina: Improving the speed and accuracy of docking with a new scoring function, efficient optimization, and multithreading. **Journal of Computational Chemistry**, 2009.

TROTT, O.; OLSON, A. J. AutoDock Vina: Improving the speed and accuracy of docking with a new scoring function, efficient optimization, and multithreading. **Journal of Computational Chemistry**, v. 31, n. 2, p. 455–461, 2010.

TUNG, S. C.; MCMILLAN, M. L. Automotive tribology overview of current advances and challenges for the future. **Tribology International**, v. 37, n. 7, p. 517–536, 2004.

TUNIO, A. A. et al. Multi enzyme production from mixed untreated agricultural residues applied in enzymatic saccharification of lignocellulosic biomass for biofuel. **Process Safety and Environmental Protection**, v. 186, p. 540–551, 2024.

TURAL, B. et al. Purification and covalent immobilization of benzaldehyde lyase with heterofunctional chelate-epoxy modified magnetic nanoparticles and its carboligation reactivity. **Journal of Molecular Catalysis B: Enzymatic**, v. 95, p. 41–47, 2013.

ULU, A. et al. Design of near-infrared light induced functionalized upconverting nanoparticles as support in enzyme immobilization: Enhanced biocatalyst activity and stability. **International Journal of Biological Macromolecules**, v. 302, p. 140581, 2025.

UPPENBERG, J. et al. The sequence, crystal structure determination and refinement of two crystal forms of lipase B from Candida antarctica. **Structure**, v. 2, n. 4, p. 293–308, 1994.

UZAR, U. Political economy of renewable energy: Does institutional quality make a difference in renewable energy consumption? **Renewable Energy**, v. 155, p. 591–603, 2020.

UZUN, S. D. et al. A novel promising biomolecule immobilization matrix: Synthesis of functional benzimidazole containing conducting polymer and its biosensor applications. **Colloids and Surfaces B: Biointerfaces**, v. 112, p. 74–80, 2013.

VAGHARI, H.; MOJGAN, H. J. Application of magnetic nanoparticles in smart enzyme immobilization. **Biotechnology Letters**, v. 38, n. 2, p. 223–233, 2016.

VALERO, F. et al. Improved catalytic performance of lipase Eversa® Transform 2.0 via immobilization for the sustainable production of flavor esters – adsorption process and environmental assessment studies. **Catalysts**, v. 12, n. 11, p. 1412, 2022.

VALLE, B. et al. Improving process sustainability in bio-oil transforming for biofuels and platform chemicals production: Valorization of the carbon residue. **Fuel**, v. 364, p. 130994, 2024.

VAMATHEVAN, J. et al. Applications of machine learning in drug discovery and development. **Nature Reviews Drug Discovery**, v. 18, n. 6, p. 463–477, 2019.

VAN ECK, N. J.; WALTMAN, L. Software survey: VOSviewer, a computer program for bibliometric mapping. **Scientometrics**, v. 84, n. 2, p. 523–538, 2010.

VÁSQUEZ-GARAY, F.; TEIXEIRA MENDONÇA, R.; PERETTI, S. W. Chemoenzymatic lignin valorization: Production of epoxidized pre-polymers using Candida antarctica lipase B. **Enzyme and Microbial Technology**, v. 112, p. 6–13, 2018.

VAZIRISERESHK, M. R. et al. Solid lubrication with MoS2: A review. **Lubricants**, v. 7, n. 7, 2019.

VEISI, H. et al. Ultrasound assisted synthesis of Pd NPs decorated chitosan-starch functionalized Fe_3O_4 nanocomposite catalyst towards Suzuki-Miyaura coupling and reduction of 4-nitrophenol. **International Journal of Biological Macromolecules**, v. 172, p. 104–113, 2021.

VERMA, K.; MOHOLKAR, V. S. Mineralization of industrial wastewater by a hybrid technique of adsorption (Fe_3O_4@AC nanocomposite) + heterogeneous Fenton + sonication and discernment of synergistic effects. **Industrial and Engineering Chemistry Research**, v. 62, n. 5, p. 5002–5016, 2023.

VERMA, M. L.; BARROW, C. J.; PURI, M. Nanobiotechnology as a novel paradigm for enzyme immobilisation and stabilisation with potential applications in biodiesel production. **Applied Microbiology and Biotechnology**, v. 97, n. 1, p. 23–39, 2013.

VILLENEUVE, P. et al. Customizing lipases for biocatalysis: A survey of chemical, physical and molecular biological approaches. **Journal of Molecular Catalysis - B Enzymatic**, v. 9, n. 4–6, p. 113–148, 2000.

WIPO. Available at: https://patentscope.wipo.int/search/en/search.jsf. Accessed on: 15 Jan. 2023.

WAGH, V. P.; SABOO, N.; GUPTA, A. Tribology as emerging science for warm mix technology: A review. **Construction and Building Materials**, v. 359, n. September, p. 129445, 2022.

WAHAB, R. A. et al. On the taught new tricks of enzymes immobilization: An all-inclusive overview. **Reactive and Functional Polymers**, v. 152, n. April, p. 104613, 2020.

WAN, J. et al. Enzyme immobilization on amino-functionalized Fe_3O_4@SiO2 via electrostatic interaction with enhancing biocatalysis in sludge dewatering. **Chemical Engineering Journal**, v. 427, p. 131976, 2022.

WANCURA, J. H. C. et al. Combined production of biofuel precursors, platform chemicals, and catalyst material from the integral processing of rice bran. **Energy Conversion and Management**, v. 317, p. 118860, 2024.

WANG, D.; XIONG, T.; MOHSIN, M. Assessing the impact of cleaner bonds on clean energy expenditure for sustainable economic recovery: A fuzzy analytical approach. **Energy Strategy Reviews**, v. 55, p. 101547, 2024.

WANG, H. et al. A bibliometric review on stability and reinforcement of special soil subgrade based on CiteSpace. **Journal of Traffic and Transportation Engineering**, v. 9, n. 2, p. 223–243, 2022a.

WANG, H. et al. Application of magnetic field (MF) as an effective method to improve the activity of immobilized Candida antarctica lipase B (CALB). **Catalysis Science & Technology**, v. 12, n. 17, p. 5315–5324, 2022.

WANG, S. et al. Affinity screening of potential anti-obesity and anti-diabetic component from pomegranate peel by co-immobilization of lipase and α -amylase using carbon nanotube and hydrogel. **Process Biochemistry**, v. 126, n. November 2022, p. 51–60, 2023.

WANG, T. et al. New Insight into Assembled Fe_3O_4@PEI@Ag Structure as Acceptable Agent with Enzymatic and Photothermal Properties. **International Journal of Molecular Sciences**, v. 23, n. 18, p. 10743, 2022.

WANG, X. Y. et al. Preparation Fe3O4@chitosan magnetic particles for covalent immobilization of lipase from Thermomyces lanuginosus. **International Journal of Biological Macromolecules**, v. 75, p. 44–50, 2015.

WANG, Z. et al. Implementation of π-π interaction in AuNPs@GDY to boost the bioelectrocatalysis in enzymatic biofuel cells. **Bioelectrochemistry**, v. 158, p. 108712, 2024.

WEBB, B.; SALI, A. Comparative protein structure modeling using MODELLER. **Current Protocols in Bioinformatics**, v. 54, n. 6, p. 1–37, 2016.

WEN, L. et al. Insight into immobilization efficiency of Lipase enzyme as a biocatalyst on the graphene oxide for adsorption of Azo dyes from industrial wastewater effluent. **Journal of Molecular Liquids**, v. 354, p. 118849, 2022.

WILLIAMSON, E. M. et al. Design of Experiments for Nanocrystal Syntheses: A How-To Guide for Proper Implementation. **Chemistry of Materials**, 2022.

WINTON, S. et al. Accelerating the Delivery of the 2030 Agenda for Sustainable Development Through the Implementation of a Sustainable Blue Economy. **Reference Module in Earth Systems and Environmental Sciences**, 2024.

WRIGHT, D. W. et al. Computing clinically relevant binding free energies of HIV-1 protease inhibitors. **Journal of Chemical Theory and Computation**, v. 10, n. 3, p. 1228–1241, 2014.

WU, Y. et al. A review on current scenario of Nanocatalysts in biofuel production and potential of organic and inorganic nanoparticles in biohydrogen production. **Fuel**, v. 338, 2023.

XIAO, N. et al. Multidimensional nanoadditives in tribology. **Applied Materials Today**, v. 29, n. September, p. 101641, 2022.

XIE, W.; HUANG, M. Immobilization of Candida rugosa lipase onto graphene oxide Fe3O4 nanocomposite: Characterization and application for biodiesel production. **Energy Conversion and Management**, v. 159, n. January, p. 42–53, 2018.

XIE, W.; HUANG, M. Fabrication of immobilized Candida rugosa lipase on magnetic Fe 3 O 4 - poly (glycidyl methacrylate- co -methacrylic acid) composite as an ef fi cient and recyclable biocatalyst for enzymatic production of biodiesel. **Renewable Energy**, v. 158, p. 474–486, 2020.

XIE, W.; WANG, J. Enzymatic production of biodiesel from soybean oil by using immobilized lipase on Fe_3O_4/poly(styrene-methacrylic acid) magnetic microsphere as a biocatalyst. **Biomacromolecules**, v. 15, n. 3, p. 836–843, 2014.

XING, M. et al. Highly efficient removal of patulin using immobilized enzymes of Pseudomonas aeruginosa TF-06 entrapped in calcium alginate beads. **Food Chemistry**, v. 377, n. August 2021, p. 131973, 2022.

XU, H.; LIANG, H. Chitosan-regulated biomimetic hybrid nanoflower for efficiently immobilizing enzymes to enhance stability and by-product tolerance. **International Journal of Biological Macromolecules**, v. 220, p. 124–134, 2022.

XU, J. et al. Nickel-carnosine complex: a new carrier for enzyme immobilization by affinity adsorption. **Chinese Journal of Chemical Engineering**, v. 38, p. 237–246, 2021.

YADAV, A. et al. Comparative study for enzymatic hydrolysis of sugarcane bagasse using free and nanoparticle immobilized holocellulolytic enzyme cocktail. **Waste Management Bulletin**, v. 2, n. 1, p. 191–202, 1 abr. 2024.

YAMAGUCHI, H.; MIYAZAKI, M. Trends in Analytical Chemistry Enzyme-immobilized micro fl uidic devices for biomolecule detection. **Trends in Analytical Chemistry**, v. 159, p. 116908, 2023.

YANAI, T.; TEW, D. P.; HANDY, N. C. A new hybrid exchange–correlation functional using the Coulomb-attenuating method (CAM-B3LYP). **Chemical Physics Letters**, v. 393, n. 1–3, p. 51–57, 2004.

YANG, G. et al. Time for a change: Rethinking the global renewable energy transition from the Sustainable Development Goals and the Paris Climate Agreement. **The Innovation**, v. 5, n. 2, p. 100582, 2024.

YANG, H. et al. Magnetic recyclable MoS2/Fe3O4 piezoelectric catalysts for highly efficient degradation of aqueous pollutants. **Surfaces and Interfaces**, v. 55, p. 105271, 2024.

YANG, K. et al. Re-examination of characteristic FTIR spectrum of secondary layer in bilayer oleic acid-coated Fe_3O_4 nanoparticles. **Applied Surface Science**, v. 256, n. 10, p. 3093–3097, 2010.

YANG, K. et al. Re-examination of characteristic FTIR spectrum of secondary layer in bilayer oleic acid-coated Fe_3O_4 nanoparticles. **Applied Surface Science**, v. 256, n. 10, p. 3093–3097, 2010.

YANG, X. et al. Advances in magnetic nanoparticles for molecular medicine. **Chemical Communications**, v. 61, n. 15, p. 3093–3108, 2025.

YOUNES, I.; RINAUDO, M. Chitin and Chitosan Preparation from Marine Sources. Structure, Properties and Applications. p. 1133–1174, 2015.

YU, D. et al. Study on the modification of magnetic graphene oxide and the effect of immobilized lipase. **International Journal of Biological Macromolecules**, v. 216, n. November 2021, p. 498–509, 2022.

ZAAK, H.; SASSI, M.; FERNANDEZ-LAFUENTE, R. A new heterofunctional amino-vinyl sulfone support to immobilize enzymes: Application to the stabilization of β-galactosidase from Aspergillus oryzae. **Process Biochemistry**, v. 64, n. September 2017, p. 200–205, 2018.

ZANG, L. et al. Preparation of magnetic chitosan nanoparticles as support for cellulase immobilization. **International Journal of Biological Macromolecules**, v. 64, p. 302–307, 2014.

ZDARTA, J.; JESIONOWSKI, T.; BILAL, M. Designing multifunctional biocatalytic cascade system by multi-enzyme co-immobilization on biopolymers and nanostructured materials. **International Journal of Biological Macromolecules**, v. 227, p. 535–550, 2023.

ZENG, X. et al. Preparation of chiral polyether dendrimer and its non-bonding immobilized CALB for high enantioselective synergy resolution of amines. **European Polymer Journal**, v. 219, p. 113389, 2024.

ZHANG, J. et al. Bionic-immobilized recombinant lipase obtained via bio-silicification and its catalytic performance in biodiesel production. **Fuel**, v. 304, n. July, p. 121594, 2021.

ZHANG, M. et al. Chain-locked precursor ion scanning based HPLC – MS / MS for in-depth molecular analysis of lipase-catalyzed transesterification of structured phospholipids containing ω -3 fatty acyl chains. **Food Chemistry**, v. 399, n. July 2022, p. 133982, 2023.

ZHANG, Q. et al. Preparation of bionanomaterial based on green reduced graphene immobilized Ochrobactrum sp. FJ1: Optimization, characterization and its application. **Separation and Purification Technology**, v. 310, n. November 2022, p. 123144, 2023.

ZHANG, Q. et al. Co-immobilization of crosslinked enzyme aggregates on lysozyme functionalized magnetic nanoparticles for enhancing stability and activity. **International Journal of Biological Macromolecules**, v. 273, p. 133180, 2024.

ZHANG, X. et al. Conformation-Dependent Coordination of Carboxylic Acids with Fe 3 O 4 Nanoparticles Studied by ATR-FTIR Spectral Deconvolution. **Langmuir**, v. 35, n. 17, p. 5770–5778, 2019a.

ZHANG, X. et al. Optimal spacer arm microenvironment for the immobilization of recombinant Protein A on heterofunctional amino-epoxy agarose supports. **Process Biochemistry**, v. 91, n. November 2019, p. 90–98, 2020.

ZHANG, Y. et al. Bioinspired Immobilization of Glycerol Dehydrogenase by Metal Ion-Chelated Polyethyleneimines as Artificial Polypeptides. **Nature Publishing Group**, n. April, p. 1–10, 2016.

ZHAO, H. et al. Biomaterials Advances Strategy based on multiplexed brush architectures for regulating the spatiotemporal immobilization of biomolecules. **Biomaterials Advances**, v. 141, n. May, p. 213092, 2022.

ZHAO, Q. et al. Condition optimization and kinetic evaluation of Novozym 435-catalyzed synthesis of aroma pyridine esters. **Molecular Catalysis**, v. 550, p. 113532, 2023.

ZHENG, D. et al. Synthesis of butyl oleate catalyzed by cross-linked enzyme aggregates with magnetic nanoparticles in rotating magneto-micro-reactor. **Journal of Biotechnology**, v. 281, n. 15, p. 123–129, 2018.

ZHENG, M. M. et al. Immobilization of Candida rugosa lipase on magnetic poly (allyl glycidyl ether-co-ethylene glycol dimethacrylate) polymer microsphere for synthesis of phytosterol esters of unsaturated fatty acids. **Journal of Molecular Catalysis B: Enzymatic**, v. 74, n. 1–2, p. 16–23, 2012.

ZHENG, Y. et al. Esterification synthesis of ethyl oleate catalyzed by Brønsted acid–surfactant-combined ionic liquid. **Green Chemistry Letters and Reviews**, v. 10, n. 4, p. 202–209, 2017.

ZHENG, Y.; SHAHSAVAR, A.; AFRAND, M. Sonication time efficacy on Fe3O4-liquid paraffin magnetic nanofluid thermal conductivity: An experimental evaluation. **Ultrasonics Sonochemistry**, v. 64, p. 105004, 2020.

ZHOU, W.; ZHANG, W.; CAI, Y. Enzyme-enhanced adsorption of laccase immobilized graphene oxide for micro-pollutant removal. **Separation and Purification Technology**, v. 294, n. March, p. 121178, 2022.

ZOUARI, N. et al. Purification and characterization of a novel lipase from the digestive glands of a primitive animal: The scorpion. v. 1726, p. 67–74, 2005.